Simulated Gastrointestinal Digestion of Collagen Hydrolysates: Assessment of Peptide Bioavailability, Bioactivity and Impact on Gut Microbial Metabolites

Christina E. Larder
School of Human Nutrition
McGill University, Montreal

February 2022

A thesis submitted to McGill University in partial fulfillment
of the requirements for the degree of Doctor in Philosophy

ABSTRACT

Osteoarthritis (OA) is the most common joint disorder, with a social and financial burden that is expected to increase in the coming years. Currently there are no effective medications to treat it. Due to limited treatment options, patients often resort to supplements, such as collagen hydrolysates (CHs). CHs have demonstrated positive results in clinical trials, such as decreased joint pain, increased mobility, and structural joint improvements. The functional components of CHs are bioactive peptides (BAPs). There are significant knowledge gaps regarding the digestion, bioavailability, and bioactivity of CH-derived BAPs, and how different CH products compare in that regard. In this dissertation, the bioaccessibility, bioavailability and bioactivity of two bovine-sourced CHs (CH-GL and CH-OPT) were assessed. In Study 1, a novel method of peptide quantification (Ala-Hyp, Pro-Hyp, Pro-Hyp-Gly, Gly-Pro-Hyp) after simulated intestinal digestion was developed using capillary electrophoresis (CE). The digesta content of Gly-Pro-Hyp and Pro-Hyp-Gly was greater in CH-GL versus CH-OPT. Furthermore, the CH-GL and CH-OPT digests had distinct peptide profiles. As amino acids (AAs) are also found in CH products and may provide health promoting properties, a concurrent method for assessing bioaccessible AA content was developed using liquid chromatography–mass spectrometry (LC-MS). No differences in AA content were observed between the two CHs. In Study 2, freeze-dried digesta from Study 1 were applied to a novel co-culture of human intestinal epithelial (HIEC-6) and hepatic (HepG2) cells to simulate in vivo absorption and first pass metabolism. Peptide content was measured from the co-culture using an adapted CE method from Study 1. A high level of transport and hepatic first pass effects on BAPs (Gly-Pro, Hyp-Gly, Ala-Hyp, Pro-Hyp, Gly-Pro-Hyp) were observed. All peptides were bioavailable (>10%) to varying degrees with both CHs, except that Gly-Pro-Hyp was transported only with CH-GL. In Study 3, the prebiotic potential of the unabsorbed CH content was investigated using a multi-stage dynamic gastrointestinal digestion model containing human fecal matter. CH-OPT increased concentrations of H_2S, short- and branched-chain fatty acids, and decreased NH_4 content in the ascending colonic vessel whereas none of these effects were observed with CH-GL. MALDI and proteomic approaches were used to assess peptide profiles (15 AA+) prior to and after small intestinal digestion. After digestion, the peptide diversity of both CHs increased significantly, and demonstrated different profiles between CHs. In Study 4, CH digests were applied to cultures of murine osteoclasts (OCs) and osteoblasts (OBs) to determine their bioactivity on bone. CH doses

used were physiologically relevant and based on peptide content after digestion (Study 1), and bioavailability (Study 2). Depending on the applied CHs, osteoclastogenesis was reduced, while osteoblast differentiation markers and mineralization were increased. Generally, CHs decreased expression of RANK and Lair-1 in OC and modulated Oscar expression, while also increasing OB differentiation markers Runx2 and Osterix. The combined approaches of using in vitro digestion models and cell culture systems provide an innovative platform to assess for the bioaccessibility and bioavailability of BAPs. Using these novel methods, this thesis demonstrates significant differences in peptide content and bioavailability between CH-GL and CH-OPT, as well as significant differences in bioactivity at the colonic level and in bone related cultures. Overall, these findings indicate the potential of CHs to exhibit prebiotic effects and to modulate the activity of bone remodeling cells, helping support the use of CHs to treat OA.

RÉSUMÉ

L'arthrose est le trouble articulaire le plus courant, avec un fardeau social et financier considérable. En raison des options de traitement limitées, les patients ont souvent recours à des compléments alimentaires, tels que les hydrolysats de collagène (CH). Les CH ont démontré des résultats positifs lors d'essais cliniques, tels que la diminution des douleurs articulaires, l'augmentation de la mobilité et l'amélioration de la structure articulaire. Les composants fonctionnels des CHs sont des peptides bioactifs (PBA). Il existe d'importantes lacunes dans les connaissances concernant la digestion, la biodisponibilité, la bioactivité des PBA dérivés des CH et les différences entre produits CH à cet égard. Dans cette thèse, la bioaccessibilité, la biodisponibilité et la bioactivité de deux CH d'origine bovine (CH-GL et CH-OPT) ont été évaluées. Dans l'étude 1, une nouvelle méthode de quantification des peptides (Ala-Hyp, Pro-Hyp, Pro-Hyp-Gly, Gly-Pro-Hyp) suivant une digestion intestinale simulée a été développée en utilisant l'électrophorèse capillaire (EC). La teneur des digesta en Gly-Pro-Hyp et Pro-Hyp-Gly était plus importante dans le CH-GL que dans le CH-OPT. Puisque les acides aminés (AA) sont également présents dans les CH et qu'ils peuvent avoir des propriétés bénéfiques pour la santé, une méthode simultanée d'évaluation de la teneur en AA bioaccessibles a été mise au point à l'aide de la chromatographie liquide-spectrométrie de masse (LC-MS). Aucune différence dans la teneur en AA n'a été observée entre les deux CH. Dans l'étude 2, les digesta lyophilisés de l'étude 1 ont été appliqués à une nouvelle co-culture de cellules épithéliales intestinales humaines (HIEC-6) et hépatiques (HepG2) pour simuler l'absorption in vivo et le métabolisme de premier passage. Le contenu en peptides résultant a été mesuré en utilisant une méthode EC adaptée de l'étude 1. Un niveau élevé de transport et d'effet de premier passage hépatique sur les PBA (Gly-Pro, Hyp-Gly, Ala-Hyp, Pro-Hyp, Gly-Pro-Hyp) a été observé. Tous les peptides étaient biodisponibles (>10%) avec les deux CH, sauf Gly-Pro-Hyp qui n'a été transporté qu'avec CH-GL. Dans l'étude 3, le potentiel prébiotique des CH a été étudié à l'aide d'un modèle de digestion gastro-intestinale dynamique à plusieurs étapes contenant des matières fécales humaines. Seul le CH-OPT a augmenté les concentrations de H_2S, d'acides gras à chaînes courte et ramifiée, et a diminué la teneur en NH_4 dans le vaisseau colonique ascendant. Des approches MALDI et protéomiques ont été utilisées pour évaluer les profils peptidiques avant et après la digestion intestinale. Suivant la digestion, la diversité peptidique des deux CH a augmenté, et des profils différents entre les CH ont été observés. Dans l'étude 4, les digesta des CH ont été appliqués à des cultures d'ostéoclastes (OC) et

d'ostéoblastes (OB) murins pour déterminer leurs effets sur les os. Les doses de CH utilisées étaient basées sur la teneur en peptides déterminée lors des études 1 et 2. Selon les CH appliqués, l'ostéoclastogenèse a été réduite et les marqueurs de différenciation des ostéoblastes et leur minéralisation ont augmenté. Les CH ont diminué l'expression de RANK et Lair-1 dans les OC et ont modulé l'expression d'Oscar, tout en augmentant les marqueurs de différenciation des OB, Runx2 et Osterix. Les approches combinées de l'utilisation de modèles de digestion in vitro et de systèmes de culture cellulaire fournissent une plateforme innovante pour évaluer la bioaccessibilité et la biodisponibilité des PBA. Cette thèse démontre des différences significatives dans la teneur en peptides et la biodisponibilité entre CH-GL et CH-OPT, ainsi que dans la bioactivité au niveau du côlon et dans les cultures liées aux os. Dans l'ensemble, ces résultats indiquent le potentiel des CH à exercer des effets prébiotiques et à moduler l'activité des cellules de remodelage osseux, contribuant à soutenir l'utilisation des CH pour traiter l'arthrose.

ACKNOWLEDGEMENTS

This dissertation is a result of all the support and guidance I received during my studies.
I would like to thank Dr. Stan Kubow for his endless enthusiasm and vital advice. I am eternally grateful that you gave me this amazing opportunity to pursue a Ph.D. with you as my supervisor. I was privileged to have your support and mentorship throughout my studies.

I would also like to thank my committee members, Dr. Elias Georges and Dr. Benjamin Simpson for their time, constructive feedback and guidance.

I wish to thank the Mitacs and NSERC funding programs, which help support students and companies to collaborate and to design and perform innovative research. These collaborations help contribute to scientific knowledge as well as make an impact for Canadian companies. These programs facilitated an amazing collaboration with a motivated and welcoming team at Genacol. A special thanks to Frederick Michaud and his family for making this project so much more than a PhD, but a lifetime achievement that I enjoyed and am proud of. Getting to know the team at Genacol made me even more passionate about my project.

A special thanks goes to Dr. Michele Iskandar. Besides providing critical and extensive editorial help, training me in cell culture, providing input on study design, helping with budgets, keeping me sane with long lab hours and thesis writing... the list goes on and on… you have become an extremely important person in my life. A mentor and friend, you were always ready with words of encouragement. I cannot express my gratitude enough.

I would like to thank the members of the McGill University Hospital Center (MUHC) Research Institute. To the members of the proteomics department, thank you to Dr. Lorne Talyor for his critical role in performing proteomics analysis, training, and guidance in data interpretation, as well as Dr. Amy Wong who facilitated the service. To all the members at the drug discovery platform: Dr. Sanjoy Kumar Das, Dr. Anne-Laure Larroque, Dr. Andrée Gravel, Dr. Nidia Lauzon, and Dr. Carine Bourget, thank you for time, patience and help in developing LC-MS methodology and well as MALDI analysis. I was extremely fortunate to also have support from Dr. Kebba Sabally from McGill

University and Patrick Sabourin from TechnoPro for their expertise in capillary electrophoresis; thank you. Further thanks to Dr. Sabally for helping me with all the various lab tasks such as changing GC tanks! I wish to also thank Dr. Norma Bautista-Lopez from McGill's parasitology department for her patience and help using the Cytation 5 instrument. Additional thanks go to Britney Phippen from Biotek for her incredible assistance in developing imaging and data extraction protocols. Thank you also to Dr. Youssef Chebli, who helped with imaging and was always ready to discuss microscopy techniques and options. I am eternally grateful that he suggested I use the Cytation 5.

To Dr. Mohd Baasir Gaisawat, who besides providing essential in-lab training, gut model support, and thesis guidance, became a good friend. I am honored to have you in my life.

To the members of Dr. Kubow's lab who have created a fun and loving work environment, I am deeply grateful. Thank you, Mr. Lucas Roldos, Ms. Fang Lu, and Ms. Xiaojiao Yang. I would also like to thank my undergraduate intern, Rackshana Sithirasenan, who helped with cell culture and was always a motivated student willing to learn.

I would also like to thank Dr. Svetlana Komarova for her generous offer to perform all bone related work in her lab. She truly was a lifesaver for me, at a time when my PhD project changed direction. I am extremely grateful. Her invitation to her lab meetings also proved to be an invigorating and educational experience. A special thanks to Dr. Josephine Tauer for her amazing, meticulous, and patient training, her wonderful efficiency suggestions, and her forceful and yet totally justifiable suggestion that I use GraphPad. It was a true pleasure to work alongside her and learn from her. Her valuable friendship is something I take away from our work together. To the members of Dr. Komarova's lab, Dr. Kerstin Tiedemann and Chrisanne Dsouza, thank you for making the lab at the Shriners Hospital so enjoyable and a place that I always wanted to go back to.

I wish to also thank all my friends and family who showed interest in my work, regardless of how many times they heard about it! Their willingness to listen helped me develop essential communication skills.

My thanks and love go out to my parents who have sacrificed so much for me. My mother, Linda Lanno, and my father, Stephen Larder, are such supportive and encouraging people that if I can be even half as great as them, I know I will have lived a good life. I love you both.

And to my wonderful husband, Ajith Airody, who went on this “thesis adventure” with me. With your support, I knew I could do it.

PREFACE

This thesis is presented in a manuscript format and consists of seven chapters. Chapter 1 presents a general introduction to osteoarthritis and the bioavailability and bioactivity of collagen hydrolysates, a supplement which is currently used by patients with joint pain to manage their condition. Chapter 2 presents a comprehensive review of current literature relating to all aspects of this thesis, notably on the limited treatments for osteoarthritis and how the use of oral supplements, such as collagen hydrolysates, may provide health benefits to patients. This section provides an in-depth review of collagen hydrolysates, their proposed bioactive components, their bioavailability, and their effects on bone and microbial fermentation products, as well as current challenges regarding methodologies available for their assessment. Chapters 3 through 6 are original research manuscripts that are linked using connecting statements. Chapter 3 has been published in LWT- Food Science and Technology. Chapter 4 has been published in Current Issues in Molecular Biology. Chapter 5 has been published in Nutrients. Chapter 6 will be submitted to Scientific Reports. Finally, the last chapter presents an overall discussion and conclusion of the work completed in this thesis as well as the implications of the main findings and recommendations for future work. This dissertation is in accordance with guidelines for thesis preparation as published by the Faculty of Graduate Studies and Research of McGill University.

CONTRIBUTION TO ORIGINAL KNOWLEDGE

A. Claims of Original Research

The aim of this doctoral thesis was to better understand the digestion, bioavailability and bioactivity of collagen hydrolysates (CHs) using novel analytical techniques and in vitro models. In Study 1, two different CH products (CH-GL and CH-OPT) underwent upper intestinal digestion and their peptide profiles, bioactive peptides (BAPs), and amino acids were assessed. Although both CHs were bovine sourced, profiles of low molecular weight peptides after digestion confirmed that the two products had different peptide compositions. Bioactive peptide content after digestion was also different between CHs products and was assessed using a novel method of targeted quantification via capillary electrophoresis. In addition, the amino acid content of the two CHs after digestion was measured using liquid chromatography–mass spectrometry (LC-MS), adapted with a hydrophilic interaction liquid chromatography and zwitterionic (HILIC-Z) column.

In Study 2, the bioavailabilities of key BAPs (Gly-Pro, Hyp-Gly, Ala-Hyp, Pro-Hyp, Gly-Pro-Hyp) from CH digesta obtained in Study 1 were assessed using a novel combination of intestinal (HIEC-6) and hepatic (HepG2) cells. This study adapted and utilized the methodology for targeted peptide quantification developed in Study 1. All peptides were transported across the intestinal cell layer to varying degrees with both CHs, but Gly-Pro-Hyp was transported only with CH-GL, and not CH-OPT. A notable difference in hepatic production was also observed; Ala-Hyp content was increased after hepatic action with both CH treatments, whereas Pro-Hyp and Gly-Pro increased with CH-GL only. In terms of overall bioavailability, no differences between CHs were observed for all peptides except that CH-GL showed significant Gly-Pro-Hyp content after first pass metabolism, whereas none was observed after CH-OPT. This study used a novel cell culture method to assess, for the first time, the bioavailability of BAPs from CH digesta.

In Study 3, an in vitro gastric and small intestinal digestion model further investigated the differences in peptide content between CH products. Proteomic analysis investigating peptides with 15 AA+ demonstrated different native peptide profiles with increased peptide diversity after digestion. This was the first study to characterize peptides before and after digestion of similarly sourced CHs. Relating to Study 1, it was confirmed that both low and high MW peptide profiles of

the CHs assessed are different. Using a dynamic computer controlled gastrointestinal (GI) model involving reactors representing the stomach, small intestine and three colonic vessels inoculated with human fecal matter, the prebiotic effects of CH treatments were assessed. In the ascending colonic reactor, CH-OPT increased H_2S, the short-chain fatty acid (SCFAs) propionic, butyric and valeric acids, as well as branched-chain fatty acids (BCFAs) and decreased NH_4, with no major changes observed with CH-GL treatment. No major effects were observed in the transverse and descending vessels for either CH. For the first time, these findings demonstrate that CHs can induce prebiotic effects in the ascending colon that are CH dependent.

In Study 4, the bioactivities of the CHs, CH-GL and CH-OPT, were evaluated on primary murine bone remodelling cells, osteoclasts (OCs) and osteoblasts (OBs). Most in vitro studies conducted to date have not accounted for GI digestion of CHs leading to altered BAP profiles, nor the bioavailability of CH-derived BAPs. To address this gap and to utilize a more physiologically representative study design, the estimated peptide bioavailabilities from Study 2 were used to determine doses of CH digesta from Study 1 that were administered to OC and OB cultures. CH-GL digests led to a significant decrease in OC size, and therefore OC activity, whereas CH-OPT did not. In addition, significant changes in osteoclastic gene expression were observed. We report, for the first time, changes to the gene expression levels of receptor activator of nuclear factor kappa-β (*Rank*), osteoclast associated Ig-like receptor (*Oscar*), leukocyte-associated immunoglobulin-like receptor-1 (*Lair-1*), and dendritic cell-specific transmembrane protein (*Dc-stamp*) after CH digesta treatment. Decreased gene activity in OCs was observed after CH-GL, more so than CH-OPT. Evaluation of osteoblastic gene expression demonstrated that levels of runt-related transcription factor 2 (*Runx2*) and transcription factor Sp7 (*Osterix*) were increased with CH-GL, although only *Runx2* was increased with CH-OPT. Expression levels of matrix metalloproteinase (*MMP)-9* and *MMP-13* from OBs after CH treatment were also reported for the first time. Notably, *MMP-9* activity was decreased after CH-GL only. Comprehensive microscopic evaluation of OBs using three stains – alizarin red, alkaline phosphatase and sirius red – supported gene expression results. Overall, CH-GL and CH-OPT exerted different effects on OBs and OCs in a CH type- and dose-dependent manner. Most in vitro models assessing the mechanisms involved in bone remodeling affected by CH treatment have focused on bone forming cells, with little work assessing the effects on OCs.

Importantly, this study demonstrated that the CH-derived peptides may alter the differentiation and activity of both OCs and OBs, and thus may impact bone health in humans.

B. Research Publications in Peer-Reviewed Scientific Journals

Larder, C. E., Iskandar, M. M., Sabally, K., & Kubow, S. (2022). Complementary and Efficient Methods for Di- and Tri-Peptide Analysis and Amino Acid Quantification from Simulated Gastrointestinal Digestion of Collagen Hydrolysate. LWT - Food Science and Technology, 155, 112880. doi:https://doi.org/10.1016/j.lwt.2021.112880

Larder, C. E., Iskandar, M. M., & Kubow, S. (2021). Assessment of Bioavailability after in Vitro Digestion and First Pass Metabolism of Bioactive Peptides from Collagen Hydrolysates. Current Issues in Molecular Biology, 43(3), 1592-1605. doi:10.3390/cimb43030113

Larder, C. E., Iskandar, M. M., & Kubow, S. (2021). Gastrointestinal Digestion Model Assessment of Peptide Diversity and Microbial Fermentation Products of Collagen Hydrolysates. Nutrients, 13(8), 2720. doi:https://doi.org/10.3390/nu13082720

III. Abstracts and Presentations

Larder, C. E., Iskandar, M. M., Sabally, K., & Kubow, S. (2018). Capillary Electrophoresis: A Fast, Cost Effective and Efficient Method Replacement for LC-MS When Identifying and Quantifying Small Peptides from Simulated Gastrointestinal Digestion of Collagen Hydrolysate. Paper presented at the BenefiQ Conference Quebec City Convention Centre, Canada

Larder, C. E., Iskandar, M. M., & Kubow, S. (2020). Dynamic Multi-Stage Gastrointestinal Digestion Model Assessment of Microbial Fermentation Products of Collagen Hydrolysates. Proceedings, 61(12), 12. doi:10.3390/IECN2020-06998

Larder, C. E., Tauer, J. T., Iskandar, M. M., Komarova, S. V., & Kubow, S. (2022). Effects of Collagen Hydrolysate Digests on Cells Involved in Bone Remodeling. To be presented at the OARSI 2022 World Congress, Berlin, Germany & Virtual - *accepted for poster presentation*

CONTRIBUTION OF AUTHORS

Christina Elizabeth Larder (Candidate) was responsible for designing, developing, and carrying out experimental protocols including in vitro digestions, cell culture, MTT, capillary electrophoresis methods for peptide analysis, amino acid analysis (LC-MS), spectrophotometric assays (antioxidant, ammonium, and hydrogen sulphide assessment), metabolic marker analysis (GC-FID), RNA extraction and qPCR analysis, fixing, staining and imaging processing. The candidate was also responsible for the interpretation of data, including proteomics and MALDI analysis, data calculation and statistical analysis. The candidate produced all tables and figures and wrote all original drafts of the manuscripts and chapters included in this thesis.

Dr. Stan Kubow (Candidate's supervisor) was responsible for the initiation of the research project, was involved in study design, methodology and provided critical feedback and guidance. Dr. Kubow supervised all aspects of the dissertation and provided extensive feedback for all manuscripts and thesis chapters.

Dr. Michele Iskandar was involved in developing the methodology for in vitro digestions and cell culture experiments and provided ongoing support for all lab experiments. Dr. Iskandar also provided critical feedback and support for data interpretations and visuals. She provided valuable input in reviewing and editing of manuscripts and thesis chapters.

Dr. Josephine Tauer provided training and support for all bone related cell culture work, staining, RNA extraction and qPCR. She provided key input in study design, methodology, data calculations and presentation, interpretations, and editorial feedback for Manuscript 4 (Chapter 6).

Dr. Svetlana Komarova provided support for all experiments included in Chapter 6. Dr. Komarova also provided critical feedback on data and results, as well as reviewing and editing for Manuscript 4 (Chapter 6).

Dr. Kebba Sabally provided training and support with GC and CE methods. Dr. Sabally helped to develop the methodology for peptide analysis.

TABLE OF CONTENTS

LIST OF TABLES

LIST OF FIGURES

ABBREVIATIONS

AA	Amino acid
ABTS	2,2'-Azino-bis-(3-ethylbenzothiazoline sulphonic acid)
ALP	Alkaline phosphatase
ANOVA	Analysis of variance
BAP	Bioactive peptide
BCFA	Branched-chain fatty acid
BMD	Bone mineral density
Caco-2	Human epithelial colorectal adenocarcinoma cells
CE	Capillary electrophoresis
CH	Collagen hydrolysate
CH-GL	Genacol Original Formula® Collagen
CH-OPT	Selection collagen hydrolysate
CIA	Collagen-induced arthritis
Col1a1	Collagen type I alpha 1 chain
CT	Computed tomography
Ctsk	Cathepsin K
CTX	C-terminal telopeptide
CTX 1	C-telopeptide of type I collagen
CZE	Capillary zone electrophoresis
Dc-Stamp	Dendritic cell-specific transmembrane protein
DMD	Disease-modifying drug
DMEM	Dulbecco's modified eagle medium
DMM	Destabilization of the medial meniscus
DPPH	2,2-Diphenyl-1-picrylhydrazyl
DPP-IV	Dipeptidyl peptidase-IV
ECM	Extracellular matrix
EDTA	Ethylenediaminetetraacetic acid
ES	External standard
ESI	Electrospray ionization

FBS	Fetal bovine serum
FD	Freeze-dried
FRAP	Ferric reducing ability of plasma
GAG	Glycosaminoglycan
GAPDH	Glyceraldehyde 3-phosphate dehydrogenase
GBD	Global burden of disease
GC	Gas chromatography
GC-FID	Gas chromatograph system equipped with a flame ionization detector
GI	Gastrointestinal
GlcN	Glucosamine
H_2S	Hydrogen sulfide
HCD	Higher-energy collisional dissociation
HepG2	Human hepatoma G2 cells
HER	English electronic heath record
HIEC	Human small intestinal epithelial cells
HILIC	Hydrophilic interaction liquid chromatography
HPLC	High performance liquid chromatography
HPLC-ESI-MS	High performance liquid chromatography–electrospray ionization tandem mass spectrometry
IDL	Instrument detection limit
IL	Interleukin
IS	Internal standard
IT	Ion trap
Lair-1	Leukocyte-associated immunoglobulin-like receptor-1
LC-MS	Liquid chromatography-mass spectrometry
LRC	Leucocyte receptor complex
M	Molar
MALDI	Matrix assisted laser desorption/ionization
MALDI-TOF	Matrix assisted laser desorption/ionization time-of-flight
M-CSF	Macrophage colony stimulating factor

MDL	Method detection limit
MEM	Minimum essential medium
MMP	Matrix metalloproteinase
MRI	Magnetic resonance imaging
MRM	Multiple reaction monitoring
MSC	Mesenchymal stem cell
MTT	3-(4,5-dimethylthiazol-2-yl)-2,5-diphenyl tetrazolium bromide
MW	Molecular weight
MWCO	Molecular weight cut off
nd	Not detectable
NFATc1	Nuclear factor activated T cells 1
NF-κB	Nuclear factor kappa B
NH_4	Ammonium
NMR	Nuclear magnetic resonance
NSAID	Non-steroidal anti-inflammatory drug
NTX	N-terminal telopeptide
OA	Osteoarthritis
OARSI	Osteoarthritis research society international
OB	Osteoblast
OC	Osteoclast
OSCAR	Osteoclast associated Ig-like receptor
Osterix	Transcription factor Sp7
OUT	Operational taxonomic unit
P1NP	Amino-terminal propeptide of type I collagen
Papp	Permeability coefficient
PBMC	Blood mononuclear cell
PCR	Polymerase chain reaction
PepT1	Peptide transporter 1
PET	Polyester
qPCR	Quantitative polymerase chain reaction

RA	Rheumatoid arthritis
RANK	Receptor activator of nuclear factor kappa-β
RANKL	Receptor activator of nuclear factor kappa-β ligand
ROS	Reactive oxygen species
RSD	Relative standard deviation
RT	Room temperature
RT-PCR	Reverse transcription-polymerase chain reaction
Runx2	Runt-related transcription factor 2
SCFA	Short-chain fatty acid
SD	Standard deviation
SEM	Standard error of mean
SF-36	Short form 36 health survey questionnaire
SI	Small intestine
SLC15A1	Solute carrier family 15 member 1
TEER	Transepithelial electrical resistance
TNF-α	Tumor necrosis factor alpha
TRAP	Tartrate-resistant acid phosphatase
UC-II	Undenatured type II collagen
UPLC	Ultra-performance liquid chromatography
VAS	Visual analogue scale
WOMAC	Western Ontario and McMaster Universities Osteoarthritis

CHAPTER 1: GENERAL INTRODUCTION

1.1 Introduction

Osteoarthritis (OA) is the most common arthritic disorder [1]. Symptoms range from joint pain and deformity, swelling, to decreased mobility and quality of life [1-3]. The social and financial burden of OA is expected to increase with a global aging population; the incidence of hip and knee OA already affects more then 303 million people globally [2]. Typically, characterized as a "wear and tear" disease associated with decreased cartilage, OA is now considered a disease of the whole joint where all articular structures play a significant role in joint health [1, 4].

With limited treatments options, and no available disease-modifying drugs (DMDs), patients often use nutraceuticals or supplements such as collagen hydrolysates (CHs), to help manage OA symptoms. As several clinical trials have shown that the oral ingestion of CHs leads to decreased pain and increased mobility [3, 5-8], CHs remains a safe, viable and easily accessible option for patients. Patient improvement after CH treatment, or its precursor gelatin, has been associated with post-digestion release of absorbable bioactive peptides (BAPs) and amino acids (AAs) that can reach the systemic circulation, then enter joint tissues [9-12]. The BAPs released after CH digestion, such as Pro-Hyp and Gly-Pro-Hyp, possess multiple health properties. These CH BAPs have been shown to help reduce pain associated with OA, stimulate wound healing and cartilage growth, regulate inflammation, as well as to exhibit angiotensin-I-converting enzyme inhibitory effects and antioxidant properties [7, 9, 10, 13]. Studies have also established that CHs have a beneficial impact on joint bone health, by decreasing bone loss, increasing bone strength and calcium content, as well as improved bone mineral density (BMD) and bone biomechanical parameters [14-17].

Despite the widespread use of CHs for the treatment of OA joint pain, studies are lacking regarding the digestion and bioavailability profiles of the key BAPs and AAs following CH digestion and the mechanisms by which they may modulate joint health. In addition, differences among CH products, attributed to collagen source, processing, and resulting BAP profiles are only recently being recognized, which may affect bioactivity [18-20]. Animal studies have been often used to estimate the BAPs bioavailability from collagen products [21-25]; however, due to species differences in intestinal permeability, predictions of bioavailability from animal models do not always correspond

with human clinical data [23, 26]. Human trials to determine bioavailability are costly with various ethical constraints and requirements. Instead, cell culture models are often used to assess the intestinal transport of food-derived BAPs [26]. To represent the physiological in vivo conditions of the small intestine [27-30], a non-tumorigenic human small intestinal epithelial cell (HIEC) line can be used for predicting transporter-mediated absorption of peptides in humans [27, 28]. In addition, it is important to also consider the subsequent hepatic first pass effects on the intestinally transported BAPs. Previous models assessing first pass have used the human hepatoma G2 (HepG2) cell line, to assess the hepatic metabolism of xenobiotics and drug transporters [31, 32]. Co-cultures of intestinal cells and hepatic cells have been used to determine first pass effects [31, 33], however combination of HIEC/HepG2 cells has not been utilized to date.

There is a significant lack of published methodologies on targeted BAP and AA quantification for protein hydrolysates, as well as bioavailability in vitro. It is therefore important to develop sensitive, rapid and cost-effective methods of measuring these bioactive compounds, as the health benefits of BAPs and AAs from collagen products have become more evident. Although previous studies have indirectly measured BAP and AA content from human blood plasma after oral ingestion of collagen products [9, 25, 34], the determination of peptides generated during in vivo digestion remains technically challenging, costly, and requires human or animal ethics approval. Instead, simulated digestion models provide a readily utilizable in vitro approach to detect BAPs and AAs released from digestive processes [26]. In vitro models designed and inoculated with human fecal matter also allow for investigations into the microbiome and microbial fermentation products.

Food components not absorbed by the intestine which include proteins, peptides, and AAs, can travel to colonic regions and be fermented by host microbiota [35, 36]. These dietary components are called prebiotics, and can induce beneficial changes in the activity, growth, or composition of microorganisms found in the gastrointestinal (GI) tract. Prebiotics have been shown to exhibit antioxidant activity, regulate inflammation, as well as reduce symptoms associated with arthritis [37-41]. Microbial fermentation products of prebiotics, such as short-chain fatty acids (SCFAs) which include acetate, propionate, and butyrate, provide several health benefits [35, 39, 42]. Branched-chain fatty acids (BCFAs) are also a product of microbial fermentation, however their impact on human health is still unclear. For example, increased production of BCFAs has been linked with

insulin resistance and obesity [43] but also associated with preventing irritable bowel syndrome [44]. As CHs contain a significant and diverse profile of peptides and AAs after digestion [45, 46], CHs may lead to the generation of microbial fermentation products in the colon, thereby potentially acting as a prebiotic. To date, the impact of CHs on the microbiome has not been investigated. As a readily accessible over-the-counter product, currently being taken by a wide population, it is important to investigate the potential impact of CHs on the generation of microbial fermentation products in the colon.

In order to study these changes at the microbiota level, the use of dynamic in vitro GI models can be applied to closely mimic human upper intestinal digestion and recreate the colonic environment similar to human in vivo conditions [47, 48]. These GI models are increasingly being utilized to predict protein and peptide digestibility and microbiome analysis [26, 49]. Assessment of microbial fermentation products such as SCFAs, BCFAs and colonic gases from these models provides information on the functional activity and compositional profiles of the gut microbiota [50-52].

Although recent clinical work has begun to demonstrate the effectiveness of CHs on BMD [53], in vitro studies are often used to investigate the molecular mechanisms and bone remodeling pathways affected by CHs. Two cell types primarily regulate bone remodeling: osteoclast (OCs) and osteoblasts (OBs). Bone resorption is orchestrated by OCs to remove bone, whereas new bone tissue is formed by OBs. Most in vitro models assessing the mechanisms involved in bone metabolism affected by CH treatment have often neglected to assess the effects on OCs; instead, studies have primarily focused only on OBs, and most work has failed to account for the digestion of CHs in the GI tract [54].

1.2 Research objectives

1. To develop sensitive and rapid methods for accurate targeted BAP and AA detection and quantification following in vitro digestion of CHs
2. To determine peptide bioavailability from two bovine-sourced CH digests utilizing a novel co-culture method of HIEC and HepG2 cells.

3. To utilize a dynamic in vitro model of digestion to assess microbial fermentation products after two different CH treatments.
4. To evaluate the possible impact and mechanisms by which two different CH digesta could affect bone remodeling cells.

1.3 Hypotheses

1. Two commercial sources of bovine CHs will differ in their peptide composition, which will lead to differences in their post-digestion peptide profiles.

2. Altered post-digestion peptide profiles between bovine CHs will lead to differences in: (a) colonic metabolite production; (b) bioavailability; and (c) bone cell remolding and differentiation.

CHAPTER 2: LITERATURE REVIEW

2.1 Osteoarthritis

2.1.1 Incidence, prevalence, and symptoms

Osteoarthritis (OA) is the most common joint disorder, and the social and financial burden of OA is only expected to increase [2, 55]. The Global Burden of Disease (GBD) project, using data up until 2017, estimated that there are over 303.1 million cases of hip and knee OA [2]. Although seemingly a large number, this GBD report is likely an underestimation, as a greater number of hand and foot cases have been diagnosed, and due to the lack of accurate data for some countries such as Central America, and sub-Saharan Africa. In fact, a commentary published in The Lancet has estimated that the global burden of OA is more then 500 million, or about 7% of the global population [56]. Other large scale approaches investigating OA, such as the English Electronic Health Record (EHR), using data from 2010 to 2015, has also shown that OA is one of most common conditions that patients seek care for [2], however, general healthcare practitioners often minimize concerns about OA, which can delay possible treatment or intervention [56]. The social and financial burden of OA depends on location, the corresponding health care system, and available services [56]. For these reasons, a direct estimation of the financial impact of OA is difficult, although data from the United States indicates that in 2016, approximately over $800 million was spent on OA alone [2]. In addition, patients with OA have increased work absence and may also exit the workforce early, thereby losing years of work that could affect personal finances [2, 57]. Patients with OA experience pain or aching in the joints, as well as stiffness, swelling and decreased mobility [1, 58]. As a result, reduced functionality and disability are common, as well a significant reduction in quality of life and mental health [1, 57].

2.1.2 Risk factors

The development of OA is not caused by a singular event and may occur or progress differently between patients. For this reason, there are a vast variety of systemic and local risk factors that affect the development, progression, and stages of OA [55]. One of the systemic risk factors for OA is genetic predisposition, where studies involving twins have suggested that 50-65% of OA onset is hereditary [55]. Age is also one of the best known and greatest risk factors for the development of OA, but it remains unclear whether the aging process itself induces OA, or whether it is the accumulation of exposures to other risk factors and biological changes as patients age, which

destabilize the joint and induce OA [55, 57]. With age, patients often have decreased muscle mass, increased oxidative damage, poor diet and decreased physical activity, which can also contribute to increased OA risk [55, 57]. Sex is another well-established systemic risk factor for OA, where women are more likely to develop OA, as well as exhibit more severe radiological and symptomatic OA [55]. Women usually develop OA during menopause and for this reason, hormonal changes have been suggested as a risk factor, but results regarding the effects of estrogen remain conflicting and inconclusive [55]. Links between OA and osteoporosis, a condition that also occurs during menopause and is caused by hormonal changes, has also been proposed as a risk factor, although further well defined and conclusive clinical work is needed. Considering the link between OA and bone health, altered bone density has also been well identified as a risk factor for OA [57]. Finally, ethnicity and race are also risk factors, linked to differences in bone structure and joint space narrowing [55, 57].

Diet can be considered both a systemic and local risk factor for OA [55]. Diet and lifestyle are key factors relating to overall human health, and healthier individuals with diets high in fiber are less likely to develop severe OA [57]. Poor dietary choices as well as reduced physical activity contribute to the development of obesity and OA [58]. Obese patients are more likely to develop OA, due to increased load bearing on joints, as well as other factors such as increased systemic inflammation [41, 59]. The incidence of OA and impact on social and individual financial burden is only expected to increase, due to a growing aging and obese population [58]. OA is also highly associated with other metabolic diseases and conditions such as diabetes, hypertension and dyslipidemia [57, 60-63], as well as an increased risk of metabolic syndrome [64, 65]. The link between metabolic diseases and OA has become increasingly significant in recent work, as shown by the 2021 Osteoarthritis Research Society International (OARSI) Virtual World Congress, which held dedicated sessions on metabolic pathways and disorders contributing to OA [66]. In a comprehensive study of the National Health and Nutrition Examination Survey III cohort, results showed that the prevalence of metabolic syndrome was increased in patients with OA, regardless of age and BMI [64]. Further studies, following approximately 1,000 patients over 20 years, have established that type 2 diabetes is a significant risk factor for severe OA, again independently of age and BMI [64]. Other local risk factors for OA include previous injury, occupation, and participation in contact sports [2, 55, 57].

Joint deformity caused by other underlying conditions as well as joint alignment may also predispose patients to develop OA [55, 57].

2.1.3 Clinical manifestations: phenotypes and stages of OA

OA is primarily diagnosed in the knees and hips, but also found often in the hands, feet, and spine [1]. As various joints can be affected and the manifestation of OA can be significantly different from patient to patient, OA is considered a heterogeneous disease with various stages and distinct phenotypes [57, 58]. To date, the definition of OA phenotypes is still heavily debated, as our knowledge of biomarkers measured in blood and urine, such as cytokine profiles, metabolomics and genomics continue to be investigated [58]. Some of the most common and generally agreed upon clinical phenotypes defined so far: 1) pain phenotypes; 2) inflammation (e.g., synovitis); 3) bone and cartilage changes; and 4) presence of biochemical markers [57, 58]. A risk factor for OA, metabolic syndrome, can also sometimes be classified as a phenotype on its own [57].

The four main stages of OA are pre-clinical, early-stage (symptomatic), established, and final end-stage OA [67]. Pre-clinical OA is often asymptomatic, with little or no radiographic evidence to support diagnosis. For this reason, biomarkers are being investigated as tools for early detection and diagnosis [67]. Symptomatic patients experience OA symptoms, without necessarily the presence of radiographical evidence to detect structural changes in the joint. During this time, significant changes in the joint may still occur and become irreversible, and so, increase the likelihood of OA onset and severity. Clinical symptoms of pain and reduced mobility are apparent at this stage and may become chronic. At some point during the disease progression, OA may develop to a point that changes and damage to the joint can be observed using various imaging methods such as radiographical, magnetic resonance imaging (MRI) or computed tomography (CT) techniques [58, 67]. At this point, any attempt to restore joint homeostasis and reverse joint damage is lost, and patients, often with knee OA, eventually undergo joint replacement surgery [67].

2.1.4 Joint tissues

OA has been classically defined as a “wear and tear” disease characterised by decreased cartilage [4]. Recent work, however, has helped establish that OA is a condition and disease of the whole joint where all articular structures form a joint and play a significant role in joint health [4]. As a

result of this shift in definition, joints are often now considered an “organ” in relation to OA disease [4, 68]. Cartilage in joints is still investigated as the primary tissue that is affected by OA, but the underlying bone, as well as the synovium have become the subjects of active research, as they can influence the onset, progression, and severity of OA [4]. For these reasons, it is important to understand how all the tissues present in a joint may regulate joint health.

2.1.4.1 Synovial joint structures (general)

Synovial joints are primarily affected by OA and are the most common joints in mammals. These types of joints contain articular cartilage, a structure with a very low coefficient of friction, which provides a smooth surface for joint motion during movement [68]. The subchondral bone is found underneath articular cartilage and provides a supporting function as well as shock absorbing qualities [4]. Another major joint structure is the synovium, and the joint cavity containing synovial fluid. Synovial fluid is a lubricating fluid that ensures joint homeostasis and health. An overview of the articular structures composing a joint can be found in **Figure 2.1.**

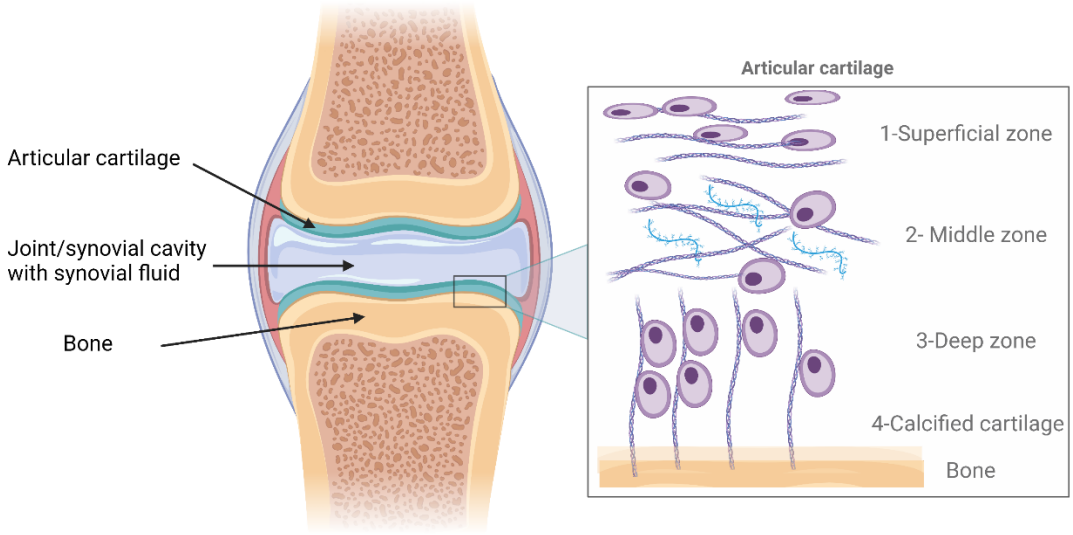

Figure 2.1. Synovial joint structures and articular cartilage zones. Created with biorender.com

There are other structures that play supporting and regulating functions in synovial joints such as ligaments, menisci, and fat pads. The contribution of these latter tissues to OA, however, is still under investigation, whereas bone, cartilage and the synovium are well-established joint structures involved in the development and severity of OA [4].

2.1.4.2 Cartilage

There are four types of cartilage: hyaline cartilage, which provides surface coverage for articular surfaces; fibroelastic cartilage, found in the meniscus; fibrocartilage, which is in the tendons and ligaments; and elastic cartilage found in the larynx [69]. Hyaline cartilage, also known as articular cartilage, is the most common and has a smooth, uniform, and glassy-like appearance. Changes in color and aberrations to the uniformity and smoothness of cartilage may occur with age, injury and other risk factors associated with OA.

Articular cartilage is comprised of an extracellular matrix (ECM) and cells that synthesize cartilage, called chondrocytes [70]. The ECM is primarily comprised of water, which represents up to 65-80% of the total weight in healthy cartilage. The remaining components of the ECM are proteins such as collagen and proteoglycans, with a very small proportion of non-collagenous proteins, lipids, phospholipids, and glycoproteins. The main proteoglycan component of the ECM is aggrecan, which aggregates with hyaluronic acid found within joints [70]. These large macromolecules are also attached to glycosaminoglycan chains, mainly chondroitin sulfate and keratan sulfate. The ECM is maintained and repaired by the resident cells, chondrocytes.

Chronotypes are highly specialized metabolically active cells originating from mesenchymal stem cells, yet they have very limited potential for replication [70]. For this reason, the healing capability of cartilage in response to injury, aging and other external and internal factors is limited [70]. These cells also seldom communicate between each other for direct signal transduction via cell-to cell contact; instead, they are sensitive to surrounding stimuli by growth factors, mechanistic load, and inflammatory signals [70]. The shape and size of chondrocytes, as well as corresponding cellular signals, are different between articular zones [70].

2.1.4.3 Cartilage zones

Articular cartilage can be divided into four zones; the superficial, middle (also know as intermediate), deep and the calcified zones [70] (**Figure 2.1**). The synthesis of different proteins, such as collagen, occurs differently depending on the articular cartilage zone. Alterations to these cells and structures in these zones may contribute to the onset, progression, and severity of OA. The superficial zone is the zone that is in contact with the synovial fluid and is characterized by

flattened chondrocytes, typically a layer about 1-3 cells thick [70]. It is the thinnest layer, but this zone protects the deeper cartilage zones from shear stress and damage during movement. Collagen components vary, but collagen types II and IX are the ones primarily found in condensed fibres parallel to the joint, and few proteoglycans are found in this zone. Below the superficial zone is the middle (or intermediate) zone [70]. A low density of typically round chondrocytes is found in this zone. The middle zone contains a significant amount of proteoglycans as well as thick collagen fibrils in a random or oblique orientation. Of the total articular cartilage volume, this middle zone can represent between 40-60%, and functions as a barrier layer regulating molecular movement and resisting stress and compression forces. The deep zone contains round chondrocytes that are arranged in columns, perpendicular to the joint [70]. The highest content of proteoglycans can be found in this layer which also has the lowest water content. Bundles of collagen fibers are found in this zone, which can be anchored to the underlying bone. These components and their orientation give this layer its unique property of resisting compression forces. Finally, the calcified zone anchors cartilage to the subchondral bone, and limits diffusion of nutrients from bone to the deeper layer of cartilage [70]. Chondrocytes in this zone are hypertrophic and express collagen X. The main mineral component of the cartilage is hydroxyapatite, which is a mineral form of calcium. Hydroxyapatite accounts for 65-75% of the mineral content in this zone although the complete mineral composition and organization of the calcified zone has not been fully elucidated [71].

2.1.4.4 Bone

Bone is a highly mineralized connective tissue [4, 54]. The contents of collagen, water and minerals vary depending on the anatomical location of the bone, as well its associated thickness. Especially in synovial joints, the bone consists of trabecular bone and the calcified cartilage zone as well as a subchondral bone plate found between these layers [72]. The subchondral bone plate is permeable to small molecules and thus is one of the main routes of providing nutrients and other essential compounds to articular cartilage. The subchondral bone is a dynamic tissue that continually undergoes remodeling. Bone remodeling involves two main cell types: osteoblasts (OBs) and osteoclasts (OCs) [4]. OBs are immature bone cells that contribute to the formation of new bone, whereas OCs are large multinucleated cells that resorb bone. The balance between the activity of OBs and OCs is essential for bone homeostasis and healthy joints [4]. Another type of bone cell are

osteocytes. These are mature bone cells that have become embedded in the calcified bone matrix and play a role in supplying nutrients and responding to soluble signalling molecules [4].

Bone remodeling is a dynamic process that is tightly regulated by crosstalk between OBs and OCs [4, 73]. The well-established receptor activator of nuclear factor kappa-β (RANK)/receptor activator of nuclear factor kappa-β ligand (RANKL) pathway plays a key role where OBs secrete RANKL, which binds to RANK found on OC precursors. This binding induces OC differentiation and fusion, which are necessary to form mature multi-nucleated OCs. The differentiation of OCs also relies on the secretion and signalling of the cytokine macrophage colony stimulating factor (M-CSF), which is excreted by OBs.

Recent research has demonstrated that, besides the RANK/RANKL pathway, co-stimulatory signals may be required for both the expression of OC-specific genes and the activation of OCs [74]. One of these co-stimulatory pathways is the activation of osteoclast associated Ig-like receptor (OSCAR). OSCAR is an immunoglobin type receptor and a member of the leucocyte receptor complex (LRC). OSCAR is conserved among species, and different isoforms as a result of alternative splicing have been found in humans and mice. Collagens act as ligands for OSCAR, and specific sequences have been shown to interact with the receptor with different levels of affinity [74]. A recent study by Park et al. (2020) demonstrated a clear link between OA and OSCAR expression [75]. Both mouse and human cartilage show increased expression of OSCAR during OA pathogenesis. Furthermore, in OA induced mice, markers of OA were significantly reduced in $OSCAR^{-/-}$ mice. The authors have suggested that a disruption of OSCAR expression or the interaction between OSCAR and collagen fragments may provide an interesting opportunity for the development of therapeutic agents for OA. Lair-1 is also a receptor that is activated by collagen fragments but unlike OSCAR, inhibits osteoclastogenesis [76, 77].

Both OSCAR and RANK signal downstream and regulate the expression of nuclear factor activated T cells 1 (NFATc1). NFATc1 is a key transcription factor regulating OC specific genes and is essential for the production of mature OCs [74]. Deletion of NFATc1 results in no OC development or production in vitro and in vivo. NFATc1 upregulates the expression of tartrate-resistant acid phosphatase (TRAP) activity, a key cytochemical marker of OC function, as well as H^+- ATPase, responsible for acidification

and demineralization of the bone being resorbed. NFATc1 also regulates cathepsin K and dendritic cell-specific transmembrane protein (DC-STAMP) expression. Cathepsin K is the main enzyme degrading collagen type I [74]. When OCs attach to the bone, the cell surface facing the bone forms a ruffed border. The ruffed border is due to the exocytosis of vesicles containing enzymes, such as cathepsin k, that degrade the organic components of the bone during bone resorption. Matrix metalloproteinase-9 (MMP-9) is also released along the ruffled boarder and helps degrade the organic component of bone [74]. It has been well established that increased levels of MMP-9 are associated with the pathogenesis of OA [78, 79]. As mentioned above, DC-STAMP is also under the regulatory control of NFATc1. DC-STAMP is a key player in OC differentiation by regulating cell-cell fusion of pre-osteoclasts [80]. Indeed, cell fusion during osteoclastogenesis is abolished in DC-STAMP knockdowns and as a result, no mature multinucleated osteoclasts can develop. DC-STAMP is also elevated and a clinical biomarker for patients with psoriatic arthritis, an inflammatory joint disease [80], although the use of DC-STAMP as a biomarker for OA has not been validated.

Osteoblasts, like OCs, are under tight regulatory and differentiation control. During osteoblastogenesis the activation of downstream transcription factors occurs. These transcription factors include runt-related transcription factor 2 (Runx2) and transcription factor Sp7 (Osterix), which both play a significant and key role in OB differentiation [81-83]. Both of these transcription factors regulate the expression of osteoblastogenic markers such as alkaline phosphatase (ALP) and Col1a1 [83]. Col1a1 is a major constituent of the ECM and responsible for the synthesis of collagen type I, alpha 1. There are numerous reports that Runx2 modulates the expression of Osterix, seeing as Runx2 is upstream of Osterix during osteoblastogenesis. Downstream from Osterix, the expression of both MMP-9 and 13 is regulated [84]. Previous work has shown that both Osterix and Runx2 regulate MMP-13 expression during endochondral ossification, which may have particular importance in the onset and development of OA [85]. Increased expression of Runx2 could help explain the increase in MMP content observed in OA synovial fluid [86].

2.1.5 Functional and cellular changes in OA joints

The onset and progression of OA can be characterized by multiple changes in morphology as well as cellular signalling in the joint **(Figure 2.2)**. The bone remodelling process can be altered in OA and may result in the formation of cysts [87], microstructure impairments and fractures [4], or bone

spurs/growths (osteophytes) that protrude out of the bone and become extremely painful [4]. Furthermore, biomarkers from plasma also indicate that pre-OA is associated with higher bone turnover, where the activity of OCs may be increased with a corresponding decrease in OB activity [4]. Notably, the resorption markers C- and N-terminal telopeptides (CTX and NTX respectively), which are both fragments of type I collagen that is mainly found in bone, are increased in the plasma of patients with early and progressive OA [4]. As a result of increased bone turnover, the thickness of the subchondral bone plate can be reduced, which in turn increases cartilage damage. This latter phenomenon has been confirmed in animals as well as humans [4]. Other evidence has also shown that OA may be the result of subchondral bone thickening causing increased stiffness and decreased mobility [4]. As a consequence, the loading capacity of the bone is reduced, so additional load is absorbed instead by the cartilage and results in cartilage degradation.

The calcified cartilage zone can become reactivated in OA, thereby calcifying unmineralized cartilage [88]. An increase in load to the remaining unmineralized cartilage occurs and stimulates cartilage degeneration, as the recovery capacity of cartilage is low. Recent work has also demonstrated that, due to the increased bone turnover, hypomineralization of the subchondral bone can occur, thereby decreasing bone loading capacity as well as joint integrity and strength [4]. It has become clear that every manifestation of pre- or established OA differs greatly between individuals and between joints affected. In addition, the changes that may occur to other joint tissues can also vary between OA stages and individuals.

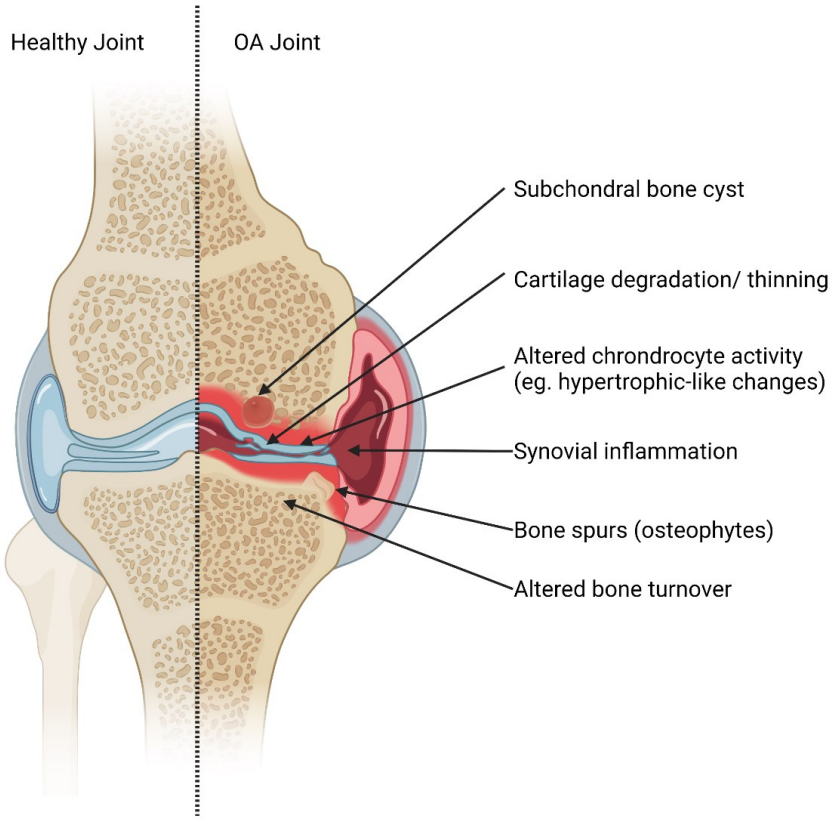

Figure 2.2. Changes to joint tissues in OA. Created with biorender.com

As described above, changes to the subchondral bone can increase loading to the joints found in cartilage, which stimulate and accelerate cartilage degeneration [4]. Changes to cartilage attributed to the onset or development of OA can vary between patients and can also differ on tissue and cellular levels. One of the hallmarks of OA is that the balance between anabolic and catabolic activity has become disrupted. The ability of cartilage to repair itself is decreased, while the catabolic activity is increased. This change in cartilage homeostasis can occur due to increased stress and loading, as well as inflammation due to injury or other metabolic factors such as obesity, in addition to an increased content of ECM proteins such as proteases that degrade the matrix components [4, 87]. Furthermore, the water content in cartilage increases while the glycosaminoglycan (GAGs) content decreases [4]. Radiographical evidence indicates that the joint space narrowing and cartilage content in OA patients decreases as the condition progresses [4].

Inflammation has been shown to play a key role in the onset and progression of OA [68]. Inflammation occurs often in the synovium, and increased levels of inflammatory cytokines have

been observed in human OA patients. The regulation of chondrocyte activity, as well as bone cell activity is directly affected by circulating levels of cytokines [68, 83, 89, 90]. Pro-inflammatory cytokines such as interleukin-1β (IL-1β) and tumor necrosis factor-α (TNF-α) function by decreasing the synthesis of ECM components while simultaneously promoting cartilage catabolism, as well as by acting as anti-osteoblastogenic agents [83, 89, 90]. On a cellular level, chondrocyte phenotype can change in OA [91]. Chondrocytes undergo hypertrophy-like changes, and although this type of abnormal cell behavior is similar to hypertrophy during growth plate development, it differs greatly due to differences in some cell signalling molecules and phenotypic characteristics [4, 91]. Chondrocytes may undergo terminal differentiation during hypertrophy in OA, which is characterized by increased resorption of proteoglycans and collagen in the ECM [91]. Specifically, biomarkers such as type X collagen, and MMP-13, a protein that degrades ECM components, are increased in hypertrophic chondrocytes. Continued changes in cellular signalling occur, and eventually chondrocytes undergo terminal degeneration characterised by the calcification of the cartilage. Crystals of calcium phosphate associated with matrix calcification can also occur [87]. On a cellular level, alkaline phosphates (ALP), Runx2, and proteins such as osteocalcin and osteopontin are increased [91]. Besides being a master regulatory transcription factor in bone, Runx2 also controls chondrocyte hypertrophic differentiation and is increased in OA [91].

Chondrocyte activity and size are altered during aging. Aging is one of the main unavoidable risk factors for OA, and cellular changes in chondrocytes are observed [70, 87, 91]. Keratin sulphate and chondroitin sulphate are the GAG components attached to core proteins, to make proteoglycans. During aging, the ratio of these components of the ECM changes, and proteoglycan size significantly decreases [70, 91]. Recent work has helped to understand some of the macroscopic and cellular changes that occur to joints in OA; however, the exact mechanisms remain to be fully elucidated. OA is a complex and dynamic condition, where patient pathology varies greatly between individuals as well as between OA stages, types, causes and anatomical locations. For these reasons, the choice and development of treatment options for patients remain extremely difficult.

2.1.6 OA Treatments

Although significant research has attempted to develop disease-modifying drugs (DMDs) for OA, all attempts have failed [58, 67], most likely due to the heterogeneity of the disease. Accordingly,

treatment options for patients are extremely limited. Current treatments often attempt to address OA symptoms such as pain, rather than improve joint structure and function. Paracetamol and non-steroidal anti-inflammatory drugs (NSAIDs) are medications often prescribed to help manage OA pain [2]. Reports have indicated that paracetamol has little benefit on reducing pain and improving function compared to a placebo and may increase the risk of abnormal liver function [92]. Similarly, NSAIDs have been shown to cause acute liver injury and are one of the main causes of acute hepatitis [93], as well as causing detrimental GI side effects [1, 94]. Although the incidence of liver injury with NSAIDs is considered low, these types of medication are one of the most prescribed, especially in OA [2, 93]. In that regard, the recommended practice of NSAIDs prescription is "lowest effective dose for the shortest duration" [2], therefore continued use for patients experiencing OA, a chronic pain disorder, remains controversial.

Weight loss both reduces the risk of developing OA, as well as reduces symptoms, improves joint function, and decreases disease progression, particularly in patients diagnosed with knee OA [59]. Strategies to decrease weight, such as increased physical activity, are also suggested as treatment options for patient with OA to strengthen joints. Notably, physical therapy and muscle strengthening exercises are suggested [2]. Weight loss for some patients, however, may not be a feasible or viable option, especially if they are underweight, but also have OA.

Patients with severe OA typically undergo joint replacement surgery, however not every type of OA can be addressed by surgery [1, 67]. This option is seen as a last resort due to the significant costs, risks associated with surgery, and the required post-operative care and therapy. Many patients have also reported that they were not satisfied with their surgical intervention [95].

2.2 Nutritional supplementation: collagen hydrolysates

With limited treatment options and no currently approved DMDs, the role of nutritional factors and supplements to treat OA warrants further investigation. This is especially true for patients with pre-clinical or symptomatic OA, as early intervention is key to stopping OA progression and eventual surgery [67]. Consumers are generally interested and open to supplementation, especially if they demonstrate and promote health improvement [96, 97]. Commonly used and readily available

supplements advertised to help manage OA are collagen-based products, such as gelatin and CHs [7, 18].

2.2.1 Collagen

Collagen is the most abundant animal protein and accounts for about 30% of total body protein [98]. It is a structural protein found in connective tissue and characterized by repeating motif "Gly-X-Y", where X is often proline (Pro) and Y is hydroxyproline (Hyp) [98, 99]. Collagen has three α-chains of approximately 1000 AAs each that coil around each other to form a triple helix structure. Collagen triple helices cross link together using telopeptides found at the ends to form collagen fibrils. Several fibrils align to form collagen fibres. This cross linking is highly conserved between collagen types. Currently, there are 29 types of collagen that have been identified, although they can vary in AA sequence, structure, function and associated distribution in tissues and organs [99]. For example, type 1 collagen is typically found in bone, skin, teeth and tendons whereas type II is found in cartilage [18].

2.2.2 Collagen products (e.g. collagen hydrolysates)

Collagen can be isolated from various sources, including porcine, bovine, as well as piscine [18, 99]. Collagen extraction is often a by-product of the meat industry, and the main source of collagen for collagen-based products remains bovine, due its high availability as well as biocompatibility and weak antigenicity [99]. Collagen can be extracted from various tissues such as bones, tendons and connective tissues [18]. Marine sources of collagen include those mentioned, but also skin and scales [18].

CHs are products with low molecular weight (MW) peptides, often between 3-6 kDa [18]. CHs are a result of industrialised processed collagen and are sold in cosmetic, pharmaceutical and food sectors [18]. Collagen is typically pre-treated using thermal treatments at temperatures usually above 40°C, which promotes collagen chain denaturation of the triple helix. Afterwards, extraction can be completed by acid and/or alkaline treatments [18, 99]. Enzymatic hydrolysis is then completed to breakdown peptide chains into lower MW peptides. The choice of processing procedure and proteolytic enzymes can vary between CH products although pepsin, papain, and Alcalase are often used [18]. The combination of processing techniques and enzymes help determine the quality and bioactivity of the final CH product. Furthermore, the source of collagen

(bovine, porcine, etc.) will have a direct effect on the AA composition of the peptides and their MW [18]. In comparison, gelatin is also a collagen-based product, but gelatin is obtained through partial hydrolysis of collagen, and is therefore processed to a lower extent than CH [100]. The conversion of collagen and gelatin into bioactive products such as CHs makes collagen sourced products valuable to pharmaceutical and cosmetic industries.

CHs are nutraceuticals that have multiple applications and are often taken as oral supplements. The health benefits of CHs have been primarily attributed to their BAP content and corresponding sequences. The peptide content of CHs is a result of the collagen source and the processing methods described above. Different processing procedures and sources will result in variable peptide sequences and content after extraction and hydrolysis, thereby affecting the overall bioactivity of the CH product. In addition to their BAP content, CHs also contain AAs which contribute to their bioactivity [7, 9, 18].

CHs have been shown to provide multiple health benefits, which include antimicrobial and antihypertensive effects, promotion of wound healing and bone synthesis, decreasing joint pain associated with OA, helping in the regulation of inflammation, improving skin health, acting as inhibitors of dipeptidyl peptidase-IV (DPP-IV), as well as having antioxidant properties and angiotensin-I-converting enzyme inhibitory effects [7, 18, 100]. The presence of BAPs such as Pro-Hyp, Ala-Hyp, Pro-Hyp-Gly and Gly-Pro-Hyp, in the blood circulation after the oral consumption of CHs and gelatin has been verified in human clinical studies [10, 11, 22, 101]. In fact, the postprandial absorption rate of Gly, Pro and Hyp were significantly greater after oral consumption of CHs compared to non-enzymatically hydrolysed collagen, suggesting that processed collagen products have increased absorption and bioavailability [9]. Besides their measurement in plasma, the CH-derived BAPs, Gly-Pro-Hyp and Pro-Hyp, were shown to be excreted in the urine after oral consumption, indicating that these peptides were well absorbed and stable post-absorptively [102]. Other clinical studies focussing on the bioactivity of BAPs have helped establish the health promoting properties of CHs after oral consumption.

2.2.3 Bioactivity and health benefits of CHs

2.2.3.1 Clinical studies on CHs and CH derived peptides

The clinical efficacy of CHs and CH-derived peptides has been demonstrated in several trials [5, 6, 8, 53, 103-109]. CHs have been shown to be a safe and effective treatment option for OA patients. The supplement primarily helps manage OA pain and increase mobility, but recent work has also demonstrated improvements in bone health and cartilage characteristics, especially in patients engaging in a physical exercise program [5, 105]. A randomized double-blind, controlled study was completed over 6 months on 250 subjects with primary knee OA to assess the efficacy of CH on OA pain and joint function [103]. Using the visual analogue scale (VAS) to assess for pain, as well as the Western Ontario and McMaster Universities Osteoarthritis (WOMAC) index pain subscale, patients showed significant improvement in knee joint pain and comfort after treatment [103]. A similar study recruited 200 patients to participate in a randomized, double-blind, placebo-controlled trial over a 6-month period to assess the efficacy of CH supplementation on patients with knee OA, but also included patients with hip, elbow, shoulder as well as hand and/or lumbar spine OA [8]. The number of clinical responders, as assessed using VAS, was significantly greater in the CH treatment group compared to the placebo group and confirmed that CHs were safe and well tolerated by patients [8]. Significant reductions in WOMAC and VAS scores were also observed in another double-blind, placebo-controlled, randomised, clinical study investigating the effectiveness of porcine and bovine CH-derived peptides in patients with knee OA [104]. Although the above study provided initial indication that the bioactive component of CHs are the peptides, the peptides were not sequenced, as only an analysis of the plasma AA content was conducted to estimate peptide profiles. Therefore, the specific CH-derived BAPS were unknown for this study [104].

Recent clinical studies have also demonstrated that collagen peptides alongside resistance training improved body composition. A randomised double-blind placebo-controlled study showed that collagen peptides increased fat-free mass, bone mass and muscle mass more so than the placebo [5]. Said collagen peptides were part of a commercial product provided by Gelita AG, however the sequences and content of the peptides were not provided nor investigated. Instead, the AA composition was assessed (no method given). In a similar study, a triple-blind placebo-controlled randomized controlled trial instructed patients with knee pain to complete a home exercise program together with a treatment with either CH or a placebo [105]. Patients treated with CH

showed significant improvement in joint structures, which included decreased cartilage abrasion and lateral meniscus protrusions as well as a significant increase in cartilage thickening in the central portion of the trochlear articular cartilage [105]. No significant differences were observed in cartilage clarity and other soft tissues such as the medical meniscus and the infrapatellar area. For the patients who were non-compliant with the home exercise program, VAS scoring still indicated that CH decreased pain [105].

Interestingly, CH supplementation also appears to improve activity related joint pain, regardless of OA diagnosis. For example, Clark et al. (2008) performed a 24-week clinical study involving 147 healthy athletes with activity-related joint pain who were physically active, fit, and had no evidence of established OA [106]. Joint discomfort and pain in the CH-treated group were significantly reduced. The authors suggested that CHs support joint health and could reduce the risk of further joint deterioration in high-risk groups (e.g., athletes), which merits further investigation. Thus, CHs could act as a preventive treatment and be recommended before potential OA diagnosis. Furthermore, athletes with knee pain also showed improvement in activity-related pain intensity after treatment with collagen BAPs over a 12-week supplementation period [6]. Accordingly, high risk groups could possibly benefit from supplementation at a young age (e.g., below 25) and possibly delay the onset of joint damage, but this remains to be assessed. More recent work by McAlindon et al. (2011) demonstrated that, in a randomized, placebo-controlled, double-blind imaging study, changes in proteoglycan content in knee cartilage were observed after 24 weeks of CH treatment as well as improvement in cartilage morphology [107].

CHs have also been shown to improve other articular structures of the joint beside cartilage, most notably in bone. In a randomized, placebo-controlled double-blinded study, König et al. (2018) concluded that bone mineral density (BMD) was increased after collagen peptide supplementation compared to placebo [53]. Furthermore, bone markers from plasma also showed significant improvement to bone remodeling homeostasis. Specifically, a biomarker for bone formation, amino-terminal propeptide of type I collagen (P1NP), was increased in the collagen peptide treatment group, whereas no changes were observed in the placebo group. In contrast, an indicator of bone resorption, C-telopeptide of type I collagen (CTX 1), was increased in the placebo group, with no changes in collagen treatment group. In summary, plasma biomarkers of bone turnover

indicated that collagen peptides increased bone formation, while also decreasing the level of bone resorption.

Another study assessing the effect of CHs in pre-pubertal children concluded that partially hydrolyzed collagen, or in other words, gelatin, could improve bone remodelling during growth and development [108]. Further studies assessing the use of CHs or similar products on young healthy participants are needed, with thorough follow up as participant grow and age. This would help determine the preventative potential of CHs on reducing the onset and severity of joint disorders.

There are very few studies that investigate the effects of CH alone on bone health. Instead, CHs are often used in association with another treatment. For example, the effects of intramuscular injection of calcitonin were compared to calcitonin treatment along with addition of CHs into the diet in postmenopausal women [109, 110]. The effects of CHs and calcitonin together increased and prolonged the effects of the calcitonin drug treatment and a greater effect in inhibiting bone collagen breakdown was observed.

2.2.3.2 In vitro and animal studies on CHs and CH derived peptides

There are numerous studies and reviews that have detailed the potential bioactivity of collagen products and CH-derived BAPs. The bioactivity of collagen products depends on the source, processing and bioavailability, i.e., the absorption of the bioactive compounds such as BAPs and AAs into the systemic circulation so they may exert their beneficial activity [18, 100]. CH and CH-derived BAPs have been shown to exhibit antioxidant activity, ACE-inhibitory activity, metal chelating abilities, anti-diabetic properties, antimicrobial potential, and beneficial effects on bone and joint health. The list of BAPs identified from CHs continues to grow, as well as the associated bioactive functions of the identified peptides. Efforts to create BAP databases have begun [111-113], although these databases remain incomplete. For the purposes of this literature review, the focus will be placed on the capacity of CH and CH-derived BAPs to exert beneficial action on cartilage, bone and OA risk factors. For a detailed list of the other potential bioactivities of CHs and related products, reviews by Fu et al. (2019), León-López et al. (2020), and Pal et al. (2016) provide comprehensive summaries of the current literature.

Previous in vitro and in vivo work by Nakatani et al. (2009) has helped establish the chondroprotective effects of porcine CHs, and its main BAP, Pro-Hyp [114]. Using an animal model, C57BL/6J mice were placed on a base AIN-93G diet, alongside a treatment of excess phosphorus to include joint damage. Different treatment diets included a negative control (no phosphorus) and control diet (gluten hydrolysate used as a control and excessive phosphorus), a CH treatment group (CH and excessive phosphorus), as well as the peptide group (Pro-Hyp and excessive phosphorus). Mice treated with phosphorus showed joint degradation, notably a decrease in chondrocyte cells and decreased articular cartilage thickness. As a result of CH and Pro-Hyp treatment, these supplements inhibited the loss of chondrocytes induced by excess phosphorus while also inhibiting cartilage thinning [114].

In the same study, an in vitro model was used where chondrocytes (ATDC5 cells) were treated with Pro, Hyp, Gly, Pro & Hyp (as a mix of individual AAs), Pro & Hyp & Gly (as a mix of individual AAs), the peptides Pro-Hyp and Pro-Hyp-Gly, as well as the same CH used in the above animal study [114]. Key findings from this study showed that CH and Pro-Hyp inhibited chondrocyte mineralization and terminal differentiation, as assessed by alizarin red and ALP staining, respectively. Changes to the ECM components were also observed, notably an increase in glycosaminoglycan which was determined by alcian blue staining. Using reverse transcription-polymerase chain reaction (RT-PCR), the mRNA content of aggrecan was increased with Pro-Hyp treatment. Additionally, the expression of RunX1 and osteocalcin was decreased with Pro-Hyp treatment. No RT-PCR analysis was done on CH treated cells. In summary, this study was one of the first to clearly establish that Pro-Hyp is one of the major bioactive components associated with the clinical efficacy of CHs towards treatment of OA, specifically on cartilage tissue [114].

Another well-established BAP derived from CHs is Gly-Pro-Hyp, which has been suggested to be involved in platelet aggregation by being recognized by platelet glycoprotein VI [115, 116]. This interaction is unique; Gly-Pro-Hyp occurs rarely in other proteins, except for collagen, and glycoprotein VI is thought to be expressed solely by platelets. Furthermore, this tripeptide has been shown to inhibit the activity of DPP-IV, which has been associated with diabetes [116]. Other peptides (Gly-Ala-Hyp and Gly-Pro-Ala) generated from CH hydrolysates were assessed for their DDP-IV activity, although only Gly-Pro-Hyp showed any activity. This peptide might prove to be an

important health modulator in OA as patients diagnosed with diabetes are at an increased risk to develop arthritis [63, 117, 118].

Most in vitro models assessing the effects of CH treatment on bone remodeling have focused on bone forming cells (OBs), with little work assessing OCs [54]. Furthermore, of the studies that have briefly investigated OCs, in depth analysis of gene profiles have not been completed. Preliminary in vitro studies using bone marrow macrophages differentiated into OCs showed that collagen decreased the number of differentiated OCs, i.e., positively tartrate-resistant acid phosphatase (TRAP) stained cells. Other reports have shown that CHs decreased OC resorption area but did not affect OC growth [15]. More recent work by N'deh et al. (2020) used osteoclast precursor RAW 264.7 cells and demonstrated that collagen extract from chicken decreased the mRNA levels of TRAP and cathepsin k [16].

The effects of CHs on OBs have been more thoroughly investigated (see review by Daneault et al. 2017 [8]), but the mechanisms of action remain to be fully established. Previous work using bovine collagen on a pre-osteoblast cell line (MC3T3-E1 cells) observed changes in gene expression, primarily an increase in Runx2 [81]. Increased expression of ALP activity and mineralization was also observed. Another in vitro study using MC3T3-E1 cells helped establish that the CH-derived BAP, Pro-Hyp, promoted osteoblastic differentiation, but not proliferation [119]. Pro-Hyp treatment was shown to upregulate both osteoblastic differentiation genes Runx2and Osterix, as well as Col1a1. The application of the collagen tri-peptide Gly-Pro-Hyp on MC3T3-E1 cells also showed upregulated protein expression of Runx2, Osterix, ALP and Col1a1 in a dose dependant manner [82]. Using the human osteoclastic MG-63 cells, CHs were shown to stimulate ALP activity, calcium deposition and collagen synthesis [120].

2.2.4 Limitations of CH supplementation

Despite the growing evidence supporting the use of CHs to treat OA, their clinical efficacy remains highly speculative for many researchers. This is primary due to: 1) the limited number of studies completed; 2) small patient sample sizes; 3) limited publications in reputed journals, seeing as conference proceedings that show clinical benefits are not included; and 4) limited treatment durations, with no long term follow up with patients. Besides some promising studies establishing

the positive health benefits of CHs, the literature also contains a significant portion of poorly designed and executed clinical studies, which decreases the credibility of CHs as a promising and potential therapeutic agent. The consensus from most of the review articles assessing the utility of CH supplementation agree that the current quality of evidence is moderate to poor [1, 121-123]. As such, independent, high-quality, long-term studies are needed and recommended, so that the therapeutic properties of CHs in both younger and older populations can be assessed. Likewise, particular emphasis and critical investigation into the processing of CHs and the resulting different peptide formulations, specifically BAP and AA content is needed, as patient and clinical outcomes could be affected [124]. Further well-designed mechanistic studies are also needed to help establish the biological plausibility of BAPs and AA content contributing to joint health.

Most clinical assessments of the effects of CHs have been completed on knee OA and assessments conducted using the WOMAC or VAS scale. More thorough investigation into cartilage and bone morphological changes as well as serum biomarkers are needed [105, 107, 125], to truly understand the impact of CHs on joints, rather then only assessing patient pain, which can often be subjective. Supplementation compliance is also critical for any treatment. A 5-year, double-blind, placebo-controlled trial in elderly women showed that calcium carbonate tablets, a treatment that prevents clinical fractures, is an ineffective public health intervention mainly because of poor long-term adherence [126]. Interestingly, the treatment remains an effective preventative measure against fracture, in those consistent with supplementation; however, this study showed that over 43% of the patients were in fact noncompliant. A recent systematic review and meta-analysis also indicated that iron and folic acid supplementation compliance is poor among targeted populations [127], and other studies have also confirmed that low adherence to nutritional supplementation remains a critical factor for public health [128, 129]. Unfortunately, compliance data for CH supplementation over long term has not been investigated. Knowing the general low observance to supplementation, as well as a low compliance of the elderly to take medication [130-132], the likelihood of patients being compliant with supplementation with CH is likely low. Compliance and pill fatigue is a major limitation of continuous CH oral supplementation, especially for the elderly who are likely to develop OA and will probably be required to take other prescribed medication at that age.

Finally, a major limitation of CH treatment for OA is that there remain significant gaps in the literature regarding the BAP components in various CH products. Investigations into the synergistic potential of BAPs in CHs are required but have gathered little attention. Furthermore, studies regarding the effect of the food matrix on the absorption of CH-derived BAPs are lacking, and there are no current recommendations or data on how the clinical benefits of CHs are altered when taken either with a meal or alone.

2.2.5 Other dietary supplements for OA

There are other dietary supplements that patients take to help manage OA symptoms besides CHs. These supplements include curcumin, ginger, polyunsaturated fatty acids, rose hip, omega-3 fatty acids (e.g., from fish oils), vitamins (e.g., vitamins D and E), essential minerals such as magnesium, as well as polyphenols [1, 122, 133]. Nutraceuticals are generally considered safe, but their clinical effectiveness remains disputed. Some reviews of pre-clinical and clinical studies have indicated that supplements may provide a safe and alternative option for patients to help address both OA pathology and symptoms [133], yet other reviews have clearly stated that the current body of evidence on nutraceuticals and supplements for OA treatment is insufficient, and therefore cannot recommend these supplements [122, 123].

Other well-known and marketed supplements for the treatment of OA include chondroitin sulfate and glucosamine, which have garnered increasing attention, as these molecules can be found in cartilage and the ECM. A recent review indicates that these supplements fall under the “probably recommended” to the patient category for disability management but not for pain treatment [123]. In contrast, CHs were deemed ineffective for disability management and not likely recommended for pain management. Contradictory evidence was demonstrated by Clegg et al. (2006) who investigated the role of glucosamine and/or chondroitin sulfate in the treatment of 1583 patients with symptomatic knee OA. Overall, glucosamine and chondroitin sulfate alone or given in combination showed no effective pain reduction in patients. A subgroup of patients with moderate-to-severe knee pain showed some pain improvement with glucosamine and chondroitin sulfate combination treatment. Also, a clinical trial assessing the effectiveness of glucosamine as compared to CH showed greater improvement with the CH treatment in OA subjects [134]. The latter result was noted in a randomised, double-blind study on patients with knee OA who were either

supplemented with CH or glucosamine sulphate [134]. Quality of life was assessed using the short form 36 health survey questionnaire (SF-36) and was improved to a greater extent with CH compared to glucosamine sulphate. WOMAC and Vas scores were also recorded, and CH demonstrated significantly better analgesic potency than glucosamine sulphate. In addition, CH treatment resulted in greater improvement in joint stiffness, and number of affected joints.

Another clinical study on knee OA assessed the effectiveness of undenatured type II collagen (UC-II) compared to a combination treatment of glucosamine and chondroitin [135]. The study demonstrated that a significant reduction in WOMAC and VAS scores were observed in the UC-II treatment group compared to glucosamine and chondroitin. Moreover, the Lequesne's functional index was also used to determine the effectiveness of the therapeutic interventions. Pain during daily activity was reduced after UC-II treatment by 20% compared to a reduction of just 6% with patients supplemented with glucosamine and chondroitin. Although clinical trials remain a highly effective tool to assess the bioactivity and effect of nutraceuticals such as CHs in humans, our understanding of the digestive processing of such products and their bioavailable bioactive components after oral consumption is limited.

2.3 Digestion and bioavailability of CHs and CH-derived peptides

2.3.1 Introduction

When consumed, CHs, BAPs, and any other nutraceuticals or medications taken orally must undergo digestion and absorption before exerting their bioactive effects [26, 54]. The GI tract extends from the mouth to the anus and functions to absorb nutrients, medications, and other food derived compounds [136]. The GI tract can be divided into two sections: the upper and lower digestive tracts. The upper digestive tract consists of the oral cavity, esophagus, stomach, and the duodenum, which is part of the small intestine. The lower digestive tract consists also of the small intestine, especially the jejunum and the ileum, as well as the large intestine, which includes the cecum, colon, rectum and anal canal. A summary of the GI tract can be found in **Figure 2.3.**

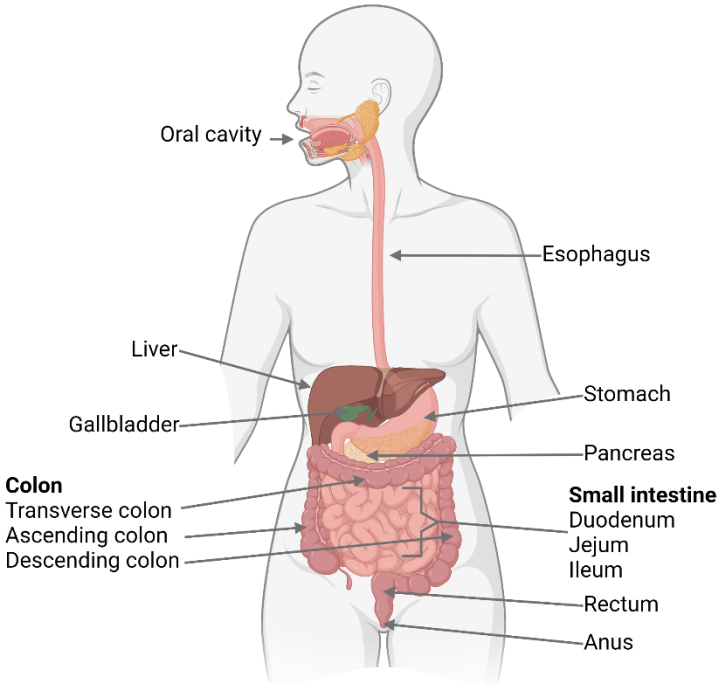

Figure 2.3. Human gastrointestinal (GI) tract. Created with biorender.com

Each section of the GI tract has a unique function. The mouth is the entry point to the GI tract, and is mainly responsible for mastication of food, and initial enzymatic breakdown of food components by enzymes such as amylase found in saliva [136]. A food bolus then forms and travels to the stomach via the esophagus. In the stomach, food and food-components are digested further by host enzymes including proteases such as pepsin as well as lipases, which digests proteins and lipids, respectively. The stomach is held at a very low pH (~ 2) to help hydrolyse the stomach contents. Afterwards, the contents are released into the SI, where digestive juices also containing enzymes are released from the pancreas, as well as bile acids from the gall bladder. The contents from the stomach also change pH in the SI, due to the presence of bicarbonate. It is mainly in the SI that proteins are broken down into peptide and AA components. This enzymatic digestion occurs within the SI, but the final breakdown of proteins to their smaller components occurs on the surface of resident intestinal enterocytes by brush border enzymes. The BAPs released after protein and peptide digestion are absorbed by villus enterocytes [136]. Nutrients are absorbed via active transporters as well as non-active transport mechanisms.

The remaining food components and nutrients that are not absorbed in the SI travel to the large intestine. In the colonic regions, non-dietary carbohydrates, proteins, peptides and AAs, can be fermented by resident microbiota. These fermented food compounds are also known as prebiotics. The human microbiome is shaped by the diet, and other resident host factors that change the microbial composition, function, and activity of the microorganisms in the GI. The microbial population impacts the types of fermented metabolites produced which have a direct effect on overall human health. The remaining components that are not absorbed, fermented, or provide any other function are eventually excreted by the anus as feces [136].

2.3.2 Absorption and hepatic first pass: bioavailability of CHs & CH-derived BAPS

After digestion, BAPs undergo first pass metabolism, which mediates the entry of bioactive molecules such as BAPs into the systemic circulation [31, 137]. This process is defined by the absorption of metabolic compounds at the level of the intestinal epithelium followed by hepatic metabolism, before being released into the blood. The additional release of BAPs after CH digestion may occur, as the CH peptide components can be broken down into smaller BAPs and AAs in the stomach and SI. Regardless of the extent of digestion, the bioactivity of CH-derived BAPs, and therefore clinical efficacy, depends heavily on the peptides' ability to reach the systemic circulation intact after oral ingestion, otherwise called bioavailability [137]. Peptide bioavailability remains one of the greatest factors regarding bio-potency, and the digestion and absorption of different CHs can differ greatly, which may lead to altered CH bioactivities [100, 138].

Large MW peptides are less effectively absorbed than lower MW peptides, so CHs with lower MWs (0.3 – 6 kDa) are more likely to be absorbed to exert their bioactivity [18, 100]. There are four main routes of peptide absorption by intestinal enterocytes: 1) paracellular transport; 2) passive diffusion; 3) transcytosis; and lastly 4) carrier-mediated transport (active transport) [26]. Some molecules may pass through cells by paracellular transport, dictated by the permeability of tight junctions between cells [26]. Peptides that pass through the intestinal layer are typically transported by diffusion or active transport. In passive transport, molecules such as peptides, may pass though the apical and basolateral membranes of the intestinal epithelium without expending energy. This type of transport depends on the properties of the peptides, such as size (MW and chain length), charge and hydrophobicity, all of which depend on AA content [18, 26]. Carrier-

mediated transport is an active type of transport, as the movement of molecules, nutrients and peptides are against their concentration gradient. Peptide transporter 1 (PepT1), also known as solute carrier family 15 member 1 (SLC15A1), is a high capacity, low affinity, protein-coupled transporter that moves peptides from the GI lumen into the intestinal epithelium [26]. Indeed, the transport of di- and tri-peptides, especially with low MW, is mainly due to the activity of PepT1. Peptides transported by PepT1 are more bioavailable than peptides transported by paracellular transport.

2.3.3 In vitro models of digestion and absorption

2.3.3.1 In vitro models of digestion

Bioaccessibility is defined as the fraction of food, molecule or compound that is released from the food matrix during digestion, and becomes available for intestinal absorption [139]. Assessing bioaccessibility remains a key component of food, nutrition and pharmaceutical research. Ideally, in vivo studies using humans provide the best evidence for measuring bioaccessibility; however, human studies are costly, lengthy, have small sample sizes, and are restricted by ethical parameters [47, 140]. Animal studies may not always reflect human studies of nutrients and bioactive food components due to differences in metabolic activity and digestive enzymes between animals and humans [23, 26, 140].

Instead, in vitro models of digestion provide a rapid, cost effective, and simple method to assess bioaccessibility [139, 140]. These models can be highly controlled, more so than animal or human studies, making them highly reproducible while providing multiple sampling options. A major advantage of using such in vitro models is that they allow for high-throughput screening of the effects of digestion on nutrients, or nutraceuticals such as CHs, to determine the BAPs that are released and those that resist digestion. This tool also allows for an initial screening among different CH products to determine potential differences in bioactivity stemming from the different BAP profiles released following digestion. In vitro models thus provide a platform for completing preclinical digestion studies to identify bioactive compounds or molecules such as a BAPs that are generated by digestive processes which could become bioavailable.

Generally, in vitro static digestions are completed in a single bioreactor, and include two or three digestion steps: oral, gastric and intestinal digestion [139]. The experimental parameters, such as the choice to include an oral digestion phase, depend on the experiment, as well as the food components of interest. Often, when assessing proteins, peptides and AAs, the oral phase is not included, as there is no significant enzymatic action in the mouth by salivary amylase to break down proteins. Instead, gastric and intestinal enzymes are applied to break down protein components, although the choice of enzymes and other experimental parameters can vary. For example, models digesting protein samples may use three enzymes (trypsin, chymotrypsin and peptidase) in a single-step digestion method, or several enzymes (pepsin and pancreatic enzymes) in a two-step process. The degree of digestion may differ between the two experimental models. Experimental parameters, such as agitation method and speed may also differ between laboratories and models.

Chen et al. (2020) utilized a simulated in vitro digestion model to determine the effect of different MW peptide fractions from tilapia skin collagen on zinc chelation capacity and bioaccessibility [19]. Pepsin and pancreatin were used to simulate the gastric and intestinal digestive phases, respectively. The results demonstrated that zinc bioaccessibility was improved by the low MW collagen-derived peptides with strong zinc chelating abilities [19]. Such studies demonstrate the utility of in vitro tools assessing the digestibility of food components and nutraceuticals before costly animal and clinical studies are undertaken. Another study demonstrated that BAPs were generated after in vitro digestion of Alaska pollock skin CH [141]. Notably, the copper-chelating activity of this CH was significantly increased after simulated digestion, which suggested that digestion contributes to the increased bioactivity potential of CHs. Another study investigating marine skin collagen identified BAPs with angiotensin-converting enzyme (ACE)-inhibitory capacity after in vitro digestion [20]. Collagenous residues from squid skins were processed and fractioned, then digested using pepsin and pancreatin to simulate upper intestinal digestion. Pepsin had almost no effect on the MW of the processed peptide fractions, whereas the digestive action of pepsin and pancreatin resulted in an increase in lower MW peptides and increased ACE-inhibitory capacity. Therefore, upper intestinal digestion may increase the bioactivity of CHs, and remains a useful screening tool before in vivo studies are completed. Also, using liquid chromatography-isoelectric focusing and tandem mass spectrometry, the decapeptide Gly-Arg-Gly-Ser-Val-Pro-Ala-Hyp-Gly-Pro was identified after digestion of squid skin collagen and demonstrated high ACE inhibitory

bioactivity [20]. The latter bioactive peptide could contribute to the overall health promoting capacity of CHs, but targeted methods of quantification of this peptide after oral CH consumption in human clinical trials are needed. Taken together, initial screenings to identify bioaccessible BAPs using in vitro gut model methods can be an effective approach to understand the potential health impacts of CH-derived digestion products to complement in vivo studies.

Although in vitro digestion models have many advantages, there are several limitations to these models [139]. For example, experimental conditions may vary greatly between experiments, although recent efforts to standardize in vitro digestion models are ongoing [47, 142]. In addition, both static and dynamic in vitro digestion models cannot always simulate the complex digestive forces, enzymatic action, and tissue interactions that occur in vivo [139]. Digestive kinetics, synergistic effects of food components and matrices, as well as different emptying times due to digestive signalling are other factors that are limited in in vitro methods, compared to in vivo [47, 139]. Regardless of the disadvantages of in vitro digestion models, these remain simple and rapid methods of assessing bioaccessibility as studies support their use for the assessment of food and nutrient digestion in terms of the release of bioactive components such as BAPs with comparable findings to in vivo results [47, 49, 139, 140, 143, 144]. Although screening for bioaccessibility of bioactives is key towards understanding the impact of digestive processes on nutraceuticals such as CHs, the bioavailability of the released bioactive components also needs to be evaluated, which is dependent upon first pass metabolism. First pass metabolism is a process defined by the hepatic metabolism of compounds following their absorption at the level of the intestinal epithelium which mediates entry into the systemic circulation [31, 137]. Since BAPs and AAs generally need to be bioavailable to exert their bioactive functions, it is important to utilize representative models to assess for bioavailability.

2.3.3.2 Models of absorption and first pass metabolism

Human clinical studies have shown that BAPs and AAs generated from orally ingested CHs and gelatin can reach the systemic circulation as well as be excreted in the urine [9-11, 102, 145]. These bioavailable BAPs and AAs have also been shown to build up in joint tissues such as cartilage and bone [3, 12, 54, 146], which likely explains why CHs demonstrate possible clinical potential. As with bioaccessibility measurements, the assessment of CH and peptide bioavailability using human trials

continues to be lengthy, costly, and with limited experimental options for sampling due to ethical restrictions, as well as limited methodologies for identifying and detecting both peptides and AAs in plasma or blood. As an alternative, animal studies have also been used to estimate the bioavailability of BAPs from collagen and collagen precursor products [21, 22, 24, 25], but these studies are also generally slow, costly, and predictions of bio-absorbability do not always align with human clinical data due to species differences in intestinal permeability as well as metabolic activity [23, 26]. Besides, bioavailability studies using animal models to assess food components and pharmaceuticals have demonstrated poor correlations between rats and humans (r^2= 0.18) and dogs and humans (r^2= 0.19) [23]. For these reasons, cell culture models have often been used instead to assess for the intestinal transport of BAPs [26].

Caco-2 cells, a human colon carcinoma cell line, has been used regularly to assess for SI absorption of drugs, nutrients, dietary components as well as CH and CH-derived peptides [13, 26, 147, 148]. For example, recent work by Song et al. (2020) assessed the bioavailability of BAPs from silver carp skin hydrolysate using a combination of in vitro digestion and Caco-2 cells [13]. They found that the transport (%) of the key peptides Hyp-Gly, Hyp-Gly-Glu and Pro-Gly-Glu-Hyp-Gly was 22.63 ± 5.19, 11.15 ± 0.52 and 18.35 ± 1.20, respectively, as measured using high performance liquid chromatography–electrospray ionization tandem mass spectrometry (HPLC-ESI-MS). Feng et al. (2017) estimated the transepithelial peptide transport efficiency of bovine CH peptides using a Caco-2 model [148]. They demonstrated that the bioavailability of CH peptides depended on the hydrolysis method used to generate the CH. Although no specific BAPs from the CHs were identified, the AA transport across the epithelial layer ranged between 15-23%, depending on the CH preparation method. The permeability of the CH-derived BAPs Gly-Pro-Hyp and Pro-Hyp was also assessed using the Caco-2 model, followed by LC-MS/MS analysis [25]. The apparent permeability coefficient (P_{app}) for Gly-Pro-Hyp and Pro-Hyp were 1.09 ± 0.03 x 10^6, and 0.13 ± 0.03 x 10^6 cm/s, respectively. Results indicated that the permeability of Gly-Pro-Hyp was greater than Pro-Hyp, even though Gly-Pro-Hyp is a larger MW peptide. Peptide transport across the intestinal layer via paracellular pathways is primarily dependent on the charge and molecular size of the compound. Since both peptides are uncharged, it is conceivable that active transporters were involved in the relatively greater transport of Gly-Pro-Hyp. For this reason, the choice of intestinal

cell line used to predict peptide bioavailability is important, especially considering the expression and activity of active peptide transporters.

Although the Caco-2 cell line is considered to be the standard to assess intestinal absorption of molecules, peptide bioavailability assessments using this cell culture model are not ideal due to the under-expression of PepT1 in these tumorigenic cells [149]. In fact, depending on the compound being assessed, especially for peptides, permeability results using Caco-2 cells do not always correlate with human intestinal permeability [23, 149]. Alternatively, a non-tumorigenic human small intestinal epithelial cell (HIEC) line can be used to overcome the limited PepT1 expression in Caco-2 cells. As HIEC cells more accurately represent the physiological in vivo conditions of the SI [27-30], these cells have been shown to be a superior alternative to Caco-2 cells for predicting transporter-mediated absorption of compounds in humans when taken orally [27, 28].

A large limitation of current in vitro studies assessing BAP bioavailability has been the sole use of intestinal cell cultures without consideration of the subsequent hepatic effects on the intestinally transported BAPs. The human hepatocellular carcinoma (HepG2) cell line has been used to assess the hepatic metabolism of xenobiotics and drug transporters [31, 32]. Specifically, previous work has utilized a Caco-2/HepG2 co-culture model of first pass metabolism, to assess the bioavailability of dietary components by applying digests from a human simulated gut digestion [31]. Similar in vitro models show very good correlations with in vivo data from humans and animal models in terms of assessing oral bioavailable of compounds such as xenobiotics [33, 150]. Furthermore, it has been shown that Pro-Gly can increase PepT1 expression in HepG2 cells, although no assessment of the hepatic effects on Pro-Gly was investigated [151]. In general, there is a major gap in the literature with respect to the study of the hepatic first pass effects on BAPs following their intestinal cell absorption. For this reason, future work assessing the bioavailability of BAPs should incorporate hepatic cellular metabolism, to truly represent in vivo conditions as much as possible.

2.4 Microbial effects of non-digested and unabsorbed CH components

2.4.1 Introduction: microbiome, prebiotics, and microbial metabolites

Prebiotics are dietary components, such as nondigested carbohydrates, proteins, peptides and AAs, that can induce beneficial changes in the activity, growth, or composition of microorganisms found

in the GI tract, otherwise known as the microbiota [152]. The microbial fermentation products of prebiotics have been implicated to provide several health benefits upon the host. Prebiotics have been shown to regulate inflammation, improve conditions such as inflammatory bowel disease, provide protection against colon cancer, exhibit antioxidant activity, as well as reduce symptoms associated with metabolic disorders, including arthritis [38, 39, 41].

Short-chain fatty acids (SCFAs) are well established bacterial fermentation products of prebiotics, and their production is an indicator of a healthy microbial community [39]. SCFAs include acetic, propionic and butyric acids, which are normally present in ratios ranging from 3:1:1 to 10:2:1 [39]. SCFA production is one of the major health benefits associated with prebiotics, such that the relative abundance of fecal SCFAs has been used as a biomarker of gut health as well as overall systemic health [39, 50, 51]. There are numerous biological functions attributed to SCFAs that are under active investigation, and the knowledge of their impact on human health status is growing. For example, butyric acid has been implicated in the control of inflammation [152, 153], appetite [154] and liver mitochondrial function [155]. Other minor SCFAs such as valeric and caproic acids also have the potential to affect human health [156, 157], although there remain significant knowledge gaps regarding their effects.

Branched-chain fatty acids (BCFAs; isobutyric, isovaleric, isocaproic acids), are microbial products derived from the fermentation of branched-chain AAs [35]. The health implications of BCFAs are still unclear, as little work regarding the health effects of these microbial products have been published. Some reports have demonstrated that BCFA production is associated with preventing irritable bowel syndrome [44] but other studies have also linked increasing exposure to BCFAs with insulin resistance and obesity [43], both of which are risk factors for OA that could exacerbate a joint condition.

Other biomarkers of large intestinal health include hydrogen sulfide (H_2S) and ammonium (NH_4). Increased production of these gases in the GI tract may adversely affect human health [35]. The production of these GI gases is attributed to an over abundant quantity of proteins and some AAs available for fermentation, which can promote dysbiosis [35, 52, 158]. Patients suffering from OA are typically prescribed NSAIDs, which can cause detrimental GI side effects as well as acute liver

injury [1, 94]. Interestingly, when taking NSAIDs, low level H_2S production was found to prevent GI damage and dysbiosis associated with this type of medication [159]. Therefore, at lower concentrations, H_2S has been reported to be a beneficial gas produced in the GI tract.

Antioxidant status also plays an essential role in maintaining overall gut health. An increased antioxidant capacity protects against DNA damage caused by reactive oxygen species (ROS) produced in the body and gut and helps to regulate inflammation [94, 160]. Clinical studies have shown that an increased fecal antioxidant content is associated with improved gut function and health [161]. Antioxidant capacity is one of the major bioactivities that CH-derived peptides are screened for, as this could reduce ROS damage affecting some of the metabolic diseases associated with OA [94, 160, 162]. BAPs and AAs from CH products have already been shown to exhibit antioxidant properties [18, 160], however, their contribution at the level of the colon has not been investigated.

Digestion of proteins in the SI can yield peptides that bypass intestinal absorption to be fermented by colonic bacteria [45]. Consequently, it is possible that the rich content and variety of peptides and AAs present in CHs may act as prebiotics that lead to the generation of microbial nitrogenous colonic fermentation products such as SCFAs, BCFAs and GI gases. In that regard, investigation into the prebiotic effects of CHs could be important for OA as gut health has been increasingly linked to joint health.

2.4.2 Relationship between OA and the gut

Interest into the vast effects that the gut microbiome and microbial metabolites have on human health have increased our understanding of the complexity of this system, but only recently has the link between the microbiome and OA begun to be recognized. Although most clinical work has focused on knee and hip OA, a recent review by Silvestre et al. (2020), discusses the link between diet, GI dysbiosis and hand OA [163]. Low grade systemic inflammation, often attributed to obesity, could explain the increased incidence of OA in non-loading bearing joints, such as in the hands. Although the review discusses possible signalling molecules that link dysbiosis with OA, the mechanisms by which gut dysbiosis may induce and develop hand OA has not been rigorously investigated and remains a matter of debate.

Schott et al. (2018) demonstrated a direct link between OA and the gut microbiome, and its effects on systemic inflammation using a murine model of diet-induced obesity [41]. Mice were supplemented with the prebiotic fiber, oligofructose, or provided with a non-prebiotic control diet. Mice also underwent the standard destabilization of the medial meniscus (DMM) surgery to induce OA. Key findings of this study showed that supplementation of the prebiotic altered the GI microbiota of the obese OA mice to a more favorable and healthier microbiota. Notably, the increase of the commensal microflora *Bifidobacterium pseudolongum* was observed in mice supplemented with oligofructose. Prebiotic treatment was also associated with the prevention of cartilage loss and improved joint structure, which was likely due to the decreased systemic inflammation and the associated beneficial microbial changes in the GI tract.

Another mouse model study demonstrated that gut health was linked to joint health in a rheumatoid arthritis (RA) mouse model. These RA models utilize the collagen-induced arthritis (CIA) process, which involves immunizing susceptible mice with type II collagen [37]. The RA condition is a chronic inflammatory disease with inflammatory profiles similar of late-stage OA. The RA mice were either treated with an antibiotic in their water or water alone (placebo). As expected, partial depletion of GI bacteria was observed in mice treated with antibiotics, as similar events have also been observed in humans. Interestingly, mice with a depleted microbiome showed increase arthritic disease severity compared to mice that received water only. Further confirmation of such studies could lead to recommendations that patients with RA and OA should take antibiotics only when necessary, as the level of inflammation and disease severity might be increased when the microbiota is depleted.

Another RA mouse model using the CIA process investigated the link between the gut microbiome and arthritis [38]. It was previously noted that in RA models using CIA, up to 20% of DBA1 mice do not develop arthritis. This lack of arthritis development was observed, yet no reason could be provided to explain this phenomenon. In 2016, Liu et al. hypothesized that host microbial communities could play a significant role in arthritis onset and development, and could account for the lack of arthritic development in some mice after CIA treatment. In their two-part study, DBA1 mice were first induced to develop arthritis, and analysis of their microbiome using 16s rRNA

sequencing was performed. The authors demonstrated that the microbiome of mice that developed arthritis showed enriched operational taxonomic units (OTUs) associated with the genus Lactobacillus before arthritis onset, whereas after the disease developed, a significant increase in the families Bacteroidaceae, Lachnospiraceae, and S24-7 was observed. Secondly, the authors then conventionalized germ-free mice with the microbiota of mice that were susceptible or resistant to arthritis induction. Mice conventionalized with the microbiota from mice susceptible to arthritis induction showed a greater frequency in arthritis onset compared to mice that were conventionalized with the microbiota of arthritis-resistant mice. Correspondingly, inflammation was also greater in the arthritis susceptible mice.

As more evidence of the link between the microbiome and OA is gathered, the impact of CHs and their potential prebiotic effects, as mediated by their peptide and AA content, warrants further investigation. In that regard, the effect of CHs on the microbiome has not been investigated but is of interest, as patients are increasingly utilizing these products to mitigate their symptoms of OA.

CONNECTING STATEMENT 1

The literature review presented in Chapter 2 summarises the growing social and financial burden of OA, and the need to find innovative solutions for patient care as no disease modifying drugs are available for OA. In that regard, CHs have been used by OA patients to help manage their symptoms and increase their mobility. Chapter 2 summarizes how the BAPs from the CH supplements may help to treat the disease and are bioavailable after oral consumption. To better understand the role of CHs and their ability to improve joint health, it is essential to be able to measure the bioactive components, i.e., peptides and AAs, after oral consumption and digestion. The ability to target and simultaneously measure BAPs and AAs from digesta can be challenging due to the limited methodological approaches available, which often include indirect measurement of the peptides. Thus, the development of simple and reliable analytical methods is required. In Chapter 3, we describe novel methods for targeted analysis of BAPs and AAs from CHs after digestion. Specifically, a novel capillary zone electrophoresis method that can analyze BAPs from digests generated via in vitro stomach and SI digestion of CHs was developed. Additionally, a concurrent method of AA analysis from CH digesta using a hydrophilic interaction liquid chromatography (HILIC) liquid chromatography-mass spectrometry (LC-MS) methodological approach was established. Chapter 3 was published in LWT - Food Science and Technology: Larder, C.E.; Iskandar, M.M.; Sabally, K.; Kubow, S. *Complementary and Efficient Methods for Di- and Tri-Peptide Analysis and Amino Acid Quantification from Simulated Gastrointestinal Digestion of Collagen Hydrolysate*. LWT, 2022. **155**: p. 112880. https://doi.org/10.1016/j.lwt.2021.112880

CHAPTER 3: RESEARCH PAPER 1

Published: LWT - Food Science and Technology, 2022; 155: p. 112880

Complementary and Efficient Methods for Di- and Tri-peptide Analysis and Amino Acid Quantification from Simulated Gastrointestinal Digestion of Collagen Hydrolysate

Affiliation:

Christina E. Larder, Michèle M. Iskandar, Kebba Sabally, Stan Kubow *

School of Human Nutrition, McGill University, Ste-Anne-de-Bellevue, QC, Canada, H9X 3V9

* Corresponding author: stan.kubow@mcgill.ca; Tel.: +1-514-398-7754

3.1 Abstract

Collagen hydrolysates (CHs) are composed of bioactive peptides (BAPs) and amino acids (AAs), which contribute to their health enhancing properties. Post digestion profiling of CHs typically evaluates either BAP or AA content in blood but not within digests. Existing methods for peptide analysis are optimized for blood samples and rely on costly methods that require substantial sample preparation and data interpretation. A capillary electrophoresis (CE) method was developed as a rapid, cost effective, and reliable method for analysis of BAPs (Ala-Hyp, Pro- Hyp, Pro-Hyp-Gly, Gly-Pro-Hyp) within digests. Coupled to LC-MS, a hydrophilic interaction liquid chromatography (HILIC) column was used to quantify 19 AAs in digests, without derivatization. Two bovine CHs (CH-GL and CH-OPT) underwent in vitro digestion and their BAP and AA content was assessed. The Gly-Pro-Hyp and Pro- Hyp-Gly content was greater in CH-GL versus CH-OPT with values of 19.82 ± 4.25 and 8.969 ± 2.742 μg/mL respectively. The two CHs had distinct peptide profiles; 13 unidentified peptide peaks from each CH were not found in the other. No differences in AA content were observed. The present work describes sensitive and rapid methodology for concurrent analysis of BAPs and AAs after digestion of CHs, which can support further understanding of the bioactive components of CHs.

Keywords: capillary electrophoresis, peptides, amino acids, collagen hydrolysate, hydrophilic interaction liquid chromatography (HILIC)

3.2 Introduction

Collagen hydrolysates (CHs) have been indicated to provide health enhancing properties in multiple human clinical studies, which has been attributed to their content of bioactive peptides (BAPs) and amino acids (AAs) (Bernardo & Azarcon, 2012; Bruyère et al., 2012; Feliciano et al., 2017; Pal & Suresh, 2016). Several reports have demonstrated that collagen products, such as gelatin, as well as collagen hydrolysates, contain peptide sequences that lead to post-digestive release of BAPs and AAs (Osawa et al., 2018; Skov, Oxfeldt, Thøgersen, Hansen, & Bertram, 2019; Udenigwe & Aluko, 2012; Yazaki et al., 2017). The BAPs identified in the blood circulation after oral ingestion of CHs and CH precursors such as gelatin include Ala-Hyp, Pro-Hyp-Gly and Gly-Pro-Hyp (Shigemura, Suzuki, Kurokawa, Sato, & Sato, 2018; L. Wang, Wang, Liang, et al., 2015). The proposed health benefits of collagen-derived BAPs include the improvement and maintenance of articular cartilage, acting as second messengers for extracellular degradation, regulation of inflammatory processes, antioxidant properties, stimulation of wound healing, learning facilitation and improved memory (Léon-López et al., 2019; Pal & Suresh, 2016). In addition to BAPs, multiple health benefits have been attributed to the digestive release of AAs from CHs, which include stimulation of protein synthesis, angiotensin converting enzyme (ACE) inhibitory activity, and anti-inflammatory and antioxidant effects (Gómez-Guillén, Giménez, López-Caballero, & Montero, 2011; Li et al., 2016; Wang et al., 2014). Furthermore, AAs can be biotransformed to other bioactive compounds within the body such as the conversion of methionine to S-adenosylmethionine, which has been shown to improve joint health (Li et al., 2016). As with BAPs, an increase in postprandial plasma AAs has been demonstrated after CH ingestion. Notably, an increase in plasma Pro, Hyp, Gly, Lys, and Ala was observed after CH ingestion, which was measured by ^{1}H nuclear magnetic resonance (NMR) spectroscopy (Skov et al., 2019).

Both human and animal CH feeding trials have primarily used liquid chromatography-mass spectrometry (LC-MS) to detect BAPs in plasma or serum (Osawa et al., 2018; Sontakke, Jung, Piao, & Chung, 2016; Taga, Kusubata, Ogawa-Goto, & Hattori, 2016; Yazaki et al., 2017). Analysis identifying lower MW peptides, however, is not often completed, largely due to limitations of "peptide-centric" proteomic work as di- and tri-peptides are too small for sequencing. Other methods of quantification include the use of ultra-performance liquid chromatography (UPLC) and high-performance liquid chromatography (HPLC) (Shigemura et al., 2018; Wang, Wang, Liang, et al.,

2015). Alemán, Gómez-Guillén, and Montero (2013), investigated the ACE-inhibitory capacity of squid collagen after in vitro digestion. They found that, after pepsin and pancreatin digestion, the ACE-inhibitory capacity of the fractionated collagen product was significantly increased. The AA composition of the fractionated hydrolysates was measured using an amino acid analyser, and peptide concentrations were calculated indirectly based on the AA results. Key BAPs of the fractions were then identified using LC-electrospray ionization (ESI)-ion trap (IT)-MS/MS; however, quantification was not done. As with other LC-MS methods, identification of di-and tri-peptides is not easily completed, so the smallest ACE-inhibitory BAP identified was nine AAs in length. Di- and tri-BAPs continue to be overlooked in the literature due to limited availability of sensitive methods for detection of lower molecular weight (MW) peptides. Accordingly, there is need for sensitive and cost-effective methods to detect and measure BAPs from digesta, particularly as lower MW peptides from CHs have greater bioactivities and bioavailabilities relative to greater MW peptides (León-López et al., 2019).

Capillary electrophoresis (CE) is a well-established tool for qualitative and quantitative measurement of peptides and peptide metabolites (Popa, Mant, & Hodges, 2003; Scriba, 2016; Verpillot, Otto, Klafki, & Taverna, 2008; Zhang, Zhu, & Gong, 2017). A commonly used type of CE is capillary zone electrophoresis (CZE), where compounds, such as peptides, migrate through a narrow-fused silica capillary where the flow is dependent upon the applied electric field, buffer and pH (Scriba, 2016). A flow-gated capillary electrophoresis method has been successfully utilized to measure BAPs such as Pro-Hyp, Pro-Pro, Pro-Gly and Pro-Leu in urine samples (Zhang et al., 2017); however, CE has not been applied towards the detection of peptides in gastrointestinal (GI) digesta.

AA analysis, primarily from plasma, has often involved derivatization followed by HPLC, gas chromatography (GC)-MS or LC-MS methods (Prinsen et al., 2016). Sample preparation associated with derivatization often makes these methods difficult and time consuming, along with underlying issues in reliability and derivative stability (Prinsen et al., 2016). Such derivative yield problems can lead to insufficient reproducibility of the derivative. Other established methods used for AA analysis from plasma or urine such as ^{1}H NMR have few sample preparation steps (Emwas et al., 2018; Skov et al., 2019), but can be difficult to adapt to different types of biological fluids due to significant spectra interpretation issues (Emwas et al., 2018). In that regard, data analyses require multiple

processing steps that make interpretation difficult, due to issues such as spectral alignment, baseline correction, scaling and normalization as well as chemical shift referencing. Accordingly, data processing of ^{1}H NMR spectra remains a highly debated topic with little consensus on the processing steps and data interpretation, especially for complex biological fluids such as urine. Biological fluids such as plasma are more easily analysed due to the extensive spectral libraries available. Additionally, sample pH, salt concentration and the choice of temperature gradients can also affect the spectral output of ^{1}H NMR.

As an alternative, tissue analysis of underivatized AA using hydrophilic interaction liquid chromatography (HILIC), often coupled to LC-MS, has become a well-established and reliable method of detection and quantification (Bellvert et al., 2018; Kennedy & Bivens., 2017; Prinsen et al., 2016). For example, HILIC methods coupled to LC-MS/MS are robust enough to separate and detect isomers of leucine and isoleucine as separate peaks from human serum (Prinsen et al., 2016). HILIC-MS has also been used to quantify 36 AAs and their metabolites from human plasma without the need to utilize a derivatization procedure during sample preparation (Prinsen et al., 2016).

Current research often focuses on the detection and quantification of either BAPs or AAs, although previous work has often used indirect measures of AAs to quantify BAPs. To our knowledge, no published literature has targeted and quantified both sets of compounds concurrently from gut digesta, even though they can both exert significant health promoting properties. Due to the large compositional peptide complexity and the number of AAs found in CHs, there is a knowledge gap regarding the low MW sequences of BAPs and the quantities of AAs released from CHs post-digestion. A major technical challenge has been the lack of published methodology for concurrent BAP and AA analysis from GI digesta after CH digestion. As the health benefits of BAPs and AAs from collagen products has become more evident, it is important to develop sensitive, rapid and cost-effective methods of measuring both sets of these bioactive compounds. Since determination of peptides generated during in vivo digestion is technically difficult, costly and requires human or animal ethics approval, simulated digestion models provide a readily utilizable in vitro approach to detect BAP and AA release from digestive processes (Amigo & Hernández-Ledesma, 2020).

The aim of this research was to describe a novel CZE and HILIC-MS methodological approach that can concurrently analyze BAPs and AAs, respectively, in digests generated from in vitro stomach and small intestine (SI) digestion of CHs.

3.3 Materials and methods

3.3.1 Standards

Peptide standards Ala-Hyp and Pro-Hyp-Gly were ordered and synthesized by CanPep Inc. (Montreal, QC, CN). Peptides Pro-Hyp (4001630) and Gly-Pro-Hyp (4008512) were purchased from Bachem (Bubendorf, Switzerland). Peptides were 98% pure with peptide purification validation completed by HPLC and mass spectra analysis. Peptide stocks of 1 mg/mL were made in ddH_2O, and subsequently diluted for calibration curves which were used for method verification, and as external standards for peptide quantification. The pH of the peptide stock solutions and CZE buffers were measured using a pH meter (Fisher Science Education, Cat no. 2253250, Saint-Laurent, QC, CN) and adjusted using either 1 M NaOH (Sigma-Aldrich, 1310-73-2, St. Louis, MO, USA) or 1 M HCl (Fisher Scientific, 7647-01-0, Waltham, MA, USA). Amino acids standards (Sigma-Aldrich, LAA21, St. Louis, MO, USA) were prepared in ddH_2O and subsequently diluted for calibration curves and used as external standards for AA quantification.

3.3.2 Simulated digestion

Two bovine-sourced CH products were used for this study: Original Formula® (Genacol, Blainville, QC) (CH-GL) and Selection (Uniprix, QC, CN) (CH-OPT). Upper intestinal digestion involving the stomach and SI was adapted from Alemán et al. (2013), and Miranda, Deusser, and Evers (2013). CHs (1200 mg) were digested in reactor vessels placed in a 37°C water bath (Cole-Parmer Advantec, TBS181SA, Montreal, QC, CN) with continuous stirring (Corning, hot plate laboratory stirrer PC351, Corning, NY, USA) and the pH was monitored and adjusted throughout digestion (Fisher Scientific, S90528, Waltham, MA, USA). A 4% (w/w) pepsin solution (Sigma-Aldrich, P7125, St. Louis, MO, USA) was prepared in 0.1 M HCl and added to the reactor vessel. The pH was adjusted to 2 and the solution incubated for 30 min. Following this, a 4% (w/w) pancreatin solution (Sigma-Aldrich, P7545, St. Louis, MO, USA) was added. The pH was adjusted to 8 and the solution incubated for 120 min. Afterwards, digesta were rapidly cooled on ice, the pH increased to 10, and then frozen to stop the enzymatic processes. Subsamples of the digesta were filtered using a 0.45 µm Millipore syringe-driven filter and stored at -20°C until analysis. Three independent digestions were completed for

each CH treatment. A blank was also completed, without the addition of the CH treatment, also in triplicate. This was used as a method blank in subsequent analyses (Harris, 2009).

3.3.3 Targeted peptide quantification

A capillary electrophoresis system (Capel 105 M and Capel 205 M; Lumex Instruments, Fraserview Place, BC, CN) was used for the targeted quantification of four peptides (Ala-Hyp, Pro-Hyp, and Pro-Hyp-Gly and Gly-Pro-Hyp). Methodology is based on our previous CE work (Larder, Iskandar, Sabally, & Kubow, 2018). In brief, the separation capillary (Molex, 2000019, Lisle, Illinois, USA) was 60 cm in total length, 53 cm effective length, and 75 µm inside diameter, similar to previous CE methods for collagen analysis (Mikulíková, Eckhardt, Pataridis, Mikšík, & Paris, 2007). Pressure injections were completed using 30 mbar for 10 s at 0 kV and analysis with 0 mbar for 1199 s at 20 kV and 205 nm. The instrument was set for 20°C. A 0.1 M phosphate buffer (pH 2.4) was used for rinsing and as a sample carrier, otherwise known as running buffer. The electropherogram was processed using the software package Elforun (Lumex Instruments Canada, Version 4.2.4, Mission, BC, CN) and baseline correction using OriginPro Version 2021b (OriginLab Corporation, Northampton, MA, USA). The filtered digesta samples were diluted 1:1 with 0.1 M phosphate buffer (pH 2.4) before injection. Before every run, the capillary was rinsed with MilliQ water, 0.5 M NaOH and running buffer, each for 5 min, as previously suggested for proline- and hydroxyproline-containing peptide CE analysis (Hamrníková, Mikšík, Deyl, & Kašicka, 1999). For each treatment and digestion replicate, three injections were performed. Quantification of each peptide, based on peak area, was performed using external standards and corresponding calibration curves. An internal standard (IS) was not used; this was because an IS is primarily used for methods when there are multiple dilutions required or when there are many sample preparation steps before injection or analysis (Dolan, 2012; Harris, 2009). In our case, sample preparation was extremely simple; digesta were only filtered and diluted with running buffer before being injected. Thus, the method developed benefited by using an external standard (ES) rather than an IS. Furthermore, the use of an ES rather than IS eliminates the potential uncertainty and variability of integrating the peak area of the IS. A minimum of six points of calibration were used to produce standard curves and the linearity was assessed by the correlation coefficient, R^2. Acceptability of the method included investigation of residual plots, calculation of the relative standard deviation (RSD) to determine precision (n = 8), and accuracy determined through recovery (n = 8). As with previous CE method development

publications (Gibbons, Wang, & Ma, 2011), linearity and instrument detection limit (IDL) were determined through serial dilution of the standard mixture and the method detection limit (MDL) was also assessed. Due to the lack of an extraction step, matrix effects were not assessed. The mean of three measurements were taken to assess methodology. Previous capillary zone electrophoresis method papers have also utilized three measurements (Hsiao, Ko, & Lo, 2001).

3.3.4 Targeted AAs quantification

The analyses of underivatized AAs (alanine, arginine, asparagine, glutamic acid, glutamine, glycine, histidine, hydroxyproline, isoleucine, leucine, lysine, methionine, phenylalanine, proline, serine, threonine, tryptophan, tyrosine, and valine) were adapted from Bellvert et al., 2018 and Kennedy and Bivens (2017). SI digesta were filtered using a 10 kDa molecular weight cut-off (Millipore, Nepean, ON, USA) in a stirred ultrafiltration membrane reactor (Amicon Ultrafiltration Cell, model 8050) at 4°C while under nitrogen gas at a pressure of 40 psi (Iskandar et al., 2015), then filtered using a 0.2 µm Millipore syringe-driven filter and stored at -20°C until analysis (Bellvert et al., 2018). Analyses of AAs using SI digesta were completed in positive mode on a triple quadrupole MS system (EVOQ Elite, Bruker, Billerica, MA) coupled with an UHPLC pump (Advance, Bruker, Billerica, MA) and equipped with a hydrophilic interaction chromatography column, Agilent Infinity Lab Poroshell 120 HILIC-Z (2.1 × 100 mm, 2.7 µm). The LC-MS grade solvents, acetonitrile and water (EMD Millipore), formic acid (Fisher Scientific) and ammonium formate (Sigma Aldrich) were used for the preparation of mobile phases. Mobile phases were prepared as follows: a 200 mM ammonium formate stock solution was prepared in water and adjusted to pH 3 with formic acid. The mobile phase A (aqueous) was prepared by diluting the stock solution 9:1 in water, and the mobile phase B (organic) was prepared by diluting the stock solution 9:1 in acetonitrile (final mobile phases at 20 mM ammonium formate). Mobile phases were sonicated for 15 min each time before use. The column temperature was set to 30°C and the flow rate was 0.8 mL/min. The LC method started at 100% B and reached 70% B over 10 min, then the gradient changed to 30% B in 0.1 min for 2.9 min. For reconditioning, the gradient was returned to initial conditions at 13.1 min until 37 min. Each SI digesta sample and AA standard was injected three times at a volume of 10 µL. The operating parameters of the mass spectrometer were: positive spray voltage 4000 V, cone temperature 350 ◦C, cone gas flow 20 (arbitrary units), heated probe temperature 400°C, probe gas flow 40 (arbitrary units), nebulizer gas flow 60 (arbitrary units). The mass spectrometer was used in the multiple

reaction monitoring (MRM) mode; transitions are presented in **Table 1**, and examples of chromatograms are presented in **Fig. S1**. AA quantification was performed using external calibration curves, based on peak area. A minimum of five points of calibration were used to produce a standard curve and the linearity was assessed by the correlation coefficient, R^2. Each curve had an R^2 greater than 0.98, and CV for each injection replicate of both CH digesta samples and standards was less than 25%. Samples were diluted with buffer B, at 1000x or 200x, to be in the middle of the standard curve range.

Table 3.1. MS transition parameters for the analysis of AAs on SI digesta. Completed in positive mode on a triple quadrupole MS system coupled with an ultrahigh performance liquid chromatography pump and equipped with a hydrophilic interaction chromatography column (HILIC).

			Product ions		
Compound	Precursor ion (m/z)	Quantification ion (m/z)	Collision energy (V)	Qualitative ion (m/z)	Collision energy (V)
Alanine	90.0	44.9	8		
Arginine	175.1	70.6	19	116.2	12
Asparagine	133.0	74.5	13	87.4/116.1	8/8
Glutamic Acid	148.0	84.4	14	130.10	7
Glutamine	147.0	84.1	15	130.1	7
Glycine	76.0	76.0	3		
Lysine	147.0	84.4	15	130.2	8
Methionine	150.0	104.3	9	56.7/133.1	14/7
Histidine	156.00	110.30	12		
Hydroxyproline	132.0	86.4	12	68.6	18
Proline	116.0	70.5	12		
Serine	106.0	60.7	9		
Threonine	120.0	74.5	9	56.7/102.3	14/6
Tryptophan	205.0	188.0	8		
Tyrosine	182.0	136.1	11	165.7/91.4	7/26
Valine	118.0	72.6	8	55.7	17
Isoleucine	132.0	86.4	8		
Leucine	132.0	86.4	8		
Phenylalanine	166.0	120.2	11	103.3/77.5	24/36

3.3.5 Statistical analysis

Peptide data is reported as mean ± standard deviation (SD). Amino acid data is reported as mean ± standard error (SEM). For each peptide and AA, differences between CH treatments were assessed

using a two tailed *t*-test and considered significant if $p < 0.05$. All analyses and figures were completed using GraphPad Prism (Version 9.0.1 for Windows, GraphPad Software, San Diego, California USA), except for baseline correction of the chromatograms which was completed using OriginPro (Version 2021b. OriginLab Corporation, Northampton, MA, US). Differences in CZE peptide area for unidentified peaks was assessed using t-tests and considered significant if $p < 0.05$.

3.4 Results and discussion

3.4.1 CZE method justification

Previous LC-MS and LC-MS/MS studies have primarily used columns such as Zorbax SB-Aq, Inert-sustain peptide C18, and Ascentis Express F5 to detect BAPs in plasma or serum after feeding CHs in human and animal trials (Osawa et al., 2018; Sontakke et al., 2016; Taga et al., 2016; Yazaki et al., 2017). To detect and quantitate BAPs in the SI samples after CH digestion, adaptations of the above MS methodologies were attempted using a variety of columns (Zorbax Eclipse Plus C18, Ace C18 PFP and Zorbax SB-C8, Synergi™ 4 µm Fusion-RP, InfinityLab Poroshell 120 Hilic Z). The resulting LC-MS chromatograms demonstrated sub-optimal peak shape, significant signal-to-noise ratios, and peak splitting (see **Supplemental Fig. S2** for examples of chromatograms). Further method development was considered to be costly, time consuming, and without assurance that the peptides of interest would be sufficiently detectable and measurable. Consequently, CE was applied as an alternative accurate, rapid and cost-effective approach, particularly since this was a well-established tool for qualitative and quantitative measurement of peptides and peptide metabolites (Popa et al., 2003; Scriba, 2016; Verpillot et al., 2008; Zhang et al., 2017). A further advantage was that CZE method development for peptide analysis is relatively straightforward, rapid, and reliable while using low sample volumes along with negligible consumable costs (Zanaboni et al., 1996).

3.4.2 CZE method validation and verification

The linear range was determined for each peptide (from 0.012 to 0.25 mg/mL), and the coefficient of determination (R^2) calculated (**Fig. 1, Table 2**). All curves generated R^2 greater than 0.990. Residuals of the calibration curves were calculated; all were lower than 20%. Residual plots were also distributed randomly. Excellent selectivity for peptides was obtained with phosphate buffer at pH 2.5 for all peptides, allowing for simultaneous analysis. Previous CE methods have also found that this buffer allows for robust analysis of peptides (Janini, Metral, & Issaq, 2001; Mikšík, Sedláková, Mikulíková, & Eckhardt, 2006; Mikulíková et al., 2007; Popa et al., 2003; Sun, Zhu, et al.,

2016). Running a phosphate buffer at low pH is suggested to avoid peptides adhering to the capillary wall (Hamrníková et al., 1999; Mikšík et al., 2006).

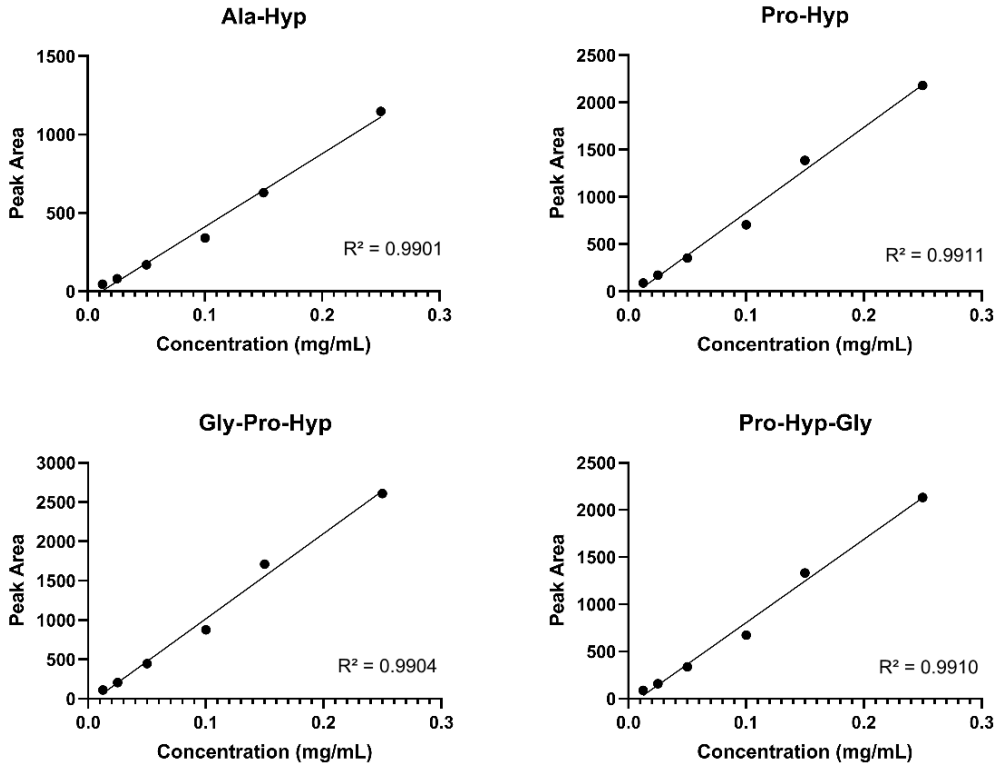

Figure 3.1. Linear calibration curves for peptide standards Ala-Hyp, Pro-Hyp, Gly-Pro-Hyp and Pro-Hyp-Gly for the range of 0.012–0.25 mg/mL (n = 8/calibration point). SEM bars are too small to appear on the figure.

Table 3.2. Method Parameter Validation

	Ala-Hyp	Pro-Hyp	Gly-Pro-Hyp	Pro-Hyp-Gly
Retention time range (min)	13.907-14.187	14.187-14.895	15.018-15.190	15.320-15.978
Linearity (R^2)	0.9901	0.9911	0.9904	0.9910
Precision (RSD %)	2.237	4.493	5.358	4.909
Accuracy (%)	101.5	96.69	106.9	114.5
IDL (ppm)	0.0750	0.0143	0.0058	0.0194
MDL (ppm)	2.626	2.844	2.198	10.99

Linearity is reported using the coefficient of determination (R^2). Repeatability is reported as precision in relative standard deviation (RSD) (%) between repeated analyses over 3 days (n=8). Accuracy is determined though recovery. IDL and MDL are reported in parts per million (ppm).

The wavelength (205 nm) was selected as it has been used in previous reports investigating peptide mapping (Heiger, Grimm, & Herold, 2008). CE methods investigating collagen peptides are flexible and can vary in voltage between 8 and 25 kV (Mikšík et al., 2006), therefore optimization for different sample types is necessary. The use of 20 kV herein provided optimal peptide peak separation. Using these buffer and CE parameters, peptides were injected individually, as well as in a standard mix. Peptides were detected as individual and sharp peaks if they were injected separately or as a mix, thereby allowing for simultaneous analysis (**Fig. 2**). The retention times of each peptide were consistent between day-to day injections and with the application of newly prepared phosphate buffer. The retention times of Ala-Hyp ranged from 13.904 to 14.187, Pro-Hyp from 14.187 to 14.895, Gly-Pro-Hyp from 15.018 to 15.190 and Pro-Hyp-Gly from 15.320 to 15.978 (**Table 2**). Despite some variability in retention times, these ranges are lower than previously reported ranges from other published CE methods (Hsiao et al., 2001). Variability in retention times is often inherent to CE analysis, as differing ionic strengths of running buffers and buffer strengths may interfere with peak migration.

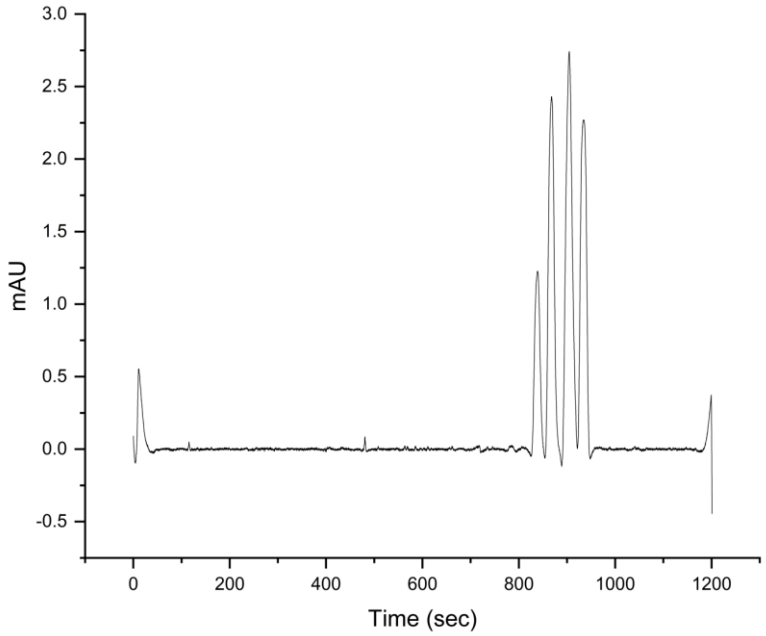

Figure 3.2. Example electropherogram of peptide mix. Each peak represents an individual peptide.

Precision was expressed as relative standard deviation (RSD %) and was 2.237, 4.493, 5.358, 4.909% for Ala-Hyp, Pro-Hyp, Gly-Pro-Hyp, and Pro-Hyp-Gly, respectively (**Table 2**). IDL and MDL were determined using dilutions of the standard mixture (Section 2.1) (**Table 2**). As with other CE methods, IDL was based on the 3σ criterion (Gibbons et al., 2011). Peak area less than three times the standard deviation was considered noise. All peptide signals for the linear and working range were above noise levels. MDL was calculated using the digestive blank (Harris, 2009). As with IDL, all peptide signals between 0.012 and 0.25 mg/mL were above criterion levels.

3.4.3 Identification and quantification of BAPs from CHs

Four peptides (Ala-Hyp, Pro-Hyp, Gly-Pro-Hyp, and Pro-Hyp-Gly) were identified after simulated gastrointestinal digestion (**Fig. 3**). Peptide content was significantly greater after CH treatment (CH-GL and CH-OPT) compared to the method blank containing no CH product (data not shown), except for Gly-Pro-Hyp after CH-OPT treatment (27.66 ± 1.84 µg/mL).

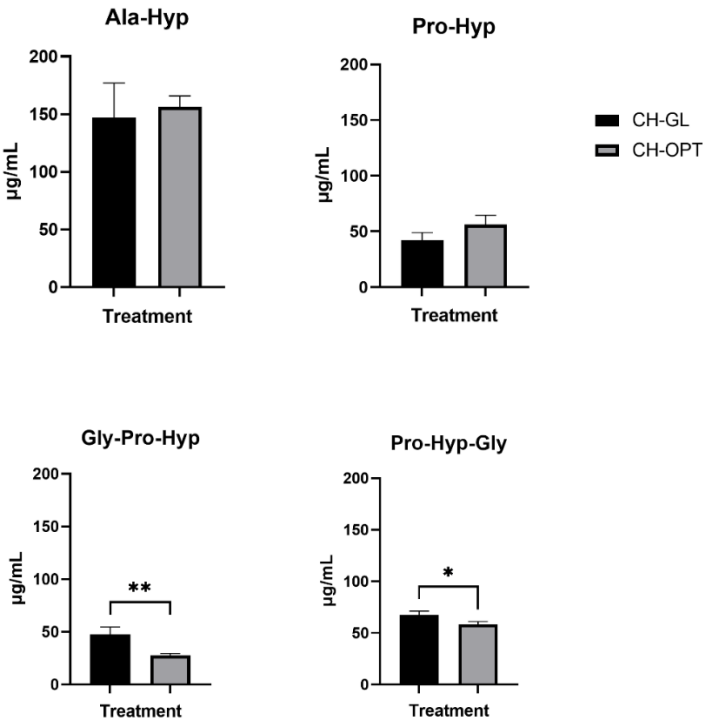

Figure 3.3. Peptide content of CH-GL and CH-OPT after upper intestinal digestion (n = 3/treatment). Values are expressed as mean ± SD in µg/mL. For each peptide, a *t*-test was completed to detect differences between CH treatments, where $p < 0.05$ was considered significant. Columns with asterisks are significantly different (*$p < 0.05$, **$p < 0.01$).

There were no differences in peptide content (µg/mL) after simulated digestion between CH-GL and CH-OPT for Ala-Hyp and Pro-Hyp respectively (CH-GL: 147.01 ± 29.87, 42.07 ± 7.06, CH-OPT: 156.45 ± 9.33, 56.04 ± 8.53). A greater tri-peptide content was observed with CH-GL. Specifically, Gly-Pro-Hyp (µg/mL) was 47.48 ± 7.13 after CH-GL treatment, whereas only 27.66 ± 1.84 was measured after CH-OPT. The tri-peptide Pro-Hyp-Gly (µg/mL) was also greater in CH-GL (67.33 ± 3.85) compared to CH-OPT (58.36 ± 2.78).

Previous work has consistently reported significantly different peptide compositions and bioactivities among CH products that varied according to the type of processing method used and source to generate the CHs (Gómez-Guillén et al., 2011; Simons et al., 2018). Additionally, we have previously shown major differences in the diversity of larger MW peptides (more than 15 AAs)

between pre- and post-digested forms of CH-GL and CH-OPT despite their similarity as bovine-sourced products (Larder, Iskandar, & Kubow, 2021). Similarly, in the present work, the post-digestion peptide content from CH-GL and CH-OPT was significantly different, which could also be attributed to differences in the preparation and processing of the CHs (Gómez-Guillén et al., 2011; Simons et al., 2018). As the di- and tri-peptides released from in vitro digestion were too small for sequencing using proteomics, the CZE methodology described herein was applied to describe post-digestion differences in the small BAP content between the two CH products.

Previous work has identified peptides (Ala-Asn, Ala-Hyp-Gly, Asp- Glu, Glu-Asn, Glu-Asp, Glu-Met, Gly-Pro-Hyp, Leu-Hyp, Leu-Met, Phe- Gly-Asn, Pro-Gly-Leu, Pro-Leu, Ser-Gly-Met, Ser-Hyp, Ser-Pro-Gly, Tyr- Met) in rat plasma after the administration of collagen products (Wang, Wang, Qian, et al., 2015). Quantitative analysis, however, was not completed except for general bioavailability of the collagen product, which was indirectly calculated by measuring the bioavailability of plasma Hyp. Quantitative analysis using LC-MS of BAPs from porcine skin hydrolysates including Pro-Hyp, Pro-Hyp-Gly and Ala-Hyp was completed in a different rat trial using intestinal perfusate and plasma (Osawa et al., 2018). The reported levels of Pro-Hyp, Pro-Hyp-Gly and Ala-Hyp from intestinal perfusate were much lower than reported here (24.62 ± 1.73, 14.03 ± 1.41 and 3.15 ± 0.43 nmol/L, respectively). These differences in peptide content could be attributable to species differences in digestion process, bioavailability and metabolic capacity between humans and animals that often occur (Cao et al., 2006; Musther, Liu, Rostami Hodjegan, Olivares-Morales, & Hatley, 2014; Punt, Peijnenburg, Hoogenboom, & Bouwmeester, 2017). Other studies using rats after fish collagen supplementation using LC-MS/MS have also reported peptide values from plasma below those measured herein. Peptides Gly-Pro-Hyp and Pro-Hyp ranged between 10 and 0.05 μg/mL and 8–0.3 μg/mL respectively over the course of 5 h (Sontakke et al., 2016)

As most food components such as peptides typically have a threshold of bioactivity, there is a gap in the literature on the quantity of BAPs released after digestion which have been identified to have a significant health impact. Such assessments are particularly useful via the application of in vitro models representative of human digestion, which could provide more physiologically relevant information for the human context than animal studies. The present work has described optimized methods using CZE that can easily and rapidly assess BAPs from simulated human digestive fluids,

while also being cost-effective. Well established BAPs (Pro-Hyp, Pro-Pro, Pro-Gly, Pro-Leu) have already been measured using flow-gated capillary electrophoresis, although using urine samples rather than GI digesta (Zhang et al., 2017). Pro-Hyp content from human urine samples ranged from 15.81703 to 28.82671 μg/mL, which is lower than reported here after digestion. This is most likely because peptides must first enter the blood stream and then are likely to be utilized by the body before being excreted into the urine. Other urinary analyses measuring X-Pro and X-Hyp peptides have also used CZE (Zanaboni et al., 1996). As with our developed method, key highlights of the CZE method developed by Zanaboni et al., 1996 was that it was rapid, straightforward, reliable, and minimal sample volumes and preparation steps were necessary for analysis. Our recent work demonstrated that CZE continues to be a relevant analytical choice for the analysis of small peptides from complex biological fluids

Future method optimization could include coupled CE-MS analysis (Zanaboni et al., 1996); however, associated costs should be considered, as well as accessibility to instrumentation. Instead, further optimization for the current developed CZE method could include modifying the inner surface of the capillary by dynamic coating to ensure peptides with proline at the carboxy terminus do not adhere to the capillary wall (Mikšík et al., 2006). Future work to adapt CZE methods to assess for the bioavailability of BAPs after absorption is also needed and is currently being investigated by our group. In fact, previous work investigating bioavailability of egg ovalbumin hydrolysate peptides by combining digestion and intestinal transport has already been completed, however, peptide analysis was performed by LC-MS (Grootaert et al., 2017).

3.4.4 Peptide peak profile of CHs; unidentified peaks

Analyses of the peptide profiles of CH-GL and CH-OPT by CZE demonstrate distinct quantitative differences in the relative abundances of peaks, as well as qualitative differences shown by the appearance of novel peaks in either CH product, which are absent in the other (**Table 3**). A total of 51 unidentified peptide peaks were observed. Specifically, 21 peptides peaks were found in both CHs, whereas 13 unknown peptide peaks were only found in CH-GL. CH-OPT also had 13 peptide peaks not found in CH-GL. Of the common peaks, analysis of peak area showed that peaks 11, 12, 25 and 26 were significantly greater in CH-GL compared to CH-OPT. In contrast, peaks 14, 16, 20, 27,

32-34, 38, 39, 42, 48 were greater in CH-OPT. All other common peaks between CHs did not significantly differ in peak area between treatments.

CZE can measure the complete peptide profile of the digesta, although peaks are unidentified, and the bioactivity of each peptide peak remains unknown. Previous work, although not using CH, has also used CZE to obtain the profile of peptides after simulated digestion of whey protein hydrolysates (Iskandar et al., 2015). Peptide profiles of collagen and collagen-incubated mixtures have also been compared using CZE. Similar to our methodology and results, qualitative differences were observed (Mikulíková et al., 2007). In the present work, differences among CH-GL and CH-OPT treatments were observed both by the appearance of novel and distinct peptide peaks, and via quantitative differences in the relative abundance of peaks. Peptide diversity remains important to assess as it may exert a significant effect on CH bioactivity, particularly as the identification and bioactivity of unknown peaks can become clearer in the future. Further work to characterize unknown peptide peaks, considering their possible bioactivity, is required. Additionally, individual peptides may not always exhibit bioactivity themselves, but could provide synergistic effects. There were 13 unidentified peaks found in each CH that were unique to each product, which could partly explain differences in bioactivity, and possibly contribute to differences in clinical efficacy. Previous clinical trials have been completed on CH-GL (Bernardo & Azarcon, 2012; Bruyère et al., 2012; Feliciano et al., 2017), although none on CH-OPT, to our knowledge.

This work has shown that CZE is a versatile tool for qualitative and quantitative assessment of post-digestive peptide profiles. Although both CH-GL and CH-OPT were sourced from bovine collagen, the present study shows that digestion of these CHs resulted in the generation of different peptide sequences in varying relative quantities. Further work implementing optimized new CZE methods in conjunction with models to assess bioavailability of small BAPs is required, to comprehensively understand the physiological impact of CHs considering their extensive consumption.

Table 3.3. Differences in peak area between CH-GL and CH-OPT, as assessed by CZE. Differences in CZE peptide peak abundance was assessed using t-tests and considered significant if $p < 0.05$.

	Peak Area		*P* Value
Peak number	CH-GL	CH-OPT	
1		7.08±0.57	Only in GR
2		16.59±1.09	Only in GR
3		58.31±6.92	Only in GR
4		58.22±17.37	Only in GR
5		60.18±4.60	Only in GR
6		126.59±31.42	Only in GR
7		63.08±6.35	Only in GR
8		17.35±5.79	Only in GR
9		34.06±3.23	Only in GR
10	49.06±3.44		Only in GL
11	260.40±17.69	57.94±6.26	0.0004
12	368.65±41.82	141.22±15.61	0.0070
13	152.97±4.85		Only in GL
14	16.99±2.1	96.19±25.99	0.0385
15	57.15±14.53	27.85±12.55	0.2018
16	7.65±1.02	35.61±5.67	0.0083
17		52.95±29.78	Only in GR
18		79.2±14.13	Only in GR
19	186.73±7.61	149.18±21.99	0.1819
20	13.08±0.26	23.84±0.15	0.0001
21		7.29±0.20	Only in GR
22	65.06±24.31		Only in GL
23	94.52±5.52	146.40±48.64	0.3489
24	169.48±15.97	135.33±1.23	0.1000

Table 3.3. continued

	Peak Area		*P* Value
Peak number	CH-GL	CH-OPT	
25	122.77±11.43	44.82±12.74	0.0104
26	269.97±15.28	133.10±20.46	0.0058
27	64.50±2.05	214.10±18.59	0.0013
28	241.70±28.45		Only in GL
29	222.170±21.61		Only in GL
30	148.90±24.22		Only in GL
31	32.61±1.04	73.3±19.71	0.1082
32	175.52±11.16	257.28±10.15	0.0056
33	272.03±48.4	520.27±29.15	0.0118
34	137.01±2.22	213.32±12.05	0.0165
35	107.89±46.52		Only in GL
36	160.48±25.24		Only in GL
37	307.15±50.69	240.1±25.30	0.3975
38	235.77±14.44	626.63±14.92	0.0000
39	119.20±9.2	264.37±9.76	0.0021
40	391.78±30.7		Only in GL
41	163.48±22.62	237.82±30.44	0.1215
42	186.67±12.09	796.75±79.45	0.0022
43	205.80±4.6		Only in GL
44		554.05±180.15	Only in GR
45	270.60±35.32		Only in GL
46	195.33±6.68		Only in GL
47	1290.58±125.64		Only in GL
48	298.40±154.5	1090.83±74.26	0.0132
49	289.20±186.72	276.77±34.63	0.9509
50	212.25±8.51		Only in GL
51		169.88±54.88	Only in GR

3.4.5 Identification and quantification of AAs using LC-MS

For each CH treatment, 19 AAs were detected and quantified. No significant differences for the content of individual AAs were noted in the digesta between CH-GL and CH-OPT, as measured by LC-MS (**Table 4**). The sum of key collagen precursors (alanine, glycine and proline) was calculated and compared between CH-GL and CH-OPT; no significant differences in AA content were found (**Fig. 4**).

Table 3.4. AA content (µg/mL) after in vitro digestion of CH-GL and CH-OPT (n=3/treatment) as assessed by LC-MS. Values are expressed as mean ± SEM. A t-test was completed, and differences were considered significant if $p < 0.05$; no differences between treatments among all AA were found.

Amino Acid	CH-GL	CH-OPT
Alanine	111.2208±15.0327	108.7583±33.5617
Arginine	241.3068±5.579	256.0998±18.5932
Asparagine	62.5012±11.335	62.8609±21.9216
Glutamic Acid	66.6557±15.0764	80.1583±41.9639
Glutamine	604.4817±100.9561	371.8237±24.812
Glycine	213.2236±55.1827	99.447±33.2505
Histidine	53.6139±4.9257	57.9085±13.6274
Hydroxyproline	2.4438±0.4474	3.3153±2.3666
Isoleucine	37.1382±10.6105	23.8331±6.2949
Leucine	105.1608±29.9644	82.9924±22.6337
Lysine	85.5931±30.2977	161.6047±122.9828
Methionine	25.9292±6.5025	17.2651±4.2559
Phenylalanine	129.1348±40.9681	129.0537±37.2171
Proline	10.8636±2.2861	12.6146±1.8895
Serine	44.2141±6.4473	42.4004±10.9691
Threonine	136.722±29.9011	98.4888±30.3788
Tryptophan	10.3131±3.1744	16.9088±7.1777
Tyrosine	23.2444±6.7786	33.6753±9.2143
Valine	50.7051±13.2648	28.6092±5.0246

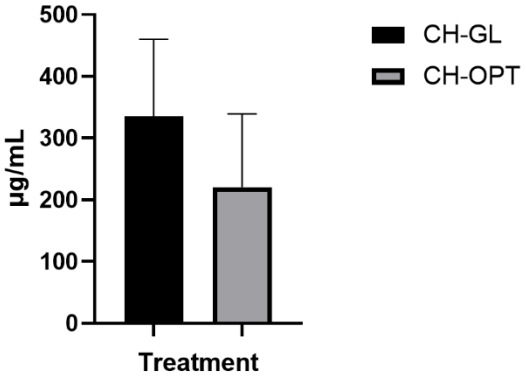

Figure 3.4. Collagen Linked AAs. Sum of collagen-linked AA content of CH-GL and CH-OPT after upper intestinal digestion. Values are expressed as mean ± SEM in µg/mL. A t-test was completed and the difference considered significant if $p < 0.05$; no significant difference was found between treatments.

Amino acid analysis has often included derivatization, followed by analysis using HPLC, GC-MS or LC-MS methods. Derivatization can increase costs, sample preparation time, and experimental error. In our study, only a simple filtration step is required before diluting and injecting, rendering this method rapid with less room for error. Other methods of AA analysis include NMR, which has been used to quantify AAs from blood samples after CH treatment (Skov et al., 2019); however, as mentioned earlier, these methods can be difficult to adapt for digesta samples. As AA analysis using HILIC, often coupled to LC-MS, has become a well-established method of detection and quantification, this method was readily adaptable for assessment of the AAs in SI digesta. Initial attempts by our group to detect and quantify AAs from SI digesta using C18 columns resulted in chromatograms showing poor peak shape, even after method optimization (See **Fig. S3** for example chromatogram). Previous work using HILIC-MS for detecting AAs from broth culture utilized only a few sample preparation steps whereby the samples were collected, centrifuged, filtered (0.2 µm), and then diluted before direct injection into the LC-MS (Bellvert et al., 2018). Accordingly, the HILIC-Z column was chosen to measure AAs from the SI digesta and our initial HILIC-MS method development to assess AA from SI digesta was carried out without additional sample preparation steps. Overall, our developed HILIC-MS approach demonstrated AA detection with optimal peak shapes that were readily obtained requiring minimal method optimization without derivatization.

It is important to note that due to the complex nature of SI digesta, dynamic range. Thus, method optimization including desalting procedures may be necessary depending on the complexity of the sample (Flick, Cassou, Chang, & Williams, 2012; Jehmlich et al., 2014). The presence of salts, such as sodium chloride, found in digesta fluid and buffers, may affect ionization efficiency and so reduce the quality of the MS data. Sample preparation of biological fluids for LC-MS analysis using available techniques for removing interfering compounds and salts is a critical step. Devices for peptide purification (i.e., µC18 ZipTip® tips, C18 ZipTip® tips, TopTip C-18 tips, OASIS® HLB µElution microplates) allow for a relatively easy desalting to eliminate low MW contaminates and so produce reliable and reproducible LC-MS data (Jehmlich et al., 2014). Alternate methods, such as solution additives, can be also used to lower sodium ion interference with protein and peptide analysis, as desalting procedures may sometimes adversely affect the structure of molecules of interest and their respective binding affinity (Flick et al., 2012). For example, solution additives such as ammonium bromide and ammonium iodide have been used in MS analyses of samples containing 1 mM NaCl to increase the relative abundances of ubiquitin by 72 and 56, respectively as compared to untreated samples (Flick et al., 2012). A decrease in sodium ion adduction using solution additives containing anions with a low proton affinity was also shown to improve signal abundance (Flick et al., 2012). Further investigations towards the use of desalting devices and solution additives to control for interfering and harmful salts found in SI digesta could be warranted to avoid continuous damage to the MS detector from repeated analyses. Overall, future work is needed to adapt LC-MS methods to assess for the bioavailability of AAs after CH consumption to gain further insights into the breakdown of BAPs into AA components, and their physiological impact. Such studies could involve the use of in vitro models of digestion coupled to human intestinal cell cultures to determine intestinal transport (Grootaert et al., 2017).

3.5 Conclusion

This work has provided a rapid, simple, and cost effective CZE method for the qualitative and quantitative assessment of BAPs after upper intestinal CH digestion. Simultaneous analysis for AA release after simulated digestion of CHs was also completed using the same simulated GI fluid, without derivatization, via use of a HILIC column. A comparison of two bovine sourced CHs showed qualitative and quantitative differences in peptide content, most likely due to differences in processing and CH preparation methods; however, no differences in AA profiles after digestion

were observed. Further research is needed to evaluate the clinical and biological significance of the differences in BAP profiles following digestion, which should also consider evaluation of the bioavailability of the BAPs.

3.6 Funding

This work was supported by a MITACS Accelerate Program PhD studentship (IT10556) collaboration between McGill University and Genacol Canada Corporation and the Collaborative Research Development Grant Program from the Natural Sciences and Engineering Council of Canada to S.K. (535744-18).

3.7 Acknowledgments

We would like to acknowledge the Drug Discovery Platform at the Research Institute of the McGill University Health Centre (RI-MUHC) for their support in performing the LC-MS work. We also wish to thank Patrick Sabourin from Technopro (www.technopro-labo.com) for support in the CE operation.

3.8 Supplementary data

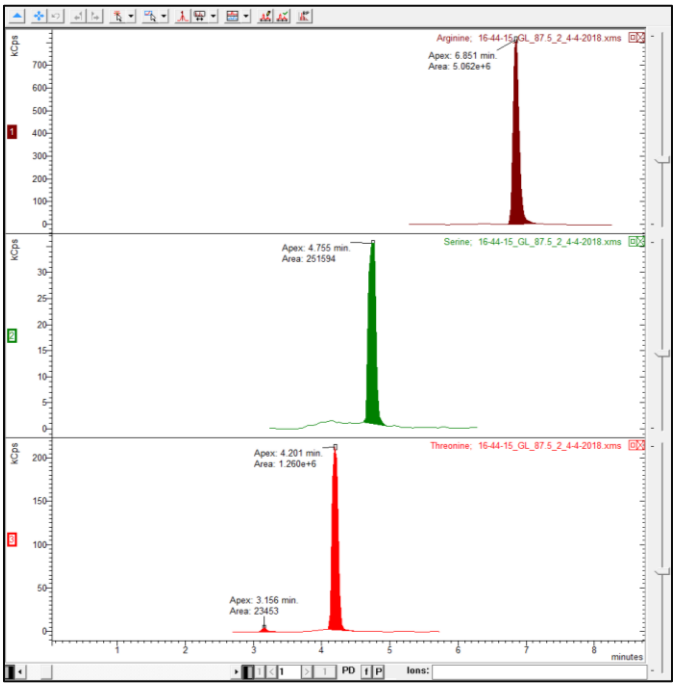

Figure S3.1. Example chromatographs of three amino acids (arginine, serine and threonine) obtained in positive mode on a triple quadrupole MS system coupled with an UPLC pump and equipped with a hydrophilic interaction chromatography column, Agilent Infinity Lab Poroshell 120 HILIC-Z.

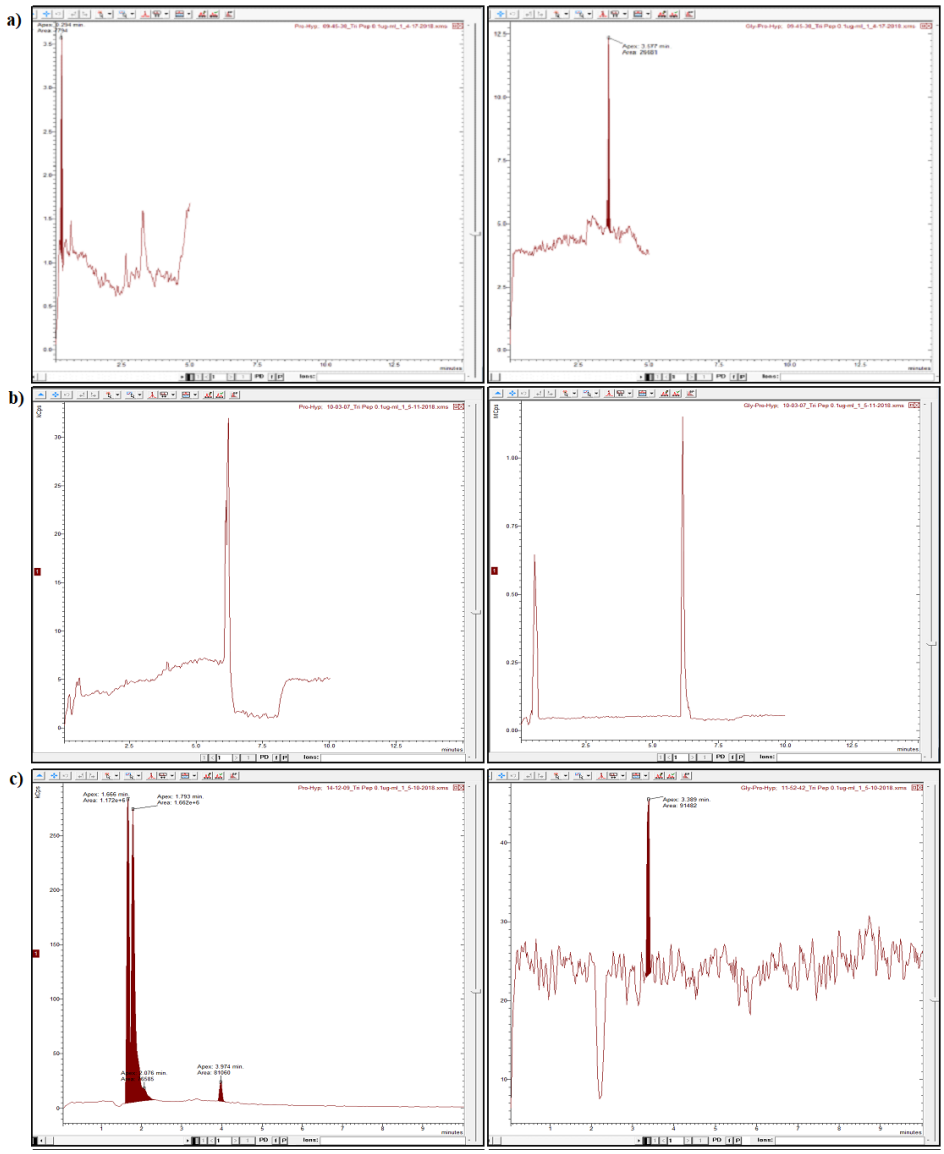

Figure S3.2. Example LC-MS chromatographs of Pro-Hyp (left) and Gly-Pro-Hyp (right) using the columns InfinityLab Poroshell 120 Hilic Z, Zorbax Eclipse Plus C18, Ace C18 PFP, Zorbax SB-C8, Synergi™ 4 µm Fusion-RP. After initial optimization attempts, columns were rejected due to unacceptable signal-to-noise ratio, peak shape, large injections peaks, and spilt peaks for either peptide. Further method development would have been possible although costly, time consuming, and without necessarily obtaining one method which would be able to detect and measure all peptides of interest.

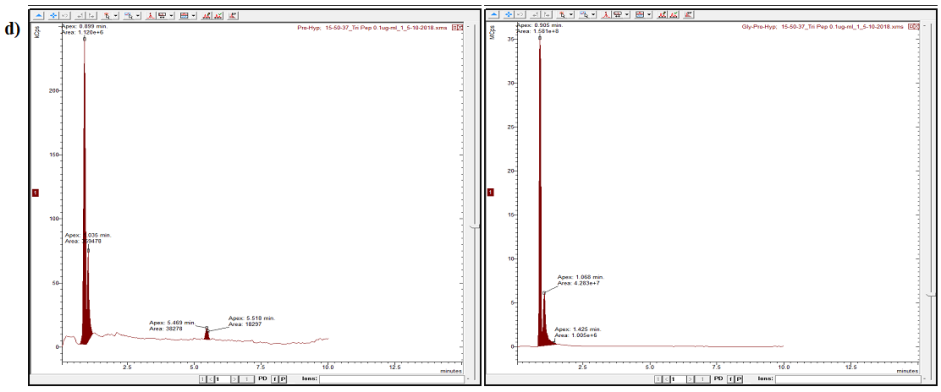

Figure S3.2. continued Example LC-MS chromatographs of Pro-Hyp (left) and Gly-Pro-Hyp (right) using the columns InfinityLab Poroshell 120 Hilic Z, Zorbax Eclipse Plus C18, Ace C18 PFP, Zorbax SB-C8, Synergi™ 4 µm Fusion-RP. After initial optimization attempts, columns were rejected due to unacceptable signal-to-noise ratio, peak shape, large injections peaks, and spilt peaks for either peptide. Further method development would have been possible although costly, time consuming, and without necessarily obtaining one method which would be able to detect and measure all peptides of interest.

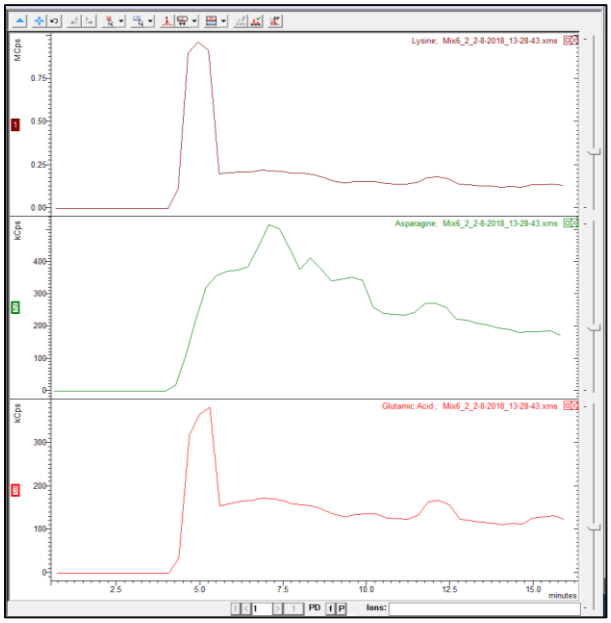

Figure S3.3 Example chromatographs of three amino acids (lysine, asparagine and glutamic acid) obtained in positive mode on a triple quadrupole MS system coupled with an UPLC pump and equipped with an Ace C18 PFP column, after multiple optimization trials.

3.9 References

Alemán, A., Gómez-Guillén, M. C., & Montero, P. (2013). Identification of ace-inhibitory peptides from squid skin collagen after in vitro gastrointestinal digestion. *Food Research International, 54*(1), 790-795. https://doi.org/10.1016/j.foodres.2013.08.027.

Amigo, L., & Hernández-Ledesma, B. (2020). Current evidence on the bioavailability of food bioactive peptides. Molecules, 25(19), 4479.

Bellvert, F., Barbier, H.K., Galy, O., Amoyal, X., Francois, J-M., Malbert, Y., . . . Bivens, A. (2018). Monitoring of 20 amino acids and other key compounds in fermentation processes. Retrieved from https://www.agilent.com/cs/library/applications/application-amino-acids-hilic-5991-9301en-agilent.pdf Accessed August 4, 2021

Bernardo, M. L. R., & Azarcon Jr., A.C. (2012). A randomized controlled trial on the effects of oral collagen treatment on the medial knee joint space and functional outcome among veterans medical center patients diagnosed with osteoarthritis of the knee. *Philippine Academy of Rehabilitation Medicine Processings 4*, 1-8.

Bruyère, O., Zegels, B., Leonori, L., Rabenda, V., Janssen, A., Bourges, C., & Reginster, J. Y. (2012). Effect of collagen hydrolysate in articular pain: A 6-month randomized, double-blind, placebo controlled study. *Complementary Therapies in Medicine, 20*(3), 124-130. https://doi.org/10.1016/j.ctim.2011.12.007

Cao, X., Gibbs, S. T., Fang, L., Miller, H. A., Landowski, C. P., Shin, H. C., . . . Sun, D. (2006). Why is it challenging to predict intestinal drug absorption and oral bioavailability in human using rat model. *Pharmaceutical Research, 23*(8), 1675-1686. https://doi.org/10.1007/s11095-006-9041-2

Dolan, J. W. (2012). When should an internal standard be used? *LC-GC Europe*, *25*(6), p316-322.

Emwas, A.-H., Saccenti, E., Gao, X., McKay, R. T., Dos Santos, V. A. P. M., Roy, R., & Wishart, D. S. (2018). Recommended strategies for spectral processing and post-processing of 1D ^{1}H-NMR data of biofluids with a particular focus on urine. *Metabolomics, 14*(3), 31. doi: 10.1007/s11306-018-1321-4

Feliciano, D. D. S., Gonzalex-Suarez, C. B., Bernardo-Bueno, M. M., Malvar, A. K. G., Cua, R. C. A., Tan-Sales, B. G. K., . . . Reyes, F. D. L. (2017). Effect of collagen hydrolysate as adjuvant treatment to exercise for knee osteoarthiritis. *Philippine Academy of Rehabilitation Medicine, 9*(1), 4-15.

Flick, T. G., Cassou, C. A., Chang, T. M., & Williams, E. R. (2012). Solution Additives That Desalt Protein Ions in Native Mass Spectrometry. *Analytical Chemistry, 84*(17), 7511-7517. doi:10.1021/ac301629s

Gibbons, S. E., Wang, C., & Ma, Y. (2011). Determination of pharmaceutical and personal care products in wastewater by capillary electrophoresis with UV detection. *Talanta, 84*(4), 1163-1168. doi: https://doi.org/10.1016/j.talanta.2011.03.030

Gómez-Guillén, M. C., Giménez, B., López-Caballero, M. E., & Montero, M. P. (2011). Functional and bioactive properties of collagen and gelatin from alternative sources: A review. *Food Hydrocolloids, 25*(8), 1813-1827. https://doi.org/10.1016/j.foodhyd.2011.02.007.

Grootaert, C., Jacobs, G., Matthijs, B., Pitart, J., Baggerman, G., Possemiers, S., . . . Voorspoels, S. (2017). Quantification of egg ovalbumin hydrolysate-derived anti-hypertensive peptides in an in vitro model combining luminal digestion with intestinal Caco-2 cell transport. *Food Research International: Part 1, 99*(Part 1), 531-541. doi: 10.1016/j.foodres.2017.06.002

Hamrníková, I., Mikšík, I., Deyl, Z., & Kašicka, V. (1999). Binding of proline- and hydroxyproline-containing peptides and proteins to the capillary wall. *Journal of Chromatography A, 838*(1), 167-177. doi: 10.1016/S0021-9673(99)00160-0

Harris, D. C. (2009). *Exploring chemical analysis* (4th ed.). New York: W.H. Freeman and Company (Chapter 5).

Heiger, D., Grimm, R., & Herold, M. (2008). Peptide mapping and analysis using capillary electrophoresis. Retrieved from https://www.agilent.com/cs/library/applications/5989-9807EN.pdf Accessed August 4, 2021

Hsiao, Y. M., Ko, J. L., & Lo, C. C. (2001). Determination of tetracycline and streptomycin in mixed fungicide products by capillary zone electrophoresis. *Journal of Agricultural and Food Chemistry, 49*(4), 1669-1674. https://doi.org/10.1021/jf0009192

Iskandar, M., Lands, L., Sabally, K., Azadi, B., Meehan, B., Mawji, N., . . . Kubow, S. (2015). High hydrostatic pressure pretreatment of whey protein isolates improves their digestibility and antioxidant capacity. *Foods, 4*(2), 184. https://doi.org/10.3390/foods4020184

Janini, G. M., Metral, C. J., & Issaq, H. J. (2001). Peptide mapping by capillary zone electrophoresis: How close is theoretical simulation to experimental determination. *Journal of Chromatography A, 924*(1), 291-306. doi: https://doi.org/10.1016/S0021-9673(01)00919-0

Jehmlich, N., Golatowski, C., Murr, A., Salazar, G., Dhople, V. M., Hammer, E., & Völker, U. (2014). Comparative Evaluation of Peptide Desalting Methods for Salivary Proteome Analysis. *Clinica Chimica Acta, 434*, 16-20. doi:10.1016/j.cca.2014.04.003

Kennedy, A. & Bivens, A. (2017). Methods for the analysis of underivatized amino acids by LC-MS. Retrieved from https://www.agilent.com/cs/library/applications/5991-8582EN_HILIC_Underivatized_Amino_Acid_application.pdf Accessed August 4, 2021

Larder, C. E., Iskandar, M. M., Sabally, K., & Kubow, S. (2018, October). *Capillary electrophoresis: A fast, cost effective and efficient method replacement for LC-MS when identifying and quantifying small peptides from simulated gastrointestinal digestion of collagen hydrolysate.* Poster presentation at the BenefiQ Conference Quebec City Convention Centre, QC, Canada. doi: 10.13140/RG.2.2.14188.90249

Larder, C. E., Iskandar, M. M., & Kubow, S. (2021). Gastrointestinal Digestion Model Assessment of Peptide Diversity and Microbial Fermentation Products of Collagen Hydrolysates. *Nutrients*, *13*(8), 2720. doi:https://doi.org/10.3390/nu13082720

León-López, A., Morales-Peñaloza, A., Martínez-Juárez, V. M., Vargas-Torres, A., Zeugolis, D. I., & Aguirre-Álvarez, G. (2019). Hydrolyzed collagen-sources and applications. *Molecules, 24*(22). doi: 10.3390/molecules24224031

Li, Y., Xiao, W., Luo, W., Zeng, C., Deng, Z., Ren, W., . . . Lei, G. (2016). Alterations of amino acid metabolism in osteoarthritis: Its implications for nutrition and health. *Amino Acids, 48*(4), 907-914. https://doi.org/10.1007/s00726-015-2168-x

Mikšík, I., Sedláková, P., Mikulíková, K., & Eckhardt, A. (2006). Capillary electromigration methods for the study of collagen. *Journal of Chromatography B, 841*(1-2), 3-13. doi: 10.1016/j.jchromb.2006.02.043

Mikulíková, K., Eckhardt, A., Pataridis, S., Mikšík, I., & Paris, F. (2007). Study of posttranslational non-enzymatic modifications of collagen using capillary electrophoresis/mass spectrometry and high performance liquid chromatography/mass spectrometry. *Journal of Chromatography A, 1155*(2), 125-133. doi: 10.1016/j.chroma.2007.01.020

Miranda, L., Deusser, H., & Evers, D. (2013). The impact of in vitro digestion on bioaccessibility of polyphenols from potatoes and sweet potatoes and their influence on iron absorption by human intestinal cells. *Food & Function, 4*(11), 1595-1601. https://doi.org/10.1039/c3fo60194c

Musther, H., Liu, B., Rostami Hodjegan, A., Olivares-Morales, A., & Hatley, O. J. D. (2014). Animal versus human oral drug bioavailability: Do they correlate? *European Journal of Pharmaceutical Sciences, 57*(1), 280-291. https://doi.org/10.1016/j.ejps.2013.08.018

Osawa, Y., Mizushige, T., Jinno, S., Sugihara, F., Inoue, N., Tanaka, H., & Kabuyama, Y. (2018). Absorption and metabolism of orally administered collagen hydrolysates evaluated by the vascularly perfused rat intestine and liver in situ. *Biomedical Research, 39*(1), 1-11. https://doi.org/10.2220/biomedres.39.1

*Pal, G. K., & Suresh, P. V. (2016). Sustainable valorisation of seafood by-products: Recovery of collagen and development of collagen-based novel functional food ingredients. *Innovative Food Science & Emerging Technologies, 37*, 201-215. doi: https://doi.org/10.1016/j.ifset.2016.03.015 **This review provides a clear overview of collagen-based products, their sources from seafood, and details on extraction, processing, and purification methods. The bioactivity of collagen hydrolysates and peptides is extensively explored, with specific emphasis with regards to human health and supplementation.**

Popa, T. V., Mant, C. T., & Hodges, R. S. (2003). Capillary electrophoresis of synthetic peptide standards varying in charge and hydrophobicity. *Electrophoresis, 24*(24), 4197-4208. doi: 10.1002/elps.200305576

*Prinsen, H. C. M. T., Schiebergen-Bronkhorst, B. G. M., Roeleveld, M. W., Jans, J. J. M., de Sain-van der Velden, M. G. M., Visser, G., . . . Verhoeven-Duif, N. M. (2016). Rapid quantification of underivatized amino acids in plasma by hydrophilic interaction liquid chromatography (HILIC) coupled with tandem mass-spectrometry. *Journal of Inherited Metabolic Disease, 39*(5), 651-660. doi: 10.1007/s10545-016-9935-z **This article discusses the use of a hydrophilic interaction liquid chromatography (HILIC) column coupled with tandem mass-spectrometry to measure amino acids without the need for derivatization. Amino acid measurements provide an indicator of health, where inborn errors of metabolism can be easily identified in patients using a rapid and sensitive method, compared to current methods often using HPLC, GC-MS and LC-MS/MS not equipped with a HILIC column.**

Punt, A., Peijnenburg, A., Hoogenboom, R., & Bouwmeester, H. (2017). Non-animal approaches for toxicokinetics in risk evaluations of food chemicals. *Alternatives to Animal Experimentation, 34*(4), 501-514. https://doi.org/10.14573/altex.1702211

Scriba, G. K. E. (2016). Separation of Peptides by Capillary Electrophoresis. In P. Schmitt-Kopplin (Ed.), *Capillary Electrophoresis : Methods and Protocols Methods* in Molecular Biology (2nd ed. pp.365-391). New York: Humana Press.

Shigemura, Y., Suzuki, A., Kurokawa, M., Sato, Y., & Sato, K. (2018). Changes in composition and content of food-derived peptide in human blood after daily ingestion of collagen hydrolysate for 4 weeks. *Journal of the Science of Food and Agriculture, 98*(5), 1944-1950. doi: 10.1002/jsfa.8677

Simons, V. S., Lochnit, G., Wilhelm, J., Ishaque, B., Rickert, M., & Steinmeyer, J. (2018). Comparative Analysis of Peptide Composition and Bioactivity of Different Collagen Hydrolysate Batches on Human Osteoarthritic Synoviocytes. *Scientific Reports, 8*(1), 17733. doi:10.1038/s41598-018-36046-3

*Skov, K., Oxfeldt, M., Thøgersen, R., Hansen, M., & Bertram, H. C. (2019). Enzymatic hydrolysis of a collagen hydrolysate enhances postprandial absorption rate-A randomized controlled trial. *Nutrients, 11*(5). doi: 10.3390/nu11051064 **This clinical study provides key information regarding the increased bioavailability of amino acids from hydrolysed vs non hydrolyzed collagen. AAs measured included Pro, Hyp and Gly.**

Sontakke, S. B., Jung, J. H., Piao, Z., & Chung, H. J. (2016). Orally available collagen tripeptide: Enzymatic stability, intestinal permeability, and absorption of gly-pro-hyp and pro-hyp. *Journal of Agricultural and Food Chemistry, 64*(38), 7127-7133. doi: 10.1021/acs.jafc.6b02955

Sun, L., Chang, W., Ma, Q., & Zhuang, Y. (2016). Purification of antioxidant peptides by high resolution mass spectrometry from simulated gastrointestinal digestion hydrolysates of Alaska pollock (*Theragra chalcogramma)* skin collagen. *Marine Drugs, 14*(10). https://doi.org/10.3390/md14100186

Sun, L., Zhu, G., Yan, X., Zhang, Z., Wojcik, R., Champion, M. M., & Dovichi, N. J. (2016). Capillary zone electrophoresis for bottom-up analysis of complex proteomes. *Proteomics, 16*(2), 188-196. doi: 10.1002/pmic.201500339

Taga, Y., Kusubata, M., Ogawa-Goto, K., & Hattori, S. (2016). Efficient absorption of x-hydroxyproline (hyp)-gly after oral administration of a novel gelatin hydrolysate prepared using ginger protease. *Journal of Agricultural and Food Chemistry, 64*(14), 2962-2970. doi: 10.1021/acs.jafc.6b00609

Udenigwe, C. C., & Aluko, R. E. (2012). Food protein-derived bioactive peptides: Production, processing, and potential health benefits. *Journal of Food Science, 77*(1), 11-24. doi: 10.1111/j.1750-3841.2011.02455.x

Verpillot, R., Otto, M., Klafki, H., & Taverna, M. (2008). Simultaneous analysis by capillary electrophoresis of five amyloid peptides as potential biomarkers of Alzheimer's disease. *Journal of Chromatography A, 1214*(1-2), 157-164. doi: 10.1016/j.chroma.2008.10.051

Wang, L., Wang, Q., Liang, Q., He, Y., Wang, Z., He, S., . . . Ma, H. (2015). Determination of bioavailability and identification of collagen peptide in blood after oral ingestion of gelatin. *Journal of the Science of Food and Agriculture, 95*(13), 2712-2717. https://doi.org/10.1002/jsfa.7008

Wang, L., Wang, Q., Qian, J., Liang, Q., Wang, Z., Xu, J., . . . Ma, H. (2015). Bioavailability and bioavailable forms of collagen after oral administration to rats. *Journal of Agricultural and Food Chemistry, 63*(14), 3752-3756. doi: 10.1021/jf5057502

Wang, W., Wu, Z., Lin, G., Hu, S., Wang, B., Dai, Z., & Wu, G. (2014). Glycine stimulates protein synthesis and inhibits oxidative stress in pig small intestinal epithelial cells. *The Journal of Nutrition, 144*(10), 1540-1548.

Yazaki, M., Ito, Y., Yamada, M., Goulas, S., Teramoto, S., Nakaya, M. A., . . . Yamaguchi, K. (2017). Oral ingestion of collagen hydrolysate leads to the transportation of highly concentrated gly-pro-hyp and its hydrolyzed form of pro-hyp into the bloodstream and skin. *Journal of Agricultural and Food Chemistry, 65*(11), 2315-2322. https://doi.org/10.1021/acs.jafc.6b05679

* Zanaboni, G., Grimm, R., Dyne, K. M., Rossi, A., Cetta, G., & Iadarola, P. (1996). Use of capillary zone electrophoresis for analysis of imidodipeptides in urine of prolidase-deficient patients. *Journal of Chromatography B: Biomedical Sciences and Applications, 683*(1), 97-107. doi: 10.1016/0378-4347(95)00583-8 **This article discusses the many benefits of using a novel capillary zone electrophoresis to measure X-Pro and X-Hyp peptides from urine samples. Method development was rapid, straightforward, reliable, and minimal sample volumes and preparation steps were necessary for analysis. This article clearly demonstrates that capillary electrophoresis is a relevant analytical choice for the analysis of small peptides from complex biological fluids.**

*Zhang, N., Zhu, Q., & Gong, M. (2017). Rapid determination of free prolyl dipeptides and 4-hydroxyproline in urine using flow-gated capillary electrophoresis. *Analytical and Bioanalytical Chemistry, 409*(30), 7077-7085. doi: 10.1007/s00216-017-0666-2 **This article discusses a novel method developed to measure free prolyl compounds in unhydrolyzed urine samples using flow-gated capillary electrophoresis. Unhydrolyzed prolyl hydroxyproline (Pro-Hyp) and (Hyp) have been suggested to act as biomarkers for disease. Measuring these compounds from complex biological fluids could help define healthy vs unhealthy profiles.**

CONNECTING STATEMENT 2

As described in Chapter 3, a novel capillary electrophoresis method was developed that showed promising results in providing a simple, cost effective and reliable measurement of BAPs after simulated in vitro digestion of CHs. In this subsequent study, a co-culture of intestinal (HIEC-6) and hepatic (HepG2) cells was developed. This model was established to simulate the absorption and subsequent hepatic action of the liver that CH-derived BAPs must undergo before being released into the systemic circulation. Only after being released into the systemic circulation, can CH-derived BAPs exert their potential health promoting properties. Digesta from Study 1 (Chapter 3) were applied to the co-culture and the transport, first pass effects, and bioavailability of the BAPs (Gly-Pro, Hyp-Gly, Ala-Hyp, Pro-Hyp, Gly-Pro-Hyp) were determined using an adapted capillary electrophoresis method developed in Study 1 (Chapter 3). This cell culture model, utilizing HIEC cells, was employed to more accuracy predict in vivo peptide transport, as previous in vitro studies have typically used only Caco-2 cells, which under-express a key peptide transporter, PepT1. In addition, the hepatic metabolic potential is also accounted for in this co-culture model. Chapter 4 has been published in Current Issues in Molecular Biology: Larder, C.E.; Iskandar, M.M.; Kubow, S. *Assessment of Bioavailability after In Vitro Digestion and First Pass Metabolism of Bioactive Peptides from Collagen Hydrolysates*. Curr. Issues Mol. Biol, 2021. **43** (3): p. 1592-1605. https://doi.org/10.3390/cimb43030113

CHAPTER 4: RESEARCH PAPER 2

Published: Current Issues in Molecular Biology, 2021; 43, 1592–1605

Assessment of Bioavailability after In Vitro Digestion and First Pass Metabolism of Bioactive Peptides from Collagen Hydrolysates

Affiliation:

Christina E. Larder, Michèle M. Iskandar, Stan Kubow *

School of Human Nutrition, McGill University, Ste-Anne-de-Bellevue, QC, Canada, H9X 3V9

* Corresponding author: stan.kubow@mcgill.ca; Tel.: +1-514-398-7754

4.1 Abstract

Collagen hydrolysates (CHs) are composed of bioactive peptides (BAPs), which possess health enhancing properties. There is a knowledge gap regarding the bioavailability of these BAPs that involves intestinal transport and hepatic first pass effects. A simulated gastrointestinal model was used to generate digesta from two CHs (CH-GL and CH-OPT), which were applied to a novel transwell co-culture of human intestinal epithelium cell line-6 (HIEC-6) and hepatic (HepG2) cells to simulate in vivo conditions of absorption and first pass metabolism. Peptide transport, hepatic first pass effects, and bioavailability were determined by measuring BAPs (Gly-Pro, Hyp-Gly, Ala-Hyp, Pro-Hyp, Gly-Pro-Hyp) using an innovative capillary electrophoresis method. All peptides were transported across the intestinal cell layer to varying degrees with both CHs; however, Gly-Pro-Hyp was transported only with CH-GL, but not CH-OPT. Notable hepatic production was observed for Ala-Hyp with both CH treatments, and for Pro-Hyp and Gly-Pro with CH-GL only. All peptides were bioavailable (>10%), except for Gly-Pro-Hyp after CH-OPT. Overall, a high degree of transport and hepatic first pass effects on CH-derived BAPs were observed. Further research is needed to explore the hepatic mechanisms related to the production of BAPs and the bifunctional effects of the bioavailable BAPs noted in this study.

Keywords: bioavailability; digestion; bioactive peptides; first pass metabolism; collagen hydrolysate; cell culture; capillary electrophoresis; human intestinal epithelial cells (HIEC-6); permeability

4.2 Introduction

Collagen hydrolysates (CHs) have been shown to provide multiple health benefits, which have been primarily attributed to their bioactive peptide (BAP) content [1–3]. These BAPs can be found in the hydrolysate products, although an increase in the diversity and content of peptides can result from gastrointestinal (GI) digestion [4,5]. The BAPs released after the digestion of collagen products, such as Pro-Hyp and Gly-Pro-Hyp, can possess multiple health properties, which include antimicrobial and antihypertensive effects, regulating inflammation, reducing pain associated with osteoarthritis, promoting bone synthesis, stimulating wound healing, as well as antioxidant properties and angiotensin-I-converting enzyme inhibitory effects [3,4,6,7].

After digestion, BAPs undergo first pass metabolism, a process defined by hepatic metabolism of compounds following their absorption at the level of the intestinal epithelium that mediates entry into the systemic circulation [8,9]. The bioactivity of BAPs depends heavily on their ability to reach the general circulation intact after oral ingestion, otherwise called bioavailability [9]. Clinical studies have consistently shown that peptides generated from orally ingested collagen precursors, such as gelatin, or collagen hydrolysates, can reach the systemic circulation and be excreted in the urine [4,6,10–12]. Importantly, the clinical efficacy of CHs has been demonstrated in multiple trials showing reduction of joint discomfort in athletes with functional knee problems and decreased joint pain in osteoarthritis patients [1,3,13]. The BAPs in the bloodstream identified after oral ingestion of CHs and CH precursors, such as gelatin, include Ala-Hyp, Pro-Hyp and Gly-Pro-Hyp [4,6,10,14].

The assessment of peptide bioavailability using human trials remains costly, lengthy and with limited experimental options for sampling due to ethical restrictions. Instead, animal studies have been used to estimate the bioavailability of BAPs from collagen and collagen precursor products [14–17]; however, predictions of bio-absorbability do not always align with human clinical data due to species differences in intestinal permeability and metabolic activity [2,18]. Bioavailability studies of food components and pharmaceuticals using animal models have demonstrated poor correlations between rats and humans ($r^2 = 0.18$) as well as dogs and humans ($r^2 = 0.19$) [18]. Due to such species differences in intestinal permeability and metabolic activity, intestinal cell culture

models, rather than animal models, are often used to assess the intestinal transport of food-derived BAPs [2].

Caco-2 cells, a human colon carcinoma cell line, has been used regularly to assess for small intestinal (SI) permeability [2]. Previous work by Feng et al. (2017) [19] used the Caco-2 model to estimate the transepithelial peptide transport efficiency of bovine CHs. The bioavailability of the CHs, as determined by amino acid (AA) transport, ranged between ~15 and 23%, depending on the hydrolysis method used to generate the CH. Recent work by Song et al. (2020) assessed the bioavailability of BAPs from silver carp skin hydrolysate using in vitro digestion and Caco-2 cells [7]. They found that, using high-performance liquid chromatography–electrospray ionization tandem mass spectrometry (HPLC-ESI-MS), the transport (%) of Hyp-Gly, Hyp-Gly-Glu and Pro-Gly-Glu-Hyp-Gly was 22.63 ± 5.19, 11.15 ± 0.52 and 18.35 ± 1.20, respectively.

Although in vitro intestinal permeability measures have typically used Caco-2 cells, peptide bioavailability assessments using this cell culture model are not ideal due to the under-expression of peptide transporters such as peptide transporter 1 (PepT1) in these tumorigenic cells. Hence, depending on the compound being assessed, permeability results using Caco-2 cells do not always correlate with human intestinal permeability [18,20]. PepT1, otherwise known as SLC15A1, is the main transporter for di- and tri-peptides, which are predominant in CHs and have been indicated to be primarily responsible for the CH-mediated bioactivities [7,10,15]. To overcome the limited PepT1 expression in Caco-2 cells, a non-tumorigenic human small intestinal epithelial cell (HIEC) line can be used. HIEC cells have been shown to be a superior alternative to Caco-2 cells for predicting transporter-mediated absorption of compounds in humans when taken orally [21,22]. The HIEC cell model also more accurately represents the physiological in vivo conditions of the SI [22–24]. To the best of our knowledge, no study has investigated the transport of CH-derived BAPs using HIEC cells. One study investigating salmon protein hydrolysate peptides and their regulation of oxidative protective genes was investigated using HIEC cells; however, no analysis of peptide bioavailability was completed [25].

Methods to accurately quantify di- and tri-peptides to determine their bioavailability have been lacking. Using plasma samples from clinical studies, quantification methods of BAP bioavailability

are often calculated using an indirect calculation of Hyp-containing peptides and/or AAs [4,10,14]. Cell culture models also suffer from such limitations in terms of peptide analysis. Feng et al. (2017) assessed the bioavailability of bovine CHs involving Caco-2 cells using an indirect calculation based on the total AAs transported [19] but peptides were not identified or measured. In the present study, our novel method for targeted BAP quantification using capillary electrophoresis (CE) [26,27] was adapted for cell culture media to determine peptide content.

Another limitation to previous in vitro studies investigating BAP bioavailability has been the sole use of intestinal cell cultures without consideration of the subsequent hepatic first pass effects on the intestinally transported BAPs. Some reports have used liver cell culture models, often using human hepatocellular carcinoma (HepG2) cell line, to assess the hepatic metabolism of xenobiotics and drug transporters [8,28]. Previous work has also shown that Pro-Gly can increase PepT1 expression in HepG2 cells, although no assessment of the hepatic effects on Pro-Gly was investigated [29]. Previous studies from our laboratory have assessed the bioavailability of dietary components using a Caco-2/HepG2 co-culture model of first pass metabolism by applying digests from a human simulated gut digestion model [8]. Similar in vitro models have assessed the oral bioavailability of compounds, such as xenobiotics, and have shown very good correlations with in vivo data from humans and animal models [30,31]. In general, there is a major gap in the literature with respect to the study of the hepatic first pass effects on BAPs following their intestinal cell absorption.

In this study, a combination of in vitro gut digestion together with HIEC-6/HepG2-mediated transport and metabolism was used to investigate the bioavailability of BAPs generated after CH digestion. Direct quantification of BAP bioavailability was performed using CE. The aim of this study was to use this novel combination of techniques and cell lines to improve our understanding of the bioavailability and metabolism of CH-derived BAPs that have postulated health promoting properties.

4.3 Materials and methods

4.3.1 Peptide standards

Peptide standards Gly-Pro, Hyp-Gly, and Ala-Hyp were ordered and synthesized by CanPep Inc. (Montreal, QC, Canada). Peptides Gly-Pro-Hyp (4008512) and Pro-Hyp (4001630) were purchased

from Bachem (Hauptstrasse, Bubendorf, Switzerland). Peptides were 98% pure with peptide purification validation completed by HPLC and mass spectra analysis, provided by the suppliers.

4.3.2 Cells

HIEC-6 (ATCC® CRL-3266™) and HepG2 (ATCC® HB-8065™) cells were purchased from American Type Culture Collection (ATCC, Manassas, Virginia, USA). HIEC-6 cells were cultured using OptiMEM 1 Reduced Serum Medium (Thermo Fisher Scientific, Gibco No. 31985, Waltham, MA, USA) with 20 mM HEPES, 10 mM GlutaMAX (Thermo Fisher Scientific, Gibco No. 35050, Waltham, MA, USA), 10 ng/mL Epidermal Growth Factor, and 4% fetal bovine serum (FBS). HepG2 cells were grown using ATCC-formulated Eagle's Minimum Essential Medium (Thermo Fisher Scientific, Gibco No. 30-2003, Waltham, MA, USA), with 10% FBS. Cells were maintained at 37 °C with 90% relative humidity and 5% CO_2 in culture medium.

4.3.3 Treatments

Two bovine-sourced CH products were used in this study: Genacol Original Formula® (Blainville, QC, Canada) (CH-GL) and Selection (Uniprix, QC, Canada) (CH-OPT).

4.3.4 Simulated digestion

Simulated human digestion was completed to provide digests for first pass metabolism studies in cell culture (see Section 2.6). Upper intestinal digestion involving the stomach and SI was adapted from Alemán et al. (2013), Miranda et al. (2013) and Larder et al. (2021) [5,32,33]. Based on a previous clinical study using CH-GL [13] and previous in vitro digestion models [5], 1,200 mg of CHs were digested in reactor vessels placed in a water bath (Cole-Parmer Advantec, TBS181SA, Montreal, QC, CN) at 37°C, and mounted on a stir plate (Corning, hot plate laboratory stirrer PC351, Corning, NY, USA), where the pH was monitored and adjusted throughout digestion (Fisher Scientific, S90528, Waltham, MA, USA). A 4% w/w pepsin solution (Sigma-Aldrich, P7125, St. Louis, MO, USA) prepared in 0.1 M HCl was added, and the pH of the solution adjusted to 2. The solution was incubated for 30 min. Afterwards, a 4% w/w pancreatin solution (Sigma-Aldrich, P7545, St. Louis, MO, USA) was added. The pH was adjusted to 8 and the solution incubated for 2 h. To stop the enzymatic processes, the resulting digesta were rapidly cooled on ice and the pH increased to 10. Digesta were then frozen at −20 °C for temporary storage, until the digesta were filtered using a membrane filter with a molecular weight cut off (MWCO) of 10 kDa in a stirred Amicon

ultrafiltration membrane reactor at 4 °C and under nitrogen gas pressure of 40 psi [34]. The filtrates were freeze-dried at −50–−60 °C and 0.85 mBar (0.64 mm Hg) (Gamma 1–16 LSC, Christ, Osterode am Harz, Germany) and stored at −80 °C until used in cell culture. Three independent digestions were completed for each CH treatment.

4.3.5 3-(4,5-dimethylthiazol-2-yl)-2,5-diphenyl tetrazolium bromide (MTT) assay

HIEC-6 cells were seeded in a 24-well plate at a density of 1×10^5 cells/well and maintained as described above (Section 2.2). Once confluent, the 3-(4,5-dimethylthiazol-2-yl)-2,5-diphenyl tetrazolium bromide (MTT) assay was performed [35]. Cells were incubated for 3 h with a 0.5 mg/mL thiazolyl blue tetrazolium bromide (Sigma-Aldrich, M5655, St. Louis, MO, USA) solution made in phosphate buffer solution. Afterwards, a lysis solution (0.4 N HCl in 100% isopropanol) was added to dissolve the purple formazan crystals that were produced by viable and metabolically active cells. The absorbance was measured at 570 nm and cell viability expressed as survival (%) of untreated cells.

4.3.6 Co-culture

A HIEC-6/HepG2 cell co-culture system was used to determine the bioavailability of targeted BAPs from CHs after digestion (Figure 1). HIEC-6 cells and HepG2 were cultured separately but then later combined in a transwell system using polyester (PET) ThinCerts (Greiner Bio-One, Cat no. 662641, Monroe, NC, USA) and corresponding 24 multiwell cell culture plates (Greiner Bio-One, Cat no. 662160, Monroe, NC, USA). The co-culture methods were adapted from Sadeghi Ekbatan et al. (2018) and Takenaka et al. (2016) [8,22]. HIEC-6 cells were seeded onto ThinCerts at 1×10^5 cells/well. The medium was changed every 2 days and cells were grown for a total of 8–9 days. Transepithelial electrical resistance (TEER) was measured using a volt-ohmmeter to assess the integrity of the monolayer and experiments were conducted when the TEER reached 100 ohm/cm^2, which has been shown to be appropriate for HIEC-6 cells [22]. HepG2 cells were then added to the basolateral side of the transwell (1 million cells/mL). Preliminary studies in terms of cell viability were completed using MTT to assess for optimal peptide dose range (see Section 2.5). At time 0, the apical medium was replaced with media containing 2 mg/mL reconstituted freeze-dried (FD) CH digesta (either CH-GL and CH-OPT), or only media (blank). The co-culture and treatments were incubated for 2 h at 37 °C, 5% CO_2. After 2 h, the inserts containing HIEC-6 cells were removed, and the plates containing HepG2 cells were incubated for another 3 h. Samples were taken from the

apical and basolateral sides at times 0, 2 and 5 h, and microcentrifuged at 2000 rpm for 15 min. The supernatant was collected and used for subsequent peptide analysis (see Section 2.7). Three independent experiments assessing bioavailability were completed. Controls included inserts without seeded cells (TEER control) and seeded wells with no CHs treatment (only media; negative control).

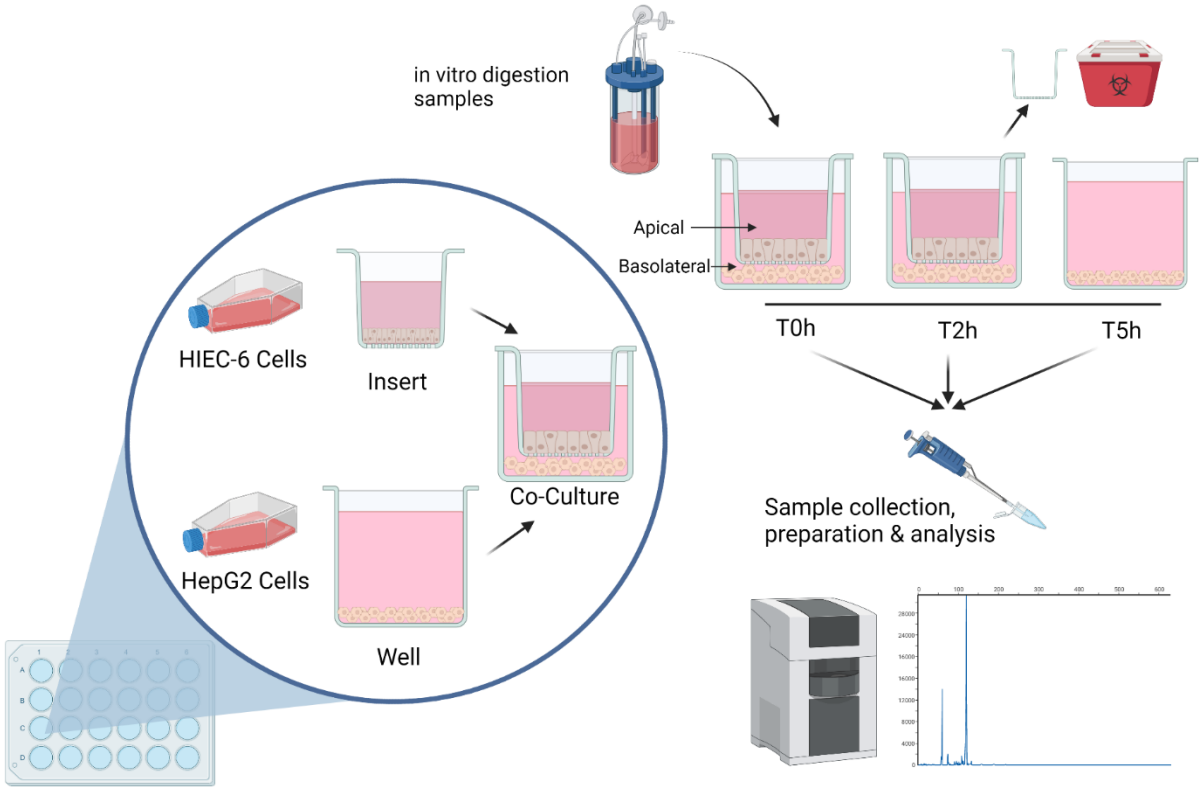

Figure 4.1. Assessment of first pass metabolism in cell culture. HIEC-6 and HepG2 cells were seeded in a 24-well transwell plate. Freeze-dried gastrointestinal digesta from a simulated digestion model were applied to the apical compartment of the co-culture and incubated for 2 h. The transwell insert was removed and the incubation continued for another 3 h. Subsamples from the apical and basolateral side were taken at times 0, 2 and 5 h, followed by peptide analysis using capillary electrophoresis. Figure created with BioRender.com

4.3.7 Targeted peptide quantification using capillary electrophoresis (CE)

Peptide analysis was completed using an adapted protocol from Larder et al. (2018) and Larder et al. (2021) (submitted) [26,27]. Samples were purified from cellular and protein debris by adapting the use of Amicon® Ultra-0.5 Centrifugal Filter Devices (Millipore, UFC501096, Burlington, Massachusetts, USA). Samples from cell culture were processed as per the manufacturer's instructions, however, the filtrate (comprising of peptides) was not discarded and instead used for analysis. A CE system (Capel 205M; Lumex Instruments, Fraserview Place, BC) was used for the targeted quantification of 5 peptides (Gly-Pro, Hyp-Gly, Ala-Hyp, Pro-Hyp, Gly-Pro-Hyp). The instrument was set for 20 °C and the separation capillary (Molex, 2000019, Lisle, Illinois, US) was similar to previous CE methods for collagen analysis [36]; 60 cm in total length, 53 cm effective length, and 75 µm inside diameter. Injections were completed using pressure (30 mbar for 10 s) at 0 kV and analysis was completed at 20 kV using 0 mbar for 1199 s at 205 nm. A 0.1 M phosphate buffer (pH 2.4) was used for rinsing and as running buffer. Filtered samples were diluted with running buffer before injection. Before sample injection, the capillary was rinsed with MilliQ water, 0.5 M NaOH and running buffer, each for 5 min. The electropherograms were processed to determine peak area using the software Elforun (Lumex Instruments Canada, Version 4.2.4, Mission, BC, Canada). Quantification of each peptide, based on peak area, was performed using external standards and corresponding calibration curves, where the linearity was assessed by the coefficients of determination, R^2. The mean of three measurements for each treatment was taken. Previous CE method papers have also utilized three measurements [37].

The apparent permeability coefficient (P_{app}) was calculated similarly to Song et al. (2020) [7], using the standard equation:

$$P_{app} = \Delta Q/(\Delta t \times A \times C_0)$$

where Δt is the incubation time (s), A is the surface area of the insert filter membrane (cm^2), C_0 is the initial concentration of peptides in the apical compartment at time 0 h (µM), and ΔQ is the amount of peptide transported within a given period (µmol/s). The incubation timepoint (Δt) used was representative of the intestinal transport phase (2 h timepoint). Data is reported as mean ± SEM. An assessment of the basolateral compartment at time 0 h showed no peptide presence. Therefore, it was assumed that for each well, treatment and plate, the peptide content off the basolateral compartment at time 0 h was 0.

Transport (%) was assessed using the same equation as Song et al. (2020) [7]. It is a fraction of the amount of transported peptide in the basolateral compartment compared to the initial apical compartment peptide content.

Transport (%) = Transported peptide content (Basolateral 2 h)/
Initial peptide content (Apical 0 h) × 100

Hepatic first pass effect (%) was calculated as:

Hepatic effect (%) = Peptide content after incubation with HepG2 (Basolateral 5 h)/
Content of peptide available for liver metabolism (Basolateral 2 h) × 100

Bioavailability, after first pass metabolism, was expressed as a percentage of final and initial peptide digesta values, as described in Sadeghi Ekbatan et al. (2018) [8].

Bioavailability (%) = Peptide content after HepG2 incubation (Basolateral 5 h)/Initial amount of peptide (Apical 0 h) × 100

4.3.8 Statistical analysis

For each peptide, a t-test was completed to assess differences between CH treatments in terms of peptide transport, hepatic effect, and first pass metabolism, where differences were considered significant if $p < 0.05$. MTT was assessed using a two-way ANOVA using dose and treatment as factors, followed by Tukey-HSD. Differences were considered significant if $p < 0.05$. All analyses and figures were completed using GraphPad Prism (Version 9.0.1 for Windows, GraphPad Software, San Diego, CA, USA). Data is reported at mean ± SEM.

4.4 Results

Two bovine-sourced CHs (CH-GL and CH-OPT) underwent simulated human digestion. Filtered digests were applied to a HIEC-6/HepG2 co-culture in a transwell system to determine the transport, hepatic first pass effects and bioavailability of BAPs (Gly-Pro, Hyp-Gly, Ala-Hyp, Pro-Hyp, Gly-Pro-Hyp).

4.4.1 MTT assay

Before CH treatments were applied to the HIEC-6/HepG2 co-cultures, a dose response study to assess possible cytotoxicity of the CH treatments was completed (**Figure 2**). Cell survival was not

significantly different between the control (0 mg/mL) and any of the peptide doses (0.125, 0.25, 0.5, 1, 2 mg/mL) for either CH treatment. This work verified that up to 2 mg/mL of reconstituted peptides from simulated CH digestion caused no adverse cytotoxic effects on HIEC-6 cells. The assessment of cytotoxicity helped establish the dose used for subsequent bioavailability studies, as a dose large enough was required to ensure that BAPs would be quantifiable after first pass metabolism.

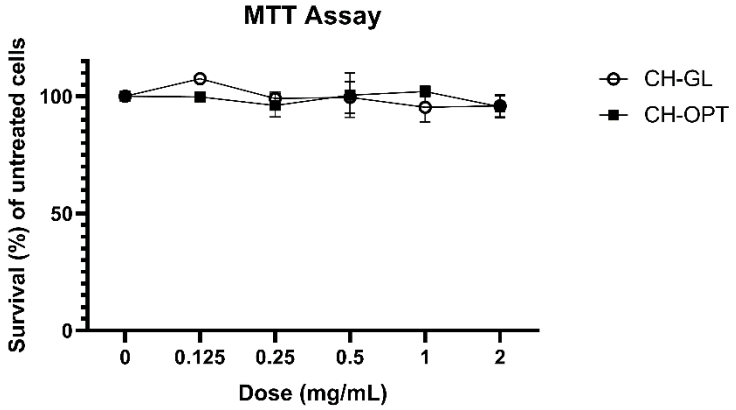

Figure 4.2. Cell survival (%) using (3-[4,5-dimethylthiazol-2-yl]-2,5-diphenyl tetrazolium bromide) (MTT) method on HIEC-6 cells. A two-way ANOVA, using dose and treatment as factors, followed by Tukey-HSD was completed where differences were considered significant if $p < 0.05$. No significant differences between CH doses or treatments were observed.

4.4.2 Peptide transport

Upper intestinal digests of CHs (CH-GL and CH-OPT) were applied to a HIEC-6/HepG2 transwell co-culture. Samples were collected from the apical and basolateral compartments at time 0 h and after 2 h to determine peptide transport (%) across the intestinal epithelium and apparent permeability (Papp). After 2 h, sub-samples were again collected, the insert containing HIEC-6 cells was discarded, and the hepatic cells allowed to incubate for another 3 h to determine the hepatic effects on CHs peptides. Samples were taken at the final timepoint (5 h) from the basolateral compartment. No detectable peptide content for either cell culture compartment at any timepoint was observed using the cell culture blank (i.e., no CH added, negative control) (data not shown).

After CH-GL treatment (2 h), 59.44 ± 11.32% of Gly-Pro-Hyp was transported across the intestinal HIEC-6 layer (Table 1). No observable content of Gly-Pro-Hyp was measured in the basolateral compartment of the transwell system after CH-OPT. Transport across the intestinal epithelium was observed for all other peptides (Gly-Pro, Hyp-Gly, Ala-Hyp, and Pro-Hyp) for both CHs. The peptide and treatment with the greatest transport (%) was Hyp-Gly after CH-OPT treatment (82.53 ± 36.53). The greatest transport (%) for CH-GL was also observed with Hyp-Gly (62.41 ± 11.11). The peptides with the least transport (%) were Ala-Hyp after CH-GL (9.27 ± 2.49) and Pro-Hyp after CH-OPT (24.15 ± 1.42).

No differences in peptide transport (%) across the epithelial layer were observed between treatments (CH-GL and CH-OPT) for any of the di-peptides (Gly-Pro, Hyp-Gly, Ala-Hyp, and Pro-Hyp).

Table 4.1. Peptide transport (%) from CH-GL and CH-OPT across intestinal epithelium.

Peptide / Treatment	Gly-Pro	Hyp-Gly	Ala-Hyp	Pro-Hyp	Gly-Pro-Hyp
CH-GL	33.11 ± 3.08	62.41 ± 11.11	9.27 ± 2.49	19.18 ± 4.81	59.44 ± 11.32
CH-OPT	40.35 ± 2.85	82.53 ± 36.53	26.4 ± 5.78	24.15 ± 1.42	nd

Values represent peptide concentration after transport (2 h timepoint) as a percentage of peptides of initial digesta values. For each peptide, a t-test was performed to determine differences in peptide transport between treatments, which were considered significant if $p < 0.05$. No significant differences in peptide transport were seen between treatments, however, no Gly-Pro-Hyp was detected in the basolateral compartment with CH-OPT (nd = not detectable).

The apparent permeability coefficients (Papp) were also assessed (**Figure S1**). Similar to the transport (%) results, the peptide Hyp-Gly had the greatest Papp compared to all the other di-peptides assessed, for both CH treatments. Specifically, P_{app} (cm/s) for CH-GL was 6.740 ± 1.200 × 10^{-6} and CH-OPT was 5.593 ± 2 .476 × 10^{-6}. The peptide with the lowest Papp was Ala-Hyp, where CH-GL was 0.725 ± 0.195 × 10^{-6} cm/s and CH-OPT was 1.033 ± 0.226 × 10^{-6} cm/s.

No differences in P_{app} were observed between treatments (CH-GL and CH-OPT) for any of the di-peptides. In contrast, P_{app} was measurable for Gly-Pro-Hyp after CH-GL treatment, but no apparent permeability coefficient could be determined for CH-OPT, due to a lack of quantifiable peptide content in the basolateral compartment after 2 h.

4.4.3 Hepatic first pass effects

Hepatic first pass effects were observed for the peptide Pro-Hyp (Table 2). An increase in Pro-Hyp following hepatic production by HepG2 cells after CH-GL (151.4 ± 24.3%) compared to CH-OPT (63.63 ± 8.63%) was observed. The peptides Ala-Hyp (304.9 ± 57.2%) and Gly-Pro (109.2 ± 9.6%) increased following hepatic production by HepG2 cells after CH-GL. An increase in Ala-Hyp content was also observed following hepatic production after CH-OPT treatment (198.0 ± 107.6%), although not for Gly-Pro (86.12 ± 14.09%). Hyp-Gly following hepatic action was the least affected (55.16 ± 16.01% after CH-GL and 28.23 ± 6.55% after CH-OPT) compared to the other di-peptides.

There were no differences in hepatic production or metabolism between treatments (CH-GL and CH-OPT) for Gly-Pro, Hyp-Gly, and Ala-Hyp. No hepatic first pass effects for Gly-Pro-Hyp were seen with CH-OPT, as no peptides were transported by the intestinal layer to be available for hepatic action.

Table 4.2. Hepatic effects on peptide content from CH-GL and CH-OPT following HepG2 incubation.

Peptide / Treatment	Gly-Pro	Hyp-Gly	Ala-Hyp	Pro-Hyp	Gly-Pro-Hyp
CH-GL	109.2 ± 9.6	55.16 ± 16.01	304.9 ± 57.2	151.4 ± 24.3*	22.32 ± 5.09
CH-OPT	86.12 ± 14.09	28.23 ± 6.55	198.0 ± 107.6	63.63 ± 8.63	nd

Values represent peptide concentration after hepatic action (5 h timepoint) as a percentage of peptides available for HepG2 action (2 h timepoint). For each peptide, a t-test was completed to determine the effect of CH treatment, where differences were considered significant if $p < 0.05$. Asterisks represent significant differences between treatments (* $p < 0.05$), nd = not detectable.

4.4.4 Peptide bioavailability

The bioavailability of the CH-GL and CH-OPT peptides after first pass metabolism was calculated in terms of a percentage of the peptide content observed after hepatic first pass effects when compared to the initial digesta peptide values. Peptide bioavailability was >32% for Gly-Pro and Hyp-Gly after both CH treatments (**Figure 3**). Ala-Hyp showed an average bioavailability of >20%. Although the bioavailability of Pro-Hyp after CH-GL treatment (26.81 ± 3.97%) appeared to be greater than CH-OPT (15.43 ± 2.60%), this difference did not reach statistical significance ($p = 0.0745$).

The bioavailability of the di-peptides Gly-Pro, Hyp-Gly, and Ala-Hyp after first pass metabolism did not differ between CH treatments. As no tri-peptide content was detected after intestinal transport using CH-OPT treatment, this peptide did not undergo detectable first pass metabolism. After CH-GL treatment, the bioavailability of Gly-Pro-Hyp was 12.24 ± 1.12%.

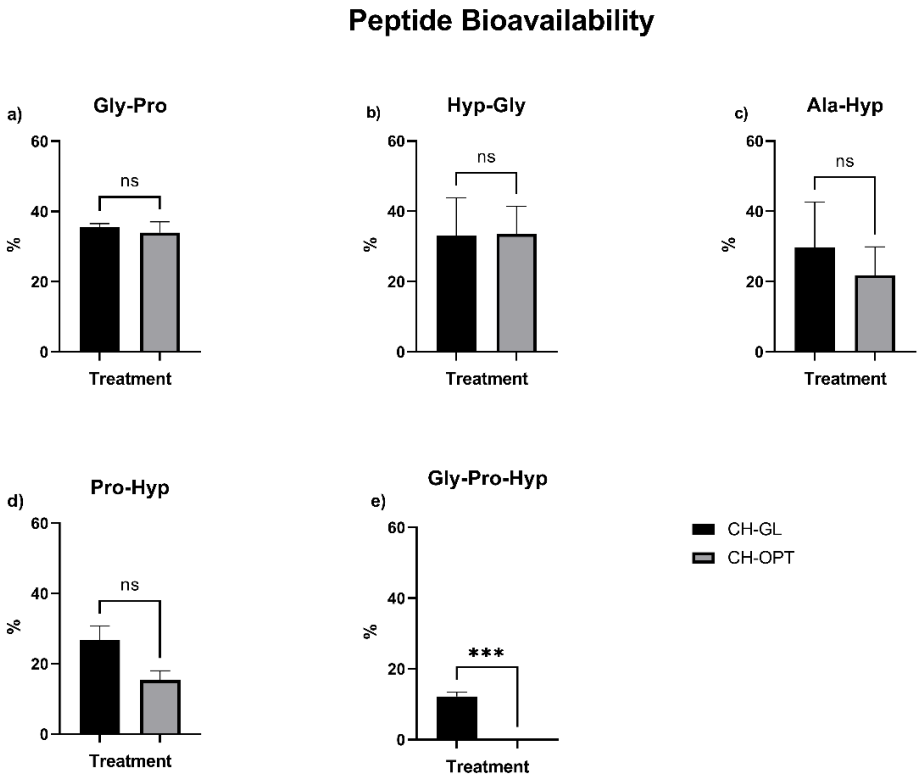

Figure 4.3. Bioavailability of CH-GL and CH-OPT peptides after first pass metabolism: (a) Gly-Pro; (b) Hyp-Gly; (c) Ala-Hyp; (d) Pro-Hyp; and (e) Gly-Pro-Hyp. Values are expressed as the final peptide content after hepatic effect as a percentage of initial digesta values. For each peptide, a t-test was completed to determine the effect of CH treatment, where differences were considered significant if $p < 0.05$. Columns with asterisks are significantly different (*** $p < 0.001$). Columns with ns are not significantly different.

4.5 Discussion

This work was the first to utilize a HIEC-6/HepG2 co-culture to predict the bioavailability of BAPs after the digestion of two CHs using an optimized CE method. This novel combination of cell lines provided further insight into the high degree of BAP transport by utilizing HIEC-6 cells, which more accurately represents the physiological in vivo conditions than previously utilized Caco-2 cells. In terms of the key observations related to di-peptide transport, the P_{app} for all the di-peptides measured for both CHs were between 1 and 10×10^{-6} cm/s. Previous work, establishing the

relationship between in vitro (P_{app}) and in vivo absorption, have ranked compounds as poorly, moderate, or well absorbed to corresponding P_{app} ranges [7,38]. Poorly absorbed compounds are below 1×10^{-6} cm/s, moderately between 1 and 10×10^{-6} cm/s, and well absorbed compound are above 10×10^{-6} cm/s. Thus, the di-peptides measured in the present study can be considered moderately bioavailable, except for Ala-Hyp after CH-GL treatment, which was $0.7254 \pm 0.1947 \times 10^{-6}$ cm/s. It is possible that the moderate and high degree of bioavailability of collagen-derived BAPs are related to the clinically significant health benefits associated with CH intake.

A relatively high (59%) monolayer transport of Gly-Pro-Hyp with a P_{app} value of approximately 9×10^{-6} cm/s was noted after CH-GL treatment. The P_{app} of Gly-Pro-Hyp observed with the CH-GL treatment could thus be in the range of a moderately to well absorbed compound. The above P_{app} value was much greater than previously reported for Gly-Pro-Hyp by Sontakke et al. (2016), who using Caco-2 cells followed by LC-MS/MS analysis, showed relatively low cumulative amounts of the tri-peptide transported across the monolayer with a P_{app} value of $1.09 \pm 0.03 \times 10^{-6}$ cm/s [15]. The Gly-Pro-Hyp peptide exhibits multiple health promoting properties, most notably inhibition of dipeptidylpeptidase-IV (DPP-IV) [39]. In patients with type 2 diabetes, DPP-IV inhibitors are used to control postprandial glycemia [39]. Future work is needed assessing the in vivo bioavailability and health modulating properties of this peptide in association with the CH-GL treatment.

In the present work, a markedly lower degree of transport for Pro-Hyp ($P_{app} = 1.912 \pm 0.4794 \times 10^{-6}$) as compared to Gly-Pro-Hyp was observed with the CH-GL treatment. Similarly, the apparent permeability reported by Sontakke et al. (2016) for Pro-Hyp ($0.13 \pm 0.03 \times 10^{-6}$ cm/s) was significantly lower than their value for Gly-Pro-Hyp [15]. The P_{app} of Pro-Hyp observed in the present study, however, was greater than the values reported by Sontakke et al. (2016) [15] and Feng et al. (2017) ($1.45 \pm 0.17 \times 10^{-6}$ cm/s) [40]. As noted by the above, the permeation of Gly-Pro-Hyp was greater than Pro-Hyp, even though Gly-Pro-Hyp is a larger molecular weight peptide. Peptide transport across the intestinal layer via paracellular pathways is primarily dependent on the charge and molecular size of the compound. Since both peptides are uncharged, it is conceivable that active transporters were involved in the relatively greater transport of Gly-Pro-Hyp. Overall, there is a paucity of research pertaining to bioactive peptide intestinal transporters, which requires more research using representative physiological models. Pro-Hyp has been shown to decrease the loss of

chondrocytes, which synthesize articular cartilage [41]. In animal models designed to promote cartilage damage, Pro-Hyp inhibited cartilage thinning [41]. Accordingly, Pro-Hyp is considered to be one of the major bioactive components linked with the clinical efficacy of CHs towards treatment of osteoarthritis.

Our work assessing Hyp-Gly demonstrated transport (%) values of 62.41 ± 11.11 and 82.53 ± 36.53 for CH-GL and CH-OPT, respectively. Song et al. (2020) showed lower transport of Hyp-Gly (22.63 ± 5.19%) from silver carp skin hydrolysate after in vitro digestion and Caco-2 assessment using HPLC-ESI-MS analysis [7]. The greater degree of transport observed in our study may be attributed to the more physiologically relevant cell culture model used; the under expression of PepT1 in Caco-2 cells could significantly decrease the amount of peptide traveling across the intestinal layer. In contrast, the P_{app} values for Hyp-Gly (6.740 ± 1.200 × 10^{-6} after CH-GL and 5.593 ± 2.476 × 10^{-6} after CH-OPT) were lower compared to Song et al. (2020), which was 10.00 × 10^{-6} cm/s [7]. Apart from the different intestinal cell types used, variances in the quality of the established monolayer due to differences in passage number, cell conditions, and culture duration could impact the intestinal transport coefficients [42]. The high bioavailability of Hyp-Gly in the present work coincides with in vivo studies showing that this antiplatelet peptide is present in blood after CH ingestion and thereby could provide anti-thrombotic protection [7].

Although there were no differences in di-peptide bioavailability between the two tested CHs, CH-GL showed significant Gly-Pro-Hyp content after first pass liver metabolism, whereas none was observed after CH-OPT. This difference in bioavailability could be attributed to the presence of other peptides found within the CHs, as the digestion and bioavailability of BAPs can be affected by the presence of other peptides, proteins, or food components [2]. Increased peptide absorption could also occur due to synergisms with other peptides present in the digests as dietary AAs and protein hydrolysates can increase PepT1 expression [2]. Previous work by our group has established that CH-GL and CH-OPT have different peptide profiles, both pre- and post-digestion, with some peptide sequences being found in one CH and not the other [5]. The synergistic effects of BAPs are still under investigation; however, hormonal responses can be influenced by the presence of other proteins or peptides consumed. For example, the glucose-dependent insulinotropic polypeptide response and gastric emptying were greater when milk protein hydrolysates were ingested

compared to whole milk protein sources [2]. Furthermore, colonic motility contractions were increased after whey hydrolysates compared to whey protein concentrates [2]. Further work on identifying and understanding synergistic effects affecting peptide transport, bioavailability and bioactivity, is required, particularly for CH-derived BAPs.

To our knowledge, the present study has been the first to determine the impact of hepatic first pass effects on BAPs after their intestinal transport. A direct and targeted method of BAPs quantification using CE allowed for an in-depth analysis of BAP content following their first pass effects. The presence of HepG2 cells in the basolateral compartment could potentially have affected permeability assessments, as previous work reporting P_{app} has used only intestinal cell monolayers. The effect of HepG2 cells in a co-culture on P_{app} has not been fully established. Some preliminary reports have demonstrated that the presence of Pro-Gly increases PepT1 expression in HepG2 cells [29], although further work is needed assessing peptide transport as affected by modulation of PepT1 expression by di-peptides. The use of a co-culture of intestinal and hepatic cell lines has been well established to understand bioavailability (%), although assessments of P_{app} were not reported [8,29,43]. Future work to incorporate hepatic effects on peptide transport should be investigated, especially considering that the expression of PepT1 may be regulated by the presence of BAPs [29]. The hepatic first pass effects on BAPs have not been well studied. Most published work discussed above investigating "bioavailability" only used Caco-2 cells thereby determining intestinal transport only, but this does not represent systemic availability. The degree that hepatic first pass effects affected peptide content in this study was unexpected; however, such studies investigating BAPs have not been previously performed. In that regard, it has been well established that there is high hepatic metabolism for small peptides [44], but hepatic upregulation of BAPs has not been studied previously. The importance of assessing the contribution of hepatic action is clearly demonstrated in our work. For example, Ala-Hyp was increased after incubating with HepG2 cells up to 304.9 ± 57.2% after treatment with CH-GL digests. Although both CHs were derived from bovine collagen, there was a significant difference in the hepatic first pass effects on Pro-Hyp. Hepatic action on Pro-Hyp was greater after CH-GL treatment (151.4 ± 24.3%) compared to CH-OPT (63.63 ± 8.63%); this was surprising as the content of Pro-Hyp that traversed across the intestinal layer was not significantly different between the treatments. The difference in hepatic first pass effects on Pro-Hyp might be due to the presence of Gly-Pro-Hyp that was solely noted to be intestinally

transported after CH-GL treatment; this tri-peptide could conceivably be metabolized further by hepatic cells to contribute to the Pro-Hyp content. Such hepatic production of Pro-Hyp would not be expected with CH-OPT as Gly-Pro-Hyp was not appreciably transported across the intestinal layer with this treatment. The increase in BAP production for all the di-peptides during hepatic action could also have occurred due to the metabolism of unidentified longer chain peptides that travelled across the epithelium. In that respect, further work into identifying and assessing other collagen-derived BAPs is needed.

No previous studies have combined simulated digestion together with HIEC-6/HepG2-mediated transport and metabolism to investigate the bioavailability of CH-derived BAPs. A notable finding was that Gly-Pro-Hyp had a 12.24 ± 1.12% bioavailability with the CH-GL treatment after intestinal transport and hepatic first pass effects. A possible comparison might be made with the in vivo studies by Skov et al. (2019), which determined the postprandial plasma concentration of Gly-Pro-Hyp in a human clinical trial using ^{1}H NMR analysis [4]. The initial Gly-Pro-Hyp content in the plasma was ~ 400 µM, and the Gly-Pro-Hyp content increased after 2 h to ~ 1050 µM, which would represent a 162.5% increase. It should be noted, however, that the method by which plasma Gly-Pro-Hyp was calculated by Skov et al. (2019), involved summing the individual AA measurements of Gly, Pro and Hyp, as no peptide sequencing or targeted quantification of Gly-Pro-Hyp was done. As digestion breaks down peptides into their AA components, it is possible that the summed plasma content of Gly, Pro, and Hyp indicated a greater apparent bioavailability of Gly-Pro-Hyp than provided via direct measurement of the tri-peptide.

To further understand the bioactivity of specific BAPs, rapid, accurate and efficient methods of identification and quantification are necessary. Previous work assessing CH-derived peptide bioavailability using Caco-2 cells have had significant limitations in terms of endpoint analysis. Feng et al. (2017) [19] assessed bovine CH bioavailability according to an indirect calculation of total AA transported. Furthermore, no peptide sequencing using proteomics methods or quantification was done. Three major AAs found in collagen are Gly, Pro and Hyp, but no Pro content was detected for all the hydrolysates assessed [19]; therefore, established BAPs sequences such as Pro-Hyp, Gly-Pro-Hyp, Gly-Pro, were likely not found. Future studies can utilize emerging technologies such as the CE methodology described herein towards the identification and quantitation of BAPs.

Despite their limitations, cell culture models continue to provide a platform to predict the bioavailability of BAPs, as animal studies often to do not correlate with human data, and human trials are long, associated with increased costs and have ethical restrictions [2]. Comparisons of cell culture models to human in vivo data generally support the use of the former to assess intestinal transport [22–24]. Discrepancies involving in vitro assessments of kinetics and peptide activity may occur, however, if the digestive and metabolic processes are not sufficiently considered [2]. Cell culture models must therefore accurately replicate the digestion, transport, and metabolism of the bioactive components of interest. For this reason, in this study, the bioavailability of CH-derived BAPs after in vitro digestion was determined using a novel co-culture of HIEC-6/HepG2 cells rather than a Caco-2 monolayer, as the expression of a key peptide transporter PepT1 is under-expressed in Caco-2 cells and predictions of peptide bioavailability could be misleading. Previous work has confirmed that HIEC cells more accurately represent the physiological in vivo conditions of the SI compared to Caco-2 cells [22–24]. Further studies can adopt and standardize this HIEC-6/HepG2 co-culture method, which could be adapted to investigate the first pass effects of bioactive food components, nutraceuticals and supplements.

As demonstrated in this study, similarly sourced and marketed CH products can contain different peptide profiles [5] and have varying degrees of peptide bioavailability. These findings are pertinent since BAPs must undergo first pass metabolism [9] for CHs and collagen-derived peptides to exert their bioactivity, such as on joint tissues including bone, cartilage and muscle. The bioavailability of collagen BAPs has been related to the clinically significant health benefits associated with CH intake, such as decreasing pain associated with OA, improving joint discomfort, and increasing bone mineral density [1,3,13,45]. Therefore, the different degree of BAP bioavailability seen after hepatic first pass effects between the CH products could modify their clinical efficacy. As consumers continue to use an increasing variety of over-the-counter CHs, assessing the bioavailability and bioactivity of BAPs from various CHs using higher throughput models is advantageous. This model provides a higher throughput method to assess peptide bioavailability before clinical studies are undertaken, which are often costly, long and have various ethical constraints.

4.6 Conclusion

The present study demonstrated the use of a more physiologically relevant model using a HIEC-6/HepG2 co-culture to assess the bioavailability of CH-derived BAPs after first pass metabolism. Furthermore, this study utilized an optimized CE method for the targeted assessment of BAPs from cell culture. Although both CHs were bovine sourced, differences in transport, hepatic effects and bioavailability were observed for different BAPs, which could potentially lead to different clinical results. Further clinical assessments of CHs are required to understand the impact of bioavailable BAPs. Overall, this study demonstrated a novel combination of techniques and cell lines that can be adapted to assess for the bioavailability of other drugs, nutraceuticals, and supplements, as well as their corresponding health promoting properties.

4.7 Funding

The present study was supported by a MITACS Accelerate Program PhD studentship (IT10556) collaboration between McGill University and Genacol Canada Corporation and the Collaborative Research Development Grant Program from the Natural Sciences and Engineering Council of Canada to S.K. (535744-18).

4.8 Acknowledgments

We would like to thank Patrick Sabourin from Technopro for his help and expertise in CE.

4.9 Supplementary data

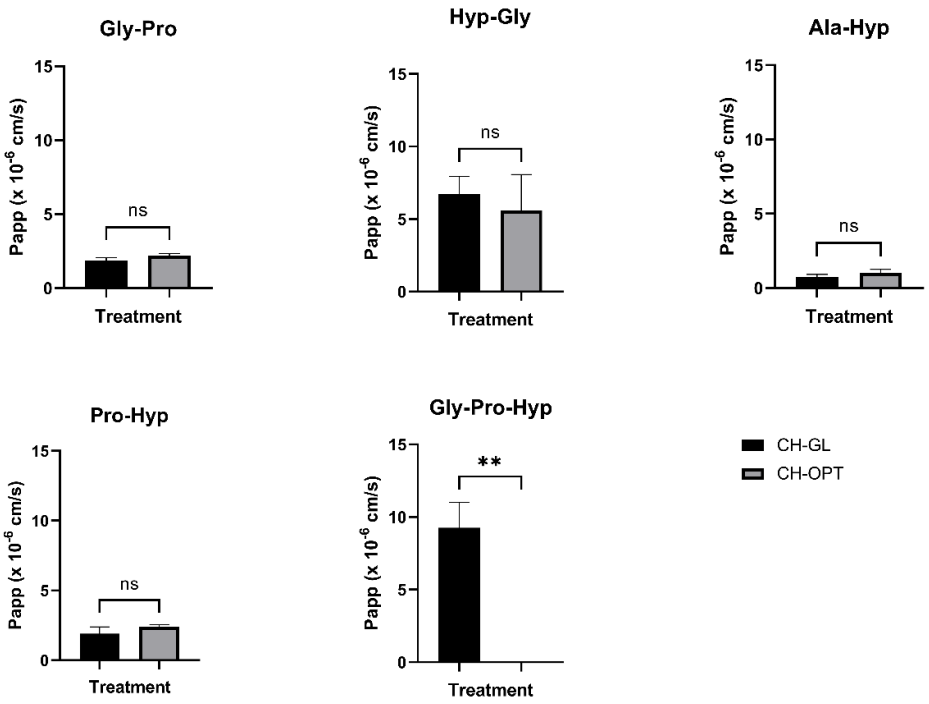

Figure S4.1. Apparent permeability coefficient (P_{app}) of CH-GL and CH-OPT peptides. Values are expressed as mean ± SEM in cm/s. For each peptide, a t-test was completed to determine the effect of CH treatment, where differences were considered significant if $p < 0.05$. Columns with asterisks are significantly different. Columns with ns are not significantly different.

4.10 References

1. Zdzieblik, D.; Oesser, S.; Gollhofer, A.; König, D. Improvement of activity-related knee joint discomfort following supplementation of specific collagen peptides. *Appl. Physiol. Nutr. Metab.* **2017**, *42*, 588–595, doi:10.1139/apnm-2016-0390.
2. Amigo, L.; Hernández-Ledesma, B. Current evidence on the bioavailability of food bioactive peptides. *Molecules* **2020**, *25*, 4479, doi:10.3390/molecules25194479.
3. Pal, G.K.; Suresh, P.V. Sustainable valorisation of seafood by-products: Recovery of collagen and development of collagen-based novel functional food ingredients. *Innov. Food Sci. Emerg. Technol.* **2016**, *37*, 201–215, https://doi.org/10.1016/j.ifset.2016.03.015.
4. Skov, K.; Oxfeldt, M.; Thøgersen, R.; Hansen, M.; Bertram, H.C. Enzymatic hydrolysis of a collagen hydrolysate enhances postprandial absorption rate-a randomized controlled trial. *Nutrients* **2019**, *11*, 1064, doi:10.3390/nu11051064.
5. Larder, C.E.; Iskandar, M.M.; Kubow, S. Gastrointestinal digestion model assessment of peptide diversity and microbial fermentation products of collagen hydrolysates. *Nutrients* **2021**, *13*, 2720, https://doi.org/10.3390/nu13082720.
6. Iwai, K.; Hasegawa, T.; Taguchi, Y.; Morimatsu, F.; Sato, K.; Nakamura, Y.; Higashi, A.; Kido, Y.; Nakabo, Y.; Ohtsuki, K. Identification of food-derived collagen peptides in human blood after oral ingestion of gelatin hydrolysates. *J. Agric. Food Chem.* **2005**, *53*, 6531–6536, doi:10.1021/jf050206p.
7. Song, H.; Tian, Q.; Li, B. Novel Hyp-Gly-containing antiplatelet peptides from collagen hydrolysate after simulated gastrointestinal digestion and intestinal absorption. *Food Funct.* **2020**, *11*, 5553–5564, doi:10.1039/D0FO00219D.
8. Sadeghi Ekbatan, S.; Iskandar, M.M.; Sleno, L.; Sabally, K.; Khairallah, J.; Prakash, S.; Kubow, S. Absorption and metabolism of phenolics from digests of polyphenol-rich potato extracts using the Caco-2/HepG2 co-culture system. *Foods* **2018**, *7*, 8.
9. Brayden, D.J. Evolving peptides for oral intake. *Nat. Biomed. Eng.* **2020**, *4*, 487–488, http://dx.doi.org/10.1038/s41551-020-0559-0.
10. Shigemura, Y.; Suzuki, A.; Kurokawa, M.; Sato, Y.; Sato, K. Changes in composition and content of food-derived peptide in human blood after daily ingestion of collagen hydrolysate for 4 weeks. *J. Sci. Food Agric.* **2018**, *98*, 1944–1950, doi:10.1002/jsfa.8677.

11. Yamamoto, S.; Deguchi, K.; Onuma, M.; Numata, N.; Sakai, Y. Absorption and urinary excretion of peptides after collagen tripeptide ingestion in humans. *Biol. Pharm. Bull.* **2016**, *39*, 428–434.
12. Shigemura, Y.; Nakaba, M.; Shiratsuchi, E.; Suyama, M.; Yamada, M.; Kiyono, T.; Fukamizu, K.; Park, E.Y.; Nakamura, Y.; Sato, K. Identification of food-derived elastin peptide, prolyl-glycine (Pro-Gly), in human blood after ingestion of elastin hydrolysate. *J. Agric. Food Chem.* **2012**, *60*, 5128–5133.
13. Bruyère, O.; Zegels, B.; Leonori, L.; Rabenda, V.; Janssen, A.; Bourges, C.; Reginster, J.Y. Effect of collagen hydrolysate in articular pain: A 6-month randomized, double-blind, placebo controlled study. *Complement. Ther. Med.* **2012**, *20*, 124–130, https://doi.org/10.1016/j.ctim.2011.12.007.
14. Wang, L.; Wang, Q.; Liang, Q.; He, Y.; Wang, Z.; He, S.; Xu, J.; Ma, H. Determination of bioavailability and identification of collagen peptide in blood after oral ingestion of gelatin. *J. Sci. Food Agric.* **2015**, *95*, 2712–2717, https://doi.org/10.1002/jsfa.7008.
15. Sontakke, S.B.; Jung, J.H.; Piao, Z.; Chung, H.J. Orally available collagen tripeptide: Enzymatic stability, intestinal permeability, and absorption of Gly-Pro-Hyp and Pro-Hyp. *J. Agric. Food Chem.* **2016**, *64*, 7127–7133, doi:10.1021/acs.jafc.6b02955.
16. Taga, Y.; Kusubata, M.; Ogawa-Goto, K.; Hattori, S. Identification of collagen-derived hydroxyproline (Hyp)-containing cyclic dipeptides with high oral bioavailability: efficient formation of cyclo(X-Hyp) from X-Hyp-Gly-type tripeptides by heating. *J. Agric. Food Chem.* **2017**, *65*, 9514–9521.
17. Wang, L.; Wang, Q.; Qian, J.; Liang, Q.; Wang, Z.; Xu, J.; He, S.; Ma, H. Bioavailability and bioavailable forms of collagen after oral administration to rats. *J. Agric. Food Chem.* **2015**, *63*, 3752–3756, doi:10.1021/jf5057502.
18. Punt, A.; Peijnenburg, A.; Hoogenboom, R.; Bouwmeester, H. Non-animal approaches for toxicokinetics in risk evaluations of food chemicals. *ALTEX* **2017**, *34*, 501–514, https://doi.org/10.14573/altex.1702211.
19. Feng, M.; Betti, M. Transepithelial transport efficiency of bovine collagen hydrolysates in a human Caco-2 cell line model. *Food Chem.* **2017**, *224*, 242–250, doi:10.1016/j.foodchem.2016.12.044.
20. Larregieu, C.A.; Benet, L.Z. Drug discovery and regulatory considerations for improving in silico and in vitro predictions that use Caco-2 as a surrogate for human intestinal permeability measurements. *Am. Assoc. Pharm. Sci. J.* **2013**, *15*, 483–497.

21. Takenaka, T.; Harada, N.; Kuze, J.; Chiba, M.; Iwao, T.; Matsunaga, T. Human small intestinal epithelial cells differentiated from adult intestinal stem cells as a novel system for predicting oral drug absorption in humans. *Drug Metab. Dispos.* **2014**, *42*, 1947–1954.
22. Takenaka, T.; Harada, N.; Kuze, J.; Chiba, M.; Iwao, T.; Matsunaga, T. Application of a human intestinal epithelial cell monolayer to the prediction of oral drug absorption in humans as a superior alternative to the Caco-2 cell monolayer. *J. Pharm. Sci.* **2016**, *105*, 915–924.
23. Pászti-Gere, E.; Pomothy, J.; Jerzsele, Á.; Pilgram, O.; Steinmetzer, T. Exposure of human intestinal epithelial cells and primary human hepatocytes to trypsin-like serine protease inhibitors with potential antiviral effect. *J. Enzym. Inhib. Med. Chem.* **2021**, *36*, 659–668, doi:10.1080/14756366.2021.1886093.
24. Zhao, X.; Xu, X.-X.; Liu, Y.; Xi, E.-Z.; An, J.-J.; Tabys, D.; Liu, N. The in vitro protective role of bovine lactoferrin on intestinal epithelial barrier. *Molecules* **2019**, *24*, 148.
25. Framroze, B.; Havaldar, F.; Misal, S. An in vitro study on the regulation of oxidative protective genes in human gingival and intestinal epithelial cells after treatment with salmon protein hydrolysate peptide. *Funct. Foods Health Dis.* **2018**, *8*, 398–411, doi:10.31989/ffhd.v8i8.529.
26. Larder, C.E.; Iskandar, M.M.; Sabally, K.; Kubow, S. Capillary electrophoresis: A fast, cost effective and efficient method replacement for LC-MS when identifying and quantifying small peptides from simulated gastrointestinal digestion of collagen hydrolysate. Presentation at the BenefiQ Conference, Quebec City Convention Centre, Québec, QC, Canada, 2–4 October 2018, doi:10.13140/RG.2.2.14188.90249
27. Larder, C.E.; Iskandar, M.M.; Sabally, K.; Kubow, S. Complementary and efficient methods for di- and tri- peptide analysis and amino acid quantification from simulated gastrointestinal digestion of collagen hydrolysate. **2021**, Manuscript submitted for publication.
28. Louisa, M.; Suyatna, F.D.; Wanandi, S.I.; Asih, P.B.S.; Syafruddin, D. Differential expression of several drug transporter genes in HepG2 and Huh-7 cell lines. *Adv. Biomed. Res.* **2016**, *5*, 104–104.
29. Zhang, M.; Xu, J.; Wang, T.; Wan, X.; Zhang, F.; Wang, L.; Zhu, X.; Gao, P.; Shu, G.; Jiang, Q., et al. The dipeptide Pro-Gly promotes IGF-1 expression and secretion in HepG2 and female mice via PepT1-JAK2/STAT5 pathway. *Front. Endocrinol.* **2018**, *9*, 424.
30. Cheng, K.C.; Li, C.; Hsieh, Y.; Montgomery, D.; Liu, T.; White, R. Development of a high-throughput in vitro assay using a novel Caco-2/rat hepatocyte system for the prediction of oral plasma area

under the concentration versus time curve (AUC) in rats. *J. Pharmacol. Toxicol. Methods* **2006**, *53*, 215–218.

31. Lau, Y.; Chen, Y.; Liu, T.; Li, C.; Cui, X.; White, R.; Cheng, K. Evaluation of a novel in vitro Caco-2 hepatocyte hybrid system for predicting in vivo oral bioavailability. *Drug Metab. Dispos*. **2004**, *32*, 937–942
32. Alemán, A.; Gómez-Guillén, M.C.; Montero, P. Identification of ace-inhibitory peptides from squid skin collagen after in vitro gastrointestinal digestion. *Food Res. Int.* **2013**, *54*, 790–795, https://doi.org/10.1016/j.foodres.2013.08.027.
33. Miranda, L.; Deusser, H.; Evers, D. The impact of in vitro digestion on bioaccessibility of polyphenols from potatoes and sweet potatoes and their influence on iron absorption by human intestinal cells. *Food Funct.* **2013**, *4*, 1595–1601, https://doi.org/10.1039/c3fo60194c.
34. Iskandar, M.; Lands, L.; Sabally, K.; Azadi, B.; Meehan, B.; Mawji, N.; Skinner, C.; Kubow, S. High hydrostatic pressure pretreatment of whey protein isolates improves their digestibility and antioxidant capacity. *Foods* **2015**, *4*, 184, https://doi.org/10.3390/foods4020184.
35. Mosmann, T. Rapid colorimetric assay for cellular growth and survival: Application to proliferation and cytotoxicity assays. *J. Immunol. Methods* **1983**, *65*, 55–63, doi:10.1016/0022-1759(83)90303-4.
36. Mikulíková, K.; Eckhardt, A.; Pataridis, S.; Mikšík, I.; Paris, F. Study of posttranslational non-enzymatic modifications of collagen using capillary electrophoresis/mass spectrometry and high performance liquid chromatography/mass spectrometry. *J. Chromatogr.* **2007**, *1155*, 125–133, doi:10.1016/j.chroma.2007.01.020.
37. Hsiao, Y.M.; Ko, J.L.; Lo, C.C. Determination of tetracycline and streptomycin in mixed fungicide products by capillary zone electrophoresis. *J. Agric. Food Chem.* **2001**, *49*, 1669–1674, https://doi.org/10.1021/jf0009192.
38. Yee, S. In vitro permeability across Caco-2 cells (colonic) can predict in vivo (small intestinal) absorption in man--fact or myth. *Pharm. Res.* **1997**, *14*, 763–766, doi:10.1023/a:1012102522787.
39. Hatanaka, T.; Kawakami, K.; Uraji, M. Inhibitory effect of collagen-derived tripeptides on dipeptidylpeptidase-iv activity. *J. Enzym. Inhib. Med. Chem*. **2014**, *29*, 823–828.
40. Feng, M.; Betti, M. Both PepT1 and GLUT intestinal transporters are utilized by a novel glycopeptide Pro-Hyp-CONH-GlcN. *J. Agric. Food Chem.* **2017**, *65*, 3295–3304, doi:10.1021/acs.jafc.7b00815.

41. Nakatani, S.; Mano, H.; Sampei, C.; Shimizu, J.; Wada, M. Chondroprotective effect of the bioactive peptide prolyl-hydroxyproline in mouse articular cartilage in vitro and in vivo. *Osteoarthr. Cartil.* **2009**, *17*, 1620–1627.
42. Ting, Y.; Zhao, Q.; Xia, C.; Huang, Q. Using in vitro and in vivo models to evaluate the oral bioavailability of nutraceuticals. *J. Agric. Food Chem.* **2015**, *63*, 1332–1338, doi:10.1021/jf5047464.
43. Li, C.; Liu, T.; Cui, X.; Annette, U.; K. C., C. Development of in vitro pharmacokinetic screens using Caco-2, human hepatocyte, and Caco-2/human hepatocyte hybrid systems for the prediction of oral bioavailability in humans. *J. Biomol. Screen* **2007**, *12*, 1084–1091.
44. Amidon, G.L.; Lee, H.J. Absorption of peptide and peptidomimetic drugs. *Annu. Rev. Pharmacol. Toxicol.* **1994**, *34*, 321–341, doi:10.1146/annurev.pa.34.040194.001541.
45. König, D.; Oesser, S.; Scharla, S.; Zdzieblik, D.; Gollhofer, A. Specific collagen peptides improve bone mineral density and bone markers in postmenopausal women-a randomized controlled study. *Nutrients* **2018**, *10*, 97, doi:10.3390/nu10010097

CONNECTING STATEMENT 3

The findings from Chapter 4 showed a high degree of transport and hepatic first pass effects on CH-derived peptides. Two bovine-sourced CHs were investigated (CH-GL and CH-OPT). Peptide bioavailability was measured by targeted analysis of the BAPs (Gly-Pro, Hyp-Gly, Ala-Hyp, Pro-Hyp, Gly-Pro-Hyp) in the apical and basolateral compartments of the co-culture containing intestinal cells and hepatic cells, respectively. All peptides were bioavailable (>10%), except for Gly-Pro-Hyp after CH-OPT; however, a profile analysis of other peptide sequences which may also contribute to CH bioactivity was not conducted. In Chapter 5, proteomic analysis was completed to investigate bioaccessible peptides found within the CHs prior to digestion as well as after stomach and small intestinal digestive processes. Furthermore, enzymatic hydrolysis of proteins and peptides in the small intestine can yield peptides that bypass intestinal absorption to travel to the large intestine where there they may be fermented by colonic bacteria. In that regard, in Chapter 5, the prebiotic potential of CHs to generate microbial fermentation products in the colon was investigated, as these products can provide significant health promoting properties. The prebiotic potential of CHs is particularly important for patients with OA as gut health has been increasingly linked to joint health. Chapter 5 was published in Nutrients: Larder, C.E.; Iskandar, M.M.; Kubow, S. *Gastrointestinal Digestion Model Assessment of Peptide Diversity and Microbial Fermentation Products of Collagen Hydrolysates*. Nutrients, 2021. **13** (8): p. 2720. https://doi.org/10.3390/nu13082720

CHAPTER 5: RESEARCH PAPER 3

Published: Current Issues in Nutrients, 2021; 13, 2720

Gastrointestinal Digestion Model Assessment of Peptide Diversity and Microbial Fermentation Products of Collagen Hydrolysates

Affiliation:

Christina E. Larder, Michèle M. Iskandar, Stan Kubow *

School of Human Nutrition, McGill University, Ste-Anne-de-Bellevue, QC, Canada, H9X 3V9

* Corresponding author: stan.kubow@mcgill.ca; Tel.: +1-514-398-7754

5.1 Abstract

Osteoarthritis (OA), the most common form of arthritis, is associated with metabolic diseases and gut microbiome dysbiosis. OA patients often take supplements of collagen hydrolysates (CHs) with a high peptide content. Following digestion, some peptides escape absorption to induce prebiotic effects via their colonic fermentation to generate short-chain fatty acids (SCFAs), branched-chain fatty acids (BCFAs) and colonic gases (NH_4 and H_2S). The capacity of CHs to generate microbial metabolites is unknown. Proteomic analysis of two CHs (CH-GL and CH-OPT) demonstrated different native peptide profiles with increased peptide diversity after in vitro gastric and small intestinal digestion. Subsequent 24 h fermentation of the CH digests in a dynamic gastrointestinal (GI) digestion model containing human fecal matter showed that CH-OPT increased ($p < 0.05$) H_2S, SCFAs (propionic, butyric and valeric acids), BCFAs, and decreased NH_4 in the ascending colon reactor with no major changes seen with CH-GL. No major effects were observed in the transverse and descending vessels for either CH. These findings signify that CHs can induce prebiotic effects in the ascending colon that are CH dependent. More studies are needed to determine the physiological significance of CH-derived colonic metabolites, in view of emerging evidence connecting the gut to OA and metabolic diseases.

Keywords: nutraceutical; in vitro digestion; collagen hydrolysate; short-chain fatty acids; branched-chain fatty acids; osteoarthritis; ammonium; hydrogen sulfide; antioxidant; peptide sequencing

5.2 Introduction

Osteoarthritis (OA) is the most common form of arthritis, affecting 50% of people over 75 years old, and accounting for 25% of visits to family doctors [1–3]. OA results in pain, mobility limitations and significant swelling in joint areas, most often in the knees and hips. Risk factors include aging, genetic predisposition, previous injuries, sex, but is also highly associated with metabolic diseases and conditions such as obesity, diabetes, hypertension and dyslipidemia [4–8]. The link between metabolic diseases and OA has become increasingly significant, such that the 2021 Osteoarthritis Research Society International (OARSI) Virtual World Congress held dedicated sessions on metabolic pathways and disorders contributing to OA [9]. Additionally, OA is also associated with an increased risk of metabolic syndrome [10,11]. In a comprehensive study of the National Health and Nutrition Examination Survey III cohort, results showed that the prevalence of metabolic syndrome was increased in patients with OA, regardless of age and BMI [10]. Further studies, following approximately 1000 patients over 20 years, have established that type 2 diabetes is a significant risk factor for severe OA, again independent of age and BMI [10].

The treatment options for OA are currently limited; however, several clinical trials have shown that ingestion of collagen hydrolysates (CHs) allows for decreased pain and increased mobility [12–18]. CH supplements contain a cocktail of peptides and amino acids (AAs); however, it is possible that these peptides are further broken down into bioactive peptides (BAPs) in the stomach and small intestine (SI) [19–23]. BAPs found in collagen products, such as Pro-Hyp, have been shown to decrease the loss of chondrocytes, prevent cartilage thinning, regulate genes associated with joint integrity, reduce the loss of subchondral bone as well as regulate inflammation by inhibiting cytokines such as tumor necrosis factor-α [24–26]. Other BAPs noted in CHs, such as Gly-Pro-Hyp, also have a variety of biological functions which include acting as an inhibitor of dipeptidylpeptidase-IV (DPP-IV), a protein linked to type 2 diabetes, as well as being involved in platelet aggregation [27,28]. Antioxidant capacity is another bioactivity of CH-derived peptides that is screened, as this could reduce reactive oxygen species damage affecting the metabolic diseases associated with OA such as type 2 diabetes [23,29–33]. This could be also relevant as clinical studies have shown that an increased fecal antioxidant content is associated with improved gut function and health [34].

Despite the potential impact of BAPs on human health, a recent review has highlighted the need for more detailed studies on the production of BAPs during digestive processes in view of the sparse information on this topic [35]. Previous work involving in vitro digestion of aged beef meat demonstrated generation of BAPs, although a comprehensive characterisation of the peptides generated was not performed [36]. To date, the impact of digestive processes on the breakdown of CH-derived peptides has been sparsely investigated. Hydrolysates of Alaska pollock skin collagen that underwent simulated gastrointestinal (GI) digestion showed the generation of low-molecular-mass peptides as assessed by reverse phase high performance liquid chromatography HPLC [21]. The digests were associated with increased metal-chelating activity, angiotensin-converting enzyme (ACE) and DPP IV-inhibitory activities as well as enhanced antioxidant capacity [21].

Prebiotics are dietary components that can induce beneficial changes in the growth, activity or composition of microorganisms found in the GI tract, otherwise known as the microbiota. Microbial fermentation products of prebiotics have been implicated to provide several health benefits upon the host [37]. Prebiotics have been shown to regulate inflammation, exhibit antioxidant activity as well as reduce symptoms associated with metabolic disorders such as arthritis [5,38–41]. Enzymatic hydrolysis of proteins in the SI can yield peptides that bypass intestinal absorption of the host to be fermented by colonic bacteria [42]. Consequently, it is conceivable that the rich content of peptides and AAs present in CHs leads to the generation of microbial nitrogenous fermentation products in the colon. As the definition of a prebiotic now includes fermented proteins, peptides and AAs [43], investigation into the prebiotic effects of CHs could be important for OA as gut health has been linked to joint health [5,38]. In that regard, a recent study on obesity showed a direct link between OA and the gut microbiome, and its effects on systemic inflammation [5]. Supplementation of the prebiotic oligofructose altered the GI microbiota of OA and obese mice to a more favorable and healthier microbiota, which was associated with prevention of cartilage loss and improved joint structure [4]. Therefore, further insights as to how CHs impact on gut microbial fermentation is warranted, particularly as patients are increasingly utilizing these products to mitigate the symptoms of OA [44,45].

Short-chain fatty acids (SCFAs) are well established products of fermentation of prebiotics and their production is an indicator of a healthy microbial community [46]. SCFA assessment includes acetic, propionic and butyric acids, which are normally present in ratios ranging from 3:1:1 to 10:2:1 [40]. SCFA production is considered one of the major benefits associated with prebiotics and the relative abundance of fecal SCFAs has been used as a biomarker of gut health as well as overall systemic health [47,48]. Although only a small fraction of SCFAs is absorbed, there are numerous biological functions attributed to SCFAs that are under active investigation. For example, butyric acid has been implicated in the control of inflammation [49], appetite [50] and liver mitochondrial function [51]. Although less is known about minor SCFAs such as valeric and caproic acids, they also have the potential to affect human health [52,53].

CH supplementation could also lead to increased microbial production of branched-chain fatty acids (BCFAs; isobutyric, isovaleric, isocaproic acids), which are products derived from colonic microbial fermentation of branched-chain AAs. The health impact of BCFAs is still under debate. Increased production of BCFAs has been associated with preventing irritable bowel syndrome [54] whereas other studies have increasingly linked exposure to BCFAs with insulin resistance and obesity [55]. Other biomarkers of large intestinal GI health include ammonium (NH_4) and hydrogen sulfide (H_2S), which are often attributed to an over abundant quantity of proteins and some AAs available for fermentation, which can promote dysbiosis [46,56,57]. Increased production of these gases in the GI tract can adversely affect human health [46], although recent reports have indicated that low levels of H_2S may help to avoid GI damage associated with taking nonsteroidal anti-inflammatory drugs (NSAIDS) [58].

For discovery-related investigations pertaining to nutrient and microbial metabolite assessment, human trials are limiting and impractical [59,60]. Furthermore, animal studies, often using rodents, are generally slow, costly and predictions of digestion and microbiota changes do not always align with human clinical data due to species differences in nutrient utilization, metabolic activity and host microbiota [61–63]. As an alternative, dynamic in vitro GI models can closely mimic human upper intestinal digestion and recreate the colonic environment similar to human in vivo conditions [59,60]. Accordingly, such models are increasingly being utilized to predict peptide digestibility and microbiome analysis [35,64], and assessment of SCFAs, BCFAs and colonic gases that provide

information on the functional activity and compositional profiles of the gut microbiota [47,48,56]. As CHs continue to be widely available for OA patients, our study was designed to address the significant gaps in the literature concerning the digestibility of CHs and their potential prebiotic effects, which could impact human health. To determine the peptide profile of two commercially available CH products, upper intestinal digestion followed by proteomics analysis was completed. To observe the production of colonic microbial metabolites after CH digestion and fermentation, a dynamic multistage computer-controlled GI model was used to determine the SCFA, BCFA, NH_4 and H_2S content as well as changes in antioxidant capacity.

5.3 Materials and Methods

5.3.1 Upper intestinal in vitro digestion of collagen hydrolysates

The two bovine-sourced CH products used for this study were Original Formula® (Genacol, Blainville, QC, Canada) (CH-GL) and Selection (Uniprix, Saint-Léonard, QC, Canada) (CH-OPT). Upper intestinal digestion involving the stomach and SI was adapted from Alemán et al., 2013 and Miranda et al., 2013 [20,65]. CHs (1200 mg) were digested in reactor vessels placed in a Versa Water Bath at 37 °C (Fisher Scientific, model 224, Waltham, MA, USA), with continuous stirring and the pH was monitored and adjusted throughout digestion (Fisher Scientific, S90528, Waltham, MA, USA). Exactly 1 mL of an enzyme solution of α-amylase (0.70783 g in 1.5 mL ddH_2O; Sigma-Aldrich, A3176, St. Louis, MO, USA) was added to each vessel and incubated for 15 min at a pH of 6.9. A pepsin solution (1.167 g; Sigma-Aldrich, P7125, St. Louis, MO, USA) was prepared in 0.1 M HCL, of which 2 mL was added and the pH was adjusted to 2. The vessels were incubated for 30 min. Following this, 2 mL of a bile solution (0.9 g/L pancreatin (Sigma-Aldrich, P7545, St. Louis, MO, USA), 6 g/L bile extract (Sigma-Aldrich, B8631, St. Louis, MO, USA), and 12 g/L sodium bicarbonate) prepared in ddH_2O was added. The pH was adjusted to 8 and the solution incubated for 120 min. The digesta was then rapidly cooled on ice and frozen to stop the enzymatic processes. Subsamples of the digesta were filtered using a 0.45 µm Millipore syringe-driven filter and stored at −20 °C until analysis.

5.3.2 Peptide profile

5.3.2.1 Matrix Assisted Laser Desorption/Ionization (MALDI)

Upper intestinal digesta were processed using Matrix Assisted Laser Desorption/Ionization Time-of-Flight (MALDI-TOF). Samples were centrifuged for 10 min to eliminate floating particles and then

ZipTiped (ThermoFisher Scientific 87782, Waltham, MA, USA), as per the manufacturer's instructions. From the ZipTiped samples, 1 µL was placed onto a MALDI target (MTP 384 target ground steel BC) and left to fully air dry. Once dried, 1 µL of matrix (10 mg/mL α-cyano-4-hydroxycinnamic acid, with 1:1 acetonitrile and 0.1% trifluoroacetic acid) was added on top of the sample and again left to air dry completely. The loaded plates were then inserted in the MALDI-TOF/TOF instrument. Profiling was performed on a MALDI-TOF/TOF Ultraflextreme mass spectrometer equipped with a SmartBeam II Nd:YAG 355 nm laser operating at 2000 Hz (Bruker Daltonics, Billerica, MA, USA). MS data were acquired by accumulating 1500 laser shots per spot in a mass range of 300–4000 Da. External calibration was carried out using a homemade standard peptide mix. Data analysis was performed with FlexAnalysis 3.4 (Bruker Daltonics).

5.3.2.2 Proteomic Analysis

Both CH samples before and after upper intestinal digestion were assessed for peptide diversity. Samples were reduced and alkylated with dithiothreitol (Sigma-Aldrich, 10197777001, St. Louis, MO, USA) and iodoacetic acid (Sigma-Aldrich, I4386, St. Louis, MO, USA) respectively, then digested with mass spectrometry (MS)-grade trypsin (Thermo Fisher Scientific 90057, Waltham, MA, USA). Samples in 2% acetonitrile, 98% water, 0.1% formic acid were loaded onto a Thermo Acclaim Pepmap precolumn (Thermo, 75 µM ID X 2 cm, C18, 3 µM beads) and then onto an Acclaim Pepmap Easyspray analytical column separation (Thermo, 75 µM X 15 cm, C18, 2 µM beads) using a Dionex Ultimate 3000 uHPLC at 220 nL/min with a 120 min analytical gradient of 2–35% organic solvent (0.1% formic acid in acetonitrile). The column was flushed using 80% organic solvent for 20 min before re-equilibrating back to 2% organic solvent for 20 min. Blank solvent was injected in between samples and the column was then flushed for 60 min at 80% organic solvent and equilibrated with 2% organic solvent for 20 min. Peptides were sequenced using a Thermo Orbitrap Fusion mass spectrometer (120,000 FWHM resolution at 200 amu in MS1; mass range 375–2000, sprayer voltage +1850V). MS/MS sequencing was performed using higher-energy collisional dissociation (HCD) fragmentation (30%; 15,000 resolution, 1.8 amu wide quadrupole isolation) at top speed for all peptides with a charge of 2+ or greater using a cycle time of 3 sec before the next MS1. An MS/MS exclude time of 12 sec was used. Peptide data was searched and compared using the Mascot 2.3 search engine (Matrix Science, Boston, MA, USA) against bovine sequences (Uniprot), corresponding to the source of the materials. Database search results were loaded onto

Scaffold Q+ Scaffold_4.4.8 (Proteome Sciences, Addlestone, Surrey, UK) for analysis. Peptide sequences determined were from 300 to 4000 m/z. BIOPEP-UWM database was used to search for BAP sequences [66].

5.3.3 Dynamic in vitro gastrointestinal digestion of collagen hydrolysates

An established dynamic computer-controlled GI model was used to digest the CH products, which has been previously validated [67,68]. The model consists of five bioreactor vessels: stomach, SI, ascending colon, transverse colon and descending colon. For each vessel, the pH was continuously measured and adjusted by a computer system, with either the addition of 0.2 M NaOH or 0.5 M HCl. The temperature of the GI model was kept at 37 °C and was monitored and controlled by flowing water through double-jacketed reactor vessels in which the GI bioreactor components are found. The model components are attached by plastic tubing and the contents of the reactor vessels were moved by peristaltic pumps. The vessel contents were continuously agitated using magnetic stir plates. The colonic vessels were inoculated with fecal matter and allowed to stabilize over a two-week period to allow for optimal bacterial growth. The two bovine-sourced CH products (CH-GL and CH-OPT) used for upper intestinal digestion (Section 2.1) were again used in the dynamic digestion model. A CH treatment dose of 1200 mg was added to a GI food mixture, as previously described by Ekbatan et al., (2016) [68] and Gaisawat et al., (2019) [69], and which was slowly pumped into the stomach vessel. The treatment dose was based on the daily dose of the Genacol Original Formula® that was shown to reduce joint pain in clinical trials [12,13,18] and the same dose was used for the upper intestinal digestions (see Section 2.1). To our knowledge, no information is available regarding the clinical efficacy of the Selection CH product. An enzyme solution of α-amylase (Sigma-Aldrich, A3176, St. Louis, MO, USA) prepared in sterile deionized water was added to the GI food mixture to replicate salivary digestion. Pepsin (Sigma-Aldrich, P7125, St. Louis, MO, USA) prepared in 0.1 M HCl was added to the stomach vessel and 35 mL of a bile solution composed of pancreatin (Sigma-Aldrich, P7545, St. Louis, MO, USA), bile extract (Sigma-Aldrich, B8631, St. Louis, MO, USA) and sodium bicarbonate were added to the SI, as described by Ekbatan et al., (2016) and Gumienna et al., (2011) [68,70]. Sub-samples from each vessel were obtained at times 0, 8, 16 and 24 h and filtered using a 0.45 µm Millipore syringe-driven filter. Two separate digestion runs were completed for each treatment, with a washout/re-

stabilization period of 3 days between treatments. Previous in vitro fermentation experiments have also utilized two separate digestion runs [71].

5.3.4 Colonic gases

5.3.4.1 Ammonium (NH_4) content

The following method was adapted from Gaisawat et al., (2019) [72]. A 1000 ppm stock solution of NH_4 (Sigma-Aldrich, A4418, St. Louis, MO, USA) was prepared in water, along with subsequent dilutions for the standard curve. Samples (50 µL) or standards were pipetted into a 96-microplate well in triplicate. To each well, 25 µL of a citrate reagent, 25 µL of freshly prepared hypochlorite reagent and 145 µL of deionized water were added. The citrate reagent comprised of 5 g trisodium citrate (Sigma-Aldrich, 1110371000, St. Louis, MO, USA) with 2 g of NaOH in 100 mL deionized water with 30 µL of salicylate nitroprusside reagent (7.813 g sodium salicylate (Sigma-Aldrich, S3007, St. Louis, MO, USA) with 0.125 g sodium nitroprusside (Sigma-Aldrich, 1614501, St. Louis, MO, USA) in 100 mL of deionized water, and adjusted to pH 6.5). The hypochlorite reagent was made with 1 g Na_3PO_4 with 2 mL 2 M NaOH, 10 mL Javex bleach in 100 mL deionized water and pH adjusted between 12 and 13. The microplate was covered, gently rocked back and forth, and allowed to sit at room temperature (RT) for 30 min. The absorbance of the samples and standards was read using a microplate reader (µQuant, 140084, BioTek Instruments, Winooski, VT, USA) at 650 nm. The concentrations of the samples were calculated using an external calibration curve, where linearity was assessed using R^2.

5.3.4.2 Hydrogen sulfide (H_2S) content

The following spectrophotometric method was used to determine inorganic sulfide concentration and was adapted from Gaisawat et al., (2019) [72]. A standard stock solution of 0.1 mM sodium sulfide in oxygen free water was prepared, along with subsequent dilutions for the standard curve. Solution A was prepared using a 5:1 ratio of zinc acetate (2.5% in water) to NaOH (6% in water). Inside a 15 mL centrifuge tube, 0.5 mL of Solution A was added to 0.3 mL of digesta. The tubes were shaken and centrifuged at 3000 *g* for 10 min. The supernatant was carefully decanted, and the pellet washed once with 5 mL of 1.5 M NaCl (pH 8), and then with 5 mL of distilled water (pH 8). The pellet was resuspended in 0.7 mL of water and vortexed. To each sample, 0.25 mL of 0.1% N,N-dimethyl-p-phenylenediamine monohydrochloride (Sigma-Aldrich, D5004, St. Louis, MO, USA) in 5.5 N HCL was added and shaken. Exactly 0.1 mL of 1.15 mM ferric chloride (Sigma-Aldrich, 157740, St.

Louis, MO, USA) in 0.6 N HCl was added. A volume of 200 µL of each sample and standard was pipetted into a 96-well microplate in duplicate and allowed to incubate for 30 min at RT. The absorbance of the samples and standards was read at 650 nm using a microplate reader (µQuant, Bio-tek Instruments, model: 140084, Winooski, VT, USA). The concentration of the samples was calculated using an external calibration curve, where linearity was assessed using R^2.

5.3.5 Short-and branched-chain fatty acids

The SCFA and BCFA content was measured using a gas chromatograph system equipped with a flame ionization detector (GC-FID) (6890A series, Agilent Technologies, Santa Clara, CA, USA) using an adapted method from Ekbatan et al., (2016) and Gaisawat et al., (2019) [68,69]. Pre-filtered subsamples from the GI model for each colonic vessel were obtained, and then diluted 1:1 with methanol. A 1 µL volume was injected into the GC-FID system. An HP-INNOWAS 30 m fused capillary column (Agilent Technologies, Santa Clara, CA, USA) with a 250 µm ID and a film thickness of 0.25 µm was used to separate the SCFAs and BCFAs from both the standard mixes and samples. A flow rate of 1 mL/min of helium gas was used. The inlet and detector temperatures were set at 220°C and 230°C, respectively. The oven temperature was originally set at 150 °C and held for 10 min and then increased by 10 °C/min to 180 °C and held for 5 min. SCFAs and BCFAs were identified based on retention times using a standard mix (Sigma-Aldrich, 46975-U, St. Louis, MO, USA) and quantified (mM) using an external calibration curve, based on peak area and dilutions of the standard mix (**Figure S1**). Linearity of SCFA and BCFA calibration curve was assessed using R^2; all were above 0.99.

5.3.6 Antioxidant capacity

5.3.6.1 Ferric reducing ability of plasma (FRAP) assay

The following method was adapted from Gaisawat et al., (2019) [69] and Benzie and Strain (1996) [73]. A 1 mM stock solution of ascorbic acid (Sigma-Aldrich, A7506, St. Louis, MO, USA) was made and subsequent dilutions completed to obtain a standard curve. A 96-well microplate was used, where 10 µL of either sample or standard was pipetted into a well, along with 30 µL of deionized and 200 µL of a previously made FRAP solution (acetate buffer, 2,4,6-tri(2-pyridyl)-s-triazine and ferric chloride solution combined in a ratio of 10:1:1). The samples and standards were mixed by pipetting for 10 sec and then incubated at RT for 8 min. The absorbance was measured at 593 nm using a µQuant microplate reader (BioTek Instruments, Winooski, VT, USA). The antioxidant

capacity of the samples was calculated using an external calibration curve, where the linearity of the curve was assessed using R^2.

5.3.6.2 DPPH (2,2-diphenyl-1-picrylhydrazyl) assay

The method was adapted from Gaisawat et al., (2019) [69] and is based on the reduction of the free radical 2,2-diphenyl-1-picrylhydrazyl (DPPH). A standard curve was made from a 50 mM Trolox stock solution, with subsequent dilutions using methanol. A 1 mM stock DPPH solution was diluted with methanol to obtain an absorbance between 0.9–0.5 to form a working solution. Exactly 100 µL of gut digesta sample or standard was pipetted into a 96 well plate, along with 150 µL of DPPH working solution and left to incubate at room temperature for 30 min in the dark. Absorbance was measured at 517 nm using a µQuant microplate reader (BioTek Instruments, Winooski, VT, USA). The antioxidant capacity of the samples was calculated using an external calibration curve, where the linearity of the curve was assessed using R^2.

5.3.7 Statistical analysis

Data is reported as mean ± standard error of the mean (SEM). For each treatment, differences between timepoints were assessed using a one-way ANOVA, followed by Dunnett's post hoc test, using time 0 h as control. All analyses were completed using JMP Pro (JMP®, Version 15.1.0, 2019 SAS Institute Inc., Cary, NC, USA) and results were considered statistically significant if $p < 0.05$. Figures were made using GraphPad Prism (Version 9.0.1 for Windows, GraphPad Software, San Diego, CA, USA.)

5.4 Results

5.4.1 Peptide profile

Before digestion, CH-GL had 62 peptide sequences not shared with CH-OPT, whereas CH-OPT had 17 peptide sequences not found in CH-GL (Table S1). Additionally, 3 peptide sequences were shared between the two types of CH brands. After upper intestinal digestion, both CH products had an increase in peptide diversity (**Table S2**). CH-GL had 300 peptide sequences not found in CH-OPT after digestion, whereas CH-OPT had 574 sequences not observed in CH-GL. After digestion, 138 peptide sequences were shared between CH-GL and CH-OPT.

Sequences released after digestion were searched using the BIOPEP-UWM^{TM} database to determine the bioactivity of the peptides metabolized; no bioactive peptide sequences were found, regardless of CH treatment. However, some sequences known to be bioactive registered in BIOPEP were found within the peptides, and often at the c-terminus of the peptide sequences, which could be released upon further digestion. Specifically, the BAPs PR and PQ which have ACE-inhibitory activity, and GPV which shows ACE-inhibitory activity as well as DPPIV inhibitory activity were found at the c-terminus of multiple peptides post-digestion (**Table S2**) [36,60].

The general peptide profile of both CH products was also determined using MALDI. Although from the same collagen source, the peptide profile, distribution, and content of both CH products were different both before and after digestion (**Figures S2–S5**). After both CH products were digested in the stomach and SI, an increase in peptide peaks was observed. The general peptide profile and intensity of the peptide peaks were different between CH-GL and CH-OPT for low and higher molecular weight peptides after digestion (**Figures S4–S5**).

5.4.2 Colonic gases

For each colonic vessel, no significant differences in NH_4 and H_2S were observed between baseline control (time 0 h) and each timepoint (8, 16, 24 h) after the digestion of CH-GL (**Figure 1**). In the ascending colon, a significant decrease ($p < 0.05$) in NH_4 (ppm) content was observed after 8, 16 and 24 h (11.64 ± 0.25, 4.71 ± 0.35, 3.81 ± 0.11, respectively) following CH-OPT supplementation compared to 30.71 ± 3.92 at baseline (time 0 h) (**Figure 1**). In the transverse colon, a decrease in NH_4 (ppm) content was also observed after CH-OPT supplementation but only after 24 h of digestion (9.55 ± 1.24), and no difference in NH_4 content was observed in the descending colon. There were no significant changes in H_2S (μM) content after digestion of CH-OPT for each timepoint and colonic vessel except for an increase in H_2S (μM) content in the ascending colon from 3.333 ± 1.238 at baseline (time 0 h) to 12.238 ± 2.810 after 16 h ($p < 0.05$).

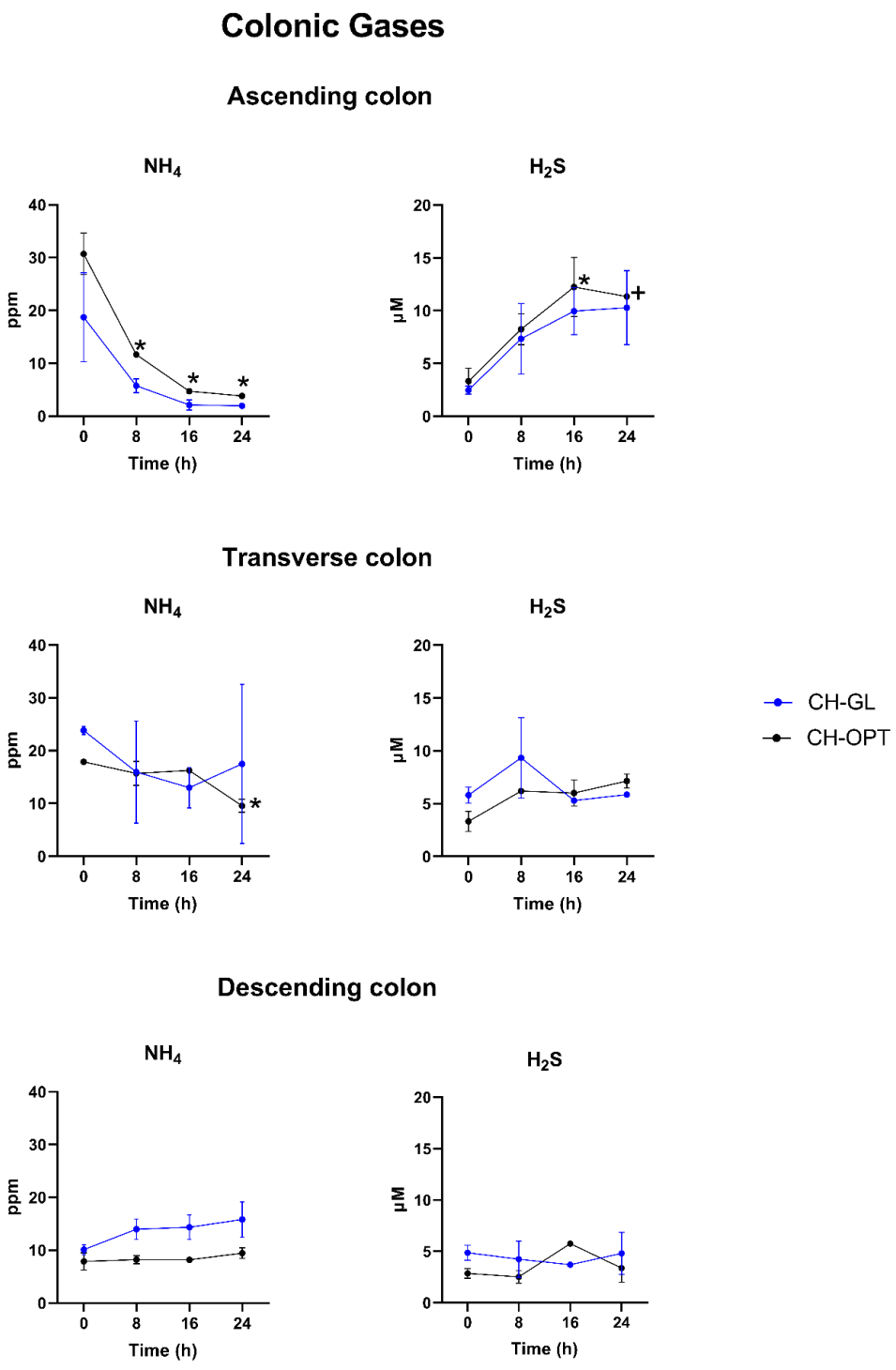

Figure 5.1. NH_4 and H_2S content for CH-GL and CH-OPT over time for each colonic region. Values are expressed as mean ± SEM in ppm for NH_4 and µM for H_2S. The * symbol indicates a significant difference from control (time 0 h) ($p < 0.05$) for each treatment and colonic region. The symbol + indicates a possible trend ($p = 0.0654$).

5.4.3 SCFAs and BCFAs

In the ascending colon, no changes in SCFAs were observed after CH-GL digestion (**Table 1)** whereas individual SCFA profiles showed variability between baseline control (time 0 h) and after the digestion of CH-OPT (**Table 2**). Specifically, propionic acid (mM) content increased from a baseline value of 0.50 ± 0.47 to 7.59 ± 0.59 and 6.53 ± 1.71 after 16 h and 24 h, respectively. Similarly, a significant ($p < 0.05$) increase in butyric acid (mM) was also observed after 16 and 24 h (6.97 ± 0.20 and 5.78 ± 1.21, respectively) from time 0 (2.92 ± 0.21). Valeric acid also increased after 8, 16 and 24 h after CH-OPT fermentation. No significant changes in acetic acid were reported for CH-OPT, for any timepoint. No changes in caproic acid or heptanoic acid were observed in the ascending colon for either CH treatment. Furthermore, for both CHs, no changes in SCFA or BCFA content were observed in the transverse and descending colon compared to baseline (time 0 h).

No increase in BCFA content was observed after digestion of CH-GL, although a significant decrease in isobutyric acid (mM) was detected in the ascending colonic reactor (**Table 1**). Isobutyric acid (mM) decreased from 0.40 ± 0.05 at baseline to 0.19 ± 0.01 after 24 h ($p < 0.05$). A trend for isobutyric acid to decrease relative to control time 0 h was also observed at 8 h (0.23 ± 0.04) ($p = 0.0531$).

An increase in BCFAs in the ascending colonic reactors was observed only with CH-OPT supplementation (**Table 2**). Specifically, isovaleric acid (mM) increased from 2.20 ± 0.09 at baseline to 3.69 ± 0.34 after 16 h ($p < 0.05$). Although not significant, a trend for an increase in isovaleric acid was observed after 24 h ($p = 0.0588$).

Similarly, as observed for SCFAs, there were no changes in BCFAs in the transverse and descending colon vessels for either CH treatment.

Table 5.1. SCFA and BCFA for CH-GL at times 0, 8, 16 and 24 h for each colonic region.

	SCFA						BCFA		
Time (h)	**Acetic Acid**	**Propionic Acid**	**Butyric Acid**	**Valeric Acid**	**Caproic Acid**	**Heptanoic Acid**	**Isobutyric Acid**	**Isovaleric Acid**	**Isocaproic Acid**
Ascending colon									
0	12.43 ± 4.43	0.08 ± 0.07	0.05 ± 0.02	0.00 ± 0.00	0.00 ± 0.00	0.00 ± 0.00	0.40 ± 0.05	0.04 ± 0.01	0.00 ± 0.00
8	24.83 ± 1.84	0.16 ± 0.05	0.05 ± 0.02	0.00 ± 0.00	0.00 ± 0.00	0.00 ± 0.00	0.23 ± 0.04^{+}	0.04 ± 0.00	0.00 ± 0.00
16	25.17 ± 1.95	0.18 ± 0.04	0.05 ± 0.00	0.00 ± 0.00	0.00 ± 0.00	0.00 ± 0.00	0.26 ± 0.01	0.04 ± 0.00	0.01 ± 0.01
24	21.48 ± 0.20	0.22 ± 0.06	0.05 ± 0.00	0.00 ± 0.00	0.01 ± 0.01	0.00 ± 0.00	0.19 ± 0.01*	0.03 ± 0.01	0.01 ± 0.00
Transverse colon									
0	3.10 ± 0.67	1.34 ± 1.27	4.67 ± 3.21	1.56 ± 1.24	0.43 ± 0.43	0.00 ± 0.00	0.54 ± 0.17	0.35 ± 0.18	0.01 ± 0.01
8	6.87 ± 2.68	1.52 ± 1.49	5.26 ± 2.65	1.74 ± 1.12	0.41 ± 0.38	0.00 ± 0.00	0.55 ± 0.09	0.43 ± 0.22	0.01 ± 0.01
16	10.56 ± 6.86	1.74 ± 1.72	3.85 ± 2.35	1.42 ± 1.09	0.29 ± 0.03	0.00 ± 0.00	0.40 ± 0.23	0.35 ± 0.27	0.02 ± 0.01
24	12.2 ± 10.56	1.29 ± 0.51	2.16 ± 1.14	0.85 ± 0.54	0.14 ± 0.12	0.00 ± 0.00	0.32 ± 0.10	0.26 ± 0.16	0.02 ± 0.01
Descending colon									
0	4.50 ± 1.73	2.08 ± 1.90	4.56 ± 3.54	1.09 ± 1.60	0.46 ± 0.42	0.00 ± 0.00	0.79 ± 0.33	0.50 ± 0.26	0.01 ± 0.01
8	5.56 ± 1.12	1.75 ± 1.51	4.70 ± 1.98	1.80 ± 0.99	0.41 ± 0.32	0.00 ± 0.00	1.00 ± 0.53	0.60 ± 0.11	0.01 ± 0.01
16	3.83 ± 0.13	1.49 ± 1.44	3.83 ± 2.04	1.49 ± 0.98	0.40 ± 0.28	0.00 ± 0.00	0.60 ± 0.02	0.50 ± 0.17	0.02 ± 0.02
24	6.80 ± 2.98	1.51 ± 1.43	4.63 ± 0.92	1.68 ± 0.69	0.38 ± 0.26	0.00 ± 0.00	0.76 ± 0.23	0.60 ± 0.07	0.02 ± 0.02

Values are expressed as mean ± SEM in mM; SCFA: short-chain fatty acids; BCFA: branched-chain fatty acids; * indicates significant differences from control (Time 0 h) ($p < 0.05$); + indicates a possible trend ($p = 0.0531$).

Table 5.2. SCFA and BCFA for CH-OPT at times 0, 8, 16 and 24 h for each colonic region.

	SCFA						BCFA		
Time (h)	**Acetic Acid**	**Propionic Acid**	**Butyric Acid**	**Valeric Acid**	**Caproic Acid**	**Heptanoic Acid**	**Isobutyric Acid**	**Isovaleric Acid**	**Isocaproic Acid**
Ascending colon									
0	3.96 ± 2.18	0.50 ± 0.47	2.92 ± 0.21	2.12 ± 0.05	1.80 ± 0.22	1.50 ± 0.08	4.27 ± 1.39	2.20 ± 0.09	1.56 ± 0.05
8	8.55 ± 3.71	5.05 ± 0.43	4.90 ± 0.26	4.42 ± 0.21*	3.65 ± 0.10	2.87 ± 0.54	3.80 ± 0.22	3.20 ± 0.13	2.66 ± 0.55
16	14.12 ± 2.73	7.59 ± 0.59*	6.97 ± 0.20*	5.91 ± 0.37*	4.44 ± 1.13	3.10 ± 0.36	5.19 ± 0.13	3.69 ± 0.34*	2.80 ± 0.18
24	14.20 ± 7.02	6.53 ± 1.71*	5.78 ± 1.21*	5.07 ± 0.70*	3.83 ± 0.08	3.12 ± 0.49	4.65 ± 0.61	2.81 ± 0.17^{+}	2.55 ± 0.47
Transverse colon									
0	3.27 ± 2.13	0.16 ± 0.03	1.68 ± 0.38	1.29 ± 0.21	0.89 ± 0.03	0.78 ± 0.16	2.67 ± 1.26	0.86 ± 0.04	0.64 ± 0.19
8	2.75 ± 0.41	0.82 ± 0.72	1.77 ± 0.50	1.52 ± 0.26	1.11 ± 0.47	0.76 ± 0.13	2.20 ± 0.10	0.98 ± 0.36	0.59 ± 0.10
16	2.94 ± 1.46	1.06 ± 1.00	1.37 ± 0.18	1.09 ± 0.03	0.82 ± .0.23	0.57 ± 0.08	2.20 ± 0.07	0.82 ± 0.10	0.52 ± 0.05
24	6.63 ± 2.54	1.52 ± 1.46	2.17 ± 0.18	1.84 ± 0.12	1.20 ± 0.37	0.91 ± 0.05	5.64 ± 0.87	1.09 ± 0.17	0.73 ± 0.02
Descending colon									
0	2.43 ± 0.37	0.85 ± 0.68	2.23 ± 0.39	1.35 ± 0.17	0.83 ± 0.23	0.46 ± 0.10	1.97 ± 0.09	1.09 ± 0.07	0.40 ± 0.13
8	4.34 ± 1.07	1.21 ± 0.92	3.70 ± 0.60	2.26 ± 0.40	1.4 ± 0.0.41	0.61 ± 0.21	2.35 ± 0.11	1.76 ± 0.17	0.45 ± 0.18
16	3.84 ± 1.16	0.37 ± 0.08	3.72 ± 1.27	2.01 ± 0.05	1.34 ± 0.06	0.54 ± 0.11	3.38 ± 0.73	1.73 ± 0.15	0.52 ± 0.17
24	3.39 ± 3.39	0.43 ± 0.12	3.95 ± 1.45	2.12 ± 0.12	1.32 ± 0.01	0.54 ± 0.11	4.17 ± 0.95	1.76 ± 0.24	0.46 ± 0.13

Values are expressed as mean ± SEM in mM; SCFA: short-chain fatty acids; BCFA: branched-chain fatty acids; * indicates significant differences from control (Time 0 h) ($p < 0.05$); + indicates a possible trend ($p = 0.0588$).

5.4.4 Antioxidant capacity

After upper intestinal digestion, there was a significant increase in ferric-reducing antioxidant capacity (FRAP) between a control digestion (with no CH supplementation), CH-GL and CH-OPT (**Figure 2**). Both CH treatments were significantly greater in antioxidant capacity compared to control. Furthermore, the antioxidant capacity of CH-GL in the SI was greater than that of CH-OPT.

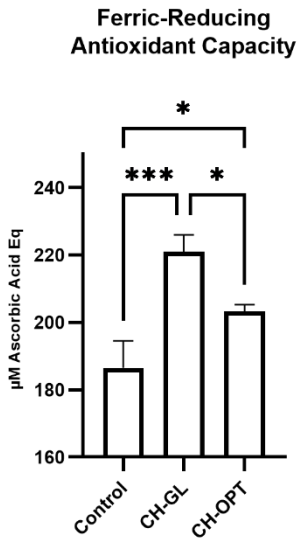

Figure 5.2. Ferric-reducing antioxidant capacity of CH-GL and CH-OPT after upper intestinal digestion. Values are expressed as mean ± SEM in µM ascorbic acid eq. One-way ANOVA followed by Tukey-HSD was completed where $p < 0.05$ was considered significant. Columns with asterisks are significantly different (* $p < 0.05$, *** $p < 0.001$).

There were no significant differences in antioxidant capacity (DPPH and FRAP) after CH-GL supplementation at any timepoint (8, 16, 24 h) for the ascending, transverse and descending colonic vessels (**Table S3**). Conversely, after CH-OPT supplementation, a significant increase ($p < 0.05$) in DPPH radical scavenging activity (mM Trolox Eq) from baseline (17.53 ± 0.68) was seen after 16 and 24 h of digestion (28.25 ± 0.85 and 26.88 ± 1.28, respectively), although only in the ascending colon (**Table S3**). No changes in DPPH capacity were seen in the transverse and descending colon. Furthermore, no changes in FRAP were seen after CH-OPT supplementation.

5.5 Discussion

This work addressed significant gaps in the literature concerning the upper intestinal digestibility of bovine CHs and well as their potential prebiotic effects at the level of the colon. Differences in the peptide profiles before and after upper intestinal digestion between the two CH products were observed, as supported through MALDI and proteomics analyses. Before digestion, three peptide sequences were shared between the two CHs, whereas 62 sequences were only found in CH-GL, and 17 sequences seen only in CH-OPT. Although the CH products shared 138 peptide sequences after digestion, peptidomic results characterized the vast heterogeneity of peptide sequences generated after CH-OPT and CH-GL digestion as exemplified by MALDI profiles as well as 300 peptides being found only in CH-GL and 574 peptide sequences noted solely in CH-OPT. The difference in peptide diversity can result from differing collagen hydrolysate preparation or purification methods as well as upper intestinal digestion [23,31,32]. The contrasting peptide profiles seen post-digestion between the two supplements could provide partial explanation as to why the antioxidant capacity of CH-GL was greater after upper intestinal digestion compared to CH-OPT. Previous studies have indicated that digestion of tuna skin collagen hydrolysates leads to an increase in antioxidant capacity, which was associated with lower molecular weight peptides [74]. Although the peptide sequences released after digestion did not match any peptides from the database BIOPEP-UMW, this was the first study to characterize peptides before and after digestion of bovine sourced CHs. Furthermore, known BAPs such as PR, PQ, and GPV from collagen were found within the peptides sequenced in both CH products, often at the c-terminals. It is conceivable that further metabolism could occur in the colonic regions, easily cleaving c-terminal amino acids, thereby releasing these BAPs. Verification of further proteolytic metabolism in the colon remains to be tested. Future use of dynamic gastrointestinal models could provide a platform to investigate the release of BAPs after colonic metabolism and the potential physiological significance of the BAPs. It is also important to note that novel research into identifying bioactive peptides is still ongoing and current databases are continuously updated. Thus, although no sequences post-digestion were identified as being bioactive, future research might establish bioactivities for some of those sequences.

Using the in vitro dynamic GI model, new insights were obtained in terms of the production of microbial metabolites generated via fermentation of the SI digestion end-products of hydrolyzed

collagen by human gut microbiota. Dynamic GI models, such as the one used herein, allow for multiple and simultaneous sampling from each colonic region, which is not possible to perform with in vivo studies due to ethical and accessibility issues. Dynamic GI models provide a platform for higher throughput analysis of the post-digestive end-products of nutrients, food components and their microbial metabolites. These models provide an alternative to costly and potentially non-representative animal studies, particularly as differences in metabolism and host microbiota can often affect results. Such GI models have certain limitations, such as variability of fecal matter used to inoculate the colonic vessels that can lead to differences in host microbiota composition and metabolism. Additionally, these models do not provide information of the crosstalk between gut microbiota and intestinal cells, which affects host inflammatory pathways and the innate immune system.

Although both hydrolysates were derived from bovine collagen, only the CH-OPT treatment was associated with an increase in colonic SCFA and BCFA content. Furthermore, only CH-OPT showed an increase in H_2S and antioxidant capacity with a corresponding decrease in NH_4, although those outcomes were primarily seen in the ascending colonic region. These findings are most likely due to differences in the SI peptide profiles between the two CH products as discussed above. In support of this contention, greater amounts of peptide sequences larger then 6 AA residues totalling 574 in CH-OPT versus 300 in CH-GL, remained intact following upper GI digestive processes to promote changes in antioxidant capacity in the ascending region of the colon and induce microbial generation of SCFAs in terms of butyric, propionic and valeric acids and the BCFA, isovaleric acid. As no changes in SCFAs, BCFAs, H_2S and antioxidant capacity were observed in the transverse or descending colonic vessels for either CH, it is likely that insufficient amounts of peptides reached those vessels to support further microbial fermentation and changes to the microbiota. Studies investigating the bioavailability of CHs are needed, to verify if peptides from CH-GL formed during digestion are absorbed locally at the GI tract and survive after they permeate across the intestinal epithelium to enter the systemic blood circulation. Furthermore, investigations focusing on lower MW CH peptides are needed, as di- and tri-peptides from collagen have known bioactivity, and increased bioavailability compared to greater MW CH peptides [19,22,35]. Analysis identifying lower MW peptides continues to be a limitation of “peptide-centric” proteomic work, seeing as di- and tri-peptides are too small for sequencing. These small MW peptides only generate 1+ ions, and

the signal interference from other ions coming from solvents, plasticizers, silicates, etc., overwhelm the peptide response. Larger MW peptides (15 AA+) provide stronger signals, with mainly 2+ ions and background ionic noise does not interfere. For this reason, many peptide sequencing approaches mainly focus on higher MW peptides. Methodologies adapted from urine samples using liquid chromatography-MS and capillary electrophoresis-MS/MS could provide novel approaches to detect lower MW peptide from simulated GI digestion, but require further development and verification [75]. However, current efforts by us to assess for lower MW BAPs, such as the di- and tri-peptides Pro-Hyp and Gly-Pro-Hyp, are ongoing and preliminary methodology results using capillary electrophoresis are encouraging [76].

Although there are no analogous studies involving CH fermentation, an increase in butyrate and propionate content was observed from fermentation of casein hydrolysates using single stage, anaerobic fermentation chambers inoculated with human fecal matter [77]. In contrast to the present work, the latter study did not include stomach and SI digestive processes that can modify peptide profiles prior to their exposure to microbial metabolism. Other reports have shown that wheat arabinogalactan peptides were associated with an increase in SCFAs after 24 h, although this was assessed using in vitro batch fermentation rather than a dynamic GI model system.

There are possible metabolic health benefits that might accrue from increased colonic generation of propionic and butyric acids that was associated with CH-OPT supplementation [47,48], and a decrease in NH_4 content [46,56], seeing as when NH_4 levels are greater then 5–10 mM, this can have negative health consequences by altering the metabolism of intestinal cells, impairing DNA synthesis and reducing the life expectancy of cells [46]. These changes encourage the multiplication of damaged cells in the intestine with altered metabolism. Levels of NH_4 reported in this paper are closer to the lower levels reported in the literature [46], and were decreased further after CH-OPT supplementation whereas no change was reported with CH-GL. Besides NH_4 in the colon, dysbiosis is also observed with a high production of H_2S content, which is another microbial biomarker of the large intestine and associated with high levels of fermented protein and sulfur containing amino acids [46,56]. Levels of H_2S measured after CH supplementation were much lower than levels shown to cause significant DNA damage (250 μM) [46]. Furthermore, H_2S at low concentrations has

recently been reported to be a beneficial gas produced in the GI tract, by helping to prevent dysbiosis and avoid GI damage associated with taking NSAIDS [58].

The benefits of SCFA production and improvements to GI gas content seen with the CH-OPT treatment could be partially offset by the corresponding increase in isovaleric acid, since enhanced gut exposure to BCFAs has been linked to an increased risk for diabetes and obesity [55]. Furthermore, although not much information is currently known about the health modulatory properties of minor SCFAs, recent research has suggested that fecal valeric acid may serve as an indicator of gut microbial dysbiosis [52]. Hence, the increase in valeric acid concentrations observed with CH-OPT could be indicative of adverse changes in gut microbial composition. An additional potential concern are reports that fecal valeric acid is positively correlated with the pro-inflammatory C-reactive protein in patients with ischemic stroke [78]. Conversely, the conjugated base of valeric acid has been associated with enhancing interleukin-10 production and suppressing Th17 cells, which could provide anti-inflammatory benefits [79]. The immunomodulatory effects of valeric acid need further investigation, particularly in relation to OA and rheumatoid arthritis as these are conditions associated with an increase in joint and whole body proinflammatory processes [80]. Interestingly, the lack of effect of the CH-GL on the SCFA and BCFA production and other microbial biomarkers of NH_4 and H_2S indicates that this supplement has neither prebiotic nor dysbiotic properties in contrast to CH-OPT.

As CH supplements continue to grow in popularity and are widely available for OA patients, our study was designed to address the significant literature gaps concerning the digestibility of CHs and their potential prebiotic effects. The effects of microbial metabolite production after CH supplementation may not only depend on the CH product fermented, but also on the initial dose of supplement. The treatment dose used in this study was based on the daily dose of the Genacol Original Formula® that was shown to reduce joint pain in clinical trials [12,13,18]. Other clinical studies, however, have used much greater doses ranging from 5 to 35 g of hydrolyzed collagen products [14,15,17,19,81,82]. It is conceivable that with a higher initial dose of CHs, greater microbial fermentation could have occurred due to more substrate availability for fermentation with subsequent greater increases in SCFAs, BCFAs, colonic gas production and antioxidant capacity. The effective dose regarding pain management but also colonic metabolite production needs to be further

investigated, as there is currently no standardized treatment dose. Our work is the first to establish that CH products utilized by OA patients can exert prebiotic effects, particularly in the ascending colon. Further research is needed using 16S rRNA gene amplicon sequencing to profile gut microbiota community structure and composition as affected by CH supplementation. It is possible that an increase in beneficial colonic metabolites could improve joint structure as well as prevent cartilage loss, as recent research has suggested a connection of the gut microbiome to OA [4]. Supplementation using the prebiotic oligofructose to obese OA mice changed the host microbiota to a healthier profile, notably by supporting the growth of *Bifidobacterium pseudolongum*. Beneficial changes to the microbiome were associated with decreased systemic inflammation, which decreased OA progression by regulating joint inflammation, chondrocyte hypertrophy, osteophyte formation, as well as joint mineralization.

5.6 Conclusion

To date, there is limited information regarding the digestion of food-derived peptides and the effects on the gut microbiome and microbial fermentation products such as SCFAs, BCFAs, NH_4 and H_2S. The present study provides the first evidence and characterization of peptides released after upper intestinal digestion. Furthermore, this study also provides first evidence that CHs can lead to the generation of SCFAs and BCFAs, although this microbial metabolic activity appears to be dependent on the nature of the CH tested, which corresponds to differing peptide diversities after upper intestinal digestion. Interestingly, changes to biomarkers of microbial health primarily only affect the ascending colon, indicating that CH products provide insufficient peptide and AA material to the transverse and descending colon. A recent review has highlighted that, long-term dietary choices such as greater protein content could exert effects on GI microbial populations, which has implications towards development of metabolic diseases such as obesity and diabetes [43]. This review emphasized that important knowledge gaps exist concerning dietary protein-mediated generation of colonic microbial molecules that could exert bioactivities towards gut inflammation and permeability. Accordingly, it is possible that CH supplements, which have a rich peptide content, can impact the structure and function of gut microbial communities. Dynamic GI model platforms, such the one utilized in the present study, can be a useful tool to further investigate the impact of CH supplementation on the gut microbiota to more fully understand the impact of these nutraceuticals on GI and systemic health.

5.7 Funding

The present study was supported by a MITACS Accelerate Program Ph.D. studentship (IT10556) collaboration between McGill University and Genacol Canada Corporation and the Collaborative Research Development Grant Program from the Natural Sciences and Engineering Council of Canada to S.K. (535744-18).

5.8 Acknowledgments

We would like to thank Mohd Baasir Gaisawat for his support in the operation of the dynamic GI model. We would also like to acknowledge the McGill University Health Center (MUHC) drug discovery platform and proteomics department for their support in performing the MALDI and proteomics analyses, respectively.

5.9 Supplementary data

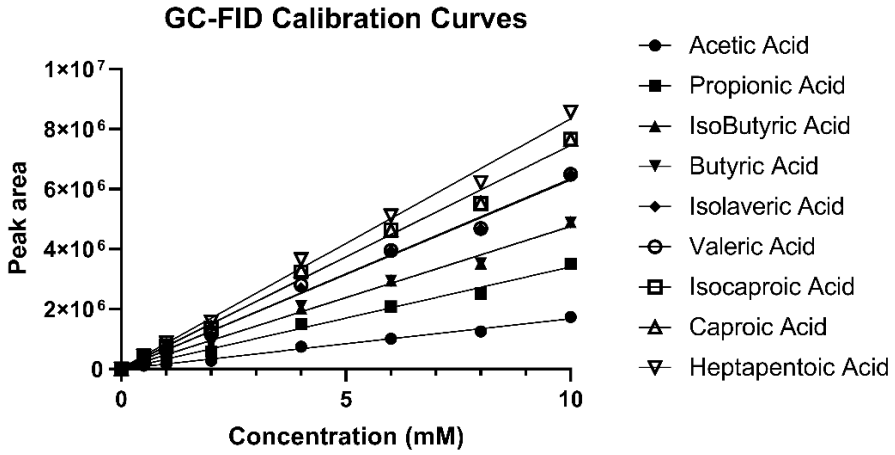

Figure S5.1. SCFA and BCFA standard curves based on peak area and concentration. Linearity was assessed using R^2; all were above 0.99.

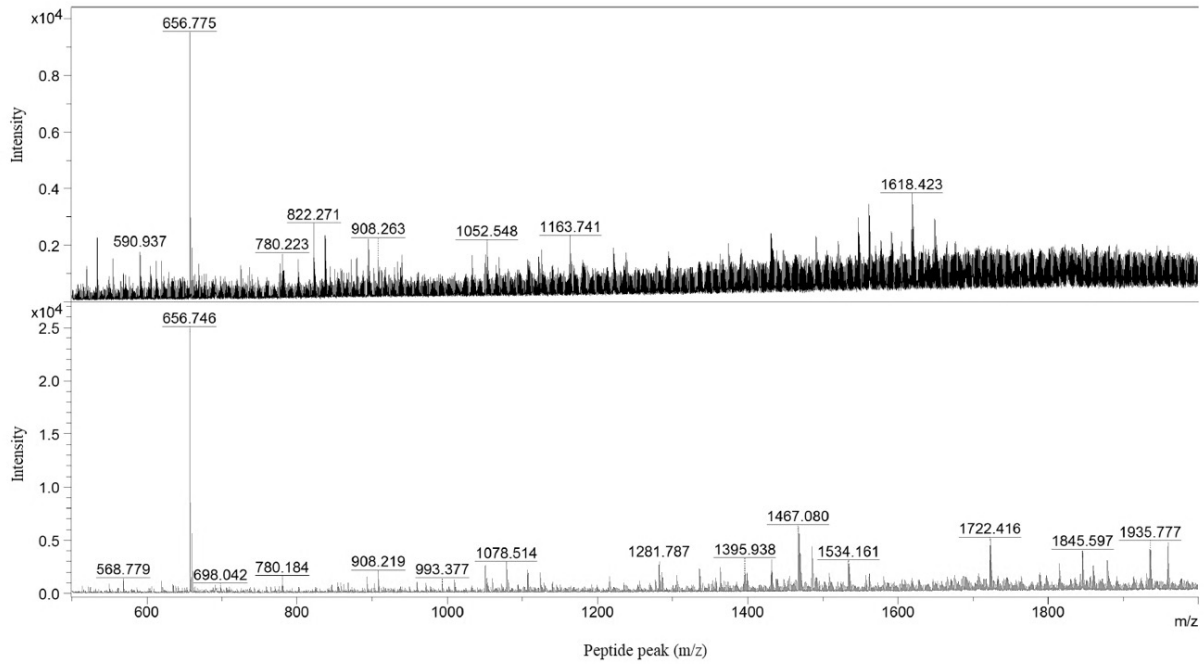

Figure S5.2. Peptide profile and content. Lower molecular mass chromatograms (500-2000 m/z) of CHs before upper GI digestion. Top chromatogram CH-GL, bottom chromatogram CH-OPT.

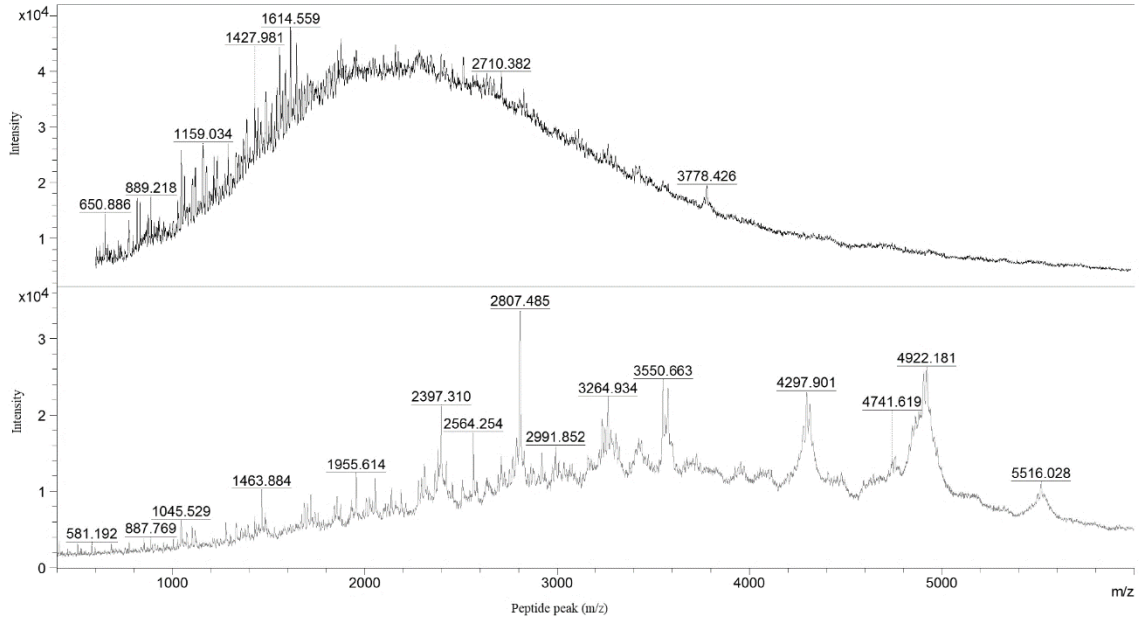

Figure S5.3. Peptide profile and content. Higher molecular mass chromatograms (100-5000 m/z) of CHs before upper GI digestion. Top chromatogram CH-GL, bottom chromatogram CH-OPT.

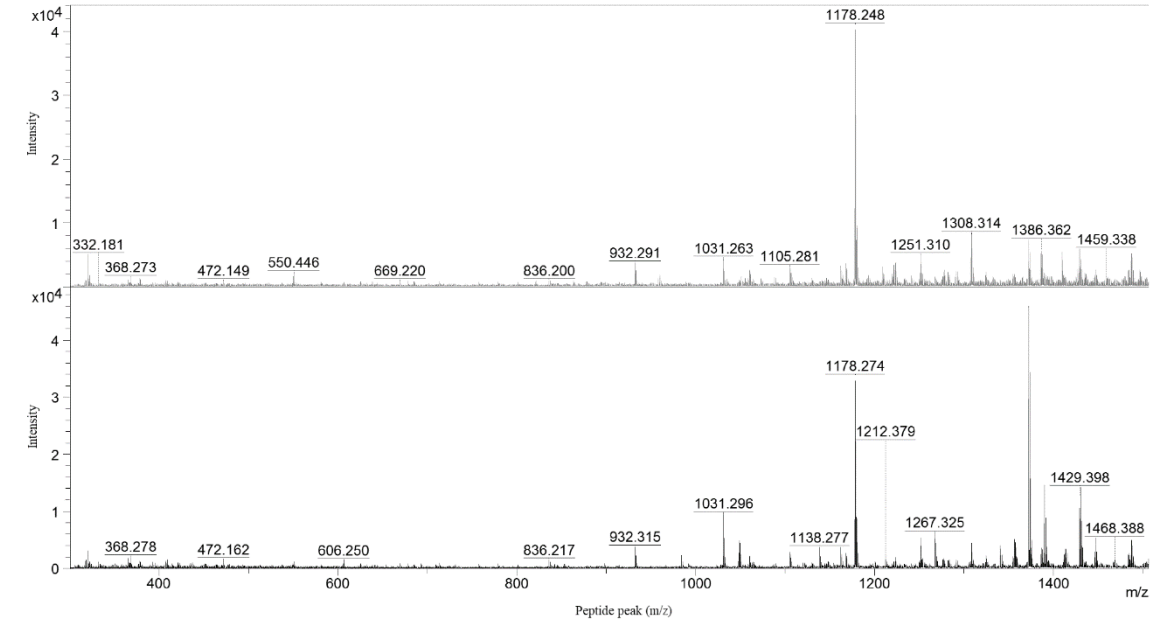

Figure S5.4. Peptide profile and content. Lower molecular mass chromatograms (300-1500 m/z) of CHs after upper GI digestion. Top chromatogram CH-GL, bottom chromatogram CH-OPT.

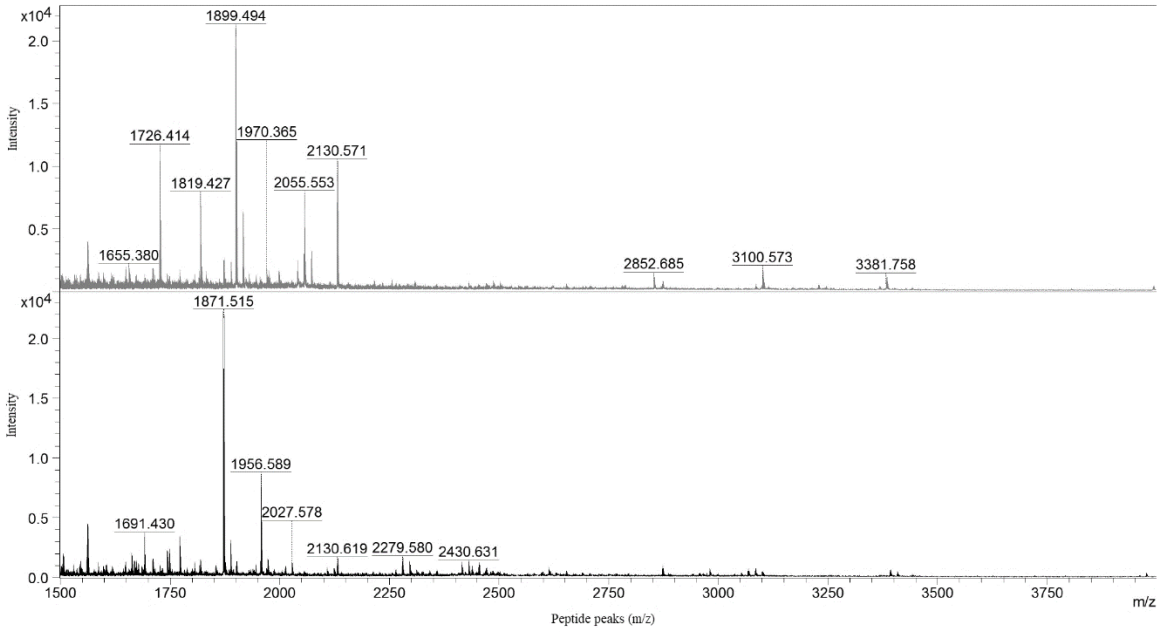

Figure S5.5. Peptide profile and content. Higher molecular mass chromatograms (1500-4000 m/z) of CHs after upper GI digestion. Top chromatogram CH-GL, bottom chromatogram CH-OPT.

Table S5.1. List of the peptide sequences from CH-GL and CH-OPT before upper intestinal digestion. Each letter is indicative of an amino acid.

Peptide Sequences		
CH-GL	CH-OPT	Shared sequences
AAGPTGPIGSR	AGPAGPAGPAGPR	AGPSGPAGPTGAR
AGPPGADGQPGAK	GPAGPAGPAGPR	GPAGPAGPRG
AGPSGPSGLPGER	GPAGPAGPAGPRG	GRPGPIGPA
AGPSGPSGLPGERG	GPAGPQGPR	
AIGPSGPAGKD	GPAGPQGPRG	
ARGSDGSVGPVGPA	GPMGPSGPRG	
AVGPAGKDGEAGAQ	GPRGPSGPQG	
AVGPAGPRGPAGPSGPAGKDGR	GPVGAPGRP	
AVGPRGPSGPQG	GPVGAPGRPG	
DGAPGKDGVRG	GSPGPQGPPGSIGPQ	
FDGDFYR	GSPGPQGPPGSIGPQG	
FSGLDGAKGD	PAGPQGPRG	
GAAGPTGPIGSR	SGPPGPPGPA	
GADGAPGKDGVRG	SPGPQGPPGSIGPQ	
GADGAPGKDGVRGL	VGSPGPAGPRG	
GDRGEAGPAGPAGPAGPR	VPGPMGPSGPR	
GDRGETGPAGPA	VPGPMGPSGPRG	
GDRGETGPAGPAGPIGPVGAR		
GDRGETGPAGPS		
GEGGPQGPRGS		
GEGGPQGPRGSEGPQG		
GEPGKQGPSGASGE		
GERGEQGPA		
GERGFPGLPGPS		
GGPQGPRGSEGPQG		
GKDGEAGAQGPPGPAGPA		
GKSGDRGETGPAGPA		
GKSGDRGETGPAGPAGPIGPV		
GKSGDRGETGPAGPAGPIGPVG		
GKSGDRGETGPAGPAGPIGPVGAR		
GPAGKSGDRGETGPAGP		
GPAGPSGPAGKDGR		
GPIGPVGAR		
GPQGPPGSIGPQ		
GPQGPPGSIGPQG		
GPSGLPGERG		
GPTGPIGSR		

Table S5.1. continued List of the peptide sequences from CH-GL and CH-OPT before upper intestinal digestion. Each letter is indicative of an amino acid.

Peptide Sequences		
CH-GL	CH-OPT	Shared sequences
GPVGPSGPPGKD		
GQGDPGRPGIPA		
IDGRPGPIGPA		
IGPSGPAGKD		
IQGPPGPAGEEGKRG		
ISVPGPMGPSGPR		
LDGAKGDAGPAGPK		
LGPVGNPGPAGPAGPR		
LMGPRGPPG		
PGDKGEAGPSGPAGPTGA		
PGPAGPAGPR		
QGDPGRPGIPA		
RGPRGDQGPVGR		
SGDRGETGPAGPA		
SGDRGETGPAGPS		
TAGPSGPSGLPGERG		
TGPAGPAGPIGPVGAR		
VGPAGPRGPA		
VGPAGPRGPAGPS		
VGPAGPRGPAGPSGPAGKDGR		
VGPRGPSGPQG		
VMGPAGSRG		
VQGPPGPAGPR		
VQGPPGRPGPQ		
VVGLPGQR		

Table S5.2. List of the peptide sequences from CH-GL and CH-OPT after upper intestinal digestion.

Peptide Sequences		
CH-GL	CH-OPT	Shared Sequences
AAGPPGPTGPAGPPGFPGAVGAK	AAGEPGKAGER	AAGAPGPQGPVGPVGK
AAGPPGPTGPAGPPGFPGAVGAKGEGGPQGPR	AAGEPGKNGAK	AAGLPGVAGAPGLPGPR
AFLSIHS	AAGLPGPKGDRGDAGPK	AGAPGAPGSQGAPGLQGMPGER
AGPPGLLGPPGPR	AAGPSGPNGLPAGSR	AGAPGPQGPVGPVGK
AGPPGPTGPAGPPGFPG	AAGPTGPIGSR	AGEAGKPGER
ANGIPGPIGPPGPR	AAGPTGPIGSRG	AGLPGVAGAPGLPGPR
APGAPGPVGPA	AAGQPGAKGER	AGPPGFPGAPGPK
AVGPAGAVGPR	ADGPAGAPGTPGPQG	AGPPGPTGPAGPPGFPGAVGAK
DARPNSWPWQ	AGAPGIPGGK	AGPPGPTGPAGPPGFPGAVGAKGEGGPQGPR
DGANGIPGPIGPPGPR	AGAPGIPGGKGDSGAPGER	AGPSGPSGLPGER
DGATGAAGPPGPTGPAGPPGFPGAVGAK	AGAPGLPGPR	AGPSGPSGLPGERG
DGDPGLRGPPGLPGPL	AGAPGPPGPPGSDGSPGGK	DGEAGAQGPPGPAGPAGER
DGIPGQPGLPGP	AGEDGHPGKPGRPGE	DGLNGLPGPIGPPGPR
DGLPGLPGLPGPP	AGEDGHPGKPGRPGERG	DGLNGLPGPIGPPGPRG
DGRPGPIGP	AGEPGKAGER	DGPRGPTGPIGPPGPA
DGRPGPIGPA	AGEPGRDGNPGSDGLPGR	DKGEPGDKGPR
DGSPGAKGDRGETGPAGPPGAPGAPGAPGPVGPAGK	AGFPGSPGAK	DTEYFGTIGIGTPAQDF
DLGPRGPPGIPGREGPK	AGPAGAAGQPGAKGER	EGPVGLPGIDGRPGPIGPA
DLSFLPQPPQ	AGPAGPAGPAGPR	ERGPPGNPGLP
DLSFLPQPPQE	AGPAGPKGEPGSPGENGAPGQMGPR	EVGPRGLPGEPGP
DNIWDQGLVSQDL	AGPAGPPGPPGAIGPSGPAGK	FGLPGPAGAR
DQGLVSQDLFS	AGPIGSAGPPGFPG	FQGPPGEPGEPGASGPMGPR
DRGETGPAGPAGPIGPVG	AGPPGADGQPGA	FRNVVDGQPF
DRGETGPAGPAGPIGPVGA	AGPPGADGQPGAK	GAAGEPGKAGER
DTEYFGTIGIGTPAQD	AGPPGESGR	GAAGLPGVAGAPGLPGPR
DTGSSNLWVPS	AGPPGPAGPAGPPGP	GANGAPGIAGAPGFPGAR
DTVQVGGISDTNQIFG	AGPPGPPGPAGK	GAPGDRGEPGPPGPAGF
EFGFDGDFYR	AGPPGPSGPPGEK	GAPGPQGPVGPVGK

Table S5.2. continued List of the peptide sequences from CH-GL and CH-OPT after upper intestinal digestion.

Peptide Sequences		
CH-GL	CH-OPT	Shared Sequences
EFGFDGDFYRA	AGPTGPIGSR	GAPGTAGPSGPSGLPGER
EGIGKPGAP	AGPTGPIGSRG	GARGEPGPAGLPGPPGE
EGPVGLPGIDGR	AGQPGAKGER	GDGGPPGATGFPGAAG
EGPVGLPGIDGRPGPI	AGRPGEAGLPGAK	GDRGETGPAGPAGPIGPV
EGPVGLPGIDGRPGPIG	AGSPGKDGLNGLPGPIGPPGPR	GDRGETGPAGPAGPIGPVG
EGPVGLPGIDGRPGPIGPAG	AIGFPGPK	GDRGETGPAGPAGPIGPVGA
EGPVGLPGIDGRPGPIGPAGA	AIGPSGPAGK	GDRGETGPAGPPGAPGAPGAPG PVGPAG
EGPVGLPGIDGRPGPIGPAGAR	AKGDPGPR	GEPGNIGFPGPK
EGSPGPLGPIGPPGVR	AKGEPGDAGAK	GEPGPAGAVGPAGAVGPR
EPGPLGIAGPPGAR	ANGLPGEKGPPGDR	GEPGPAGLPGPP
ERGPPGPMGPPGLAGPPGESGR	APGPKGAR	GEPGPAGLPGPPG
ETGPAGPAGPIGPV	AQGPPGPAGPAGER	GEPGPAGLPGPPGE
ETGPAGPAGPIGPVG	ARGEPGPAGLPGPPGER	GEPGPAGLPGPPGER
ETGPAGPAGPIGPVGA	ARGPAGPQGPR	GEPGPLGIAGPPGAR
FDGDFYR	ARGPPGPPGK	GEPGPTGIQGPPGPAGEEGK
FDNIWDQGLVS	ARGPPGPPGTNGVPGQR	GEQGPAGSPGF
FDNIWDQGLVSQ	ARGPSGPQGPSGPPGPK	GERGPPGESGAAGPTGPIGS
FGFDGDFYR	ARGPSGPQGPSGPPGPKGNSGE PGAPGSK	GETGPAGPAGPIGPVG
FGFDGDFYRA	ARGSDGSVGPVGPA	GFPGADGVAGPK
FGTIGIGTPA	ARGSDGSVGPVGPAGP	GFPGADGVAGPKGPAGE
FGTIGIGTPAQD	ASGHPGPIGPPGPR	GFPGADGVAGPKGPAGER
FLGLPGSR	ASGPAGPRGPPGSAGSPGK	GFPGLPGPSGEPGK
FPGERGLPGA	ASGPAGPRGPPGSAGSPGKDG	GFPGLPGPSGEPGKQ
FPGLPGPSGEPGK	ASGPMGPR	GFPGLPGPSGEPGKQGAPGA
FPGPKGANGEPGK	AVAGPPGPSGPPGEK	GFPGLPGPSGEPGKQGPSGA
FPGYPGPK	AVGPAGKDGEAG	GFPGLPGPSGEPGKQGPSGASG ER
GAAGPPGPTGPAGPPGFPGAVG AK	AVGPAGKDGEAGAQ	GFQGPPGEPGEPGASGPMGPR
GAPGAIGAPGPAGANGDRGEA GPAGPAGPAGPR	AVGQPGPPGPSGEEGK	GFSGLDGAK
GAPGFLGLPGSR	AVGSPGPAGPR	GFSGLDGAKGDAGPAGPK
GAPGFPGPK	DGAKGDAGPAGPK	GFSGLQGPPGPPGSPGEQGPSG ASGPAGPR

Table S5.2. continued List of the peptide sequences from CH-GL and CH-OPT after upper intestinal digestion.

Peptide Sequences		
CH-GL	CH-OPT	Shared Sequences
GAPGIAGAPGFPGAR	DGAKGDAGPAGPKGEPGSPGENGAPGQMGPR	GHGAGGASIL
GAVGPAGAVGPR	DGASGHPGPIGPPGPR	GHNGLDGL
GDAGPPGPAGPAGPPGPIG	DGEAGAQGPPGPAGPA	GIDGRPGPIGPA
GDGGPPGATGFPGAAGR	DGEAGAQGPPGPAGPAGE	GIPGPFGPR
GDLGPRGPPGIPGREGPK	DGEAGAQGPPGPAGPAGERGEQGPAGSPGF	GIRGPPGLP
GDPGMPGLPGLKGDEGIQGLP	DGNPGSDGLPGR	GISVPGPMGPSGPR
GDRGETGPAGPPGAPGAPGAPGPVGPAGK	DGPRGPTGP	GLNGLPGPIGPPGPR
GDTGAKGEPGPTGIQGPPGPAGEEGK	DGRPGPPGPPGAR	GLPGAKGAAGLPGVAGAPGLPGPR
GDVGPLGPLGKEGPPGPR	DGSPGAKGDR	GLPGLKGHNGLQGLPGL
GEIGPAGPPGPPGLR	DGSPGAKGDRGETGPAGPPGAPGAPGAPGPVGPA	GLPGLKGHNGLQGLPGLA
GENGVPGEDGAPGPMGPR	EAGPAGPAGPAGPR	GLPGPIGPPGPR
GEPGPPGLDQP	EGAPGAEGSPG	GLPGPPGAPGPQGF
GEPGPTGIQGPPGPAGEEGKR	EGAPGAEGSPGR	GLPGPPGAPGPQGFQGPPGEPGEPGASGPMGPR
GETGPAGPAGPIGPV	EGAPGAEGSPGRDGSPGA	GLPGVAGSVGEPGPLGIAGPPGA
GETGPAGPAGPIGPVGA	EGAPGAEGSPGRDGSPGAK	GLPGVAGSVGEPGPLGIAGPPGAR
GETGPAGPAGPIGPVGAR	EGLRGPR	GLTGPIGPPGPAGAPGDK
GETGPAGPPGAPGAPGAPGPVGPAGK	EGPQGPPGPVGSPGER	GNDGATGAAGPPGPTGPAGPPGFPGAVGAK
GEVGFQGKTGPPGPPG	EGSKGPRG	GPAGLPGPPGER
GEVGLPGLSGPVGPPGNPGANGLPGAKGAAGLPGVAGAPGLPGPR	EPGSSGVDGAPGKDGPRGPTGPIGPPGPAGQPGDK	GPIGPPGPR
GEVGPAGPNGF	FAGPAGAAGQPGAKGER	GPPGEPGEPGASGPMGPR
GFDGDFYRA	FAGPPGADGQPGAK	GPPGESGAAGPTGPIGS
GFDGLDFDWEYPGSR	FDNIWDQGLVSQDL	GPPGESGAAGPTGPIGSR
GFLLPASQIIPTAQ	FLPQPPQEK	GPPGPMGPPG
GFMPSDR	FSGLDGAK	GPPGPMGPPGL
GFPGLPGPS	FSGLDGAKG	GPPGPMGPPGLAGPPGESG
GFPGPPGPIGL	FSGLDGAKGD	GPPGPMGPPGLAGPPGESGR
GFPGPPGPK	GAAGEPGKAGE	GPPGPPGPPGPPGPPSG
GFPGSPGNIGPAGK	GAAGEPGKNGAK	GPPGPPGPPGPPGPPSGGY

Table S5.2. continued List of the peptide sequences from CH-GL and CH-OPT after upper intestinal digestion.

Peptide Sequences		
CH-GL	CH-OPT	Shared Sequences
GFPGTPGLPGFK	GAAGIPGGKGEK	GPPGPPGPPGPPGPPSGGYD
GFPGTPGLPGFKG	GAAGIPGGKGEKGETGL	GPPGPSGLPGLP
GFPGTPGLPGFKGI	GAAGLPGPK	GPPGSAGSPGKDGLNGLPGPIGPPGPR
GFPGTPGLPGFKGIR	GAAGLPGPKGD	GPPGSAGSPGKDGLNGLPGPIGPPGPRG
GFPGYPGPK	GAAGLPGPKGDR	GPSGPSGLPGER
GGGYEFGFDGDF	GAAGLPGPKGDRGD	GPSGPSGLPGERG
GGGYEFGFDGDFYR	GAAGLPGPKGDRGDAGPK	GPTGPIGPPGPA
GGISDTNQIF	GAAGPTGPIGSR	GRTGDAGPAGPPGPPGPPGPPGPPS
GGISDTNQIFG	GAAGQPGAKGER	GRTGDAGPAGPPGPPGPPGPPGPPSG
GGPGPMGLMGPR	GADGAPGKDG	GSAGPPGATGFPGAAG
GGYDLSFLPQPPQE	GADGAPGKDGV	GSAGPPGATGFPGAAGR
GGYEFGFDGDF	GADGAPGKDGVR	GSPGERGEVGPAGPNGF
GHPGPPGPVGPA	GADGAPGKDGVRG	GSVGEPGPLGIAGPPGAR
GIDGRPGPIGP	GAKGDAGAPGAPGSQGAPGLQGMPGER	GVPGDLGAPGPSGAR
GIDGRPGPIGPAGA	GAKGEPGDAGAK	GVPGPPGAVGPAGK
GIPGEFGLPGPAGA	GANGAPGNDGAK	GVPGPPGAVGPAGKDGEAGAQGPPGPAGPAGE
GIPGEFGLPGPAGAR	GANGAPGNDGAKGDAGAPGAPGSQGAPGLQGMPGER	GVPGPPGAVGPAGKDGEAGAQGPPGPAGPAGER
GIPGEFGLPGPAGARGER	GANGDRGEAGPAGPAGPAGPR	GVVGLPGQR
GIPGLPGPR	GAPGADGPAGAPG	HMWPGDIK
GIPGLPGPRG	GAPGADGPAGAPGTPGPQ	IDGRPGPIGP
GIPGPVGAAGATGAR	GAPGADGPAGAPGTPGPQG	IDGRPGPIGPA
GISVPGPMGPSGPRG	GAPGADGPAGAPGTPGPQGIAGQ	IGFPGPKGPSGDPGK
GIVGLPGQR	GAPGAIGAPGPA	IGPAGPPGPPGLR
GLLGLPGQPG	GAPGAPGAPGPVGPA	ILGDVFIR
GLLGPKGPPGIPGPPGV	GAPGAPGPVGPA	ISVPGPMGPSGPR
GLLGPKGPPGPPGPPGVTGM	GAPGAVGPAGPR	LNGLPGPIGPPGPR
GLPGADGRAGVMGPAGSR	GAPGDKGEAGPSGPAGPT	LPGPIGPPGPR
GLPGEMGRP	GAPGDRGEPGPPGPA	LQGPPGPPGSPGEQGPSGASGPAGPR

Table S5.2. continued List of the peptide sequences from CH-GL and CH-OPT after upper intestinal digestion.

Peptide Sequences		
CH-GL	CH-OPT	Shared Sequences
GLPGLKGHNGLQGLPGLAGHHGDQGAPGAVGPAGPR	GAPGDRGEPGPPGPAG	LSFLPQPPQE
GLPGLPGEKGHT	GAPGEKGEGGPPGAAGPA	NGDDGEAGKPGRPGER
GLPGLPGPK	GAPGFPGPR	NGLPGPIGPPGPR
GLPGPAGPPGE	GAPGIPGGK	PGADGVAGPK
GLPGPIGPKG	GAPGNDGAK	PGFGLPGK
GLPGPIGPPGPRG	GAPGPAGPK	PGPMGPSGPR
GLPGPLGPPGP	GAPGPAGPKGSPGEAGRPGEAGLPGA	QGLPGPAGPPGEAGKPGEQGVPGDLGAPGPSGAR
GLPGPPGAP	GAPGPAGPKGSPGEAGRPGEAGLPGAK	QGPPGEPGEPGASGPMGPR
GLPGPPGAPGP	GAPGPAGPKGSPGEAGRPGEAGLPGAKG	RGEPGNIGFPGPK
GLPGTAGLPGMK	GAPGPAGSRGPPGPQGPR	RGETGPAGPAGPIGPVG
GLPGVAGAPGLPGPR	GAPGPMGPR	RGETGPAGPAGPIGPVGA
GLPGVAGSVGEPGPL	GAPGPQGPPGAPGP	RGPPGPMGPPGLAGPPGESGR
GLPGVAGSVGEPGPLGI	GAPGPQGPPGAPGPL	SGATPVFDNIWDQGLVSQDL
GLQGLPGLAGHHGDQGAPGAVGPAGPR	GAPGPQGPPGAPGPLG	SGDRGETGPAGPAGPIGPV
GLSGLPGPPGPPGPR	GAPGSKGDTGAK	SGDRGETGPAGPAGPIGPVG
GLTGPIGPPGPAGAPGDKGEAGPSGPAGPT	GAPPGEGPGEQK	SGDRGETGPAGPAGPIGPVGA
GLTGPIGPPGPAGAPGDKGEAGPSGPAGPTGA	GARGEPGPAGLPGPPGER	SGLQGPPGPPGSPGEQGPSGASGPAGPR
GLTGPIGPPGPAGAPGDKGEAGPSGPAGPTGAR	GARGEPGPAGLPGPPGERGGPGS	SVPGPMGPSGPR
GNIGFPGPK	GASGHPGPIGPPGPR	TGDAGPAGPPGPPGPPGPPGPPS
GNPGQPGQPGLP	GAVGQPGPPGPSGEEGK	TGISVPGPMGPSGPR
GPAGLPGVPGR	GDAGAPGAPGSQGAPGLQGMPGER	TGPPGPSGISGPPGPPGPAGK
GPAGPAGPIGP	GDAGPAGPK	VALRGPPGP
GPAGPAGPIGPV	GDAGPAGPKGEPGSPGENGAPGQMGPR	VGGISDTNQIF
GPAGPAGPIGPVG	GDAGPPGPAGPA	VPGPMGPSGPR
GPAGPAGPIGPVGA	GDAGPPGPAGPAGPPGP	
GPAGPIGPV	GDAGPPGPAGPAGPPGPI	
GPAGPIGPVG	GDAGPPGPAGPAGPPGPIGN	

Table S5.2. continued List of the peptide sequences from CH-GL and CH-OPT after upper intestinal digestion.

Peptide Sequences		
CH-GL	CH-OPT	Shared Sequences
GPAGPIGPVGA	GDIGSPGRDGA	
GPAGPPGLLGP	GDKGEPGDKGPR	
GPAGPPGLLGPPGPR	GDKGEPGSSGVDGAPGK	
GPAGPPGLLGPPGPRG	GDKGEPGSSGVDGAPGKDGPR	
GPAGPPGPPGLR	GDKGEQGPPGPTGPQGPIG	
GPAGPPGPPGLRG	GDKGETGEQGDR	
GPGPMGLMGPR	GDKGETGEQGDRG	
GPIGFPGPK	GDQGAPGAVGPAGPR	
GPIGPPGIP	GDRGDAGPK	
GPIGPPGIPGPK	GDRGDAGPKGADGAPGKDGV	
GPIGPPGPRG	GDRGEAGPA	
GPIGPPGRP	GDRGEAGPAGPA	
GPMGLMGPR	GDRGEAGPAGPAGPAGPR	
GPPGAPGLPG	GDRGENGSPGAPGAPGHPGPP GPVGPA	
GPPGAPGLPGQ	GDRGETGPAGPA	
GPPGAPGPLGI	GDRGETGPAGPAGPIGP	
GPPGASGAPGPQGF	GDRGETGPAGPPGAP	
GPPGEPGEPGA	GDRGETGPAGPPGAPGAPGAPG PVGPA	
GPPGFGLPGK	GDRGETGPAGPSGAPGPAGSR	
GPPGFPGPK	GDSGAPGERGPPGAGGPPGPR	
GPPGFQGLP	GDSGAPGERGPPGAGGPPGPRG	
GPPGHPGLP	GDSGPPGER	
GPPGLLGPPGPR	GDSGPPGERGAPGPQG	
GPPGLPGLPGFK	GDSGRPGEPGLMGPR	
GPPGLPPPRVVGASP	GEAGAPGIPGGK	
GPPGPPGFPGKP	GEAGAPGIPGGKGDSGAPGER	
GPPGPPGLPGPK	GEAGAPGIPGGKGDSGAPGERG PPG	
GPPGPPGPPGPK	GEAGAPGIPGGKGDSGAPGERG PPGAGGPPGPR	
GPPGPPGPPGPPGLR	GEAGAQGPPGPAGPAGER	
GPPGPPGPPGPPGPPS	GEAGKPGER	
GPPGPPGPPGPPGPPSGGYDL	GEAGPAGPAGPAGPR	
GPPGPTGPAGPPGFPG	GEAGSPGIAGPK	

Table S5.2. continued List of the peptide sequences from CH-GL and CH-OPT after upper intestinal digestion.

Peptide Sequences		
CH-GL	CH-OPT	Shared Sequences
GPPGQPGLP	GEDGKDGSPGEPGANGLPG	
GPSGPQGPSGPPGP	GELGPVGNPGPAGPAGPR	
GPTGLPGPAGPPGL	GENGPVGPTGPVGAAGPSGPNGPPGPAGSR	
GPTGPIGPPGP	GEPGAKGER	
GPTGPIGPPGPAG	GEPGAVGQPGPPGPSGEEGK	
GPVGPAGPIG	GEPGDAGAK	
GPVGPTGPVGAAGPSGPNGPPGPAGSR	GEPGPAGLPGPPGERGGPGS	
GRPGAPGPAGAR	GEPGPPGQP	
GRPGLPGPI	GEPGPQGH	
GSDGSVGPVGPAGPI	GEPGPRGPPGA	
GSDGSVGPVGPAGPIG	GEPGRDGNPGSDGLPGR	
GSDGSVGPVGPAGPIGSAGPPG	GEPGSPGENGAPGQMGPR	
GSDGSVGPVGPAGPIGSAGPPGF	GEQGPAGPPGFQ	
GSDGSVGPVGPAGPIGSAGPPGFPGAPGPK	GEQGPPGPAGFPGAPGQNGEPGAK	
GSDGSVGPVGPAGPIGSAGPPGFPGAPGPKGEL	GEQGPSGASGPAGPR	
GSTGEIGPAGPPGPPGL	GERGEAGSPGIAGPK	
GSTGEIGPAGPPGPPGLR	GERGPPGESG	
GSVGPVGPAGPIGSAGPPGFPGAPGPK	GERGPPGESGAAGPT	
GTAGPSGPSGLPGER	GERGPPGESGAAGPTGPIG	
GTGSMTGILGYDTVQVGGI	GERGPPGESGAAGPTGPIGSR	
GTGSMTGILGYDTVQVGGISDTNQ	GERGPPGNPGLP	
GTGSMTGILGYDTVQVGGISDTNQIFG	GERGSPGGP	
GVDGLPGQPGPR	GESGAPGVPGIAGPR	
GVMGFPGPK	GESGNKGEPGAVGQPGPPGPSGEEGK	
GVMQGPMGPMGPR	GETGAPGLKGENGVPGENGAPGPMGPR	
GVPGPPGAVGPAGKDGEA	GETGPAGPPG	
GYDLSFLPQPPQ	GETGPAGPPGAPGAPGAPGPVGPA	

Table S5.2. continued List of the peptide sequences from CH-GL and CH-OPT after upper intestinal digestion.

Peptide Sequences		
CH-GL	CH-OPT	Shared Sequences
GYDTVQVGGI	GETGPAGPSGAPGPAGSR	
GYPGNAGPVGAAGAPGPQGPV GPVGK	GETGPAGRPGEVGPPGPPGPA	
IAGAPGFPGAR	GETGPQGPPGPTGPSGDKGD	
IDGRPGPIGPAG	GEVGAPGDPG	
IGQPGAVGPAGI	GEVGPAGPNGFAGPAGAAGQP GAKGE	
IGQPGAVGPAGIR	GEVGPAGPNGFAGPAGAAGQP GAKGER	
IGQPGAVGPAGIRG	GEVGPRGLPGEPGP	
ILGDVFIRQ	GFMPSDRA	
ILGDVFIRQY	GFPGAPGQNGEPGAK	
ILGPPGPR	GFPGLPGPSGEPGKQGAPG	
IPGLPGVPGPRGP	GFPGLPGPSGEPGKQGAPGAS	
ISGPSGPIGPPGIPGPK	GFPGLPGPSGEPGKQGPS	
ISVPGPMGPSGPRG	GFPGLPGPSGEPGKQGPSG	
KGEPGVVGAPGTAGPSGPSGLP GER	GFPGLPGPSGEPGKQGPSGAS	
KNWGEGW	GFPGLPGPSGEPGKQGPSGASG E	
LDTEYFGTIGIGTPAQDF	GFPGNPGAPGSPGPA	
LGAPGFLGLPGSR	GFPGNPGAPGSPGPAGH	
LGFPGER	GFPGNPGAPGSPGPAGHQGAV GSPGPAGPR	
LGPLGAPGEDGRPGPPGSIGI	GFPGPKGAAGEPGKAGER	
LGSLGSPGLPGLPGPPG	GFPGPPGMKGPA	
LGVPGLPGYPGR	GFPGSPGAK	
LPASQIIPTAQ	GFSGLDGAKGD	
LPGDRGPPGPPGI	GFSGLDGAKGDAGPAGPKGEPG SPGENGAPGQMGPR	
LPGLPGPK	GGAGPPGPEGGK	
LTGPIGPPGPAGAPGDKGEAGPS GPAGPTGAR	GGPGERGEQGPPGPA	
MGFPGPK	GGPGERGEQGPPGPAGFPGAPG QNGEPGAK	
MGIKGHRGFPGNPGAPGSPGPA GHQGAVGSPGPAGPR	GGPGERGEQGPPGPAGFPGAPG QNGEPGAKGE	

Table S5.2. continued List of the peptide sequences from CH-GL and CH-OPT after upper intestinal digestion.

Peptide Sequences		
CH-GL	CH-OPT	Shared Sequences
MGPPGEPGLPG	GGPGGPGPKGDKGEPGSSGVDGAPGK	
MMGPPGPPGPLGIPGR	GGPGGPGPQGPAG	
MQGPMGPMGPR	GGPGGPGPQGPAGK	
MWPGDIK	GGPGPAGPR	
PAGPAGPIGPV	GGPGSRGFPGADGVAGPK	
PAGPAGPIGPVG	GGQGPPGSPGPK	
PAGPAGPIGPVGA	GHNGLDGLKGQPGAPGVKGEPGAPGENGTPGQTGA	
PAGPPGLLGPPGPR	GHNGLQGLPGLAGH	
PGADGVAGPKGPAGER	GHPGPIGPPGPR	
PGAPGFPGPK	GIAGPPGAR	
PGEPGEPGVSGPMGPR	GIPGPVGEQGLPGAP	
PGEPGPQGPIGVP	GIQGPPGPAGEEGK	
PGFPGLPGK	GISGPPGPPGPAGK	
PGGPPGLPGPAGPKGAK	GIVGLPGQRGE	
PGLAGSPGLPGIHGLQ	GKDGEAGAQ	
PGLHGLPGEKGDPGPPGFDVSGPPGERGSPGIPGAPGPMGPPGSPGLPGK	GKEGSKGPR	
PGLPGGQGPPGSPGPKGSPGFPGIPGPPGQPGPR	GKSGDRGETGPAGPA	
PGPMGLMGPR	GKSGDRGETGPAGPAGP	
PGPPGPPGPPGLR	GKSGDRGETGPAGPAGPIGP	
PGPQGPPGL	GKSGDRGETGPAGPAGPIGPV	
PGPQGPPGLA	GKSGDRGETGPAGPAGPIGPVG	
PGPSGISGPPGPPGPAGKEGLR	GKSGDRGETGPAGPAGPIGPVGA	
PGPVGAAGATGAR	GLAGPAGPQ	
PGTPGLPGFKGIR	GLAGPPGESGR	
PGVVGAPGTAGPSGPSGLPGER	GLMPGSVGPVGPR	
PIGFPGPK	GLPGAAGER	
PMGLMGPR	GLPGADGR	
PPGFGLPGK	GLPGADGRA	
PPGLLGPPGPR	GLPGADGRAG	
PQGLPGLPGEP	GLPGADGRAGVM	
PTGFPGPK	GLPGAPGPR	

Table S5.2. continued List of the peptide sequences from CH-GL and CH-OPT after upper intestinal digestion.

Peptide Sequences		
CH-GL	CH-OPT	Shared Sequences
PVFDNIWDQGLVS	GLPGEKGPPGDR	
QGPSGASGERGPPGPMGPPGL	GLPGEKGPPGDRGGPGPAGPR	
QGPSGASGERGPPGPMGPPGLAGPPGESGR	GLPGEPGPR	
QVGGISDTNQIF	GLPGGGPPGLGLPGPKG	
QVIGGEGPGLPGQKGDPGPPGPPGSR	GLPGLKGH	
RGEPGPAGAVGPAGAVGPR	GLPGLKGHNGL	
RGETGPAGPAGPIGPV	GLPGLKGHNGLQGLPG	
RGETGPAGPAGPIGPVGAR	GLPGLKGHNGLQGLPGLAG	
RGETGPAGPPGAPGAPGAPGPVGPAGK	GLPGLKGHNGLQGLPGLAGH	
RGPVGPPGAP	GLPGPKGDR	
RGSTGEIGPAGPPGPPGL	GLPGPKGDRGDAGPK	
RGSTGEIGPAGPPGPPGLR	GLPGPPGAPGPQ	
RNVVDGQPF	GLPGPPGAPGPQG	
RPGPPGPPGPK	GLPGPPGER	
SAGPPGFPGAPGPK	GLPGPRGPQ	
SGATPVFDNIWDQGLV	GLPGPSGEPGK	
SGDRGETGPAGPAGPIG	GLPGQPGIPGE	
SGDRGETGPAGPAGPIGPVGAR	GLPGTSGPPGENGKPGEPGPK	
SGETGASGPPGF	GLQGPPGPPGSPGEQGPSGASGPAGPR	
STGISVPGPMGPSGPR	GLTGPIGPPGPA	
SVGPVGPAGPIGSAGPPGFPGAPGPK	GLTGSPGSPGPDG	
TAGPSGPSGLPGER	GLTGSPGSPGPDGK	
TAILPGLGR	GLVGEPGPAGSK	
TGPAGPAGPIGPV	GNAGPPGPPGPAGK	
TGPAGPAGPIGPVG	GNDGATGAAGPPGPTGPAGPPGF	
TGPAGPAGPIGPVGAR	GNPGPAGPAGPR	
TGPIGPPGPAGAPGDKGEAGPSGPAGPTGAR	GNPGSDGLPGR	
TGPPGPSGISGPPGPPGPAGKEGL	GNSGEPGAPGSK	
TVQVGGISDTNQIF	GNSGEPGAPGSKGDTGAK	
VGEPGPLGIAGPPGAR	GPAGANGLPGEK	

Table S5.2. continued List of the peptide sequences from CH-GL and CH-OPT after upper intestinal digestion.

Peptide Sequences		
CH-GL	CH-OPT	Shared Sequences
VGGISDTNQI	GPAGAPGTPGPQ	
VGGISDTNQIFG	GPAGAPGTPGPQG	
VGLMPGSVGPVGPR	GPAGPAGPAGPR	
VMGFPGPK	GPAGPAGPR	
VPGEDGAPGPMGPR	GPAGPPGLPGSVGAPGPR	
VPGLPGYPGR	GPAGPPGPAGE	
VPGPMGPSGPRG	GPAGPPGPIGN	
VPVVTGIR	GPAGPPGPR	
VVGGEDARPNSWPWQ	GPAGPQGPR	
WGFMPSDRA	GPAGPQGPRGD	
YDLSFLPQPPQE	GPAGPQGPRGDKGETGEQ	
YEFGFDGDFYRA	GPAGPQGPRGDKGETGEQGD	
	GPAGPQGPRGDKGETGEQGDR	
	GPAGPSGPAGK	
	GPAGPSGPAGKDG	
	GPAGPSGPAGKDGR	
	GPAGSRGATGPAGV	
	GPAPGAADGGPQ	
	GPEGLPGPQGPK	
	GPIGPPGRA	
	GPKGENGPVGPTGPV	
	GPKGENGPVGPTGPVG	
	GPKGENGPVGPTGPVGAAGPSGPNGPPGPAGS	
	GPKGENGPVGPTGPVGAAGPSGPNGPPGPAGSRGDGGPPGATGFPGAAG	
	GPKGPPGPPGL	
	GPKGPPGPPGP	
	GPNGDSGRPGEPGLM	
	GPPGAGGPPGPR	
	GPPGAGGPPGPRG	
	GPPGDPGLPG	
	GPPGDRGGPGPAGPRG	
	GPPGEPGLPG	
	GPPGFPGAPGPK	
	GPPGKDGASGHPGPIGPPGPR	

Table S5.2. continued List of the peptide sequences from CH-GL and CH-OPT after upper intestinal digestion.

Peptide Sequences		
CH-GL	CH-OPT	Shared Sequences
	GPPGLAGPPGE	
	GPPGLAGPPGESGR	
	GPPGPAGEEGK	
	GPPGPAGPAGER	
	GPPGPAGPAGERGEQGPA	
	GPPGPAGPR	
	GPPGPEGPR	
	GPPGPMGPPGLA	
	GPPGPMGPPGLAGPPGESGRE	
	GPPGPPGAIGPSGPAGK	
	GPPGPPGIR	
	GPPGPPGKR	
	GPPGPPGLPG	
	GPPGPPGLR	
	GPPGPPGPAALPGSK	
	GPPGPPGPAGK	
	GPPGPQGLPGLAG	
	GPPGPQGPR	
	GPPGPSGEAGPPGPPGK	
	GPPGPVGPPG	
	GPPGPVGPPGLKGDS	
	GPPGQPGLPG	
	GPPGSAGSPGK	
	GPPGSAGSPGKDG	
	GPPGSAGSPGKDGL	
	GPRGPPGPAGA	
	GPSGDPGKAGEK	
	GPSGDPGKAGEKGH	
	GPSGEPGTAGPPGTPGPQG	
	GPSGLPGER	
	GPSGLPGERG	
	GPSGPNGPPGPAGSR	
	GPSGPPGPDGNKGEPG	
	GPSGPPGPDGNKGEPGV	
	GPSGPPGPDGNKGEPGVVGAPG	
	GPSGPPGPDGNKGEPGVVGAPG TAGPSGPSGLPGERG	

Table S5.2. continued List of the peptide sequences from CH-GL and CH-OPT after upper intestinal digestion.

Peptide Sequences		
CH-GL	CH-OPT	Shared Sequences
	GPSGPQGIR	
	GPSGPQGPSGPPGPK	
	GPSGPQGPSGPPGPKGN	
	GPSGPQGPSGPPGPKGNSGEPGAPGSK	
	GPTGPIGPPGPAGQPGD	
	GPTGPIGPPGPAGQPGDKG	
	GPVGNPGPAGPAGPR	
	GPVGPSGPPGK	
	GPVGPSGPPGKD	
	GPVGPSGPPGKDGAS	
	GPVGPSGPPGKDGASGHPGP	
	GPVGPSGPPGKDGASGHPGPIGPPGPR	
	GPVGPTGPVG	
	GPVGPTGPVGA	
	GPVGPTGPVGAA	
	GQAGVMGFPGPK	
	GQPGAKGER	
	GQPGPPGPPGTAGFPGSPGAK	
	GQPGVMGFPGPK	
	GRPGAPGPA	
	GRPGAPGPAGA	
	GRPGEVGPPGPPGPAGEK	
	GRPGLPGAAGA	
	GRPGPIGPAGA	
	GRPGPPGPPG	
	GRTGDAGPAGPPGPPGPPGPPGPPSGGYD	
	GRVGAPGPA	
	GRVGAPGPAGA	
	GSDGQPGPPGPPGTAGFPGSPGAK	
	GSDGSVGPVGPA	
	GSDGSVGPVGPAGP	
	GSEGPQGVR	
	GSEGPQGVRGEPGPPGPA	

Table S5.2. continued List of the peptide sequences from CH-GL and CH-OPT after upper intestinal digestion.

Peptide Sequences		
CH-GL	CH-OPT	Shared Sequences
	GSEGPQGVRGEPGPPGPAGA	
	GSPGEAGRPGE	
	GSPGEAGRPGEAGLP	
	GSPGEAGRPGEAGLPG	
	GSPGEAGRPGEAGLPGA	
	GSPGEAGRPGEAGLPGAK	
	GSPGEAGRPGEAGLPGAKG	
	GSPGERGEVGPAGPNG	
	GSPGERGEVGPAGPNGFAGPAG AAGQPGAKGE	
	GSPGERGEVGPAGPNGFAGPAG AAGQPGAKGER	
	GSPGGPGAAGFPGGR	
	GSPGPMGPR	
	GSPGPQGPPGSIGPQ	
	GSPGRDGSPGAK	
	GSPGSPGPDGK	
	GSQGSQGPAGPPGPPGPPGPPG PSGGGY	
	GSTGEIGPAGPPGPPG	
	GTKGPKGENGPVGPT	
	GTKGPKGENGPVGPTGPVG	
	GTKGPKGENGPVGPTGPVGA	
	GTKGPKGENGPVGPTGPVGAA	
	GTKGPKGENGPVGPTGPVGAAG PSGPNGPPGPAGSR	
	GVAGAPGLPGPR	
	GVAGEPGRDGLPGGP	
	GVAGEPGRDGLPGGPG	
	GVAGEPGRDGLPGGPGL	
	GVAGPKGPAGER	
	GVDGAPGKDGPR	
	GVKGDVGLPGP	
	GVPGEDGAPGPMGPR	
	GVPGEKGPIG	
	GVPGPPGAVGPAGKD	
	GVQGPPGPAGPR	

Table S5.2. continued List of the peptide sequences from CH-GL and CH-OPT after upper intestinal digestion.

Peptide Sequences		
CH-GL	CH-OPT	Shared Sequences
	GVVGLPGQRGE	
	GVVGLPGQRGER	
	GVVGPQGAR	
	HGNRGEPGPAGAVGPAGA	
	HGNRGEPGPAGAVGPAGAVGPR	
	HMWPGDIKA	
	HPGPIGPPGPR	
	IDGRPGPI	
	IGFPGPKGPSGDPGKAGEK	
	IGPAGLPGPR	
	IGPPGDPGR	
	IGPPGPAGAPGDK	
	IGPSGPAGK	
	IGPSGPAGKD	
	IPGIGKPGQDGIPGQPGFPGGK	
	IQGPPGPAGE	
	IQGPPGPAGEEGK	
	IQGPPGPAGEEGKR	
	ISGPKGDSGPPGER	
	ISGPPGPPGPAGK	
	KAGPPGPK	
	KGENGVPGEDGAPGPMGPR	
	KGENGVPGENGAPGPMGPR	
	KGEPGDKGPR	
	KGEPGSSGVDGAPGKDGPR	
	LAGPPGESGR	
	LDGAKGDAGPA	
	LDGAKGDAGPAGPK	
	LGAPGPSGAR	
	LGPVGNPGPAGPAGPR	
	LKGENGVPGEDGAPGPMGPR	
	LKGENGVPGENGAPGPMGPR	
	LQGLPGTSGPPGENGKPGEPGPK	
	LRGIPGSPGGPGSDGKPGPPGSQGETGRPGPPGSPGPR	

Table S5.2. continued List of the peptide sequences from CH-GL and CH-OPT after upper intestinal digestion.

Peptide Sequences		
CH-GL	CH-OPT	Shared Sequences
	LSGPVGPPGNPGANGLPGAK	
	LTGSPGSPGPDGK	
	LVGEPGPAGSK	
	NAGPPGPPGPAGK	
	NGDDGEAGKPGRPGE	
	NGDDGEAGKPGRPGERGPPGPQG	
	NGDDGEAGKPGRPGERGPPGPQGA	
	NGEKGETGAPGLKGENGVPGENGAPGPMGPR	
	NGETGPQGPPGPTGPSGDKGDTGPPGPQG	
	NGVPGEDGAPGPMGPR	
	NGVPGENGAPGPMGPR	
	PAGLPGPPGER	
	PAGPQGPR	
	PGAPGPPGKR	
	PGAPGTPGER	
	PGAVGPLGPR	
	PGEAGEPGLPG	
	PGEKGPPGDR	
	PGGPPGLPGPAGPK	
	PGLLGPPGPR	
	PGLPGPSGEPGK	
	PGLPGPSGEPGKQGPSGA	
	PGLPGPSGEPGKQGPSGASGER	
	PGPAGPAGPR	
	PGPIGPAGAR	
	PGPIGPPGPR	
	PGSDGLPGR	
	PGSDGLPGRD	
	PGSDGLPGRDGAPG	
	PPGARGPPGDTGKDGPR	
	PPGFDVSGPPGERGSPGIPGAPGPMGPPGSPGLPGK	
	PSGPQGPSGPPGPK	

Table S5.2. continued List of the peptide sequences from CH-GL and CH-OPT after upper intestinal digestion.

Peptide Sequences		
CH-GL	CH-OPT	Shared Sequences
	PVGNPGPAGPAGPR	
	QGAVGSPGPAGPR	
	QGLPGPAGTAGE	
	QGLPGTSGPPGENGKPGEPGPK	
	QGLPGTSGPPGENGKPGEPGPK GEAGAPGIPGGK	
	QGMPGER	
	QGPPGPAGEEGK	
	QGPPGPPGSPGEQGPSGASGPA GPR	
	QGPSGASGERGPPGPMGPPG	
	QGVPGDPGAVGPLGPR	
	QPGLPGPR	
	RGAAGLPGPK	
	RGEAGSPGIAGPK	
	RGEPGPAGLPGPPGER	
	RGETGPAGPAGP	
	RGETGPAGPPGAPGAPGAPGPV GPA	
	RGETGPAGPSGAPGPAGSR	
	RGFPGER	
	RGFPGLPGPSGEPGK	
	RGIGTPGPKR	
	RGIPGSPGGPGSDGKPGPPGSQ GETGRPGPPGSPGPR	
	RGPAGPQGPR	
	RGPLGPPG	
	RGPNGDSGRPGEPGLMGPR	
	RGPPGAGGPPGPR	
	RGPPGESGAAGPTGPIGSR	
	RGPPGPPGK	
	RGPPGPPGPR	
	RGPPGPQGPR	
	RGPSGPQGPSGPPGPK	
	RGVPGPPGAVGPA	
	RGVQGPPGPAGPR	
	SAGIPGPFGPR	

Table S5.2. continued List of the peptide sequences from CH-GL and CH-OPT after upper intestinal digestion.

Peptide Sequences		
CH-GL	CH-OPT	Shared Sequences
	SFLPQPPQEK	
	SGAAGPTGPIGS	
	SGAAGPTGPIGSR	
	SGAPGVPGIAGPR	
	SGDRGETGPAGPA	
	SGDRGETGPAGPAGPI	
	SGDRGETGPAGPAGPIGP	
	SGDRGETGPAGPS	
	SGDRGETGPAGPSGAPGPA	
	SGDRGETGPAGPSGAPGPAGS	
	SGDRGETGPAGPSGAPGPAGSR	
	SGEPGAPGSKGDTGAK	
	SGHPGPIGPPGPR	
	SGLDGAKGDAGPAGPK	
	SGLDGAKGDAGPAGPKGEPGSPGENGAPGQMGPR	
	SGPAGPRGPPGSAGSPGK	
	SGPAGPRGPPGSAGSPGKDGLNGLPGPIGPPGPR	
	SGRPGEPGLMGPR	
	SPGPQGPPGSIGPQ	
	STPVPGLPGPPGPPGR	
	TAGFPGSPGAK	
	TAGPSGPSGLPGERG	
	TGDAGPAGPPGPPGPPGPPGPPSG	
	TGDAGPAGPPGPPGPPGPPGPPSGGYD	
	TGPPGPAGQDGRPGPPGPPG	
	TGPPGPAGQDGRPGPPGPPGA	
	TGSPGSPGPDGK	
	VAGAPGLPGPR	
	VAGEPGRDGLPGGPG	
	VAGPKGPAGE	
	VAGPKGPAGER	
	VAGPPGPSGPPGEK	
	VDGAPGKDGPR	

Table S5.2. continued List of the peptide sequences from CH-GL and CH-OPT after upper intestinal digestion.

Peptide Sequences		
CH-GL	CH-OPT	Shared Sequences
	VGAPGPAGAR	
	VGEPGPAGSK	
	VGEPGPAGSKGESGNKGEPGAV GQPGPPGPSGEEGK	
	VGNPGPAGPAGPR	
	VGPAGAVGPR	
	VGPAGKDGEAGAQ	
	VGPPGPPGPAGEK	
	VGPPGPSGN	
	VGPPGPSGNAGPPGPPGPAGK	
	VGPPGPSGNAGPPGPPGPAGKE	
	VGPSGPPGKD	
	VGQPGPPGPSGEEGK	
	VGSPGPAGPR	
	VQGPPGPAGPR	
	VQGPPGPAGPRG	
	VVGAPGTAGPSGPSGLPGER	
	VVGLPGQR	
	VVGLPGQRGER	

Table S5.3. DPPH and FRAP for CH-GL and CH-OPT at times 0, 8, 16 and 24 h for each colonic region.

	CH-GL		CH-OPT	
Time (h)	**DPPH**	**FRAP**	**DPPH**	**FRAP**
	Ascending colon			
0	24.00±6.05	440.82±270.11	17.53±0.68	273.39±2.49
8	24.05±2.05	392.93±92.98	18.63±2.03	315.14±56.17
16	27.68±2.63	454.30±50.21	28.25±0.85*	370.81±43.24
24	29.10±1.20	424.08±28.36	26.88±1.28*	390.69±73.07
	Transverse colon			
0	20.65±8.75	431.06±247.33	15.40±0.45	236.11±55.67
8	21.20±3.85	392.00±40.91	21.58±3.93	255.00±31.81
16	24.08±0.43	328.78±74.38	16.13±1.28	297.74±1.99
24	17.55±4.25	292.52±66.95	23.73±0.03	323.09±55.17
	Descending colon			
0	29.35±9.85	520.32±304.04	22.50±1.10	245.05±26.84
8	24.25±11.45	699.77±99.49	19.98±0.43	170.49±39.77
16	28.28±9.43	309.25±110.65	21.15±0.50	247.54±42.25
24	20.68±3.73	492.42±71.59	19.55±0.01	278.36±23.36

Values are expressed as mean ± SEM in mM. DPPH is reported in mM Trolox Eq. FRAP is reported in µM ascorbic acid equivalents. Within a column, * symbol indicates significant differences from control (Time 0 h) ($p<0.05$).

5.10 References

1. Lane, N.; Shidara, K.; Wise, B. Osteoarthritis year in review 2016: Clinical. *Osteoarthr. Cartil.* **2017**, *25*, 209–215, doi:10.1016/j.joca.2016.09.025.
2. Li, M.; Xiao, R.; Li, J.; Zhu, Q. Regenerative approaches for cartilage repair in the treatment of osteoarthritis. *Osteoarthr. Cartil.* **2017**, *25*, 1577–1587, doi:10.1016/j.joca.2017.07.004.
3. Bello, A.E.; Oesser, S. Collagen hydrolysate for the treatment of osteoarthritis and other joint disorders:a review of the literature. *Curr. Med Res. Opin.* **2006**, *22*, 2221–2232, doi:10.1185/030079906x148373.
4. Schott, E.M.; Farnsworth, C.W.; Grier, A.; Lillis, J.A.; Soniwala, S.; Dadourian, G.H.; Bell, R.D.; Doolittle, M.L.; Villani, D.A.; Awad, H.; et al. Targeting the gut microbiome to treat the osteoarthritis of obesity. *JCI Insight* **2018**, *3*, 95997, doi:10.1172/jci.insight.95997.
5. Veronese, N.; Cooper, C.; Reginster, J.-Y.; Hochberg, M.; Branco, J.; Bruyère, O.; Chapurlat, R.; Al-Daghri, N.; Dennison, E.; Herrero-Beaumont, G.; et al. Type 2 diabetes mellitus and osteoarthritis. *Semin. Arthritis Rheum.* **2019**, *49*, 9–19, doi:10.1016/j.semarthrit.2019.01.005.
6. Eymard, F.; Parsons, C.; Edwards, M.; Petit-Dop, F.; Reginster, J.-Y.; Bruyere, O.; Richette, P.; Cooper, C.; Chevalier, X. Diabetes is a risk factor for knee osteoarthritis progression. *Osteoarthr. Cartil.* **2015**, *23*, 851–859, doi:10.1016/j.joca.2015.01.013.
7. Singh, G.; Miller, J.D.; Lee, F.H.; Pettitt, D.; Russell, M.W. Prevalence of cardiovascular disease risk factors among US adults with self-reported osteoarthritis: Data from the Third National Health and Nutrition Examination Survey. *Am. J. Manag. Care* **2002**, *8*, 383–391.
8. Baudart, P.; Louati, K.; Marcelli, C.; Berenbaum, F.; Sellam, J. Association between osteoarthritis and dyslipidaemia: A systematic literature review and meta-analysis. *RMD Open* **2017**, *3*, e000442, doi:10.1136/rmdopen-2017-000442.
9. Chun, J.-S.; Collins, K.; Rockel, J.; Iijima, H.; Werdyani, S.; Wang, F.-S.; Batushansky, A. Concurrent session 1: Metabolic osteoarthritis. In Proceedings of OARSI Connect ’21 Virtual World Congress on Osteoarthritis, Virtual, 29 April–1 May 2021.
10. Sellam, J.; Berenbaum, F. Is osteoarthritis a metabolic disease? *Jt. Bone Spine* **2013**, *80*, 568–573, doi:10.1016/j.jbspin.2013.09.007.
11. Kluzek, S.; Newton, J.L.; Arden, N.K. Is osteoarthritis a metabolic disorder? *Br. Med. Bull.* **2015**, *115*, 111–121, doi:10.1093/bmb/ldv028.

12. Bernado, M.L.R.; Azarcon, A.C., Jr. A randomized control trial on the effects of oral collagen treatment on the medial knee joint space and functional outcome among veterans medical center patients diagnosed with osteoarthritis of the knee. Philipp. *Acad. Rehabil. Med. Process*. **2012**, *4*, 1–8.
13. Bruyère, O.; Zegels, B.; Leonori, L.; Rabenda, V.; Janssen, A.; Bourges, C.; Reginster, J.-Y. Effect of collagen hydrolysate in articular pain: A 6-month randomized, double-blind, placebo controlled study. *Complement. Ther. Med.* **2012**, *20*, 124–130, doi:10.1016/j.ctim.2011.12.007.
14. Kumar, S.; Sugihara, F.; Suzuki, K.; Inoue, N.; Venkateswarathirukumara, S. A double-blind, placebo-controlled, randomised, clinical study on the effectiveness of collagen peptide on osteoarthritis. *J. Sci. Food Agric.* **2014**, *95*, 702–707, doi:10.1002/jsfa.6752.
15. Zdzieblik, D.; Oesser, S.; Baumstark, M.W.; Gollhofer, A.; König, D. Collagen peptide supplementation in combination with resistance training improves body composition and increases muscle strength in elderly sarcopenic men: A randomised controlled trial. *Br. J. Nutr.* **2015**, *114*, 1237–1245, doi:10.1017/s0007114515002810.
16. Zdzieblik, D.; Oesser, S.; Gollhofer, A.; König, D. Improvement of activity-related knee joint discomfort following supplementation of specific collagen peptides. *Appl. Physiol. Nutr. Metab.* **2017**, *42*, 588–595, doi:10.1139/apnm-2016-0390.
17. Benito-Ruiz, P.; Camacho-Zambrano, M.; Carrillo-Arcentales, J.; Mestanza-Peralta, M.; Vallejo-Flores, C.; Vargas-López, S.; Villacís-Tamayo, R.; Zurita-Gavilanes, L. A randomized controlled trial on the efficacy and safety of a food ingredient, collagen hydrolysate, for improving joint comfort. *Int. J. Food Sci. Nutr.* **2009**, *60*, 99–113, doi:10.1080/09637480802498820.
18. Feliciano, D.D.S.; Gonzalex-Suarez, C.B.; Bernardo-Bueno, M.M.; Malvar, A.K.G.; Cua, R.C.A.; Tan-Sales, B.G.K.; Aycardo, S.M.O.; Tan-Ong, M.; Chan, R.; Reyes, F.D.L. Effect of collagen hydrolysate as adjuvant treatment to exercise for knee osteoarthiritis. *Philipp. Acad. Rehabil. Med*. **2017**, *9*, 4–15.
19. Skov, K.; Oxfeldt, M.; Thøgersen, R.; Hansen, M.; Bertram, H.C. Enzymatic Hydrolysis of a Collagen Hydrolysate Enhances Postprandial Absorption Rate-A Randomized Controlled Trial. *Nutrients* **2019**, *11*, 1064, doi:10.3390/nu11051064.
20. Aleman, A.; Gómez-Guillén, M.C.; Montero, P. Identification of ace-inhibitory peptides from squid skin collagen after in vitro gastrointestinal digestion. *Food Res. Int.* **2013**, *54*, 790–795, doi:10.1016/j.foodres.2013.08.027.

21. Guo, L.; Harnedy, P.A.; Zhang, L.; Li, B.; Zhang, Z.; Hou, H.; Zhao, X.; Fitzgerald, R.J. In vitroassessment of the multifunctional bioactive potential of Alaska pollock skin collagen following simulated gastrointestinal digestion. *J. Sci. Food Agric.* **2015**, *95*, 1514–1520, doi:10.1002/jsfa.6854.
22. Fu, Y.; Therkildsen, M.; Aluko, R.E.; Lametsch, R. Exploration of collagen recovered from animal by-products as a precursor of bioactive peptides: Successes and challenges. *Crit. Rev. Food Sci. Nutr.* **2018**, *59*, 2011–2027, doi:10.1080/10408398.2018.1436038.
23. Di Bernardini, R.; Harnedy, P.; Bolton, D.; Kerry, J.; O'Neill, E.; Mullen, A.M.; Hayes, M. Antioxidant and antimicrobial peptidic hydrolysates from muscle protein sources and by-products. *Food Chem.* **2011**, *124*, 1296–1307, doi:10.1016/j.foodchem.2010.07.004.
24. Nakatani, S.; Mano, H.; Sampei, C.; Shimizu, J.; Wada, M. Chondroprotective effect of the bioactive peptide prolyl-hydroxyproline in mouse articular cartilage in vitro and in vivo. *Osteoarthr. Cartil.* **2009**, *17*, 1620–1627, doi:10.1016/j.joca.2009.07.001.
25. Kouguchi, T.; Ito, A.; Iwai, K.; Shimizu, M.; Takahata, Y.; Suzuki, T.; Morimatsu, F.; Tanabe, S. Chicken Collagen Hydrolysate-derived Peptides Inhibit Tumor Necrosis Factor-α-induced Inflammatory Response in Endothelial Cells. *Food Sci. Technol. Res.* **2012**, *18*, 667–671, doi:10.3136/fstr.18.667.
26. Ohara, H.; Ichikawa, S.; Matsumoto, H.; Akiyama, M.; Fujimoto, N.; Kobayashi, T.; Tajima, S. Collagen-derived dipeptide, proline-hydroxyproline, stimulates cell proliferation and hyaluronic acid synthesis in cultured human dermal fibroblasts. *J. Dermatol.* **2010**, *37*, 330–338, doi:10.1111/j.1346-8138.2010.00827.x.
27. Hatanaka, T.; Kawakami, K.; Uraji, M. Inhibitory effect of collagen-derived tripeptides on dipeptidylpeptidase-IV activity. *J. Enzym. Inhib. Med. Chem.* **2014**, *29*, 823–828, doi:10.3109/14756366.2013.858143.
28. Knight, C.; Morton, L.F.; Onley, D.J.; Peachey, A.R.; Ichinohe, T.; Okuma, M.; Farndale, R.W.; Barnes, M.J. Collagen-platelet interaction: Gly-Pro-Hyp is uniquely specific for platelet Gp VI and mediates platelet activation by collagen. *Cardiovasc. Res.* **1999**, *41*, 450–457, doi:10.1016/S0008-6363(98)00306-X.
29. Valko, M.; Leibfritz, D.; Moncol, J.; Cronin, M.T.D.; Mazur, M.; Telser, J. Free radicals and antioxidants in normal physiological functions and human disease. *Int. J. Biochem. Cell Biol.* **2007**, *39*, 44–84, doi:10.1016/j.biocel.2006.07.001.

30. Finkel, T.; Holbrook, N.J. Oxidants, oxidative stress and the biology of ageing. *Nature* **2000**, *408*, 239–247, doi:10.1038/35041687.
31. Ao, J.; Li, B. Amino acid composition and antioxidant activities of hydrolysates and peptide fractions from porcine collagen. *Food Sci. Technol. Int.* **2012**, *18*, 425–434, doi:10.1177/1082013211428219.
32. Sun, L.; Chang, W.; Ma, Q.; Zhuang, Y. Purification of Antioxidant Peptides by High Resolution Mass Spectrometry from Simulated Gastrointestinal Digestion Hydrolysates of Alaska Pollock (*Theragra chalcogramma*) Skin Collagen. *Mar. Drugs* **2016**, *14*, 186, doi:10.3390/md14100186.
33. Arulselvan, P.; Fard, M.T.; Tan, W.S.; Gothai, S.; Fakurazi, S.; Norhaizan, M.E.; Kumar, S.S. Role of Antioxidants and Natural Products in Inflammation. *Oxidative Med. Cell. Longev.* **2016**, *2016*, 5276130, doi:10.1155/2016/5276130.
34. Bianchi, M.A.; Scazzina, F.; Del Rio, D.; Valtueña, S.; Pellegrini, N.; Franzini, L.; Callegari, M.L.; Pellacani, C.; Buschini, A.; Zavaroni, I.; et al. Ability of a high-total antioxidant capacity diet to increase stool weight and bowel antioxidant status in human subjects. *Br. J. Nutr.* **2010**, *104*, 1500–1507, doi:10.1017/s0007114510002424.
35. Amigo, L.; Hernández-Ledesma, B. Current evidence on the bioavailability of food bioactive peptides. *Molecules* **2020**, *25*, 4479, doi:10.3390/molecules25194479.
36. Mora, L.; Bolumar, T.; Heres, A.; Toldrá, F. Effect of cooking and simulated gastrointestinal digestion on the activity of generated bioactive peptides in aged beef meat. *Food Funct.* **2017**, *8*, 4347–4355, doi:10.1039/c7fo01148b.
37. Roberfroid, M.; Gibson, G.R.; Hoyles, L.; McCartney, A.L.; Rastall, R.; Rowland, I.; Wolvers, D.; Watzl, B.; Szajewska, H.; Stahl, B.; et al. Prebiotic effects: Metabolic and health benefits. *Br. J. Nutr.* **2010**, *104*, S1–S63, doi:10.1017/s0007114510003363.
38. Dorożyńska, I.; Majewska-Szczepanik, M.; Marcińska, K.; Szczepanik, M. Partial depletion of natural gut flora by antibiotic aggravates collagen induced arthritis (CIA) in mice. *Pharmacol. Rep.* **2014**, *66*, 250–255, doi:10.1016/j.pharep.2013.09.007.
39. Liu, X.; Zeng, B.; Zhang, J.; Li, W.; Mou, F.; Wang, H.; Zou, Q.; Zhong, B.; Wu, L.; Wei, H.; et al. Role of the Gut Microbiome in Modulating Arthritis Progression in Mice. *Sci. Rep.* **2016**, *6*, 30594, doi:10.1038/srep30594.

40. Rowland, I.; Gibson, G.; Heinken, A.; Scott, K.; Swann, J.; Thiele, I.; Tuohy, K. Gut microbiota functions: Metabolism of nutrients and other food components. *Eur. J. Nutr.* **2018**, *57*, 1–24, doi:10.1007/s00394-017-1445-8.
41. Peng, M.; Biswas, D. Short chain and polyunsaturated fatty acids in host gut health and foodborne bacterial pathogen inhibition. *Crit. Rev. Food Sci. Nutr.* **2016**, *57*, 3987–4002, doi:10.1080/10408398.2016.1203286.
42. Ashaolu, T.J.; Ashaolu, J.O. Prebiotic peptides, their formation, fermentation in the gut, and health implications. *Biotechnol. Prog.* **2021**, e3142, doi:10.1002/btpr.3142.
43. Diether, N.E.; Willing, B.P. Microbial Fermentation of Dietary Protein: An Important Factor in Diet–Microbe–Host Interaction. *Microorganisms.* **2019**, *7*, 19, doi:10.3390/microorganisms7010019.
44. Sirico, F.; Miressi, S.; Castaldo, C.; Spera, R.; Montagnani, S.; Di Meglio, F.; Nurzynska, D. Habits and beliefs related to food supplements: Results of a survey among Italian students of different education fields and levels. *PLoS ONE* **2018**, *13*, e0191424, doi:10.1371/journal.pone.0191424.
45. Dickinson, A.; Mackay, D.; Wong, A. Consumer attitudes about the role of multivitamins and other dietary supplements: Report of a survey. *Nutr. J.* **2015**, *14*, 66, doi:10.1186/s12937-015-0053-9.
46. Nyangale, E.P.; Mottram, D.S.; Gibson, G.R. Gut Microbial Activity, Implications for Health and Disease: The Potential Role of Metabolite Analysis. *J. Proteome Res.* **2012**, *11*, 5573–5585, doi:10.1021/pr300637d.
47. Rahim, M.B.H.A.; Chilloux, J.; Gili, L.M.; Neves, A.L.; Myridakis, A.; Gooderham, N.; Dumas, M.-E. Diet-induced metabolic changes of the human gut microbiome: Importance of short-chain fatty acids, methylamines and indoles. *Acta Diabetol.* **2019**, *56*, 493–500, doi:10.1007/s00592-019-01312-x.
48. Rios-Covian, D.; Ruas-Madiedo, P.; Margolles, A.; Gueimonde, M.; De los Reyes-Gavilán, C.G.; Salazar, N. Intestinal Short Chain Fatty Acids and their Link with Diet and Human Health. *Front. Microbiol.* **2016**, *7*, 185, doi:10.3389/fmicb.2016.00185.
49. Matt, S.; Allen, J.; Lawson, M.A.; Mailing, L.J.; Woods, J.A.; Johnson, R.W. Butyrate and Dietary Soluble Fiber Improve Neuroinflammation Associated with Aging in Mice. *Front. Immunol.* **2018**, *9*, 1832, doi:10.3389/fimmu.2018.01832.

50. Li, Z.; Yi, C.-X.; Katiraei, S.; Kooijman, S.; Zhou, E.; Chung, C.K.; Gao, Y.; van den Heuvel, J.K.; Meijer, O.C.; Berbée, J.F.P.; et al. Butyrate reduces appetite and activates brown adipose tissue via the gut-brain neural circuit. *Gut* **2018**, *67*, 1269–1279, doi:10.1136/gutjnl-2017-314050.
51. Mollica, M.P.; Raso, G.M.; Cavaliere, G.; Trinchese, G.; De Filippo, C.; Aceto, S.; Prisco, M.; Pirozzi, C.; Di Guida, F.; Lama, A.; et al. Butyrate Regulates Liver Mitochondrial Function, Efficiency, and Dynamics in Insulin-Resistant Obese Mice. *Diabetes* **2017**, *66*, 1405–1418, doi:10.2337/db16-0924.
52. Chang, Y.; Chen, Y.; Zhou, Q.; Wang, C.; Chen, L.; Di, W.; Zhang, Y. Short-chain fatty acids accompanying changes in the gut microbiome contribute to the development of hypertension in patients with preeclampsia. *Clin. Sci.* **2020**, *134*, 289–302, doi:10.1042/cs20191253.
53. Saresella, M.; Marventano, I.; Barone, M.; La Rosa, F.; Piancone, F.; Mendozzi, L.; D'Arma, A.; Rossi, V.; Pugnetti, L.; Roda, G.; et al. Alterations in Circulating Fatty Acid Are Associated With Gut Microbiota Dysbiosis and Inflammation in Multiple Sclerosis. *Front. Immunol.* **2020**, *11*, 1390, doi:10.3389/fimmu.2020.01390.
54. Sheflin, A.; Borresen, E.C.; Wdowik, M.J.; Rao, S.; Brown, R.J.; Heuberger, A.L.; Broeckling, C.D.; Weir, T.L.; Ryan, E.P. Pilot Dietary Intervention with Heat-Stabilized Rice Bran Modulates Stool Microbiota and Metabolites in Healthy Adults. *Nutrients* **2015**, *7*, 1282–1300, doi:10.3390/nu7021282.
55. Utzschneider, K.M.; Kratz, M.; Damman, C.J.; Hullarg, M. Mechanisms Linking the Gut Microbiome and Glucose Metabolism. *J. Clin. Endocrinol. Metab.* **2016**, *101*, 1445–1454, doi:10.1210/jc.2015-4251.
56. Pietro, C.; Viviane, V.; Estefania, P.r.C.; Jerome, S.; Anna-Maria, K. Biomarkers of gastrointestinal functionality in animal nutrition and health. *Anim. Feed Sci. Technol.* **2019**, *250*, 9–31.
57. Ma, N.; Ma, X. Dietary Amino Acids and the Gut-Microbiome-Immune Axis: Physiological Metabolism and Therapeutic Prospects. *Compr. Rev. Food Sci. Food Saf.* **2019**, *18*, 221–242, doi:10.1111/1541-4337.12401.
58. Wallace, J.L.; Motta, J.-P.; Buret, A.G. Hydrogen sulfide: An agent of stability at the microbiome-mucosa interface. *Am. J. Physiol. Liver Physiol.* **2018**, *314*, G143–G149, doi:10.1152/ajpgi.00249.2017.

59. Dupont, D.; Alric, M.; Blanquet-Diot, S.; Bornhorst, G.; Cueva, C.; Deglaire, A.; Denis, S.; Ferrua, M.; Havenaar, R.; Lelieveld, J.; et al. Can dynamic in vitro digestion systems mimic the physiological reality? *Crit. Rev. Food Sci. Nutr.* **2018**, *59*, 1–17.
60. Van de Wiele, T.; Van den Abbeele, P.; Ossieur, W.; Possemiers, S.; Marzorati, M. The simulator of the human intestinal microbial ecosystem (Shime®). In *The Impact of Food Bioactives on Health: In Vitro And ex Vivo Models*; Verhoeckx, K., Cotter, P., López-Expósito, I., Kleiveland, C., Lea, T., Mackie, A., Requena, T., Swiatecka, D., Wichers, H., Eds.; Springer International Publishing: Cham, Switzerland, 2015; pp. 305–317.
61. Cao, X.; Gibbs, S.T.; Fang, L.; Miller, H.A.; Landowski, C.; Shin, H.-C.; Lennernas, H.; Zhong, Y.; Amidon, G.L.; Yu, L.X.; et al. Why is it Challenging to Predict Intestinal Drug Absorption and Oral Bioavailability in Human Using Rat Model. *Pharm. Res.* **2006**, *23*, 1675–1686, doi:10.1007/s11095-006-9041-2.
62. Musther, H.; Olivares-Morales, A.; Hatley, O.J.; Liu, B.; Hodjegan, A.R. Animal versus human oral drug bioavailability: Do they correlate? *Eur. J. Pharm. Sci.* **2014**, *57*, 280–291, doi:10.1016/j.ejps.2013.08.018.
63. Nagpal, R.; Wang, S.; Woods, L.C.S.; Seshie, O.; Chung, S.T.; Shively, C.A.; Register, T.C.; Craft, S.; McClain, D.A.; Yadav, H. Comparative microbiome signatures and short-chain fatty acids in mouse, rat, non-human primate, and human feces. *Front. Microbiol.* **2018**, *9*, 2897, doi:10.3389/fmicb.2018.02897.
64. Egger, L.; Ménard, O.; Baumann, C.; Duerr, D.; Schlegel, P.; Stoll, P.; Vergères, G.; Dupont, D.; Portmann, R. Digestion of milk proteins: Comparing static and dynamic in vitro digestion systems with in vivo data. *Food Res. Int.* **2019**, *118*, 32–39, doi:10.1016/j.foodres.2017.12.049.
65. Miranda, L.; Deußer, H.; Evers, D. The impact of in vitro digestion on bioaccessibility of polyphenols from potatoes and sweet potatoes and their influence on iron absorption by human intestinal cells. *Food Funct.* **2013**, *4*, 1595–1601, doi:10.1039/c3fo60194c.
66. Minkiewicz, P.; Dziuba, J.; Iwaniak, A.; Dziuba, M.; Darewicz, M. BIOPEP Database and Other Programs for Processing Bioactive Peptide Sequences. *J. AOAC Int.* **2008**, *91*, 965–980, doi:10.1093/jaoac/91.4.965.
67. Kubow, S.; Iskandar, M.M.; Melgar-Bermudez, E.; Sleno, L.; Sabally, K.; Azadi, B.; How, E.; Prakash, S.; Burgos, G.; Felde, T.Z. Effects of Simulated Human Gastrointestinal Digestion of Two Purple-

Fleshed Potato Cultivars on Anthocyanin Composition and Cytotoxicity in Colonic Cancer and Non-Tumorigenic Cells. *Nutrients* **2017**, *9*, 953, doi:10.3390/nu9090953.

68. Ekbatan, S.S.; Sleno, L.; Sabally, K.; Khairallah, J.; Azadi, B.; Rodes, L.; Prakash, S.; Donnelly, D.J.; Kubow, S. Biotransformation of polyphenols in a dynamic multistage gastrointestinal model. *Food Chem.* **2016**, *204*, 453–462, doi:10.1016/j.foodchem.2016.02.140.
69. Gaisawat, M.B.; Iskandar, M.M.; MacPherson, C.W.; Tompkins, T.A.; Kubow, S. Probiotic Supplementation is Associated with Increased Antioxidant Capacity and Copper Chelation in C. difficile-Infected Fecal Water. *Nutrients* **2019**, *11*, 2007, doi:10.3390/nu11092007.
70. Gumienna, M.; Lasik, M.; Czarnecki, Z. Bioconversion of grape and chokeberry wine polyphenols during simulated gastrointestinal in vitro digestion. *Int. J. Food Sci. Nutr.* **2011**, *62*, 226–233.
71. Harris, S.; Powers, S.; Monteagudo-Mera, A.; Kosik, O.; Lovegrove, A.; Shewry, P.; Charalampopoulos, D. Determination of the prebiotic activity of wheat arabinogalactan peptide (AGP) using batch culture fermentation. *Eur. J. Nutr.* **2019**, *59*, 297–307, doi:10.1007/s00394-019-01908-7.
72. Gaisawat, M.B.; MacPherson, C.W.; Tremblay, J.; Piano, A.; Iskandar, M.M.; Tompkins, T.A.; Kubow, S. Probiotic Supplementation in a Clostridium difficile-Infected Gastrointestinal Model Is Associated with Restoring Metabolic Function of Microbiota. *Microorganisms* **2019**, *8*, 60, doi:10.3390/microorganisms8010060.
73. Benzie, I.F.; Strain, J.J. The Ferric Reducing Ability of Plasma (FRAP) as a Measure of "Antioxidant Power": The FRAP Assay. *Anal. Biochem.* **1996**, *239*, 70–76, doi:10.1006/abio.1996.0292.
74. Nurilmala, M.; Hizbullah, H.H.; Karnia, E.; Kusumaningtyas, E.; Ochiai, Y. Characterization and Antioxidant Activity of Collagen, Gelatin, and the Derived Peptides from Yellowfin Tuna (*Thunnus albacares*) Skin. *Mar. Drugs* **2020**, *18*, 98, doi:10.3390/md18020098.
75. Mischak, H.; Julian, B.A.; Novak, J. High-resolution proteome/peptidome analysis of peptides and low-molecular-weight proteins in urine. *Proteom. Clin. Appl.* **2007**, *1*, 792–804, doi:10.1002/prca.200700043.
76. Larder, C.E.; Iskandar, M.M.; Sabally, K.; Kubow, S. Capillary electrophoresis: A fast, cost effective and efficient method replacement for LC-MS when identifying and quantifying small peptides from simulated gastrointestinal digestion of collagen hydrolysate. In Proceedings of BenefiQ Conference Quebec City Convention Centre, Canada Oct 2-4 2018.

77. Walker, A.; Duncan, S.; Leitch, C.; Child, M.W.; Flint, H.J. pH and Peptide Supply Can Radically Alter Bacterial Populations and Short-Chain Fatty Acid Ratios within Microbial Communities from the Human Colon. *Appl. Environ. Microbiol.* **2005**, *71*, 3692–3700, doi:10.1128/aem.71.7.3692-3700.2005.
78. Yamashiro, K.; Tanaka, R.; Urabe, T.; Ueno, Y.; Yamashiro, Y.; Nomoto, K.; Takahashi, T.; Tsuji, H.; Asahara, T.; Hattori, N. Gut dysbiosis is associated with metabolism and systemic inflammation in patients with ischemic stroke. *PLoS ONE* **2017**, *12*, e0171521, doi:10.1371/journal.pone.0171521.
79. Luu, M.; Pautz, S.; Kohl, V.; Singh, R.; Romero, R.; Lucas, S.; Hofmann, J.; Raifer, H.; Vachharajani, N.; Carrascosa, L.C.; et al. The short-chain fatty acid pentanoate suppresses autoimmunity by modulating the metabolic-epigenetic crosstalk in lymphocytes. *Nat. Commun.* **2019**, *10*, 1–12, doi:10.1038/s41467-019-08711-2.
80. Berenbaum, F. Osteoarthritis as an inflammatory disease (osteoarthritis is not osteoarthrosis!). *Osteoarthr. Cartil.* **2013**, *21*, 16–21, doi:10.1016/j.joca.2012.11.012.
81. König, D.; Oesser, S.; Scharla, S.; Zdzieblik, D.; Gollhofer, A. Specific Collagen Peptides Improve Bone Mineral Density and Bone Markers in Postmenopausal Women—A Randomized Controlled Study. *Nutrients* **2018**, *10*, 97, doi:10.3390/nu10010097.
82. Trč, T.; Bohmova, J. Efficacy and tolerance of enzymatic hydrolysed collagen (EHC) vs. glucosamine sulphate (GS) in the treatment of knee osteoarthritis (KOA). *Int. Orthop.* **2010**, *35*, 341–348, doi:10.1007/s00264-010-1010-z.

CONNECTING STATEMENT 4

In Chapter 5, proteomic analysis demonstrated that two similarly sourced CHs (CH-GL and CH-OPT) differed in their peptide profiles before and after upper intestinal digestion. This study provided first evidence that CHs can lead to the generation of microbial nitrogenous fermentation products, although this activity was dependent on the CH tested. Results from this study indicated that CHs could induce prebiotic effects in the ascending colon as shown by increased content of SCFAs, H_2S, and decreased NH_4 after CH-OPT, with no major changes observed with CH-GL. Thus, the prebiotic potential most likely depended on the diversity of peptides available for fermentation. The bioactivity of CHs is mediated by BAPs that are absorbed and enter the systemic circulation that can lead to health promoting effects in tissues, such as on bone. In Chapter 6, CH digesta were applied to primary murine osteoclast and osteoblast cultures at doses matching peptide concentrations previously determined in our digestion (Study1: Chapter 3) and bioavailability studies (Study 2: Chapter 4). The aim of this final study was to evaluate the in vitro effects of CH digesta on osteoblast and osteoclast differentiation and activity.

CHAPTER 6: RESEARCH PAPER 4

Collagen Hydrolysate Digests Modify Metabolism of In Vitro Bone Cells in a Dose- and Treatment-Dependent Manner

Affiliations:

Christina E. Larder[1], Josephine T. Tauer[2,3], Michèle M. Iskandar[1], Svetlana Komarova[2,3], and Stan Kubow[1]*

[1]School of Human Nutrition, McGill University, Ste-Anne-de-Bellevue, QC, Canada, H9X 3V9

[2]Dentistry, McGill University, Montréal, QC, Canada, H3A 1G1

[3] Shriners Hospital for Children, Montréal, Canada, H4A 0A9

***** Corresponding author: stan.kubow@mcgill.ca; Tel.: +1-514-398-7754

6.1 Abstract

Osteoarthritis (OA) is the most common joint disorder. Recent studies have indicated that an imbalance in the activity of bone-resorbing osteoclasts (OCs) and bone-forming osteoblasts (OBs) can adversely impact joint health. Collagen hydrolysates (CHs) are used for pain management of OA, which could be mediated via post-digestion release of bioactive peptides. The underlying cellular effects of CH-derived peptides on bone are poorly understood. Two bovine-sourced CHs (CH-GL and CH-OPT) were digested in vitro and applied to primary murine OC and OB cultures based on previous bioavailability data. Primary OC and OB precursors were isolated from the long bones of male and female C57BL6 mice (n=8-11). In the presence of the CH digests (0.01, 0.05, 0.1, 0.5 mg/mL), osteoclastogenesis was induced under standard and high differentiation concentrations (50, 100 ng/mL) of the receptor activator of nuclear factor kappa-B ligand (RANKL). OB cells were exposed to two doses of the CH digests (0.01, 0.1 mg/mL). Treatment with CH-GL at all doses led to an approximate 50% decrease in OC size (p<0.001) compared to untreated cells at both RANKL conditions. A significant decrease in OC size (p< 0.05) was noted only in CH-OPT digesta at 0.01 mg/mL under the high differentiation RANKL conditions (100 ng/mL). OC differentiation was increased with CH-OPT (0.01 and 0.05 mg/mL) (p<0.05). CH-OPT was associated with a decrease in *Oscar* expression (p<0.05) with 50 ng/mL RANKL whereas expression was increased (p<0.05) at 100 ng/mL RANKL. At 100 ng/mL RANKL, CH-GL and CH-OPT digests decreased (p<0.05) *Rank* expression at all doses except for 0.5 mg/mL. In OBs, CH-GL (0.1 mg/mL) was associated with increased (p<0.05) mineralization together with increased (p<0.01) *Runx2* and *Osterix* expression and decreased (p<0.05) *MMP-9* expression. OB cells treated with CH-OPT at 0.1 mg/mL showed increased (p<0.05) *Runx2* and *Col1a1* expression. These findings demonstrated increased OB activity with treatment of digesta from both CH products. The balance of bone cell remodelling appears to favor digesta obtained from CH-GL as differentiation and activity of OCs was decreased with CH-GL but enhanced with CH-OPT.

Keywords (6): osteoarthritis, collagen hydrolysate, osteoclast, osteoblast, bone formation, bone resorption

6.2 Introduction

Osteoarthritis (OA) is the most common form of arthritis and with a global aging population, the social and financial burden of OA is expected to increase[1]. Patients with OA often experience joint deformity, swelling, pain, and decreased mobility [1,2]. Although classically a "wear and tear" disease associated with cartilage degeneration, OA is now considered a disease of the whole joint[3]. Notably, the subchondral and underlying trabecular bone impact the onset, progression and severity of OA [3]. Although the cross-talk between bone and cartilage is still not fully understood, previous work has established that a disruption in bone remodelling is commonly associated with cartilage defects [3].

While cartilage and bone structure continue to deteriorate in patients with OA, there are still no approved drugs that treat or slow down the progression of the disease [1]. OA patients may use exercise, physical therapy, and weight loss to help improve their condition, but these strategies may not reverse or treat the condition itself. Patients with severe OA can eventually undergo joint replacement surgery [1,4]. However, this option is seen as a last resort due to the significant costs, risks associated with surgery, and post-operative care required. Furthermore, not every type of OA can be addressed by surgery, and of the patients who undergo joint surgery, many may still be affected by OA symptoms. OA patients often use nutritional supplements and nutraceuticals to help manage symptoms before the conditions progresses. A commonly used supplement is collagen hydrolysate (CH), which has demonstrated positive results in clinical trials, such as decreased joint pain as well as increased joint comfort and mobility [2,5-8]. The functional components of CHs are bioactive peptides (BAPs) [8], which can be detected in blood and plasma after CH oral ingestion [2]. Furthermore, bioavailable BAPs, such as Pro-Hyp, can be absorbed and detected in cartilage and bone cells such as bone-resorbing osteoclasts (OCs) and bone-forming osteoblasts (OBs) [2,9-11].

In addition to OA symptomatic relief, animal studies have established that CHs exert beneficial effects on bone health. Collagen products, such as gelatin and CHs, have been shown to decrease bone loss, increase bone strength, improve bone mineral density (BMD), as well as improve bone biomechanical parameters [12-15]. So far only a limited number of human clinical trials have investigated the effect of CHs on bone metabolism and demonstrated increased BMD after collagen treatment [9,16,17].

Bone remodeling is a dynamic process that is tightly regulated by OCs and OBs [3,18]. The receptor activator of nuclear factor kappa-β (RANK)/ receptor activator of nuclear factor kappa-β ligand (RANKL) pathway plays a central role, where OBs secrete RANKL, which binds to the RANK receptor found on OC precursors and induces their differentiation and fusion into mature multi-nucleated OCs. So far, in vitro studies assessing the effect of CHs on bone remodeling focused mainly on OBs [9]. Although some insight into the impact on OB cell activity after CH treatment has have been addressed (see review by Daneault et al., 2017 [9]), the exact mechanisms of action remain poorly understood. Previous work using bovine collagen on immortalised MC3T3-E1 pre-osteoblast cells observed increased expression of genes involved in OB differentiation, such as *Runx2* [19]. Other work, also using MC3T3-E1cells and the collagen peptide Gly-Pro-Hyp, observed increases in *Runx2*, as well as *Osterix*, another gene involved in OB differentiation, as well as alkaline phosphatase (*ALP*) [20]. As *ALP* also plays a role during stages of bone mineralization, this observed increase suggests increased bone formation. Microscopic analysis of OBs using alizarin red staining confirmed elevated OB mineralization after collagen hydrolysate and peptide treatment [9,11,21], and increased *ALP* staining in pre-osteoblasts has also been observed [19,22]. Additionally, collagen synthesis, as determined by sirius red staining and *Col1a1* gene expression, has also increased after CH treatment [21]. Regarding CH effects on OCs, research data are limited but preliminary studies have demonstrated decreased OC differentiation and function after treatment with collagen products [12-14,18]. However, up to now, the majority of in vitro studies have typically applied CHs directly on bone cells, neglecting digestion of CH peptides in the gastrointestinal (GI) tract and their subsequent first pass metabolism. Such metabolic processes generate bioavailable CH-derived BAPs, to which bone cells are exposed in vivo [9]. In that regard, researchers are now cautioned in terms of the interpretation of in vitro studies that have applied CH products directly on bone cells [9].

In our previous work, CHs were digested in vitro and applied to a cell culture model of first pass metabolism. The content [23] and bioavailability (%) [24] of released BAPs was determined. In the present study, we assessed the effect of digested CHs on primary OC and OB cultures. Specifically, digested CHs, using pre-determined doses based on BAP bioavailability, were applied to OCs and OBs, and their effect on differentiation and function assessed. Both standard and high concentrations of RANKL (50 and 100 ng/mL, respectively) were used in the osteoclastogenesis

studies. The high RANKL concentration mimics OA progression and elevated bone deterioration initiated by OBs [14,18].

6.3 Materials and methods

6.3.1 Collagen hydrolysate treatment and experimental workflow

Two bovine-sourced CH products were used: Original Formula® (Genacol, Blainville, QC) (CH-GL) and Selection (Uniprix, QC, CN) (CH-OPT). First, CHs underwent in vitro digestion [23] (**Fig. 6.1 A**) followed by first pass metabolism using a HIEC-6/HepG2 co-culture (**Fig. 6.1 B**) [24]. BAPs content after digestion and bioavailability (%) were determined. Correspondingly, these data were used to establish freeze-dried CH digesta doses for in vitro osteoclastogenesis and osteoblastogenesis studies, to replicate physiological conditions (**Fig. 6.1 C**).

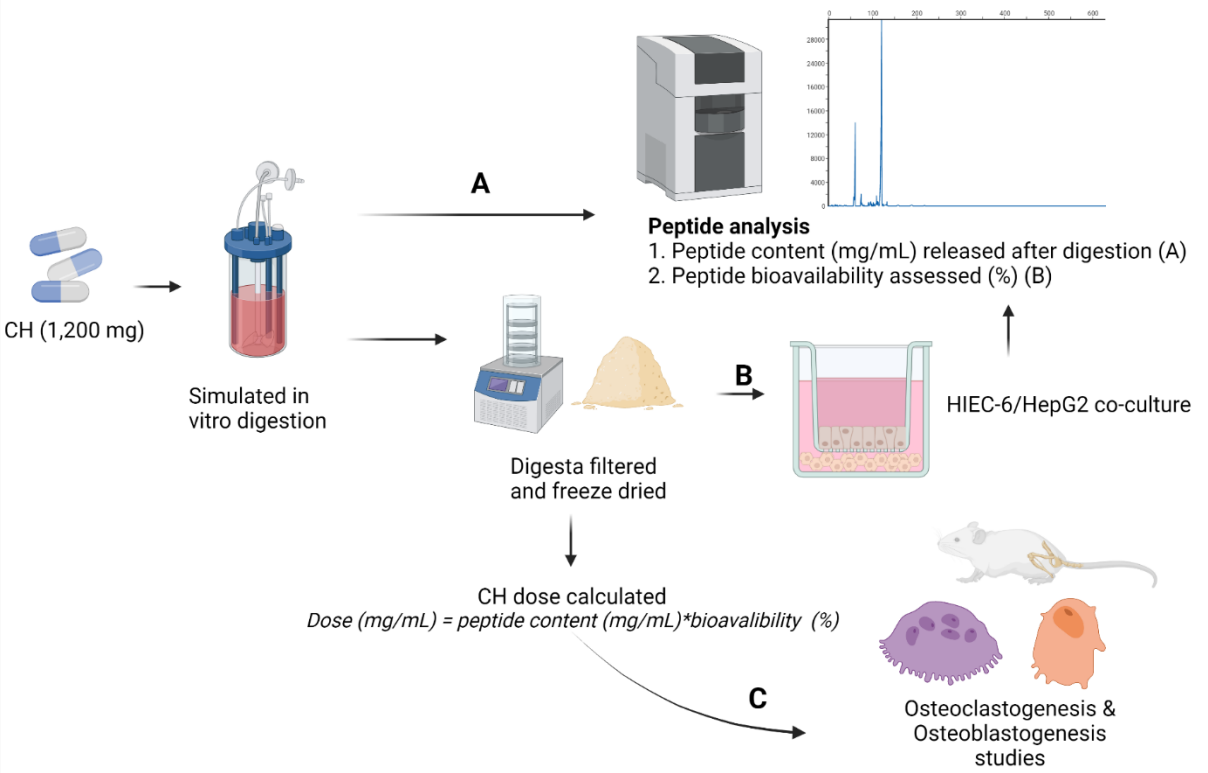

Figure 6.1. Schematic overview of experimental workflow. (A) CHs underwent in vitro digestion and peptide content was assessed [23]. (B) Filtered and freeze-dried CH digesta was applied to co-cultures of HIEC-6/HepG2 cells to determine peptide bioavailability (%) after first pass metabolism [24]. (C) Peptide content after digestion and bioavailability (%) were used to determine doses of freeze-dried CH digesta for cell cultures studies with bone remodelling cells. Created with Biorender. com.

6.3.1.1 In vitro digestion of collagen hydrolysate

Both CH products underwent simulated gastric and small intestinal digestion as described previously [24]. In brief, CHs were digested with pepsin (4 % w/w) for 30 min at pH 2.0 followed by pancreatin (4 % w/w) for 1 h 30 min at pH 8.0. Enzymatic activity was inactivated and the resulting digesta filtered using a stirred Amicon ultrafiltration reactor and a membrane filter with a molecular weight cut off 10 kDa at 4 °C and under a nitrogen gas pressure of 40 psi. The filtrates were freeze-dried at -50 to -60 °C and 0.85 mBar (0.64 mm Hg) (Gamma 1-16 LSC, Christ, Osterode am Harz, Germany) and stored at −80 °C until further use.

6.3.1.2 CH dose calculation for in vitro osteoclastogenesis and osteoblastogenesis studies

Pro-Hyp is a key BAP shown to regulate genes associated with joint integrity and bone health [24,25]. The presence of Pro-Hyp after CH-OPT and CH-GL in vitro digestion and first pass metabolism was confirmed in previous studies. The Pro-Hyp content and bioavailability data previous collected was used to calculate the freeze-dried CH concentration for bone related in vitro cell culture studies.

As no significant difference in Pro-Hyp content after both in vitro digestion and in bioavailability between CH-OPT and CH-GL were observed [23,24], the peptide content released after digestion and bioavailability after CH-GL treatment was used for dosage calculations of both CH digesta. Briefly, in vitro digestion of the currently recommended daily dose [7] of 1,200 mg CH-GL resulted in the release of ~ 42 µg/mL Pro-Hyp [23,24]. Subsequent bioavailability of Pro-Hyp after in vitro first pass metabolism was determined to be ~ 26% [24]. Applying the amount of released Pro-Hyp and bioavailability, the following CH dose for in vitro bone cultures was calculated:

*42 µg/mL *26% = 10.92 µg/mL ≈ 0.01 mg/mL*

A dose response using 0.05, 0.1 and 0.5 mg/mL was included in this study to account for inherent variability in digestion and absorption between humans [26], calculated bioavailability [24], previously published CH doses used for in vitro studies [11,14,18,21] and greater initial oral doses of CH which may translate to a potentially greater amount of substrate absorption [16,27,28]. Freeze-dried CH digesta were dissolved in α-MEM with L-glutamine (Gibco, #12 000-022), without any additives, and filter-sterilized (0.22 µm) before being used in cell culture studies.

6.3.2 Animals

All experiments were compliant with McGill University guidelines established by the Canadian Council on Animal Care. A C57BL6 mouse colony was maintained at the Animal Care Facility of the Shriners Hospitals for Children-Canada. Mice were on a 12-h alternating light and dark cycle and had unrestricted access to food and water.

6.3.3 Osteoclast isolation and in vitro osteoclastogenesis

OC precursors were obtained from long bones of eight 11-week old C57BL6 mice, using a previously established protocol [29]. In brief, femora and tibiae were isolated and cleaned of soft tissue. Bone marrow cells were collected via centrifugation and processed further for OC precursor isolation and emptied long bones were used for isolation of OBs. Red blood cells of collected bone marrow were

removed using red blood cell lysing buffer (Sigma Aldrich, #R7757) from the cell pellet, following manufacturer protocol. Red blood cell lysis was stopped by adding complete culture medium (**See supplementary Table S6.1**) and centrifuged again. The cell pellet was resuspended in complete culture medium supplemented with macrophage colony-stimulating factor (M-CSF, 50 ng/mL) and incubated overnight in a T75 cm^2 flask (Falcon, #353136). The following day, non-adherent cells were collected and plated at a cell density of 50 x 10^3 cells/cm^2 in a 48-well cell culture plate. Cells were treated with complete culture medium (**See supplementary Table S6.1**) supplemented with 50 ng/mL M-CSF and 50 or 100 ng/mL RANKL, as well as CH digesta as depicted in **Table 6.1.** Cultures were carried out at 37°C and 5% CO_2, for 5-7 days. After 3 days, supplemented OC culture media was changed, and changed onward every 2 days. Mature OCs were observed between days 5-7 and either stained for TRAP or collected for gene expression analysis. The OCs cultures were exposed to CH treatments for the duration of the experiment. For each CH supplement, four doses were assessed under two different RANKL concentrations. A negative control, CH controls, and a differentiation control was also completed. A full description of controls and treatments is depicted in **Table 6.1.**

Table 6.1. Osteoclast study design: description of controls and treatments.

Osteoclastogenesis	
Treatment	*Media supplements*
Negative Control	M-CSF
CH-GL CH control	M-CSF + CH-GL (0.01 and 0.1 mg/mL)
CH-OPT CH control	M-CSF + CH-OPT (0.01 and 0.1 mg/mL)
Differentiation Control 1 (RANKL50)	M-CSF + RANKL50
Differentiation Control 2 (RANKL100)	M-CSF + RANKL100
CH-GL	M-CSF + RANKL50 + CH-GL (0.01, 0.05, 0.1, 0.5 mg/mL)
	M-CSF+ RANKL100 + CH-GL (0.01, 0.05, 0.1, 0.5 mg/mL)
CH-OPT	M-CSF+ RANKL50 + CH-OPT (0.01, 0.05, 0.1, 0.5 mg/mL)
	M-CSF+ RANKL100 + CH-OPT (0.01, 0.05, 0.1, 0.5 mg/mL)
Osteoblastogenesis	
Treatment	*Media supplements*
Positive Control	Ascorbic acid+β-glycerophosphate
CH-GL	Ascorbic acid +β-glycerophosphate + CH-GL (0.01 mg/mL)
	Ascorbic acid +β-glycerophosphate + CH-GL (0.1 mg/mL)
CH -OPT	Ascorbic acid + β-glycerophosphate + CH-OPT (0.01 mg/mL)
	Ascorbic acid + β-glycerophosphate + CH-OPT (0.1 mg/mL)

CHs were dissolved in α-MEM with L-glutamine, without any additives, and filter-sterilized (0.22 µm) before application to cell culture. *Osteoclastogenesis*: M-CSF (50 ng/mL) was added to each control and treatment. RANKL application was with 50 ng/mL (RANKL50) or 100 ng/mL (RANKL100). Osteoclasts (OCs) were treated with 4 doses of CH-GL or CH-OPT. *Osteoblastogenesis*: Ascorbic acid (50 µg/mL) and β-glycerophosphate (4 mM) were added to each control and treatment, respectively. Osteoblasts (OBs) were treated with 2 doses of CH-GL or CH-OPT. For both OCs and OB, cells were grown in α-MEM with L-glutamine, fetal bovine serum, 1% sodium pyruvate, 1% penicillin-streptomycin, and 0.1 mg/mL ampicillin at 37°C, with 5% CO_2.

6.3.4 OC quantification and analysis

Mature OCs were fixed using 10% buffered formalin (pH 7.4) for 10 min at room temperature and stained using a TRAP commercial kit (Sigma, #387A-KT), as described previously [29]. Images were obtained using a Cytation 5 (BioTekCytation 5 Imaging Reader, Model CY5V) and processed using Gen5 Image Prime Software (BioTek Instruments, Version 3.09.07). Mature OCs were defined as large cells with more then 3 nuclei and positive TRAP staining. The number of OCs as well as cell size (area) was measured using Image J [30].

6.3.5 OB isolation and in vitro osteoblastogenesis

OBs were obtained from long bones of eight 11-week-old male and three female C57BL6 mice, as described previously [31]. In brief, femora and tibiae were isolated from mice and soft tissue and bone marrow cells removed. Bones were washed in 70% ethanol followed by 1X PBS (**See supplementary Table S6.1**). Bones were placed in physiological solution (**See supplementary Table S6.1.**) and chopped into smaller pieces using scissors. OBs were isolated by a sequential enzymatic digestion using a 3-collagenase step protocol, as described before [31]. In brief, 1 mL of stock solutions 1, 2 and 3 (**See supplementary Table S6.1**) were incubated with the bones for 15, 30 and 60 min, respectively, with shaking and the solutions removed between incubations. Afterwards, bone pieces were plated in a 10 cm petri dish with 10 mL of complete culture media (**See supplementary Table S6.1**). Cells were left to grow out of bone pieces for 5-10 days. Cells were incubated at 37°C, with 5% CO_2 with media changed every other day until cultures reached confluence. Once confluent, cells were collected using 0.25% trypsin, passed through a 40 µm cell strainer (Fisherbrand, #22363547), and resuspended in complete culture media. Cells were plated onto 6 well-plates at a cell density of 5,000 cells/cm^2 and left to acclimatize at 37 °C, 5% CO_2 for 3 days. On day 3, media was changed, and 50 µg/mL ascorbic acid and 4 mM β-glycerophosphate were added alongside CH treatment as described in **Table 6.1**. Cell culture media was changed every other day until day 28, where cells were either stained for alizarin red, alkaline phosphatase or sirius red, or collected for gene expression analysis. Treatments were compared to a positive control that induced osteoblastogenesis.

6.3.6 OB staining analysis

OBs monolayers cultures were fixed and stained with alizarin red to evaluate mineralized bone nodules, with alkaline phosphatase to evaluate OB activity, and with sirius red to evaluate

deposited collagen. Staining was performed as described previously [31,32] and with associated staining kit instructions. Images were obtained using a Cytation 5 (BioTekCytation 5 Imaging Reader, Model CY5V), visualized and processed using Gen5 Image Prime Software (BioTek Instruments, Version 3.09.07) for pixel intensity and stain area (μm^2).

6.3.6.1 Osteoblast staining: alizarin red

OB monolayer cultures were rinsed with 1X PBS (**See supplementary Table S6.1**) and fixed with 10% buffered formalin (pH 7.4) for 8-10 min at room temperature. Fixed OB monolayers were washed with 1X PBS three times and left to air dry. Once dry, wells were rinsed with 70% ethanol and left to dry. A 1% alizarin red staining solution (Sigma, #A5533) (w/v) in distilled water was made, filtered and pH adjusted to 5.5. The alizarin red staining solution was added to each cell layer and incubated for 5-15 min at room temperature. Once stained, cells were washed 3 times with 50% ethanol, followed by distilled water and 1X PBS.

6.3.6.2 OB staining: alkaline phosphatase

OB monolayer cultures were fixed with 10% buffered formalin (pH 7.4) for 8-10 min at room temperature. The staining solution was made by mixing Solution A (3.75 mL of Milli-Q water and 0.2 M Tris-HCL (pH 8.3) with 4.5 mg of Fast red violet salt (Sigma, #F3381)) with Solution B (0.75 mg naphthol (Sigma, #N5000) and 30 µL of N,N-dimenthylformamide (Fisher Scientific, #BP1160)) and filtered (0.22 µm) to remove precipitates. The staining solution was added to each cell layer for 8-15 min at room temperature in the dark. Afterwards, cells were washed with distilled water until clear.

6.3.6.3 OB staining: sirius red

Cells were rinsed with 1X PBS and fixed with ice-cold 70% ethanol for 1 h at 4°C. Afterwards, cells were washed with 1X PBS, and left to air dry at room temperature. Once dry, cells were stained using Picro-Sirius Red Stain Kit (Abcam, #ab150681) following manufacturer instructions. Briefly, cells were incubated with sirius red staining solution for 1 h with gentle agitation. Afterwards, cells were washed twice with the provided acetic acid solution followed by a washing step with double distilled water and allowed to air dry.

6.3.7 Gene expression analysis

RNA was isolated from OC and OB cultures using TRIzol™ reagent (ThermoFisher Scientific, #15596026) according to the manufacturer's instructions. Reverse transcription was performed

using the High-Capacity cDNA Reverse Transcription Kit (ThermoFisher Scientific, Applied Biosystems™, #4368813) according to the manufacturer's instructions. Quantitative real-time PCR (qPCR) was performed using a QuantStudio™ 7 Flex System (ThermoFisher Scientific, Version 1.3), SYBR™ Green PCR Select Master Mix (Fisher Scientific, #4472918,) and customized primers (**See supplementary Table S6.2**). An internal plate control was applied to every PCR plate to enable comparisons of multi-PCR runs. Actin B and glyceraldehyde 3-phosphate dehydrogenase (GAPDH) were used as endogenous controls for gene expression analysis, which was performed according to the delta-delta Ct method.

6.3.8 Statistical analysis

For each CH and RANKL treatment, OC data were assessed by one-way ANOVA with Dunnett's post-hoc test to determine differences between treatment doses and respective differentiation control (**p*<0.05, ***p*<0.01, ****p*<0.001). For OBs, the effect of CH treatment was assessed by one-way ANOVA with Dunnett's post-hoc test to determine differences between treatment doses and respective control (**p*<0.05, ***p*<0.01, ****p*<0.001). OC and OB data are reported as mean ± standard error of mean (SEM). All statistical analyses and figures were performed using GraphPad Prism software (Version 9.0.1 for Windows, GraphPad Software). OC results from gene expression analysis were logarithmic transformed for graphical illustration.

6.4 Results

6.4.1 OC differentiation, size and gene expression were affected by CHs

First, we verified that in the absence of RANKL, OC precursors do not differentiate into mature OCs (negative control; **Fig. 6.2**). We also verified that OC precursors, in the presence of either CH digesta without RANKL, do not differentiate into mature OCs (CH controls; **Supplemental Fig. S6.1**).

Next, we examined whether CH-GL and CH-OPT digesta altered OC differentiation and size under standard and high RANKL conditions. Compared to the respective differentiation controls, we observed a significant decrease ($p < 0.05$) in the number of differentiated OC by 84% with 0.05 mg/mL CH-GL under the standard RANKL condition (50 ng/mL) (**Fig. 6.2a**). In contrast, CH-OPT digesta was associated with a significant ($p < 0.05$) increase OC number at 0.01 mg/mL and 0.05 mg/mL doses under high differentiation conditions (RANKL, 100 ng/mL) **(Fig. 6.2b)**. OCs were significantly smaller ($p< 0.001$) at all CH-GL doses applied at both standard (50 ng/mL) and high

differentiation (100 ng/mL) RANKL conditions (**Fig. 6.2a**). On the other hand, CH-OPT digesta was associated with a significant decrease ($p < 0.05$) in OC size only at the 0.01 mg/mL dose at the high differentiation conditions (100 ng/mL) of RANKL (**Fig. 6.2b)**.

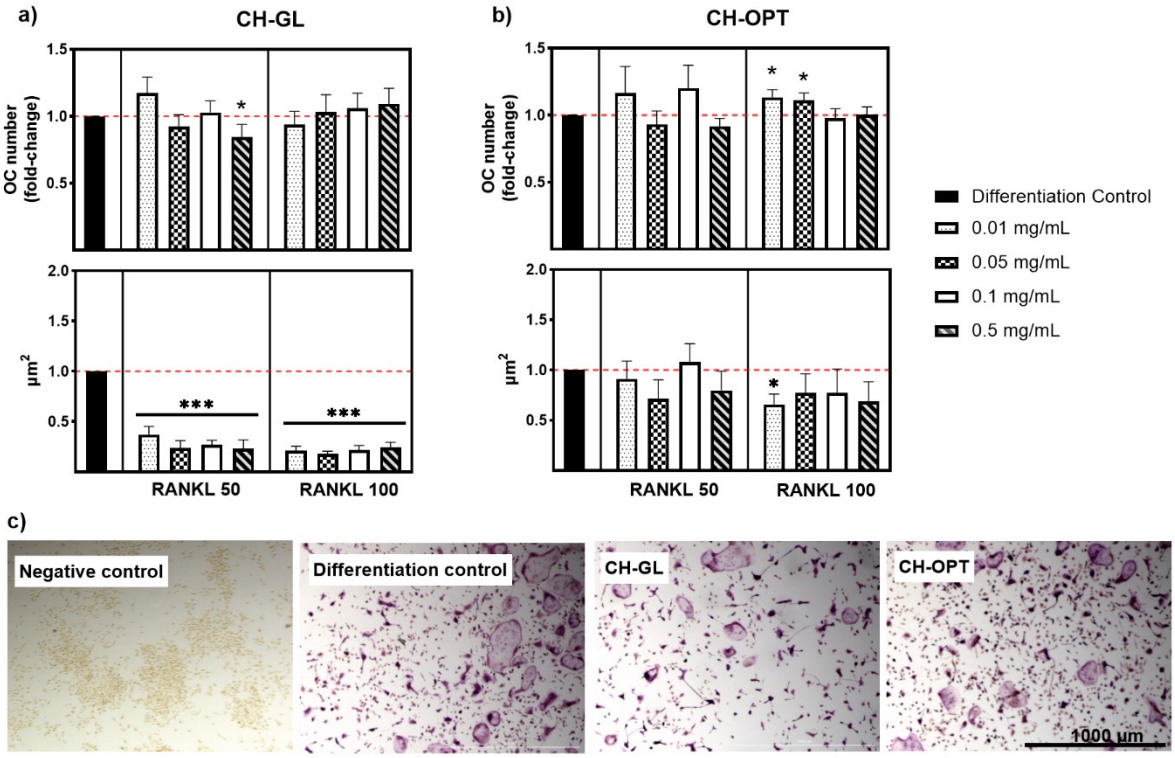

Figure 6.2. Differentiation and size of OCs were affected by CH treatment. Bone marrow cells plated and differentiated with M-CSF (50 ng/mL) and RANKL (50 ng/mL or 100 ng/mL) were used. The negative control was treated with only M-CSF (50 ng/mL) with no RANKL; no wells showed positively stained OCs. Average number and size of differentiated osteoclasts (a, b) was determined after cells were fixed and stained with tartrate-resistant acidic phosphatase (TRAP). (c) Representative images of stained OCs are presented (RANKL 50 ng/mL). Data are presented as mean ± SEM. For each RANKL and CH treatment, statistical significance was assessed by one-way ANOVA with Dunnett's post-hoc test to determine differences between treatment doses and differentiation respective controls (*<0.05, **<0.01, ***<0.001).

To verify that the OC gene expression was unaffected at the two concentrations of RANKL, we assessed the gene expression of *Rank, Lair-1, Oscar, Nfatc1, Dc-stamp* and cathepsin k (*Ctsk*) in the

two RANKL differentiation controls (50 and 100 ng/mL). No differences in gene expression were observed at the two RANKL conditions (**Table S6.3**).

As the RANK/RANKL-pathways plays a significant role in OC differentiation, we investigated the expression of the RANKL-receptor *Rank* in OCs after CH-digesta treatment. Under standard RANKL-induced osteoclastogenesis conditions (50 ng/mL), the expression of *Rank* was unchanged in the presence of either CH digesta (**Figs. 6.3 and 6.4**). Under higher RANKL, however, *Rank* expression showed an average decrease of 0.63-fold at all doses of CH-GL (**Fig. 6.3**). Similarly, *Rank* expression was decreased for CH-OPT at all doses, apart from 0.5 mg/mL **(Fig. 6.4**). To investigate effects on the downstream signals of *Rank*, we assessed the expression of transcription factor *Nfatc1*, which regulates expression of *Ctsk*, the main enzyme degrading type I collagen [33]. Additionally, *Nfatc1* regulates the expression of *Dc-stamp*, a key player in OC differentiation by regulating cell-cell fusion of pre-osteoclasts [34]. The expression of *Nfatc1* was reduced significantly (p <0.05) by 0.19-fold with CH-GL at the 0.1 mg/mL dose at RANKL standard conditions (**Fig. 6.3**). Also at standard RANKL conditions, decreases in *Dc-stamp* expression were seen at 0.01 (p < 0.05), 0.05 (p < 0.001) and 0.1 mg/mL (p < 0.01) CH-GL. Expression of *Dc-stamp* was decreased significantly (p <0.05) with CH-OPT at standard RANKL differentiation conditions, but only at the 0.1 mg/mL dose (**Fig. 6.4**). The expression of *Dc-stamp* was unaffected by both types of CH-digesta under high differentiation RANKL conditions. The expression of *Ctsk* was unaffected by either type of CH-digesta under both RANKL conditions (**Figs. 6.3 and 6.4)**.

Apart from the RANK/RANKL pathway, co-stimulatory signals may be required for the expression of osteoclast-specific genes and the activation of OCs [35]. One co-stimulatory pathway of OC differentiation involves the osteoclast-associated receptor (*Oscar*). Under the standard RANKL condition, 0.5 mg/mL of CH-GL was associated with a significant (p< 0.01) reduction of *Oscar* expression (**Fig. 6.3)**. *Oscar* expression was reduced by 0.07, 0.48 and 0.26-fold at the doses of 0.05, 0.1 and 0.5 mg/mL CH-OPT, respectively (**Fig. 6.4)**. In contrast, under the high differentiation condition (100 ng/mL RANKL), *Oscar* expression was significantly increased (p< 0.05) by 3.8-fold with the CH-OPT treatment at 0.1 mg/mL (**Fig. 6.4)**.

The expression of the collagen type I receptor, *Lair-1*, was decreased with both CH digesta treatments, but only at the high RANKL differentiation condition (100 ng/mL) (**Fig. 6.3 and 6.4)**. Specifically, *Lair-1* expression decreased significantly (p<0.05) by 0.2-fold at the 0.05 mg/mL concentration for both CH-GL and CH-OPT. At the 0.1 and 0.5 mg/mL concentrations, CH-GL was associated with significantly (p<0.05) decreased Lair-1 expression by 0.32 and 0.19-fold, respectively, while CH-OPT showed no effect at those doses.

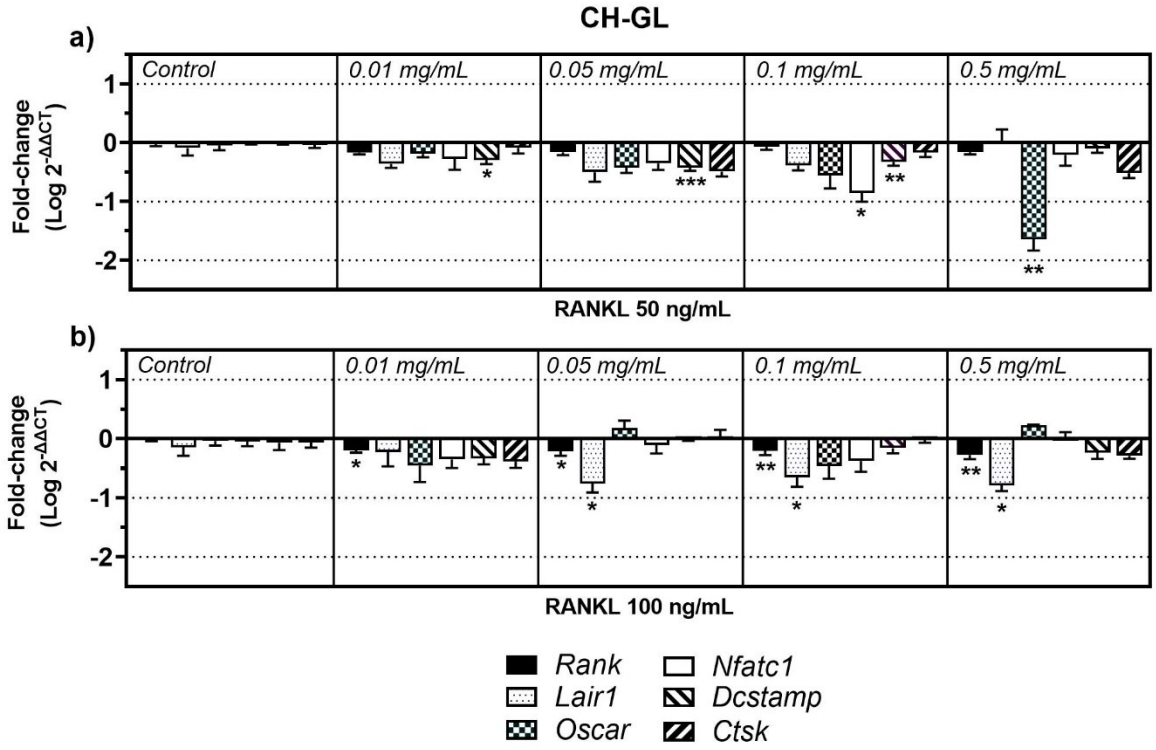

Figure 6.3. CH-GL affected gene expression in a dose dependent manner during RANKL-initiated osteoclast differentiation. Gene expression after CH-GL (0.01, 0.05, 0.1, 0.5 mg/mL) with (a) RANKL 50 ng/mL and (b) RANKL 100 ng/mL. Statistical significance was assessed by one-way ANOVA with Dunnett's post-hoc test to determine differences between treatment doses and respective control (*<0.05, **<0.01, ***<0.001). Data are reported as mean ± SEM.

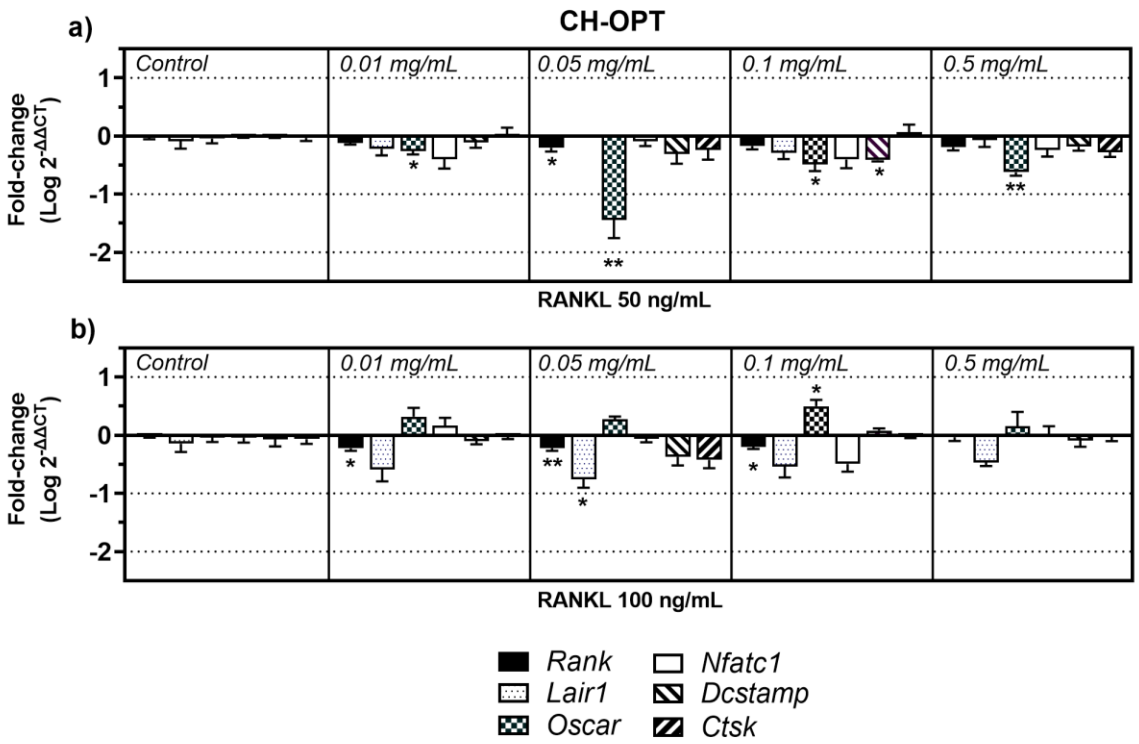

Figure 6.4. CH-OPT affected gene expression in a dose dependent manner during RANKL-initiated osteoclast differentiation. Gene expression after CH-OPT (0.01, 0.05, 0.1, 0.5 mg/mL) with (a) RANKL 50 ng/mL and (b) RANKL 100 ng/mL. Statistical significance was assessed by one-way ANOVA with Dunnett's post-hoc test to determine differences between treatment doses and respective control (*<0.05, **<0.01, ***<0.001). Data are reported as mean ± SEM.

6.4.2 Osteoblastic gene expression was affected by CH digests, in a CH type- and dose-dependent manner.

As both *Runx2* and *Osterix* play a significant role in OB differentiation [19,20,35], we investigated their expression in OBs under CH-digesta treatment. Compared to the differentiation control, *Runx2* and *Osterix* were significantly increased (p<0.01) by 2 and 1.8-fold- with 0.1 mg/mL CH-GL, respectively (**Fig.6.5**). Similarly, *Runx2* expression after CH-OPT was also increased after 0.1 mg/mL treatment, although no changes in *Osterix* levels were observed (**Fig. 6.5)**. Staining data from alkaline phosphatase to assess OB activity showed no difference between CHs treatments and control. Mineralized bone nodule aggregates observed with alizarin red staining are also indicative of osteogenic induction and a significant increase (p<0.05) in pixel intensity after staining was

observed for both doses of CH-GL compared to control (**See supplemental Fig. S6.2).** No change in pixel intensity was observed after CH-OPT; in fact, a small decrease in alizarin red stained area was observed after 0.01 mg/mL CH-OPT.

Investigating downstream signals of *Runx2* and *Osterix*, we found that *MMP-9* was significantly reduced by CH-GL at 0.01 (p<0.01) and 0.1 mg/mL (p<0.05) (**Fig. 6.5**), whereas no changes in *MMPs* were observed after CH-OPT treatment (**Fig. 6.5**). Also under the control of *Runx2* and *Osteirx*, *Col1a1,* a gene responsible for collagen synthesis, was increased after 0.1 mg/mL of CH-OPT. Interestingly, no increase in pixel intensity or stained area after sirius red analysis for deposited collagen was observed for CH-OPT to support the corresponding increase in *Col1a1* expression (**See supplemental Fig. S6.2**).

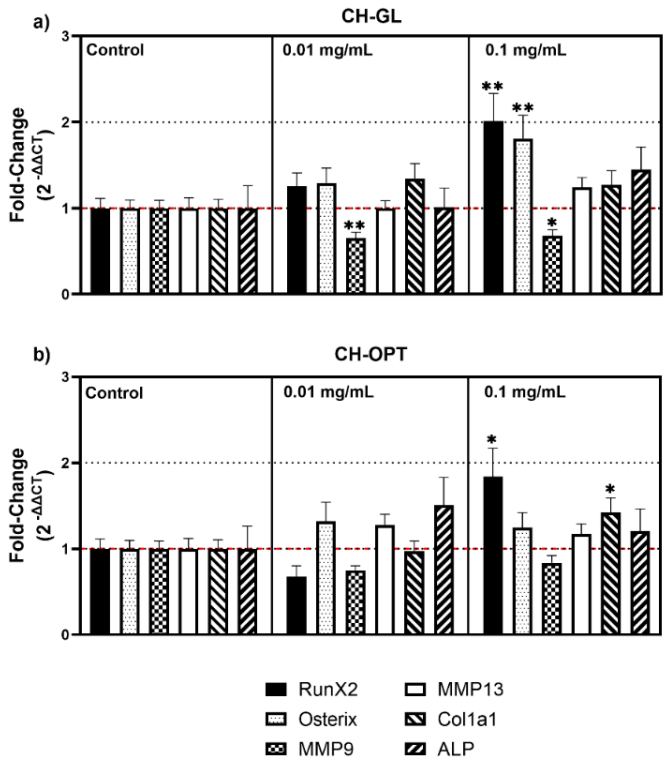

Figure 6.5. Changes in osteoblast gene expression was induced after CH treatment. Primary OBs were plated in osteogenic medium containing β-glycerophosphate and ascorbic acid. Cells were either not treated (control) or treated with 0.01 or 0.1 mg/mL of (a) CH-GL or (b) CH-OPT. Statistical significance was assessed by one-way ANOVA with Dunnett's post-hoc test to determine differences between treatment doses and respective control (*<0.05, **<0.01, ***<0.001). Data are reported as mean ± SEM.

6.5 Discussion

This work has addressed a major research gap, as the differentiation and activity of OCs and OBs was examined with CH digesta in contrast to the direct application of CHs onto these bone remodelling cells in previous work [9]. In vitro studies have typically applied CH products directly onto bone remodelling cells, primarily OBs, while neglecting the effects of GI digestion on collagen products or associated CH-derived BAP bioavailability [23,24] Physiologically relevant doses were selected based on our earlier in vitro digestion and peptide bioavailability studies using the digesta from these two CH products [23,24]. A key finding was that OC size was decreased by approximately 50% with all the CH-GL doses. In that regard, OC size has been associated with resorption activity[36] as larger OCs have been reported to resorb bone more than two-fold greater on a per cell basis as

compared to small OCs[37]. Consequently, it is conceivable that a decrease in resorption activity occurs with the CH-GL treatment. The present work extends the findings of previous OC studies involving collagen treatments, which were limited to quantitation of differentiated OCs without measurements of area or size [12-14]. OC differentiation was also decreased in the presence of CH-GL (0.5 mg/mL) and 50 ng/mL RANKL. Decreased OC differentiation after collagen treatment has been reported previously[12,14], although another report showed no effect of CH treatment on OC differentiation[13]. In our study, the effect of CH-GL on OC differentiation was accompanied with decreased expression of *Oscar*, a co-stimulatory signal needed for expression of OC-specific genes and activation of OCs [35]. Decreased *Oscar* expression is further indicative that OC activation and resorption activity was decreased. To our knowledge, this is the first time that *Oscar* expression after CH treatment has been reported.

The CH-OPT digesta treatment was not associated with any effect on OC differentiation and size under standard RANKL conditions (50 ng/mL). In contrast to CH-GL, OC differentiation was increased with 0.01 and 0.05 mg/mL CH-OPT at the higher RANKL concentration (100 ng/mL). It is possible that the increase in osteoclastogenesis was initiated in part via increased expression of *Oscar,* a receptor activated by collagen fragments [38], that promotes OC differentiation and activation. In support of this contention, *Oscar* expression showed a tendency to be elevated at all the CH-OPT concentrations, although this only reached significance at the 0.1 mg/mL dose. The increase in OC differentiation after CH-OPT treatment may have been partly favored by the concomitant reduced expression of *Lair-1*, a receptor that inhibits osteoclastogenesis and is activated by collagen fragments [38,39]. Thus, the increase in osteoclastogenesis observed with CH-OPT is partly explainable by the decreased *Lair-1* expression. Although *Lair-1* expression was similarly decreased with CH-GL, this was not accompanied with an increase in OC differentiation. It is possible that other signalling and competing pathways are involved with the decreased osteoclastogenesis seen with CH-GL exposure. For example, decreased signalling by triggering receptor expressed on myeloid cells 2 (TREM2), a receptor that regulates OC formation and function, could have compensated for the decreased *Lair-1* expression after CH-GL treatment. Previous work using a fish hydrolysate resulted in decreased expression of TREM2 from microglial signatures in the hippocampus[40].

Cathepsin K and *Dc-stamp* are genes downstream of the RANKL/RANK-signalling pathway [34]. Under standard RANKL-induced differentiation, *Dc-stamp,* a regulator of cell-cell fusion, was significantly downregulated after CH-GL digesta treatment. A reduction in cell-cell fusion signalling via *Dc-stamp* may also partly explain the decreased OC size observed with CH-GL. To our knowledge, this is the first time that the levels of *Dc-stamp* have been reported after CH treatment. The present results are in concert with previous CH studies measuring a different cell fusion marker, CD36. Specifically, in bone marrow cells isolated from C3H/HeN mice for osteoclastogenesis studies, human serum obtained from oral bovine CH treatment resulted in decreased expression levels in the cell fusion marker CD36, as assessed by Taqman Low Density Array [12]. The impact of CH-OPT on *Dc-stamp* expression was far less than that was observed with CH-GL; expression only decreased under standard RANKL and solely with 0.1 mg/mL CH-OPT. Previous work has shown that *Dc-stamp* is a biomarker of psoriatic arthritis and bone repair response [34], but research regarding direct ligands for this cell membrane receptor is still ongoing [41]. A recent review by Kodama et al, (2020) has shed light on the regulatory mechanisms of *Dc-stamp*, but our results suggest that *Dc-stamp* appears to be sensitive to CH-GL with lower circulating levels of RANKL. Further work to identify CH-derived BAPs that trigger *Dc-stamp* expression is needed, as well as an investigation into how circulating collagen fragments that result from bone turnover could affect OC fusion signalling.

As mentioned above, both *Ctsk* and *Dc-stamp* are genes downstream of the RANKL/RANK-signalling pathway [34]. Although *Dc-stamp* was modulated by CH treatment, no effect on *Ctsk* expression was observed. To our knowledge, only one other previous study has investigated the expression of *Ctsk* after collagen treatment involving OCs. Specifically, chicken collagen extract was applied directly to OC precursor RAW264.7 cells, without prior in vitro digestion. Using ImageJ, mRNA *Ctsk* levels were quantified relative to GAPDH, and were decreased by ~0.1 after collagen treatment compared to untreated controls. Our results suggests that other signalling pathways may be activated concomitantly, intervening with the RANKL/RANK-signalling pathway and downstream expression of *Ctsk*. Future work, investigating other regulatory pathways affected by collagen fragments and peptides is needed [38,39].

In terms of the OB cultures, a key finding was the enhanced collagen deposition in association with increased mineralisation seen after 0.1 mg/mL of CH-GL, which has been previously described with CH treatments [21]. The increase in collagen deposition in our study is likely due to the decreased

expression of the collagen degrading matrix metallopeptidase *MMP-9*. Although it is well established that increased levels of *MMP-9* are associated with OA pathogenesis, previous work has not investigated the impact of CHs on MMP activity in bone cells [42,43]. Interestingly, MMP expression was dependent upon the type of CH digesta applied. The CH-GL digesta was associated with decreased *MMP-9* expression whereas digesta from CH-OPT exerted no effect. In contrast to *MMP-9*, *MMP-13*, a key participant in cartilage degradation [44], showed no significant changes in expression regardless of the CH tested. Previous work has shown that *Osterix* activates the *MMP-13* promoter in a dose-dependent manner [45]. Although *Osterix* expression was increased with CH-GL, no changes in *MMP-13* were observed. A possible explanation is that a threshold of *Osterix* downstream signalling is needed for *MMP-13* activation, which was not attained with the CH treatment.

The 0.1 mg/mL dose of CH-GL was associated with an approximate two-fold increase in the key OB differentiation markers *Runx2* and *Osterix*. These results are in concert with previous work showing similar increases in *Runx2* and *Osterix* after collagen peptide treatment [11,22]. Upregulation of *Osterix,* a key regulator of bone formation and mineralization [45,46], was associated with increased mineralization following CH-GL treatment. Treatment with CH-OPT was also associated with induced *Runx2* expression at the 0.1 mg/mL dose; however, no increased mineralization in the OBs was observed. The latter observation is most likely because *Osterix* expression showed no change with CH-OPT treatment. Previous work has shown involvement of both *Runx2* and *Osterix* in the control bone mineralisation[45].

No significant changes were observed in *ALP* gene expression and specific staining after either treatment with either CH digesta. This finding contrasts with previous studies using a pre-osteoblast cell line (MC3T3-E1 cells) and murine OB cultures showing increased *ALP* activity and mineralization after collagen treatment [9,11,13,14,19,21]. This discrepancy might be due to the different collagen products applied, doses used, and the direct application of CHs onto OB cultures [23,47,48].

The balance between the activity of OCs and OBs is essential for bone homeostasis and healthy joints, which is disrupted in OA[3]. The results from the present study indicate that CH-GL digesta lead to decreased OC activity while increasing OB activity, which could improve bone turnover in OA.

Taken together, after CH-GL treatment, OC size was significantly reduced, alongside decreased expression of osteoclastogenesis markers such as *Dc-stamp*, *Oscar* and *Rank*. In concert with the above findings with CH-GL, OB mineralization was increased with corresponding increases in OB differentiation markers *Runx2* and *Osterix*, as well as a decrease in *MMP-9* expression. The above findings contrasted in several respects with regards to the bone cells exposed to the CH-OPT digesta. In particular, an increase in OC differentiation and *Oscar* expression was observed with CH-OPT under the higher RANKL conditions that mimic elevated bone deterioration. Furthermore, only *Runx2* and *Col1a1* expression were increased in OBs after CH-OPT treatment. Overall, the above results indicate that CH-OPT appears to be less likely to improve bone homeostasis in OA. The differences between the two bovine-sourced CH digesta in OCs and OBs may be due to the different molecular weights (MWs) of the collagen products [18,47] leading to differing CH peptide profiles after digestion [23,48], and differing bioavailability of key bioactive peptides [24]. The differential collagen peptide profiles of the two tested CH products [24,48] could have differentially affected other unexplored pathways or signalling receptors that recognize collagen peptides. For example, receptors such as GPVI, which promotes OC differentiation and activation, or G6B-b, a receptor that inhibits differentiation, could have been activated by collagen fragments [38] associated with CH-GL and CH-OPT digesta.

As mentioned above, in vitro studies have typically applied CHs directly onto bone remodelling cells, neglecting the effects of GI digestion and bioavailability processes [9]. A review by Daneault et al., (2017) emphasized that such in vitro studies should be interpreted with caution [9]. Recently, Wauquier et al., (2019) obtained human serum at 1 h after oral intake of 25 g of CH [12]. The CH peptide enriched serum was applied onto cultures of blood mononuclear cells and primary human umbilical cord-derived mesenchymal stem cells for the assessment of osteoclastogenesis and osteoblastogenesis, respectively. Their findings indicated that the CH peptide enriched serum decreased osteoclastogenesis and enhanced osteoblastic activity [12]. A major limitation was that BAPs were not measured in the tested serum. There is limited feasibility for collection of human serum samples for such studies as this is time consuming, costly, and requires human ethics approval. As an alternative, the content and bioavailability of key BAPs from CHs using the combination of in vitro digestion and bioavailability methods together with cell culture can be completed without the above limitations[23,24].

Previous work has established that the sequence Gly-X-Y, where X and Y are often Pro and Hyp, has a beneficial effect on bone healing processes [49] and that Gly-Pro-Hyp upregulates osteoblastic differentiation genes in a dose-dependent manner [20]. The presence of Gly-Pro-Hyp after in vitro digestion of CH-GL and CH-OPT was confirmed in previous studies [23]. as well as the presence of Pro-Hyp [23]. Pro-Hyp is a well-known bioactive peptide found in CHs that has been shown to decrease cartilage loss in clinical trials [50] and animal studies [25], as well a decrease subchondral bone loss [25]. The presence of these peptides may explain the beneficial effects of CH digesta on bone remodelling cells seen with CH-GL, particularly the decrease in osteogenic activity with a corresponding increase in OB differentiation gene markers. Previous clinical trials have also established that CH-GL treatment is beneficial for joints [7,50,51], although the exact mechanisms remain unknown. The altered gene expression in bone cells seen after CH-GL treatment might also be involved to further promote overall joint health. On the other hand, increased osteoclastogenesis noted after CH-OPT treatment could increase bone resorption, as shown by the minimal improvement in the bone forming OB cell activity. Further in vivo animal studies and clinical studies are needed to elucidate the mechanisms by which CHs affect joint health, especially in the context of bone remodelling.

6.6 Conclusion

As bone remodeling is tightly regulated by bone-resorbing OCs and bone-forming OBs, the effects of CHs were tested on both cell types. The present study demonstrated that in vitro CH-GL digesta decreased OC gene expression differentiation and size whereas OC differentiation was increased by CH-OPT digesta. Also, OB differentiation markers and mineralization was increased with CH-GL digesta to a greater extent than observed after CH-OPT treatment. Taken together, it appears that balance of bone cell remodelling favors digesta obtained from CH-GL as compared to CH-OPT. Further studies involving animal models and clinical trials are needed to gain further understanding of the impact of CHs on bone health, especially in the context of OA.

6.7 Funding

This work was supported by a MITACS Accelerate Program PhD studentship (IT19837) in collaboration between McGill University and Genacol Canada Corporation as well as the

Collaborative Research Development Grant Program from the Natural Sciences and Engineering Council of Canada to S.K. (535744 -18).

6.8 Supplementary data

Table S6.1. Cell culture media and solutions

	Components
Base media	αMEM with L-glutamine (Gibco, #12 000-022)
Complete media	Base media, 10% fetal bovine serum (FBS, Wisent, #080152), 1% sodium pyruvate (Wisent, #600-110-EL), 1% penicillin-streptomycin (Wisent, #450-201-EL), 0.1 mg/mL ampicillin (BioShop Canada Inc, #AMP201.25)
1x PBS	140 mM NaCl, 3 mM KCl, 10 mM Na_2HPO_4, 2mM KH_2PO_4, 500 mL MilliQ H_20, adjusted to pH 7.4
Physiological solution	10 mM glucose, 130 mM NaCl, 5 mM KCl, 1 mM MgCl, 1mM CaCl, 20 mM HEPES
Stock solution 1	10 mL physiological solution, 125 µL 0.25% trypsin, 5 µL collagenase P (100 mg/mL) (Thermofisher, #11213857001)
Stock solution 2	10 mL physiological solution, 125 µL 0.25% trypsin, 10 µL collagenase P (100 mg/mL) (Thermofisher, #11213857001)
Stock solution 3	10 mL physiological solution, 125 µL 0.25% trypsin, 100 µL collagenase II (100 mg/mL) (Wothington-Biochem #CollagenaseII)

Table S6.2. Primer list for qPCR analysis

Gene	Sequence ´5 -´3		NCBI Reference Sequence
Osteoclasts			
RANK	Forward	GCATCCCTTGCAGCTCAACA	NM_009399.4
	Reverse	ATGGAAGAGCTGCAGACCAC	
Oscar	Forward	TCGCTGATACTCCAGCTGTC	NM_175632.3
	Reverse	TCTGGGGAGCTGATCCGTTA	
Cathepsin K	Forward	CAGTAGCCACGCTTCCTATCC	NM_007802.4
	Reverse	ACGCCGAGAGATTTCATCCA	
Lair-1	Forward	CTGTACCCCTGGGCAACTTT	NM_001302681.1
	Reverse	TTCCATAAAGGTGCTGCCGT	
NFATc1	Forward	CCCGGAGTTCGACTTCGATT	NM_016791.4
	Reverse	TCTCTGTAGGCTTCCAGGCT	
DC-STAMP	Forward	TTTCCACGAAGCCCTAGCTG	NM_029422.4
	Reverse	GCGTTCCTACCTTCACGGAG	
Osteoblasts			
Col1a1	Forward	GAGCGGAGAGTACTGGATCG	NM_007742.4
	Reverse	GTTCGGGCTGATGTACCAGT	
ALP	Forward	CAGGCCGCCTTCATAAGCA	NM_007431.3
	Reverse	GTGCCGATGGCCAGTACTAA	
Runx2	Forward	GCTTCTCAGCTTTAGCGTCG	NM_001145920.2
	Reverse	AAGGTGCCGGGAGGTAAGT	
Osterix	Forward	GATGGCGTCCTCTCTGCTTG	NM_130458.4
	Reverse	GGGCTGAAAGGTCAGCGTAT	
MMP-9	Forward	CCAGCCGACTTTTGTGGTCT	NM_013599.4
	Reverse	TGGCCTTTAGTGTCTGGCTG	
MMP13	Forward	GCCATTACCAGTCTCCGAGG	NM_008607.2
	Reverse	GGTCACGGGATGGATGTTCA	

Table S6.2. continued. Primer list for qPCR analysis

Gene	Sequence ´5 -´3		NCBI Reference Sequence
Housekeeping Genes (endogenous controls)			
Actin-B	Forward	TGTTACCAACTGGGACGACA	NM_007393.5
	Reverse	GGGGTGTTGAAGGTCTCAAA	
GAPDH	Forward	ACCCAGAAGACTGTGGATGG	NM_001289726.1
	Reverse	CACATTGGGGGTAGGAACAC	

Table S6.3. P values of the statistical comparison of gene expression between the two RANKL controls (50 and 100 ng/mL).

Gene	P value
Rank	0.8735
Lair-1	0.9998
Oscar	0.9993
NfatC1	0.9995
Dc-stamp	0.9977
Ctsk	0.9446

For each gene, statistical significance was assessed by a t-test ($p<0.05$) to determine differences between RANKL controls (50 ng/mL versus 100 ng/mL).

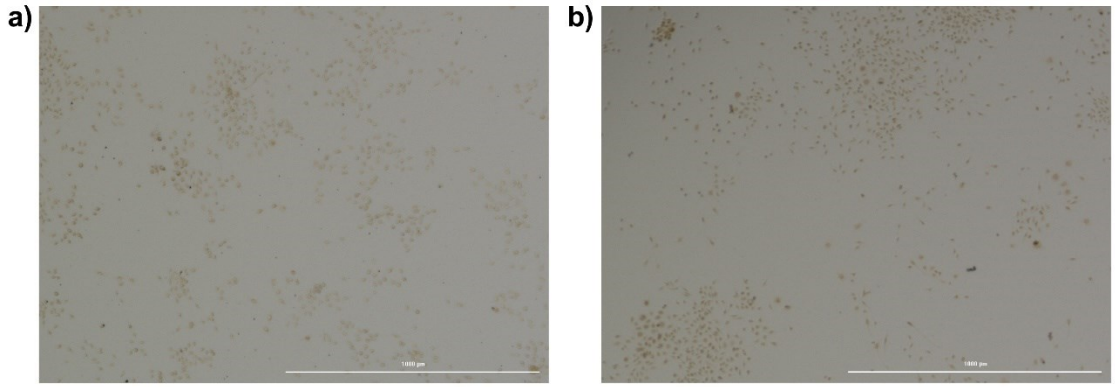

Figure S6.1. OC differentiation was not induced by CH treatment alone. Representative images of TRAP-stained OC precursor cells plated with M-CSF (50 ng/mL) and CH digests with no RANKL. No wells showed positively stained OCs after either: (a) CH-GL or (b) CH-OPT treatment.

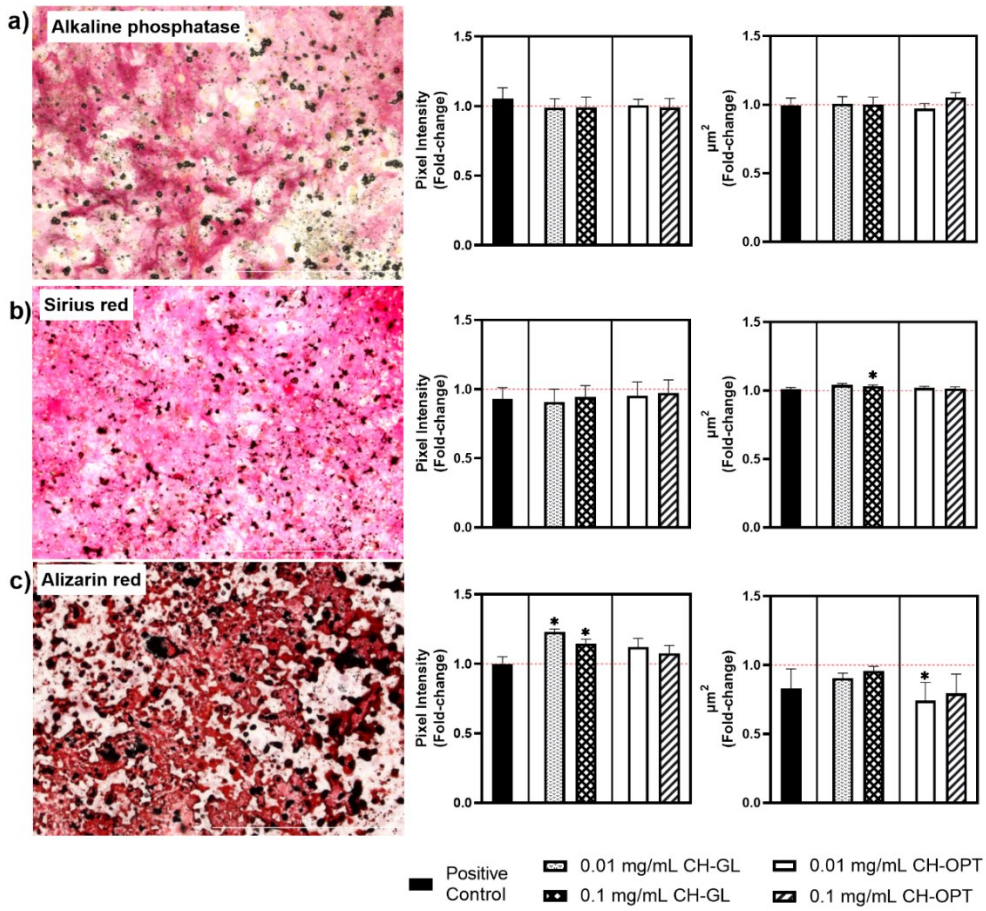

Figure S6.2 Primary OB staining with (a) alkaline phosphatase, (b) sirius red and (c) alizarin red. OBs were plated in osteogenic medium containing β-glycerophosphate and ascorbic acid. Cells were either not treated (control) or treated with CH (CH-GL or CH-OPT) at either 0.01 or 0.1 mg/mL. Representative images of stained OBs stained shown and pixel intensity and stained area were determined. Data are represented as mean ± SEM. For each stain and CH treatment, statistical significance was assessed by one-way ANOVA with Dunnett's post-hoc test to determine differences between treatment doses and respective control (*<0.05).

6.9 References

1 Mahmoudian, A., Lohmander, L. S., Mobasheri, A., Englund, M. & Luyten, F. P. Early-stage symptomatic osteoarthritis of the knee — time for action. *Nature Reviews Rheumatology* **17**, 621–632, doi:10.1038/s41584-021-00673-4 (2021).

2 Bello, A. E. & Oesser, S. Collagen hydrolysate for the treatment of osteoarthritis and other joint disorders: A review of the literature. *Curr. Med. Res. Opin.* **22**, 2221-2232 (2006).

3 Castañeda, S. & Vicente, E. F. Osteoarthritis: more than cartilage degeneration. *Clin. Rev. Bone. Miner. Metab.* **15**, 69-81, doi:10.1007/s12018-017-9228-6 (2017).

4 Lim, Y. Z., Hussain, S. M., Cicuttini, F. M. & Wang, Y. in *Bioactive Food as Dietary Interventions for Arthritis and Related Inflammatory Diseases* (eds Ronald Ross Watson & Victor R. Preedy) Ch. 6, 97-137 (Elsevier Inc., 2019).

5 Zdzieblik, D. *et al.* Collagen peptide supplementation in combination with resistance training improves body composition and increases muscle strength in elderly sarcopenic men: A randomised controlled trial. *Br. J. Nutr.* **114**, 1237-1245 (2015).

6 Zdzieblik, D., Oesser, S., Gollhofer, A. & König, D. Improvement of activity-related knee joint discomfort following supplementation of specific collagen peptides. *Appl. Physiol. Nutr. Metab.* **42**, 588-595, doi:10.1139/apnm-2016-0390 (2017).

7 Bruyère, O. *et al.* Effect of collagen hydrolysate in articular pain: A 6-month randomized, double-blind, placebo controlled study. *Complement. Ther. Med.* **20**, 124-130, doi:https://doi.org/10.1016/j.ctim.2011.12.007 (2012).

8 Pal, G. K. & Suresh, P. V. Sustainable valorisation of seafood by-products: Recovery of collagen and development of collagen-based novel functional food ingredients. *Innov. Food Sci. Emerg. Technol.* **37**, 201-215, doi:https://doi.org/10.1016/j.ifset.2016.03.015 (2016).

9 Daneault, A., Prawitt, J., Fabien Soulé, V., Coxam, V. & Wittrant, Y. Biological effect of hydrolyzed collagen on bone metabolism. *Crit. Rev. Food Sci. Nutr.* **57**, 1922-1937, doi:10.1080/10408398.2015.1038377 (2017).

10 Kawaguchi, T., Nanbu, P. N. & Kurokawa, M. Distribution of prolylhydroxyproline and its metabolites after oral administration in rats. *Biol. Pharm. Bull.* **35**, 422-427 (2012).

11 Elango, J. *et al.* Collagen peptide upregulates osteoblastogenesis from bone marrow mesenchymal stem cells through MAPK- Runx2. *Cells* **8**, doi:10.3390/cells8050446 (2019).

12 Wauquier, F. *et al.* Human enriched serum following hydrolysed collagen absorption modulates bone cell activity: from bedside to bench and vice versa. *Nutrients* **11**, doi:10.3390/nu11061249 (2019).

13 Guillerminet, F. *et al.* Hydrolyzed collagen improves bone metabolism and biomechanical parameters in ovariectomized mice: An *in vitro* and *in vivo* study. *Bone* **46**, 827-834, doi:10.1016/j.bone.2009.10.035 (2010).

14 N'deh, K. P. U. *et al.* Collagen extract derived from yeonsan ogye chicken increases bone microarchitecture by suppressing the RANKL/OPG ratio via the JNK signaling pathway. *Nutrients* **12**, 1967 (2020).

15 Guillerminet, F. *et al.* Hydrolyzed collagen improves bone status and prevents bone loss in ovariectomized C3H/HeN mice. *Osteoporosis Int.* **23**, 1909-1919, doi:10.1007/s00198-011-1788-6 (2012).

16 König, D., Oesser, S., Scharla, S., Zdzieblik, D. & Gollhofer, A. Specific collagen peptides improve bone mineral density and bone markers in postmenopausal women-a randomized controlled study. *Nutrients* **10**, 97, doi:10.3390/nu10010097 (2018).

17 Martin-Bautista, E. *et al.* A nutritional intervention study with hydrolyzed collagen in pre-pubertal spanish children: influence on bone modeling biomarkers. *J. Pediatr. Endocrinol. Metab.* **24**, 147-153, doi:10.1515/jpem.2011.009 (2011).

18 Elango, J. *et al.* Cross-talk between primary osteocytes and bone marrow macrophages for osteoclastogenesis upon collagen treatment. *Sci. Rep.* **8**, 1-11 (2018).

19 Liu, J. *et al.* Bovine collagen peptides compounds promote the proliferation and differentiation of MC3T3-E1 pre-osteoblasts. *PLoS One* **9**, e99920, doi:10.1371/journal.pone.0099920 (2014).

20 Min, G. *et al.* Collagen hydrolysate Gly-Pro-Hyp on osteoblastic proliferation and differentiation of MC3T3-E1 cells. *Journal of Clinical and Nursing Research* **1**, 40-46, doi:10.26689/jcnr.v1i3.158 (2017).

21 Kim, H. K., Kim, M.-G. & Leem, K.-H. Collagen hydrolysates increased osteogenic gene expressions via a MAPK signaling pathway in MG-63 human osteoblasts. *Food Funct.* **5**, 573-578, doi:10.1039/c3fo60509d (2014).

22 Kimira, Y. *et al.* Collagen-derived dipeptide prolyl-hydroxyproline promotes differentiation of MC3T3-E1 osteoblastic cells. *Biochem. Biophys. Res. Commun.* **453**, doi:10.1016/J.BBRC.2014.09.121 (2014).

23 Larder, C. E., Iskandar, M. M., Sabally, K. & Kubow, S. Complementary and efficient methods for di- and tri-peptide analysis and amino acid quantification from simulated gastrointestinal digestion of collagen hydrolysate. *LWT* **155**, 112880, doi:https://doi.org/10.1016/j.lwt.2021.112880 (2022).

24 Larder, C. E., Iskandar, M. M. & Kubow, S. Assessment of Bioavailability after In Vitro Digestion and First Pass Metabolism of Bioactive Peptides from Collagen Hydrolysates. *Curr. Issues Mol. Biol.* **43**, 1592-1605, doi:doi:10.3390/cimb43030113 (2021).

25 Nakatani, S., Mano, H., Sampei, C., Shimizu, J. & Wada, M. Chondroprotective effect of the bioactive peptide prolyl-hydroxyproline in mouse articular cartilage in vitro and in vivo. *Osteoarthr. Cartil.* **17**, 1620-1627 (2009).

26 Walther, B. *et al.* Gutself: Interindividual variability in the processing of dietary compounds by the human gastrointestinal tract. **63**, 1900677, doi:https://doi.org/10.1002/mnfr.201900677 (2019).

27 Kumar, S., Sugihara, F., Suzuki, K., Inoue, N. & Venkateswarathirukumara, S. A double-blind, placebo-controlled, randomised, clinical study on the effectiveness of collagen peptide on osteoarthritis. *J. Sci. Food Agric.* **95**, 702-707 (2015).

28 Skov, K., Oxfeldt, M., Thøgersen, R., Hansen, M. & Bertram, H. C. Enzymatic hydrolysis of a collagen hydrolysate enhances postprandial absorption rate-A randomized controlled trial. *Nutrients* **11**, doi:10.3390/nu11051064 (2019).

29 Boraschi-Diaz, I. & Komarova, S. V. The protocol for the isolation and cryopreservation of osteoclast precursors from mouse bone marrow and spleen. *Cytotechnology* **68**, 105-114, doi:10.1007/s10616-014-9759-3 (2016).

30 ImageJ (National Institutes of Health, Bethesda, Maryland, USA, , 1997-2018).

31 Orriss, I. R., Hajjawi, M. O. R., Huesa, C., MacRae, V. E. & Arnett, T. R. Optimisation of the differing conditions required for bone formation in vitro by primary osteoblasts from mice and rats. *Int. J. Mol. Med.* **34**, 1201-1208, doi:10.3892/ijmm.2014.1926 (2014).

32 Orriss, I. R., Taylor, S. E. & Arnett, T. R. Rat osteoblast cultures. *Methods Mol. Biol.* **816**, 31-41, doi:10.1007/978-1-61779-415-5_3 (2012).

33 Wilson, S. R., Peters, C., Saftig, P. & Brömme, D. Cathepsin K activity-dependent regulation of osteoclast actin ring formation and bone resorption. *The Journal of biological chemistry* **284**, 2584-2592, doi:10.1074/jbc.M805280200 (2009).

34 Chiu, Y.-H. & Ritchlin, C. T. DC-STAMP: A key regulator in osteoclast differentiation. *J. Cell. Physiol.* **231**, 2402-2407, doi:10.1002/jcp.25389 (2016).

35 Nedeva, I. R., Vitale, M., Elson, A., Hoyland, J. A. & Bella, J. Role of OSCAR signaling in osteoclastogenesis and bone disease. *Frontiers in cell and developmental biology* **9**, doi:10.3389/fcell.2021.641162 (2021).

36 Tiedemann, K. *et al.* Regulation of osteoclast growth and fusion by mTOR/raptor and mTOR/rictor/Akt. **5**, doi:10.3389/fcell.2017.00054 (2017).

37 Lees, R. L., Sabharwal, V. K. & Heersche, J. N. Resorptive state and cell size influence intracellular pH regulation in rabbit osteoclasts cultured on collagen-hydroxyapatite films. *Bone* **28**, 187-194, doi:10.1016/s8756-3282(00)00433-6 (2001).

38 Boraschi-Diaz, I., Wang, J., Mort, J. S. & Komarova, S. V. Collagen type I as a ligand for receptor-mediated signaling. *Frontiers in Physics* **5**, doi:10.3389/fphy.2017.00012 (2017).

39 Boraschi-Diaz, I. *et al.* Collagen type I degradation fragments act through the collagen receptor LAIR-1 to provide a negative feedback for osteoclast formation. *Bone* **117**, 23-30, doi:10.1016/j.bone.2018.09.006 (2018).

40 Chataigner, M. *et al.* Dietary fish hydrolysate improves memory performance through microglial signature remodeling during aging. *Frontiers in Nutrition* **8**, doi:10.3389/fnut.2021.750292 (2021).

41 Kodama, J. & Kaito, T. Osteoclast multinucleation: Review of current literature. *International journal of molecular sciences* **21**, 5685 (2020).

42 Jackson, M. T., Moradi, B., Smith, M. M., Jackson, C. J. & Little, C. B. Activation of matrix metalloproteinases 2, 9, and 13 by activated protein C in human osteoarthritic cartilage chondrocytes. *Arthritis Rheumatol* **66**, 1525-1536, doi:https://doi.org/10.1002/art.38401 (2014).

43 Zeng, G. Q., Chen, A. B., Li, W., Song, J. H. & Gao, C. Y. High MMP-1, MMP-2, and MMP-9 protein levels in osteoarthritis. *Genet. Mol. Res.* **14**, 14811-14822, doi:10.4238/2015.November.18.46 (2015).

44 Li, H., Wang, D., Yuan, Y. & Min, J. New insights on the MMP-13 regulatory network in the pathogenesis of early osteoarthritis. *Arthrit. Res. Ther.* **19**, 248, doi:10.1186/s13075-017-1454-2 (2017).

45 Liu, Q. *et al.* Recent advances of osterix transcription factor in osteoblast differentiation and bone formation. *Frontiers in cell and developmental biology* **8**, doi:10.3389/fcell.2020.601224 (2020).

46 Nakashima, K. *et al.* The novel zinc finger-containing transcription factor osterix is required for osteoblast differentiation and bone formation. *Cell* **108**, 17-29, doi:10.1016/s0092-8674(01)00622-5 (2002).

47 Simons, V. S. *et al.* Comparative analysis of peptide composition and bioactivity of different collagen hydrolysate batches on human osteoarthritic synoviocytes. *Sci. Rep.* **8**, doi:10.1038/s41598-018-36046-3 (2018).

48 Larder, C. E., Iskandar, M. M. & Kubow, S. Gastrointestinal digestion model assessment of peptide diversity and microbial fermentation products of collagen hydrolysates. *Nutrients* **13**, 2720, doi:https://doi.org/10.3390/nu13082720 (2021).

49 Hata, S. *et al.* Effect of oral administration of high advanced-collagen tripeptide (HACP) on bone healing process in rat. *Journal of Hard Tissue Biology* **17**, 17-22, doi:10.2485/jhtb.17.17 (2008).

50 Feliciano, D. D. S. *et al.* Effect of collagen hydrolysate as adjuvant treatment to exercise for knee osteoarthritis in *Philippine Academy of Rehabilitation Medicine* Vol. 9 4-15 (2017).

51 Bernardo, M. L. R. & Azarcon Jr., A. C. A randomized controlled trial on the effects of oral collagen treatment on the medial knee joint space and functional outcome among Veterans Medical Center patients diagnosed with osteoarthritis of the knee in *Philippine Academy of Rehabilitation Medicine Proceedings* Vol. 4 1-8 (2012).

CHAPTER 7: GENERAL SUMMARY AND CONCLUSIONS

7.1 General discussion

This thesis describes a series of studies and in vitro models that were used to investigate and follow the digestive, gut microbial and biological processes that CHs undergo following oral consumption. This thesis provides a holistic view into the bioaccessibility and bioavailability of two CHs (CH-GL and CH-OPT) and their BAP content, as well as their corresponding health promoting properties. Specifically, Study 1 (**Figure 7.1, A**) investigated the bioaccessibility of low MW peptides, whereas Study 3 (**Figure 7.1, C**) presents data on higher MW peptides (15 AA+). Study 2 (**Figure 7.1, B**) assessed the bioavailability of key di-and tri-BAPs from CH digesta collected in Study 1. Following upper intestinal digestion, there are two main routes that peptides may follow, small intestinal absorption or colonic microbial fermentation, both of which were explored in this thesis. Study 3 (**Figure 7.1, C**) investigated what occurs to the unabsorbed portion of CHs and its impact on microbial metabolite production, whereas Study 4 (**Figure 7.1, D)** investigated the bioactivity of the bioavailable CH components on bone cells. The framework of the thesis provides a system of analysis for CH investigation, replicating, in a step-by-step process, what occurs in vivo (**Figure 7.2**). This methodological approach (i.e., assessing digestion, absorption, gut microbial metabolism and then bioactivity; **Figure 7.2**), could be used as a standard investigative approach to assess the impact of other supplements and nutraceuticals on human health before costly animal and human studies are undertaken.

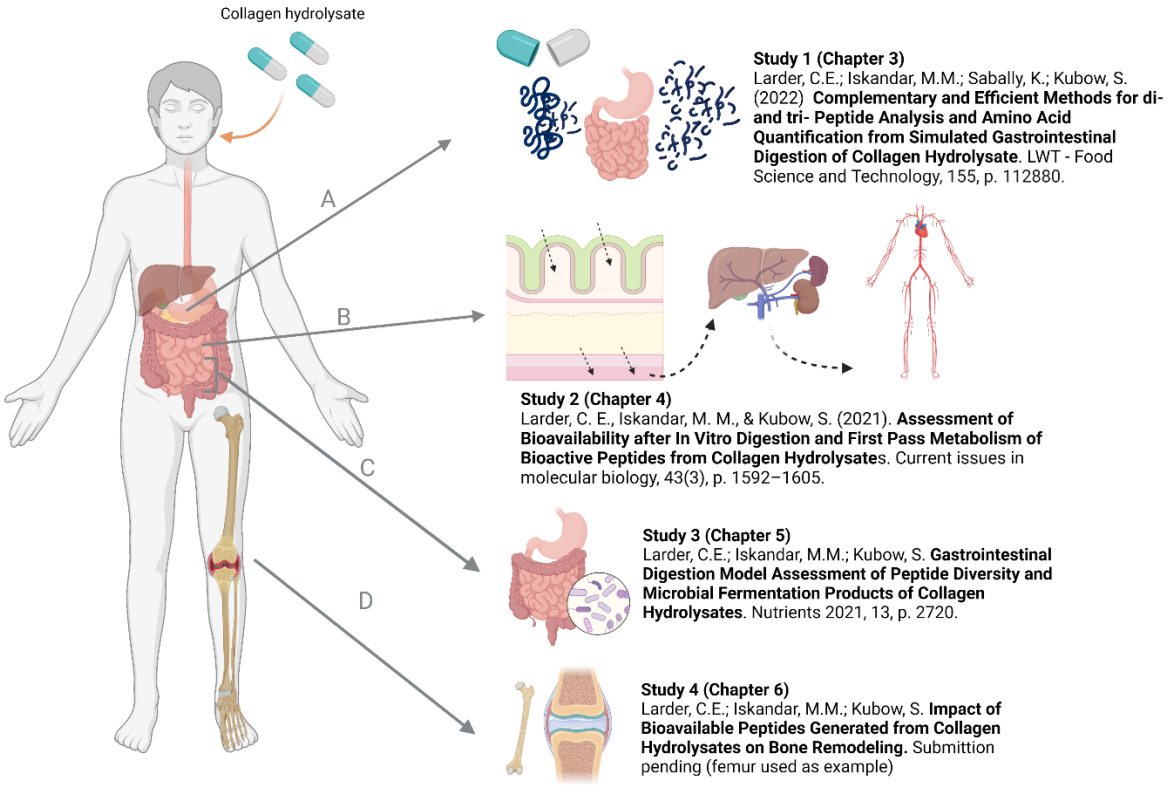

Figure 7.1. Thesis summary. Created with Biorender

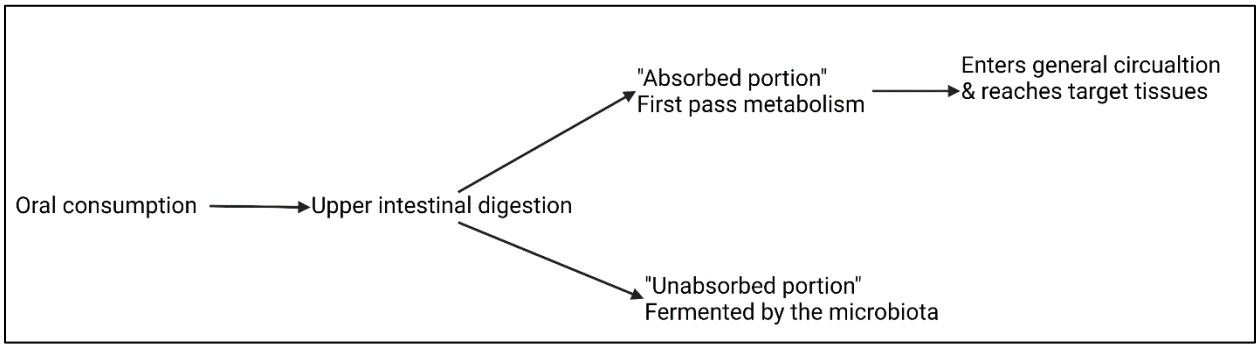

Figure 7.2. Methodological framework to investigate the bioaccessibility, bioavailability and bioactivity of food derived products, supplements or nutraceuticals. Created with Biorender

CHs are supplements that OA patients can easily access and consume to help manage OA symptoms and improve joint health [7, 18]. CHs are taken orally because this is both a cost effective and easily

accessible method of treatment for the general public, seeing as no prescription or injection by a physician are necessary. Before oral consumption, analysis of the peptide profile and compositional nature of similarly sourced CHs can be vastly different, as demonstrated by the proteomics and MALDI analysis of bovine-sourced CHs (CH-GL and CH-OPT) completed in Study 3. The peptide profiles of CH-GL and CH-OPT were different before digestion, with some sequences found in one product and not the other. Only three peptide sequences were shared between the two products before digestion. This difference in peptide diversity can result from differing CH preparation and purification methods [160, 164]. Our results are in agreement with previous work by Simon et al. (2018), who investigated the peptide composition of three different CHs (CH-Alpha®, Peptan® B 2000 and Mobiforte®) [138]. Peptide composition and profile were assessed by MALDI-TOF mass spectrometry and ICPL™-isotope labelling and showed distinctly different peptide compositions among the products, which was attributed to their different preparation methods.

Using an in vitro model of upper intestinal digestion, the peptide profiles (15 AA+) of CH-GL and CH-OPT were compared. A significant increase in peptide diversity was observed with both CHs after digestion, although significantly more sequences were released after CH-OPT digestion. Digestion efficiency and the release of different peptide sequences are a direct result of differing CH preparation or purification methods, that make certain CHs more digestible than others. This was the first study to characterize peptides before and after digestion of similarly sourced CHs. Previous work, such as the work completed by Simons et al. (2018), investigating CH composition and bioactivity has often failed to account for digestive processes [138]. A recent review by Amigo et al. (2020) also noted that cell-based experiments used to investigate the bioactivity of food peptides are often not consistent with in vivo data, principally because in vitro studies do not consider the digestive and metabolic processes that occur before BAPs reach their target tissues [26]. Our work clearly demonstrates the necessity of digesting CH products prior to subsequent analysis of bioactivity, as the peptide profiles may change significantly after digestion.

In Study 3, analysis of lower MW peptides (e.g. peptides with less than 15 AA) was not possible, due to the limitation of “peptide-centric” proteomic methodologies, as di- and tri-peptides are too small for sequencing. In addition, the complexity of the CH digesta samples rendered MALDI analysis and interpretation impossible. An investigation into lower MW peptides, such as di- and tri-peptides

from collagen was needed, as these small peptides have well-established bioactivity and increased bioavailability compared to greater MW CH peptides [9, 26, 100]. For example, CH-derived Pro-Hyp has been shown to decrease the loss of chondrocytes, prevent articular cartilage thinning and improve bone health [114, 119], which helps to improve joint integrity in OA patients [105]. The tri-peptide Gly-Pro-Hyp also promotes improved bone health, by increasing osteoblastic cell activity, specifically upregulating the protein expression of Runx2, Osterix, ALP and Col1a1 in a dose-dependent manner [82].

Although small MW peptide content significantly contributes to CH bioactivity, no methods of targeted peptide analysis have been described in the literature for CH digesta. Previous methodological approaches, developed for plasma samples, often calculated peptide content using indirect calculations of Hyp-containing peptides and/or AAs [9, 11, 22]. For example, Skov et al. (2019), determined the postprandial plasma concentration of Gly-Pro-Hyp in a human clinical trial using ^{1}H NMR analysis, but they did not target and quantify the peptide directly. Instead, they estimated the peptide content by summing the individual AA measurements of Gly, Pro, and Hyp. As digestion breaks down peptides into their AA components, it is possible that the summed plasma content of Gly, Pro, and Hyp showed a greater apparent bioavailability of Gly-Pro-Hyp than a direct measurement of the tri-peptide itself. In addition to the lack of targeted peptide methods, no methodological approach had been developed to measure free AA content after in vitro CH digestion. In response to the above needs, Study 1 utilized our standard in vitro model of digestion and addressed significant gaps in methodology as well as provided further understanding of the first biological processes that CH must undergo in the GI tract after oral consumption. The bioaccessibility of CH-derived peptides with known bioactivity was determined using a novel CE method with concurrent analysis of the free AA content determined using LC-MS equipped with a HILIC-Z column. Similar to the proteomic and MALDI analysis in Study 3, the peptide profiles of CH-GL and CH-OPT using CE was assessed in Study 1. Key results showed qualitative differences between the two CHs, which was determined by the appearance of novel peaks in either CH product, which were absent in the other. Unlike proteomic analysis, distinct quantitative differences in the relative abundances of peaks were also determined among shared peaks assessed by CE. There were 13 unidentified peaks found in each CH that were unique to each product, which could partly explain differences in bioactivity observed in our later studies (Study 4: effect of CH on

bone), and possibly contribute to differences in clinical efficacy. Peptide diversity after digestion remains important to assess as it may exert a significant effect on CH bioactivity, particularly as the identification and bioactivity of unknown peaks can become clearer in the future. These unknown peptides may also contribute to the reported health benefits of CHs seen in clinical trials. Furthermore, individual peptides may not always exhibit bioactivity themselves, but could provide synergistic effects.

Using LC-MS equipped with a HILIC-Z column, our reported free AA content measured from in vitro CH digesta was greater than previously reported plasma AA concentrations by Skov et al. (2019) after CH supplementation in humans and measured by ^{1}H NMR [9]. This difference could be due to several reasons. Firstly, AAs could have been incorporated into protein synthesis or used to synthesize other metabolites in human subjects, thereby lowering the AA content from the blood. Secondly, different CH products between their study and ours were used. Skov at al. (2019) used the CH product OmniCol™ (Essentia Protein Solutions, Graasten, Denmark), which is currently not available for sale in North America. In contrast, we used Genacol Original Formula® (Blainville, QC, Canada) (CH-GL) and Selection (Uniprix, QC, Canada) (CH-OPT) in our study. The source of raw material likely differs between the products listed above. As previously established in Study 1 and 3, the peptide content between similar sourced CHs can differ significantly. It is conceivable that the AA content can also differ between CH products from Denmark compared to products sold and distributed in Canada. Although our study showed no difference between the AA content of CH-GL and CH-OPT, differences between the CHs used in our study and the one assessed by Skov et al. (2019) could be possible, but needs to be verified. Finally, and most importantly, are the different methods of quantification used. Methods such as ^{1}H NMR have few sample preparation steps [9, 165], but data analyses require multiple processing steps that can make interpretation difficult, due to issues such as spectral alignment, baseline correction, scaling and normalization as well as chemical shift referencing. Data processing of ^{1}H NMR spectra remains a highly debated topic with little consensus from experts on the processing steps and data interpretation, especially for complex biological fluids. Additionally, sample pH, salt concentration and the choice of temperature gradients can also affect the spectral output of ^{1}H NMR. In contrast, LC-MS methods such as the one used in our study equipped with a HILIC column have little sample preparation steps and provide accurate and reliable data. Furthermore, with the use of external standards, data can be

easily interpreted with far less room for error in comparison to ^{1}H NMR, as reliance on spectral databases are not necessary.

Reported levels of the BAPs Pro-Hyp, Pro-Hyp-Gly and Ala-Hyp (24.62 ± 1.73, 14.03 ± 1.41 and 3.15 ± 0.43 nmol/L, respectively) from a rat intestinal perfusate after porcine skin hydrolysate supplementation were much lower than reported in Study 1 [34]. Other studies using rat models with fish collagen supplementation using LC-MS/MS have also reported peptide values from plasma below those measured in Study 1 [25]. Specifically, the peptides Gly-Pro-Hyp and Pro-Hyp from fish collagen ranged between 0.05-10 µg/mL and 0.3-8 µg/mL, respectively over the course of 5 h in a rat model [25]. The differences in peptide content between previous work and ours could be attributable to species differences in digestion process, bioavailability and metabolic capacity between humans and animal models that often occur [23, 166, 167]. In vitro models of digestion have been shown to represent more physiological conditions, seeing as animal models, particularly rodents, may not always reflect human in vivo conditions accurately. However, to truly understand and compare CH-derived BAPs content from plasma, an assessment of the bioavailability of the peptides (those that enter the general circulation after first-pass) using a cell-based in vitro model was necessary and completed in Study 2.

Study 2 followed the next biological step that CHs undergo after oral consumption and digestion. Study 2 assessed the contents of digested CH-derived peptides that enter the general circulation after being absorbed by the SI and undergoing first pass by the liver. These bioavailable BAPs eventually reach target tissues such as bone and cartilage, and exert health promoting properties to improve joint function in OA patients. Yet, a significant gap in the literature was the lack of targeted methodologies that could be used to measure and quantify peptides from simulated biological models. For this reason, the CE method from Study 1 was adapted for the quantification of bioavailable BAPs in Study 2.

Freeze dried digesta from Study 1 were applied to a co-culture of HIEC-6/HepG2 cells in an effort to represent physiological conditions, as recent criticism of cell-based work emphasised the fact that most studies fail to consider the digestive and metabolic processes that bioactive food peptides must undergo before absorption [26]. In addition, most published work investigating

"bioavailability" determined intestinal transport only. Intestinal absorption alone does not represent systemic availability. In Study 2, a co-culture of both intestinal and hepatic cells was used to fully understand and determine the bioavailability of CH-derived BAPs. The importance of assessing the contribution of hepatic action was clearly demonstrated in our work. Notably Ala-Hyp production was observed after incubating with HepG2 cells (up to 304.9 ± 57.2%) after CH-GL digest treatment. Furthermore, there was a significant difference in the hepatic first pass effects on Pro-Hyp between the two CHs. Hepatic action on Pro-Hyp was greater after CH-GL treatment (151.4 ± 24.3%) compared to CH-OPT (63.63 ± 8.63%). This observation was unexpected as the content of Pro-Hyp that travelled across the intestinal layer was not significantly different between the treatments. The difference in hepatic first pass effects on Pro-Hyp might be due to the presence of Gly-Pro-Hyp that was solely noted to be intestinally transported after CH-GL treatment; this tri-peptide could have been metabolized further by hepatic cells to contribute to the Pro-Hyp content. Such hepatic production of Pro-Hyp would not be expected with CH-OPT as Gly-Pro-Hyp was not appreciably transported across the intestinal layer with this treatment. The increase in BAP production for all the di-peptides during hepatic action could also have occurred due to the metabolism of unidentified longer chain peptides that travelled across the epithelium.

Previous work assessing the effects of a polyphenol-rich potato extract using a Caco-2/HepG2 co-culture has also demonstrated notable polyphenol production after HepG2 incubation [31]. Increases in ferulic, dihydrocaffeic, 3-hydroxyphenylpropionic, and coumaric acids by 166, 338, 233 and 212 % after incubation with HepG2 were observed. As shown with our work, the degree of hepatic metabolism in the previous study was surprising, as the cellular uptake of the phenolic metabolites was only 3-11%. Previous studies and our optimized cell culture method continue to support the use of co-cultures utilizing hepatic cell lines, as the generation of secondary metabolites and the breakdown of peptides is significant. Differences in P_{app} and transport (%) was observed between our work and previous literature, but this is likely due to the different cell line used as well as the co-presence of HepG2 cells. Previous in vitro work using Caco-2 cells, which have decreased expression of peptide transporters such a PepT1, should be interpreted with caution as they may not predict human in vivo bioavailability accurately and do not take into account the considerable hepatic action peptides may undergo, as explained above. Further studies can adopt and

standardize the HIEC-6/HepG2 co-culture method, which could be adapted to investigate the first pass effects of other bioactive food components, nutraceuticals and supplements.

Based on the P_{app} and transport (%) of the targeted CH-derived peptides in Study 2, a high degree of transport and bioavailability was observed compared to other food-derived peptides. In previous work assessing the transport of whey protein isolates using a Caco-2 monolayer, BAPs Leu-Pro-Tyr-Pro-Tyr and Trp-Arg, which exhibit DPP-IV activity, were shown to have very low permeability (0.05% and 0.47%, respectively) [168]. Milk-derived peptides from casein with antioxidant properties have a greater range of permeability. The permeability of the peptides Ile -Glu, Ser-Asp-Lys and Tyr-Pro-Tyr were 44.81, 21.68 and 5.56% respectively [169]. Furthermore, the permeability of a milk-derived peptide (RLSFNP) with ACE-inhibitory activity was also assessed only using Caco-2 [170]. Only 6.4% of the peptide content traveled across the intestinal layer after 2.5 h. In our work, the lowest peptide permeability was for Ala-Hyp (9.27 ± 2.49 %) after CH-GL treatment, although the greatest peptide permeability after CH-GL was Hyp-Gly with 62.41 ± 11.11 % travelling across the intestinal cell layer. Generally, our work supports previous literature that has shown CHs to be well absorbed in animal and human studies. In fact, a main feature and benefit of CH products is their bioavailability and tolerability by patients [8, 18, 100]. As a consequence of increased bioavailability, a greater amount and number of BAPs in the bloodstream may reach OA joints and exert their bioactivity. The wide range of peptide bioavailability observed in the literature and our work is most likely due to the fact that size, shape and charge may influence peptide absorption [26]. Future work to improve and develop in silico models to estimate BAP transport could provide an additional platform to our methodological approach investigating peptide bioavailability before cell culture studies are completed [144].

As demonstrated in Study 2, not all the CH peptide content was absorbed. Larger MW peptides, which are less bioavailable, may also bypass intestinal absorption [18, 100]. Following the route of CHs after oral consumption, the remaining CH content that reaches the colon had never been investigated. It was possible that the rich content of peptides (demonstrated in Studies 1 and 2) and AAs (Study 1) could survive digestion, reach the large intestine, and lead to the generation of microbial nitrogenous fermentation products. For this reason, Study 3 utilized a dynamic GI model inoculated with human fecal matter to determine the prebiotic potential of CH-GL and CH-OPT.

Insight into the microbial metabolite production potential of CHs is particularly relevant for OA patients, as gut health is being increasingly linked to joint health [37, 38, 41].

In our study, the prebiotic impact of CHs was only observed in the ascending colon. It is possible that the doses of CHs used (1.2 g) did not allow for enough substrate to survive and be available for fermentation in the transverse and descending colonic regions. Only CH-OPT demonstrated significant changes in microbial metabolite production in the ascending colon, with no obvious prebiotic or dysbiotic effects after CH-GL treatment. Compared to other reports utilizing similar digestion models and analyses of microbial metabolite production after polyphenol treatment, the changes observed after CH-OPT are only slightly lower. After the application of polyphenol compounds (chlorogenic, caffeic and ferulic acid and rutin) to a similar dynamic GI model, total SCFA content (mM) increased to approximately 30, 60 and 55 in the ascending, transverse and descending colon, respectively [171]. In another batch-type model, SCFA content after probiotic treatment over 24 h was also greater than the effect of CH-OPT [172]. SCFA content ranged between 40-50 mM after treatments, whereas the total SCFA content after CH-OPT fermentation was below 38.53 mM in the ascending colon. In the same study the content of NH_4 and H_2S, which are produced after protein fermentation, was measured using similar methods as the ones used in this thesis. When NH_4 levels are greater than 5–10 mM, this can have negative health consequences by altering the metabolism of intestinal cells, impairing DNA synthesis and reducing the life expectancy of cells [35]. These changes encourage the multiplication of damaged cells in the intestine with altered metabolism. Levels of NH_4 reported in Study 3 are closer to the lower levels reported in the literature [35] and were decreased further after CH-OPT supplementation. In a comparison, NH_4 levels were shown to increase above 15 mM after probiotic treatment (*L. rhamnosus, L. helveticus, S. boulardii and B. longum*) in a batch fermentation model [172]. The levels of proteins, peptides and AAs from CH supplementation are below the level needed to induce excessive NH_4 production and cause dysbiosis.

While Study 3 investigated the potential prebiotic effects of the unabsorbed portion of CHs, insight into the bioactivity of the absorbed portion of the BAPs remained to be explored. Therefore, in Study 4, the effects of bioavailable peptides that reach the systemic circulation and possibly joint tissue targets were investigated. Specifically, the effects of CH-GL and CH-OPT were determined on

bone remodeling cells, OCs and OBs. A review by Amigo et al. (2020), cautioned readers interpreting previous cell-based experiments that were used to determine the bioactivity of food peptides, as the doses used were generally greater than those in animal and human models, and therefore not physiological [26]. Furthermore, as mentioned above, these experiments often neglected the digestive processes that food components must undergo, before being applied to cell culture experiments. For this reason, the BAP content released after digestion of CHs from Study 1, as well as the bioavailability data from Study 2 were used to calculate physiologically representative doses of CHs for the application on bone cells in Study 4. Additionally, FD digesta from Study 1 were utilized to account for the breakdown of peptides and the different peptide diversities between undigested and digested CH (as validated in Study 3). This series of in vitro methods provides an optimal alternative to animal and human models to investigate the bioactive effects of CH-derived peptides on any downstream target tissues (e.g., bone, cartilage, or skin). This methodological approach can also be adopted and applied to investigate other food-derived bioactive compounds and nutraceuticals.

In Study 4, the effects of CHs were determined on both OC and OB cells. Previous work assessing CHs on bone health has focused on OBs, yet our work clearly demonstrates that the activity of OCs was also significantly affected by CHs. It is therefore important to assess OBs *and* OCs as they both contribute to the overall health and homeostasis of bone remodeling. Novel insight into gene modulation after CH treatment was observed in OCs in this study. To our knowledge, no previous work has assessed the impact of CH on OSCAR, Lair-1, and DC-Stamp expression in OCs in vitro. We also report for the time the levels of MMP-9 and MMP-13 in OBs after CH treatment. Our results demonstrate that these genes can be modulated by CH treatment in a type- and dose dependent manner.

Recent research demonstrated that, besides the RANK/RANKL-pathway, co-stimulatory signals such as those from OSCAR, may be required for both the expression of osteoclast-specific genes and the activation of OCs [74]. Collagen fragments act as ligands for OSCAR, and specific sequences have been shown to interact with the receptor with different levels of affinity [74], although no work assessing the signalling potential of CHs has been reported. However, recent work has demonstrated a clear link between OA and OSCAR expression [75]. Both mouse and human

cartilage show increased expression of OSCAR during OA pathogenesis. Furthermore, in OA induced mice, markers of OA were significantly reduced in OSCAR$^{-/-}$ mice. The authors have suggested that a disruption of OSCAR expression or the interaction with OSCAR and collagen fragments may provide an interesting opportunity for the development of therapeutic agents for OA. In our study, OSCAR expression was significantly decreased after CH-GL treatment, which could partly explain the therapeutic properties of CHs in terms of bone health and joint health previously demonstrated in clinical studies. In contrast, CH-OPT decreased OSCAR expression with standard RANKL conditions, whereas in pathological conditions with increased RANKL, OSCAR expression was increased. Increased OSCAR expression could contribute to increased OC differentiation, and thus increase bone resorption. The clinical implications of increased OSCAR expression, as a result of CH-OPT, are unknown as no clinical studies have been completed with CH-OPT to our knowledge. Both OSCAR and RANK signal downstream and regulate the expression of NFATc1. NFATc1 is a key transcription factor regulating OCs specific genes, and essential for the production of mature OCs [74]. NFACTc1 expression was deceased with CH-GL under standard RANKL, with no modulation after CH-OPT treatment. DC-stamp, a regulator of cell-cell fusion was downregulated with both CHs under standard RANKL. These results demonstrate that OC activity is downregulated with CHs, especially CH-GL, which may translate to clinical potency.

Other OC genes that were assessed in this study, and in previous work, were RANK, Lair-1 and Cathepsin K expression. RANK expression was decreased with CH under increased RANKL conditions. As no difference in RANKL controls were observed, the contributing factor to the observed increased RANK expression is likely due to the CH treatments, not RANKL. Decreased RANK/RANKL signalling typically decreases downstream expression of OC differentiation genes and activity, demonstrated by lower expression levels of OSCAR, NFACTc1, and DC-Stamp, although no changes in cathepsin K were observed in our study. Other competing pathways could have regulated cathepsin K expression. Gene OC modulation may partly explain the decreased OC differentiation observed with CH-GL, but more importantly, it was the size of the OCs that were significantly decreased after CH-GL treatment. Each CH-GL dose, under both RANKL conditions, decreased OC size, and as a result, would decrease OC resorption activity [173].

Novel insight into gene modulation after CH treatment in OBs was also provided in Study 4. Previous work has often assessed only one CH or collagen peptide; a comparison between different CH products and their potential to affect bone cells had not yet been assessed. Our results demonstrate that OB genes were modulated by CH treatment in a type- and dose dependent manner. The OB differentiation gene Runx2 was increased after 0.1 mg/mL CH treatment by almost 2-fold. Furthermore, CH-GL also increased another OB differentiation gene marker Osterix whereas no changes were observed after CH-OPT treatment. Enhanced collagen deposition was associated with increased mineralisation at the 0.1 mg/mL CH-GL dose, as previously described with CH treatments [120]. This increase in collagen deposition is likely due to decreased expression of the collagen degrading enzyme MMP-9 observed only with CH-GL. Although it is well established that increased levels of MMP-9 are associated with OA pathogenesis, previous work has not investigated the impact of CHs on MMP activity in bone cells [78, 79]. In contrast to CH-GL, no increase in sirius and alizarin red staining, assessing collagen deposition and mineralization respectively, were observed with CH-OPT, as well as no effect on MMP-9 expression. Interestingly, the gene expression levels of Col1a1 were increased with 0.1 mg/mL CH-OPT, however no increase in deposited collagen assessed by sirus red staining were observed. There are a few reasons as to why these conflicting results may have occurred. Firstly, gene expression precedes deposition; therefore, increased culture time may allow the observation of increased collagen deposition staining. Secondly, other pathways and regulators of collagen deposition could have affected collagen content, such as MMP-2 and 14 [174]. Increased screening for other genes associated with collagen regulation is necessary to understand the impact of CHs in OBs more fully.

Overall, the effect of CH-GL on bone cells was generally greater than CH-OPT. This could be due to the diversity of BAPs from CH-GL after digestion as well as its bioavailable peptide content. As determined in Study 1, the content of Pro-Hyp-Gly released after CH-GL digestion was greater than CH-OPT. Although no bioavailability data is available for this peptide, it is conceivable that the peptide may be metabolized further into Pro-Hyp, a CH peptide that promotes joint health [114]. Furthermore, the Gly-Pro-Hyp content after digestion of CH-GL was greater than CH-OPT, as well as only being bioavailable with CH-GL. Previous work has established that the sequence Gly-X-Y, where X and Y are often Pro and Hyp respectively, has a beneficial effect on bone healing processes [175] and that Gly-Pro-Hyp upregulated expression of Runx2, Osterix, ALP and Col1 in OB cells in a dose-

dependent manner [82]. The beneficial effects on OC and OB activity after CH-GL are therefore most likely due to the greater content of Pro-Hyp-Gly and Gly-Pro-Hyp after digestion as well as the relatively high bioavailable content of Pro-Hyp. Furthermore, the synergistic effects of unidentified BAPs are still under investigation. These synergistic phenomena could influence digestive processes as well as peptide absorption and metabolism. For example, hormonal responses can be influenced by the presence of other proteins or peptides consumed. The glucose-dependent insulinotropic polypeptide response and gastric emptying were greater when milk protein hydrolysates were ingested compared to whole milk protein sources [26]. Also, colonic motility contractions were increased with whey hydrolysates compared to whey protein concentrates [26].

Further work on identifying and understanding the synergistic effects affecting peptide transport, bioavailability and bioactivity is needed, particularly for CH-GL. Although CH-OPT has increased peptide diversity after digestion (Study 3), the bioactivity of these peptides in joint tissues appears to be low, as there were less observed effects on bone cells compared to CH-GL. Competing peptides could have also inhibited or decreased the bioactivity of some sequences. In line with improved bone remodeling cell function after CH-GL, clinical studies using CH-GL have shown that patients with joint pain had significant improvement in joint structures, which included decreased cartilage abrasion and lateral meniscus protrusions as well as a significant increase in cartilage thickening in the central portion of the trochlear articular cartilage [105]. In this study as well as two others, CH-GL was also shown to decrease joint pain [8, 105, 176]. To our knowledge, no information is available regarding the clinical efficacy of CH-OPT.

7.2 Strengths and limitations

The determination of BAPs and AAs generated during in vivo digestion is technically difficult, costly and requires human or animal ethics approval [26]. As an alternative, simulated digestion models, like the one used in Study 1, provide a relatively simple in vitro approach to detect BAPs and AAs released from digestive processes. There are many in vitro models to choose from and each has their advantages and disadvantages [139], but regardless of the model chosen, experimental conditions such as the digestive enzymes used and their concentrations may vary between laboratories, making comparing in vitro digestion studies sometimes difficult. Recent efforts to standardize in vitro digestion models, such as INFOGEST, are ongoing [47, 142]. Even using a

harmonised digestive model, in vitro digestion models cannot always simulate the complex digestive forces, enzymatic action, and tissue interactions that occur in vivo, and remain a limitation of these approaches [139]. Notwithstanding the disadvantages of in vitro digestion models, these models remain a simple and rapid method of assessing bioaccessibility, and previous studies continue to support the use of in vitro digestion models for the assessment of nutrient digestion and for BAPs when compared to in vivo results [47, 49, 139, 140, 143, 144].

Existing methods for the assessment of CH-derived BAPs are optimised for blood and plasma samples and rely on costly methods that require substantial sample preparation and data interpretation [9, 20, 165]. Furthermore, previous studies have often used indirect measures of AAs to quantify BAPs, and have focused on either metabolite, but not both. The work described in Study 1 details sensitive and rapid methodologies for concurrent analysis of BAPs and AAs after digestion of CHs, which can support further understanding of the bioactive components of CHs. In our study, a simple filtration step was required before diluting and injecting digesta samples for AA analysis, rendering this method rapid with less room for error, unlike other methods that require AA derivation before LC-MS analysis. Similarly, sample preparation for CE was also rapid and used minimal sample volume. As the methods described in Study 1 were sensitive, simple, cost-effective, and reliable, they can easily be used towards future in vitro CH digestion studies by other laboratories. There are some limitations to the current methods developed that must be considered. Due to the complex nature of SI digesta, the presence of salts, such as sodium chloride, found in digesta fluid and buffers, may affect ionization efficiency and so reduce the quality of the MS data collected by LC-MS to quantify AAs. Another limitation was that no desalting procedure was used, although this may be necessary depending on the complexity of the sample [177, 178]. A limitation of the current CE method is that only 5 BAPs were targeted while CH products contain a wide variety of peptides. Therefore, a more comprehensive assessment of other BAPs should be developed. CE is also heavily affected by ionic strength, so peptide retention time may differ from one experiment to another. Thus, a re-assessment and peak identification is required between experiments.

A major novelty of Study 2 was the assessment of CH-derived BAPS using a Transwell co-culture of HIEC-6 and HepG2 cells to simulate in vivo conditions of absorption and first pass metabolism. Cell

culture models provide an excellent platform to predict the bioavailability of BAPs, as animal studies often to do not correlate with human data, and human trials are long, expensive, and have ethical restrictions [26]. Comparisons of cell culture models to human in vivo data generally support the use of in vitro models to assess intestinal transport [28-30]. No previous work has used this combination of cells to represent more accurately what occurs in vivo. In fact, although previous work has demonstrated that HIEC cells more accurately represent the physiological in vivo conditions of the SI compared to Caco-2 cells [28-30], Caco-2 remains the standard in bioavailability studies. The results from Study 2 can encourage future studies to adopt and standardize the HIEC-6/HepG2 co-culture method to investigate the first pass effects of bioactive food components, nutraceuticals and supplements. Another strength of Study 2 was that in vitro CH digesta, rather than the CH product itself was directly dissolved in cell culture media. The CH digesta was applied to the bioavailable cell culture model thereby taking into account the breakdown and digestion of the peptides by the upper intestinal tract [26]. In contrast, one of the limitations of Study 2 was that the expression of the peptide transport PepT1 was not assessed. Previous work has shown that CH-derived BAPS such as Pro-Gly can increase PepT1 expression in HepG2 cells, although no assessment on intestinal epithelial cells was completed [151]. Whether CHs affect Pept1 expression in the SI remains to be determined.

The use of the continuous multi-stage GI model in Study 3 enabled us to perform a more physiologically relevant evaluation of the microbial metabolites produced after CH consumption in the different colonic segments, compared to in vitro batch fermentation models [47, 48]. Using models that target all 3 colonic regions is an advantage of the multi-stage GI model; and was particularly relevant for our work, seeing as the prebiotic potential of the CHs was primarily observed in the ascending colon only. Our work was the first to investigate the microbial metabolites produced by CHs. One of the main advantages from our study is that a comprehensive analysis of the major SCFAs (acetic, butyric, and propionate acids), but also the minor SCFAs (valeric, caproic and heptanoic acids) and BCFAs (isobutyric, isovaleric and isocaproic acids) was completed. Although the health implications of minor SCFAs and BCFAs are still under investigation, their contribution to overall health may become apparent in the future. A major limitation of this study is that the interaction and cross-signalling between the microbiome environment and epithelial cells are not represented in the current version of the dynamic GI model. Future work combining in vitro

GI models and cell culture could address this gap. Another limitation of the current study was that only one dose (1.2 g) based on clinical studies using CH-GL, was administered. Other trials have used much greater doses ranging from 5 to 35 g of CH products [5, 9, 53, 103, 104, 134]. As a result of a greater initial dose of CHs, increased microbial fermentation products could have occurred due to more substrate availability to the colonic regions.

So far, most in vitro studies have applied CH products directly to bone remodelling cells, neglecting the effects of GI digestion or associated CH-derived BAP bioavailability [54]. A major strength and novelty of Study 4 was that CH digesta, using pre-determined doses based on BAP bioaccessibility (Study 1) and bioavailability (Study 2), were applied to primary OB and OC cultures. This combination of methodologies can be used to determine physiologically relevant CH doses for in vitro studies thereby increasing the transferability of the generated results to the human context. Ideally, first pass extracts obtained directly from Study 2 should be applied to the bone-related cultures; however, the feasibility of obtaining sufficient first pass sample, as well as having no interfering media components are areas for future investigation.

Previous studies have used only one RANKL concentration, whereas in our work a standard (50 ng/mL) as well as a high dose of RANKL (100 ng/mL) was used to mimic OA progression and elevated bone deterioration initiated by OBs [4, 16, 73]. Complimentary analysis of both cell types allowed for a holistic approach into bone remodeling mechanisms affected by CHs. Our work was also the first to investigate the impact of CHs on multiple genes from both OCs and OBs, as previous analyses have typically focused on 1-3 gene markers only. In addition, gene expression from OCs not previously explored, such as Dc-Stamp and Lair-1 and OSCAR, were investigated and found to be modulated by CHs in a type- and dose-dependent manner. One of the limitations of this study was that inflammation and cytokine profiles, which are key factors in OA pathogenesis and regulate bone metabolic cells, were not assessed [74, 179]. In addition, the crosstalk between OCs and OBs was not investigated in a co-culture, so cell-to-cell signalling, and regulation were not accounted for.

7.3 Considerations for future research

The findings from the present thesis work provide novel information regarding the bioaccessibility of CH-derived BAPs and AAs after in vitro digestion, as well as novel methods of quantification. Furthermore, this work provides significant insights into the bioavailability and bioactivity of CH-derived BAPs. The use of novel techniques and models have helped address significant gaps in the literature, but many unanswered questions could be further investigated.

For Studies 1, 2 and 3 the choice of in vitro digestion model could be optimized for future studies. Use of the standardized static in vitro digestion method developed by the COST INFOGEST network would ensure reproducibility and comparability of the digestion protocol between laboratories, while also reflecting in vivo conditions of human digestion [49, 142, 180]. The INFOGEST digestion method is characterized by its availability and its adaptability to various food components. The method also provides a platform that researchers with limited experience can adopt to acquire endpoint digesta of food samples such as peptides and AAs [180]. Besides a general improvement to the in vitro digestion method selected, each study also has areas of future work that should be considered.

Study 1: The identification of bioaccessible BAPs was performed using a targeted approach using CE. BAPs were initially selected based on their potential bioactivity to joint health and other well-established sequences observed from CH analysis in plasma. Identification of a wider range of BAPs could provide further insight into the health benefits and bioactivities of CHs. For example, other sequences identified from bovine collagen in previous work, such as Val-Gly-Pro-Val and Gly-Pro-Arg-Gly-Phe, have been shown to exhibit antihypertensive activity, and the sequence Pro-Pro-Arg has DPP-IV inhibitory properties [100]. Besides identifying other BAPs, future method optimisation could include coupling CE with MS analysis [181]. Additionally, modifying the inner surface of the capillary by dynamic coating to ensure peptides with proline at the carboxy terminus do not adhere to the capillary wall, would ensure reproducible results for ongoing and intensive analyses of CH digesta [182].

Study 2: Transwell systems, such as the one used in Study 2 to co-culture HIEC and HepG2 cells to assess the bioavailability of CH derived BAPs, are commonly used due to their simplicity and

accessibility. These systems are often used in drug pharmacokinetic studies and drug oral bioavailability work but there are still several limitations of these systems. Transwell cultures do not reflect the real intestinal structure and microenvironment of the human GI tract [183]. Furthermore, tissue-tissue cross talk is also not represented in Transwell methods. As an alternative, 3D tissue models or gut-on-a chip models in controlled systems more accurately reflect human GI physiology [183, 184]. Traditional 2D cultures, typically using Caco-2 cells, only represent absorptive enterocytes from the GI, and lack the stem cell niche able to produce the other cell types present in the intestine. Organoids overcome such limitations and these "mini organ" cultures produce intestinal epithelial layer cells as well as goblet, enteroendocrine, tuft, and Paneth cells [184]. A key benefit of an organoid-like system compared to traditional 2D cultures is the presence of a mucus layer produced by goblet cells. Organoids still have some limitations, as they create 3D spheroids, in which access to their apical compartment is limited. Yet, recent work has enzymatically lysed organoids and seeded them into 2D substrates, allowing access to the apical and basolateral sides of the epithelium [184]. Other techniques, such as microinjection, have also been used to access the luminal component of the organoid model, but have had limited success to date [184]. Organoids are still powerful experimental tools that are also practical, as they can be frozen and repeatably thawed and grown, providing a rich source of material for experiments. Other systems utilizing microfluidics and cell biology, otherwise known as "gut-on-chip" models are also used to investigate drugs, gut-host crosstalk, the microbiome and nutrition metabolism [183]. Different "gut-on-chip" models have been developed, and current applications to replicate the intestinal environment contain epithelial, endothelial and immune type cells. "Gut-on-chip" models may also be co-cultured with the microbiome, to represent the crosstalk between microorganisms and the host. These systems have been used to understand drug efficacy and drug pharmacokinetics after oral ingestion [183]. For example, the pharmacokinetics of three drugs (propranolol, thiopentone and pentobarbital) were evaluated using a microfluidic system to mimic in vivo conditions and found that propranolol was better absorbed [185]. Previous work by Kimura et al. (2015) developed a "body-on-chip" model which included both the intestinal barrier as well as hepatic tissue and a lung model which was used to assess three anticancer drugs (epirubicin, irinotecan, and cyclophosphamide) [186]. Further work has also developed innovative intestine-liver models to assess intestinal drug absorption, and hepatic metabolism, as well as bioactivity of breast cancer cells [187]. Utilizing these culture models to assess CH-derived BAPs would more

accurately reflect in vivo conditions and better help predict bioavailability and potential bioactivity. These innovative “gut-on-chip” culture models also provide a platform to understand the link between the GI tract and inflammation [183]. As inflammation is a key component of OA, future work assessing the effects of CH-derived BAPs on inflammation is the next step to further this research. Initial assessments of cytokine production and other markers of inflammation could be completed using a co-culture of GI cells and immune cells, before implementing more advanced systems such as “gut-on-chip” to investigate OA inflammation.

Study 3: Previous studies have indicated that the microbiome plays an important role in the onset and severity of arthritis [37]. Study 3 inoculated colonic bioreactors from a dynamic GI model with fecal matter from a healthy individual. Future gut model studies to assess the impact of CH could use fecal samples from patients with OA to study the changes to microbial fermentation products. Additional biomarkers of GI health, focusing on AA fermentation, could be investigated such as p-cresol. P-cresol, as well as other indole compounds, are products of aromatic AA catabolism [35]. Future analysis using 16S rRNA gene amplicon sequencing to profile gut microbiota community structure and composition affected by CH supplementation is also another consideration for future work, as metabolite products only help to partially assess the impact on the microbiome. As mentioned previously, only one dose of CH (1.2 g) was used to assess the impact of CH on microbial metabolite productions. Other clinical trials have used greater doses (ranging 5-35 g), so future work using a dose response to CH supplementation could help predict the optimal dose required for CHs to have the most beneficial impact on the microbiome.

Study 4: Inflammation is a key factor in OA pathogenesis and cytokine secretion has been found to regulate bone metabolic cells [74, 179] and cell-to-cell signalling between OBs and OCs is a key component of the RANK/RANKL pathway. Therefore, future work utilizing a co-culture of OBs and OCs as well as macrophages to evaluate the effects of CH digesta on bone remodelling could be utilized [73]. Murine cells provide an easily accessible cell source to conduct preliminary analysis, but human-derived bone cells would more accurately reflect the changes that would occur in humans after CH treatment. Further development and harmonization between the use of first pass metabolism extracts from Study 2 and the bone cells in Study 4, would also provide a more accurate representation of the impact of bioavailable BAPs on OBs and OCs.

Improvement to the delivery system of BAPs after oral consumption of CH is also another consideration for future work to enhance their bioavailability and thus their bioactivity. Current research in structural modification such as direct PEGylation as well as conjugation with glucosamine (GlcN) to increase peptide delivery are promising methods to consider in future work [188, 189]. Other methods to facilitate oral peptide bioavailability are enzyme inhibitors as well as absorption enhancers such as chitosans, which help to increase the absorption of hydrophilic drugs [7, 189]. Another use of chitosans could be to form a part of the carrier systems adapted to increase the absorption of the identified peptides [7, 189]. Increased absorption of well-established peptides that function on bone and cartilage, such as Pro-Hyp, would increase the potential of CHs to improve OA patient joint health.

7.4 Conclusions

In summary, this dissertation has presented a series of studies that follow CHs throughout the GI tract and assess their bioactivity. The results of this thesis have demonstrated that CHs from the same source (bovine) contained very different peptide profiles, before and after digestion, as well as differences in BAP bioavailability. The bioactivity of the two CHs assessed also differed, which is most likely a result of their differing BAP content and profiles. Bioactivity at the level of the microbiome demonstrated that CHs could induce prebiotic effects in the ascending colon, and that the effects were CH-dependent. The bioactivity of CH-derived BAPs also demonstrated that CHs have a dose and treatment effect on bone remodeling cells. Bone resorbing cells showed decreased gene expression and size, while increased gene expression and mineralization was observed in bone forming cells.

This dissertation has also developed novel methods of assessment for bioaccessible peptides and AAs, as well as bioavailable peptides after first pass metabolism. The novel co-culture of HIEC/HepG2 cells provides a high-throughput method to determine bioavailability that more accurately represents the physiological in vivo conditions of the SI compared to current cell culture standards. Implementation of this co-culture could be used to investigate the first pass effects of other bioactive food components, nutraceuticals, and supplements. The use of all in vitro models described in this dissertation provides a cost-effective platform for high throughput analysis of bioactive metabolites such as BAPs generated after CHs consumption.

GENERAL REFERENCES

1. Lim, Y.Z., et al., *Chapter 6: Nutrients and Dietary Supplements for Osteoarthritis*, in *Bioactive Food as Dietary Interventions for Arthritis and Related Inflammatory Diseases*, R.R. Watson and V.R. Preedy, Editors. 2019, Elsevier Inc.: Academic Press. p. 97-137.
2. Peat, G. and M.J. Thomas, *Osteoarthritis Year in Review 2020: Epidemiology & Therapy.* Osteoarthritis and Cartilage, 2021. **29**(2): p. 180-189.
3. Bello, A.E. and S. Oesser, *Collagen Hydrolysate for the Treatment of Osteoarthritis and Other Joint Disorders:A Review of the Literature.* Current Medical Research and Opinion, 2006. **22**(11): p. 2221-2232.
4. Castañeda, S. and E.F. Vicente, *Osteoarthritis: More Than Cartilage Degeneration.* Clinical Reviews in Bone and Mineral Metabolism, 2017. **15**(2): p. 69-81.
5. Zdzieblik, D., et al., *Collagen Peptide Supplementation in Combination with Resistance Training Improves Body Composition and Increases Muscle Strength in Elderly Sarcopenic Men: A Randomised Controlled Trial.* British Journal of Nutrition, 2015. **114**(8): p. 1237-1245.
6. Zdzieblik, D., et al., *Improvement of Activity-Related Knee Joint Discomfort Following Supplementation of Specific Collagen Peptides.* Applied Physiology, Nutrition, and Metabolism, 2017. **42**(6): p. 588-595.
7. Pal, G.K. and P.V. Suresh, *Sustainable Valorisation of Seafood by-Products: Recovery of Collagen and Development of Collagen-Based Novel Functional Food Ingredients.* Innovative Food Science & Emerging Technologies, 2016. **37**: p. 201-215.
8. Bruyère, O., et al., *Effect of Collagen Hydrolysate in Articular Pain: A 6-Month Randomized, Double-Blind, Placebo Controlled Study.* Complementary Therapies in Medicine, 2012. **20**(3): p. 124-130.
9. Skov, K., et al., *Enzymatic Hydrolysis of a Collagen Hydrolysate Enhances Postprandial Absorption Rate-a Randomized Controlled Trial.* Nutrients, 2019. **11**(5).
10. Iwai, K., et al., *Identification of Food-Derived Collagen Peptides in Human Blood after Oral Ingestion of Gelatin Hydrolysates.* Journal of Agricultural and Food Chemistry, 2005. **53**(16): p. 6531-6536.

11. Shigemura, Y., et al., *Changes in Composition and Content of Food-Derived Peptide in Human Blood after Daily Ingestion of Collagen Hydrolysate for 4 Weeks.* Journal of the Science of Food and Agriculture, 2018. **98**(5): p. 1944-1950.
12. Oesser, S., et al., *Oral Administration of 14c Labeled Gelatin Hydrolysate Leads to an Accumulation of Radioactivity in Cartilage of Mice (C57/Bl).* The Journal of Nutrition, 1999. **129**(10): p. 1891-1895.
13. Song, H., Q. Tian, and B. Li, *Novel Hyp-Gly-Containing Antiplatelet Peptides from Collagen Hydrolysate after Simulated Gastrointestinal Digestion and Intestinal Absorption.* Food & Function, 2020. **11**(6): p. 5553-5564.
14. Wauquier, F., et al., *Human Enriched Serum Following Hydrolysed Collagen Absorption Modulates Bone Cell Activity: From Bedside to Bench and Vice Versa.* Nutrients, 2019. **11**(6).
15. Guillerminet, F., et al., *Hydrolyzed Collagen Improves Bone Metabolism and Biomechanical Parameters in Ovariectomized Mice: An in Vitro and in Vivo Study.* Bone, 2010. **46**(3): p. 827-834.
16. N'deh, K.P.U., et al., *Collagen Extract Derived from Yeonsan Ogye Chicken Increases Bone Microarchitecture by Suppressing the RANKL/OPG Ratio Via the JNK Signaling Pathway.* Nutrients, 2020. **12**(7): p. 1967.
17. Guillerminet, F., et al., *Hydrolyzed Collagen Improves Bone Status and Prevents Bone Loss in Ovariectomized C3H/Hen Mice.* Osteoporosis International, 2012. **23**(7): p. 1909-1919.
18. León-López, A., et al., *Hydrolyzed Collagen-Sources and Applications.* Molecules, 2019. **24**(22): p. 4031.
19. Chen, L., X. Shen, and G. Xia, *Effect of Molecular Weight of Tilapia (Oreochromis Niloticus) Skin Collagen Peptide Fractions on Zinc-Chelating Capacity and Bioaccessibility of the Zinc-Peptide Fractions Complexes in Vitro Digestion.* Applied Sciences, 2020. **10**(6): p. 2041.
20. Alemán, A., M.C. Gómez-Guillén, and P. Montero, *Identification of Ace-Inhibitory Peptides from Squid Skin Collagen after in Vitro Gastrointestinal Digestion.* Food Research International, 2013. **54**(1): p. 790-795.
21. Wang, L., et al., *Bioavailability and Bioavailable Forms of Collagen after Oral Administration to Rats.* Journal of Agricultural and Food Chemistry, 2015. **63**(14): p. 3752-3756.

22. Wang, L., et al., *Determination of Bioavailability and Identification of Collagen Peptide in Blood after Oral Ingestion of Gelatin.* Journal of the Science of Food and Agriculture, 2015. **95**(13): p. 2712-2717.
23. Punt, A., et al., *Non-Animal Approaches for Toxicokinetics in Risk Evaluations of Food Chemicals.* Alternatives to Animal Experimentation, 2017. **34**(4): p. 501-514.
24. Taga, Y., et al., *Identification of Collagen-Derived Hydroxyproline (Hyp)-Containing Cyclic Dipeptides with High Oral Bioavailability: Efficient Formation of Cyclo(X-Hyp) from X-Hyp-Gly-Type Tripeptides by Heating.* Journal of Agricultural and Food Chemistry, 2017. **65**(43): p. 9514-9521.
25. Sontakke, S.B., et al., *Orally Available Collagen Tripeptide: Enzymatic Stability, Intestinal Permeability, and Absorption of Gly-Pro-Hyp and Pro-Hyp.* Journal of Agricultural and Food Chemistry, 2016. **64**(38): p. 7127-7133.
26. Amigo, L. and B. Hernández-Ledesma, *Current Evidence on the Bioavailability of Food Bioactive Peptides.* Molecules, 2020. **25**(19).
27. Takenaka, T., et al., *Human Small Intestinal Epithelial Cells Differentiated from Adult Intestinal Stem Cells as a Novel System for Predicting Oral Drug Absorption in Humans.* Drug Metabolism and Disposition, 2014. **42**(11): p. 1947-1954.
28. Takenaka, T., et al., *Application of a Human Intestinal Epithelial Cell Monolayer to the Prediction of Oral Drug Absorption in Humans as a Superior Alternative to the Caco-2 Cell Monolayer.* Journal of Pharmaceutical Sciences, 2016. **105**(2): p. 915-924.
29. Pászti-Gere, E., et al., *Exposure of Human Intestinal Epithelial Cells and Primary Human Hepatocytes to Trypsin-Like Serine Protease Inhibitors with Potential Antiviral Effect.* Journal of Enzyme Inhibition and Medicinal Chemistry, 2021. **36**(1): p. 659-668.
30. Zhao, X., et al., *The in Vitro Protective Role of Bovine Lactoferrin on Intestinal Epithelial Barrier.* Molecules, 2019. **24**(1): p. 148.
31. Sadeghi Ekbatan, S., et al., *Absorption and Metabolism of Phenolics from Digests of Polyphenol-Rich Potato Extracts Using the Caco-2/HepG2 Co-Culture System.* Foods, 2018. **7**(1): p. 8.
32. Louisa, M., et al., *Differential Expression of Several Drug Transporter Genes in HepG2 and Huh-7 Cell Lines.* Advanced biomedical research, 2016. **5**: p. 104.

33. Lau, Y.Y., et al., *Evaluation of a Novel in Vitro Caco-2 Hepatocyte Hybrid System for Predicting in Vivo Oral Bioavailability.* Drug Metabolism and Disposition, 2004. **32**(9): p. 937-942.
34. Osawa, Y., et al., *Absorption and Metabolism of Orally Administered Collagen Hydrolysates Evaluated by the Vascularly Perfused Rat Intestine and Liver in Situ.* Biomedical research, 2018. **39**(1): p. 1-11.
35. Nyangale, E.P., D.S. Mottram, and G.R. Gibson, *Gut Microbial Activity, Implications for Health and Disease: The Potential Role of Metabolite Analysis.* Journal of Proteome Research, 2012. **11**(12): p. 5573-5585.
36. Diether, N.E. and B.P. Willing, *Microbial Fermentation of Dietary Protein: An Important Factor in Diet-Microbe-Host Interaction.* Microorganisms, 2019. **7**(1): p. 19.
37. Dorozynska, I., et al., *Partial Depletion of Natural Gut Flora by Antibiotic Aggravates Collagen Induced Arthritis (CIA) in Mice.* Pharmacological Reports, 2014. **66**(2): p. 250-255.
38. Liu, X., et al., *Role of the Gut Microbiome in Modulating Arthritis Progression in Mice.* Scientific Reports, 2016. **6**: p. 30594.
39. Rowland, I., et al., *Gut Microbiota Functions: Metabolism of Nutrients and Other Food Components.* European Journal of Nutrition, 2017. **57**(1): p. 1-24.
40. Peng, M. and D. Biswas, *Short Chain and Polyunsaturated Fatty Acids in Host Gut Health and Foodborne Bacterial Pathogen Inhibition.* Critical Reviews in Food Science and Nutrition, 2017. **57**(18): p. 3987-4002.
41. Schott, E.M., et al., *Targeting the Gut Microbiome to Treat the Osteoarthritis of Obesity.* JCI Insight, 2018. **3**(8): p. e95997.
42. Roberfroid, M., et al., *Prebiotic Effects: Metabolic and Health Benefits.* British Journal of Nutrition, 2010. **104 Suppl 2**: p. S1-63.
43. Utzschneider, K.M., et al., *Mechanisms Linking the Gut Microbiome and Glucose Metabolism.* The Journal of clinical endocrinology and metabolism, 2016. **101**(4): p. 1445-1454.
44. Sheflin, A.M., et al., *Pilot Dietary Intervention with Heat-Stabilized Rice Bran Modulates Stool Microbiota and Metabolites in Healthy Adults.* Nutrients, 2015. **7**(2): p. 1282-1300.
45. Ashaolu, T.J. and J.O. Ashaolu, *Prebiotic Peptides, Their Formation, Fermentation in the Gut, and Health Implications.* Biotechnology Progress, 2021. **37**(3): p. e3142.

46. Larder, C.E., M.M. Iskandar, and S. Kubow, *Gastrointestinal Digestion Model Assessment of Peptide Diversity and Microbial Fermentation Products of Collagen Hydrolysates.* Nutrients, 2021. **13**(8): p. 2720.
47. Dupont, D., et al., *Can Dynamic in Vitro Digestion Systems Mimic the Physiological Reality?* Critical Reviews in Food Science and Nutrition, 2018. **59**(10): p. 1546-1562.
48. Van de Wiele, T., et al., *The Simulator of the Human Intestinal Microbial Ecosystem (Shime®)*, in *The Impact of Food Bioactives on Health: In Vitro and Ex Vivo Models*, K. Verhoeckx, et al., Editors. 2015, Springer International Publishing: Cham. p. 305-317.
49. Egger, L., et al., *Digestion of Milk Proteins: Comparing Static and Dynamic in Vitro Digestion Systems with in Vivo Data.* Food Research International, 2019. **118**: p. 32-39.
50. Abdul Rahim, M.B.H., et al., *Diet-Induced Metabolic Changes of the Human Gut Microbiome: Importance of Short-Chain Fatty Acids, Methylamines and Indoles.* Acta Diabetologica, 2019. **56**(5): p. 493-500.
51. Ríos-Covián, D., et al., *Intestinal Short Chain Fatty Acids and Their Link with Diet and Human Health.* Frontiers in Microbiology, 2016. **7**: p. 185.
52. Pietro, C., et al., *Biomarkers of Gastrointestinal Functionality in Animal Nutrition and Health.* Animal Feed Science and Technology, 2019. **250**: p. 9-31.
53. König, D., et al., *Specific Collagen Peptides Improve Bone Mineral Density and Bone Markers in Postmenopausal Women-a Randomized Controlled Study.* Nutrients, 2018. **10**(1): p. 97.
54. Daneault, A., et al., *Biological Effect of Hydrolyzed Collagen on Bone Metabolism.* Critical Reviews in Food Science and Nutrition, 2017. **57**(9): p. 1922-1937.
55. Zhang, Y. and J.M. Jordan, *Epidemiology of Osteoarthritis.* Clinics in Geriatric Medicine, 2010. **26**(3): p. 355-369.
56. Hunter, D.J., L. March, and M. Chew, *Osteoarthritis in 2020 and Beyond: A Lancet Commission.* Lancet (London, England), 2020. **396**(10264): p. 1711-1712.
57. Vina, E.R. and C.K. Kwoh, *Epidemiology of Osteoarthritis: Literature Update.* Current Opinion in Rheumatology, 2018. **30**(2): p. 160-167.
58. Van Spil, W.E., et al., *Osteoarthritis Phenotypes and Novel Therapeutic Targets.* Biochemical Pharmacology, 2019. **165**: p. 41-48.
59. Wluka, A.E., C.B. Lombard, and F.M. Cicuttini, *Tackling Obesity in Knee Osteoarthritis.* Nature Reviews Rheumatology, 2013. **9**(4): p. 225-235.

60. Veronese, N., et al., *Type 2 Diabetes Mellitus and Osteoarthritis.* Seminars in Arthritis and Rheumatism, 2019. **49**(1): p. 9-19.
61. Eymard, F., et al., *Diabetes Is a Risk Factor for Knee Osteoarthritis Progression.* Osteoarthritis and Cartilage, 2015. **23**(6): p. 851-859.
62. Singh, G., et al., *Prevalence of Cardiovascular Disease Risk Factors among US Adults with Self-Reported Osteoarthritis: Data from the Third National Health and Nutrition Examination Survey.* The American Journal of Managed Care, 2002. **8**(15 Suppl): p. S383–S391.
63. Baudart, P., et al., *Association between Osteoarthritis and Dyslipidaemia: A Systematic Literature Review and Meta-Analysis.* RMD Open, 2017. **3**(2): p. e000442.
64. Sellam, J. and F. Berenbaum, *Is Osteoarthritis a Metabolic Disease?* Joint, Bone, Spine: Revue du Rhumatisme, 2013. **80**(6): p. 568-573.
65. Kluzek, S., J.L. Newton, and N.K. Arden, *Is Osteoarthritis a Metabolic Disorder?* British Medical Bulletin, 2015. **115**(1): p. 111-121.
66. Chun, J.-S., et al. *Concurrent Session 1: Metabolic Osteoarthritis*. in *OARSI Connect '21 Virtual World Congress on Osteoarthritis*. 2021. Virtual.
67. Mahmoudian, A., et al., *Early-Stage Symptomatic Osteoarthritis of the Knee — Time for Action.* Nature Reviews Rheumatology, 2021. **17**(10): p. 621–632.
68. Loeser, R.F., et al., *Osteoarthritis: A Disease of the Joint as an Organ.* Arthritis and Rheumatism, 2012. **64**(6): p. 1697-1707.
69. Lees, D. and P. Partington, *Articular Cartilage.* Orthopaedics and Trauma, 2016. **30**(3): p. 265-272.
70. Sophia Fox, A.J., A. Bedi, and S.A. Rodeo, *The Basic Science of Articular Cartilage: Structure, Composition, and Function.* Sports health, 2009. **1**(6): p. 461-468.
71. Zhang, Y., et al., *Analysis of the Mineral Composition of the Human Calcified Cartilage Zone.* International Journal of Medical Sciences, 2012. **9**(5): p. 353-360.
72. Stewart, H.L. and C.E. Kawcak, *The Importance of Subchondral Bone in the Pathophysiology of Osteoarthritis.* Frontiers in Veterinary Science, 2018. **5**: p. 178-178.
73. Elango, J., et al., *Cross-Talk between Primary Osteocytes and Bone Marrow Macrophages for Osteoclastogenesis Upon Collagen Treatment.* Scientific Reports, 2018. **8**(5318): p. 1-11.
74. Nedeva, I.R., et al., *Role of Oscar Signaling in Osteoclastogenesis and Bone Disease.* Frontiers in cell and developmental biology, 2021. **9**(641162).

75. Park, D.R., et al., *Osteoclast-Associated Receptor Blockade Prevents Articular Cartilage Destruction Via Chondrocyte Apoptosis Regulation.* Nature Communications, 2020. **11**(1): p. 4343.

76. Boraschi-Diaz, I., et al., *Collagen Type I as a Ligand for Receptor-Mediated Signaling.* Frontiers in Physics, 2017. **5**(12).

77. Boraschi-Diaz, I., et al., *Collagen Type I Degradation Fragments Act through the Collagen Receptor Lair-1 to Provide a Negative Feedback for Osteoclast Formation.* Bone, 2018. **117**: p. 23-30.

78. Jackson, M.T., et al., *Activation of Matrix Metalloproteinases 2, 9, and 13 by Activated Protein C in Human Osteoarthritic Cartilage Chondrocytes.* Arthritis Rheumatol, 2014. **66**(6): p. 1525-1536.

79. Zeng, G.Q., et al., *High MMP-1, MMP-2, and MMP-9 Protein Levels in Osteoarthritis.* Genetics and Molecular Research, 2015. **14**(4): p. 14811-14822.

80. Chiu, Y.-H. and C.T. Ritchlin, *Dc-Stamp: A Key Regulator in Osteoclast Differentiation.* Journal of Cellular Physiology, 2016. **231**(11): p. 2402-2407.

81. Liu, J., et al., *Bovine Collagen Peptides Compounds Promote the Proliferation and Differentiation of MC3T3-E1 Pre-Osteoblasts.* PloS One, 2014. **9**(6): p. e99920.

82. Min, G., et al., *Collagen Hydrolysate Gly-Pro-Hyp on Osteoblastic Proliferation and Differentiation of MC3T3-E1 Cells.* Journal of Clinical and Nursing Research, 2017. **1**(3): p. 40-46.

83. Amarasekara, D.S., S. Kim, and J. Rho, *Regulation of Osteoblast Differentiation by Cytokine Networks.* International Journal of Molecular Sciences, 2021. **22**(6): p. 2851.

84. Liu, Q., et al., *Recent Advances of Osterix Transcription Factor in Osteoblast Differentiation and Bone Formation.* Frontiers in cell and developmental biology, 2020. **8**(601224).

85. Nishimura, R., et al., *Osterix Regulates Calcification and Degradation of Chondrogenic Matrices through Matrix Metalloproteinase 13 (Mmp13) Expression in Association with Transcription Factor Runx2 During Endochondral Ossification.* Journal of Biological Chemistry, 2012. **287**(40): p. 33179-33190.

86. Wang, X., et al., *Regulation of Mmp-13 Expression by Runx2 and FGF2 in Osteoarthritic Cartilage.* Osteoarthritis and Cartilage, 2004. **12**(12): p. 963-973.

87. Poole, A.R., *Osteoarthritis as a Whole Joint Disease.* HSS journal : the musculoskeletal journal of Hospital for Special Surgery, 2012. **8**(1): p. 4-6.
88. Oegema, T.R., et al., *The Interaction of the Zone of Calcified Cartilage and Subchondral Bone in Osteoarthritis.* Microscopy Research and Technique, 1997. **37**(4): p. 324-332.
89. Amarasekara, D.S., J. Yu, and J. Rho, *Bone Loss Triggered by the Cytokine Network in Inflammatory Autoimmune Diseases.* Journal of Immunology Research, 2015. **2015**(832127).
90. Amarasekara, D.S., et al., *Regulation of Osteoclast Differentiation by Cytokine Networks.* Immune Network, 2018. **18**(1).
91. van der Kraan, P.M. and W.B. van den Berg, *Chondrocyte Hypertrophy and Osteoarthritis: Role in Initiation and Progression of Cartilage Degeneration?* Osteoarthritis and Cartilage, 2012. **20**(3): p. 223-232.
92. Leopoldino, A.O., et al., *Paracetamol Versus Placebo for Knee and Hip Osteoarthritis.* The Cochrane database of systematic reviews, 2019. **2**(2): p. Cd013273.
93. Meunier, L. and D. Larrey, *Recent Advances in Hepatotoxicity of Non Steroidal Anti-Inflammatory Drugs.* Annals of Hepatology, 2018. **17**(2): p. 187-191.
94. Arulselvan, P., et al., *Role of Antioxidants and Natural Products in Inflammation.* Oxidative Medicine and Cellular Longevity, 2016. **2016**: p. 5276130.
95. Bourne, R.B., et al., *Patient Satisfaction after Total Knee Arthroplasty: Who Is Satisfied and Who Is Not?* Clinical Orthopaedics and Related Research, 2010. **468**(1): p. 57-63.
96. Dickinson, A., D. MacKay, and A. Wong, *Consumer Attitudes About the Role of Multivitamins and Other Dietary Supplements: Report of a Survey.* Nutrition Journal, 2015. **14**: p. 66.
97. Sirico, F., et al., *Habits and Beliefs Related to Food Supplements: Results of a Survey among Italian Students of Different Education Fields and Levels.* PloS One, 2018. **13**(1).
98. Ferraro, V., M. Anton, and V. Santé-Lhoutellier, *The "Sisters" A-Helices of Collagen, Elastin and Keratin Recovered from Animal by-Products: Functionality, Bioactivity and Trends of Application.* Trends in Food Science & Technology, 2016. **51**: p. 65-75.
99. Liu, D., et al., *Collagen and Gelatin.* Annual Review of Food Science and Technology, 2015. **6**(1): p. 527-557.
100. Fu, Y., et al., *Exploration of Collagen Recovered from Animal by-Products as a Precursor of Bioactive Peptides: Successes and Challenges.* Critical Reviews in Food Science and Nutrition, 2019. **59**(13): p. 2011-2027.

101. Ohara, H., et al., *Comparison of Quantity and Structures of Hydroxyproline-Containing Peptides in Human Blood after Oral Ingestion of Gelatin Hydrolysates from Different Sources.* Journal of Agricultural and Food Chemistry, 2007. **55**(4): p. 1532-1535.

102. Yamamoto, S., et al., *Absorption and Urinary Excretion of Peptides after Collagen Tripeptide Ingestion in Humans.* Biological & Pharmaceutical Bulletin, 2016. **39**(3): p. 428-434.

103. Benito-Ruiz, P., et al., *A Randomized Controlled Trial on the Efficacy and Safety of a Food Ingredient, Collagen Hydrolysate, for Improving Joint Comfort.* International Journal of Food Sciences and Nutrition, 2009. **60**(Suppl 2): p. 99-113.

104. Kumar, S., et al., *A Double-Blind, Placebo-Controlled, Randomised, Clinical Study on the Effectiveness of Collagen Peptide on Osteoarthritis.* Journal of the Science of Food and Agriculture, 2015. **95**(4): p. 702-707.

105. Feliciano, D.D.S., et al., *Effect of Collagen Hydrolysate as Adjuvant Treatment to Exercise for Knee Osteoarthritis*, in *Philippine Academy of Rehabilitation Medicine*. 2017. p. 4-15.

106. Clark, K.L., et al., *24-Week Study on the Use of Collagen Hydrolysate as a Dietary Supplement in Athletes with Activity-Related Joint Pain.* Current Medical Research and Opinion, 2008. **24**(5): p. 1485-1496.

107. McAlindon, T.E., et al., *Change in Knee Osteoarthritis Cartilage Detected by Delayed Gadolinium Enhanced Magnetic Resonance Imaging Following Treatment with Collagen Hydrolysate: A Pilot Randomized Controlled Trial.* Osteoarthritis and Cartilage, 2011. **19**(4): p. 399-405.

108. Martin-Bautista, E., et al., *A Nutritional Intervention Study with Hydrolyzed Collagen in Pre-Pubertal Spanish Children: Influence on Bone Modeling Biomarkers.* Journal of Pediatric Endocrinology and Metabolism, 2011. **24**(3-4): p. 147-153.

109. Adam, M., et al., *Postmenopausal Osteoporosis. Treatment with Calcitonin and a Diet Rich in Collagen Proteins.* Casopis Lekaru Ceskych, 1996. **135**(3): p. 74-78.

110. Moskowitz, R.W., *Role of Collagen Hydrolysate in Bone and Joint Disease.* Seminars in Arthritis and Rheumatism, 2000. **30**(2): p. 87-99.

111. Minkiewicz, P., et al., *Biopep Database and Other Programs for Processing Bioactive Peptide Sequences.* Journal of AOAC International, 2008. **91**(4): p. 965-980.

112. Minkiewicz, P., A. Iwaniak, and M. Darewicz, *Biopep-Uwm Database of Bioactive Peptides: Current Opportunities.* International Journal of Molecular Sciences, 2019. **20**(23): p. 5978.

113. Shi, L., et al., *BioPD: A Web-Based Information Center for Bioactive Peptides.* Regulatory Peptides, 2004. **120**(1): p. 1-3.

114. Nakatani, S., et al., *Chondroprotective Effect of the Bioactive Peptide Prolyl-Hydroxyproline in Mouse Articular Cartilage in Vitro and in Vivo.* Osteoarthritis and Cartilage, 2009. **17**(12): p. 1620-1627.

115. Knight, C.G., et al., *Collagen-Platelet Interaction: Gly-Pro-Hyp Is Uniquely Specific for Platelet Gp VI and Mediates Platelet Activation by Collagen.* Cardiovascular Research, 1999. **41**(2): p. 450-457.

116. Hatanaka, T., K. Kawakami, and M. Uraji, *Inhibitory Effect of Collagen-Derived Tripeptides on Dipeptidylpeptidase-Iv Activity.* Journal of Enzyme Inhibition and Medicinal Chemistry, 2014. **29**(6): p. 823-828.

117. Piva, S.R., et al., *Links between Osteoarthritis and Diabetes: Implications for Management from a Physical Activity Perspective.* Clinics in Geriatric Medicine, 2015. **31**(1): p. 67-87 viii.

118. Louati, K., et al., *Association between Diabetes Mellitus and Osteoarthritis: Systematic Literature Review and Meta-Analysis.* RMD Open, 2015. **1**(1): p. e000077.

119. Kimira, Y., et al., *Collagen-Derived Dipeptide Prolyl-Hydroxyproline Promotes Differentiation of MC3T3-E1 Osteoblastic Cells.* Biochemical and Biophysical Research Communications, 2014. **453**(3).

120. Kim, H.K., M.-G. Kim, and K.-H. Leem, *Collagen Hydrolysates Increased Osteogenic Gene Expressions Via a MAPK Signaling Pathway in MG-63 Human Osteoblasts.* Food & Function, 2014. **5**(3): p. 573-578.

121. Van Vijven, J.P.J., et al., *Symptomatic and Chondroprotective Treatment with Collagen Derivatives in Osteoarthritis: A Systematic Review.* Osteoarthritis and Cartilage, 2012. **20**(8): p. 809-821.

122. Henrotin, Y., et al., *Nutraceuticals: Do They Represent a New Era in the Management of Osteoarthritis? - a Narrative Review from the Lessons Taken with Five Products.* Osteoarthritis and Cartilage, 2011. **19**(1): p. 1-21.

123. Liu, X., et al., *Which Supplements Can I Recommend to My Osteoarthritis Patients?* Rheumatology, 2018. **57**(suppl_4): p. iv75-iv87.

124. Mobasheri, A., et al., *A White Paper on Collagen Hydrolyzates and Ultrahydrolyzates: Potential Supplements to Support Joint Health in Osteoarthritis?* Current Rheumatology Reports, 2021. **23**(11): p. 78.

125. McAlindon, T., et al., *Determination of Serum Biomarkers in Osteoarthritis Patients: A Previous Interventional Imaging Study Revisited.* Journal of Biomedical Research, 2017. **31**(1): p. 25-30.

126. Prince, R.L., et al., *Effects of Calcium Supplementation on Clinical Fracture and Bone Structure: Results of a 5-Year, Double-Blind, Placebo-Controlled Trial in Elderly Women.* Archives of Internal Medicine, 2006. **166**(8): p. 869-875.

127. Fite, M.B., et al., *Compliance with Iron and Folic Acid Supplementation (Ifas) and Associated Factors among Pregnant Women in Sub-Saharan Africa: A Systematic Review and Meta-Analysis.* PloS One, 2021. **16**(4): p. e0249789.

128. Gonzalez-Casanova, I., et al., *Predictors of Adherence to Micronutrient Supplementation before and During Pregnancy in Vietnam.* BMC Public Health, 2017. **17**(1): p. 452.

129. Malek, L., et al., *Poor Adherence to Folic Acid and Iodine Supplement Recommendations in Preconception and Pregnancy: A Cross-Sectional Analysis.* Australian and New Zealand Journal of Public Health, 2016. **40**(5): p. 424-429.

130. Yap, A.F., T. Thirumoorthy, and Y.H. Kwan, *Medication Adherence in the Elderly.* Journal of Clinical Gerontology and Geriatrics, 2016. **7**(2): p. 64-67.

131. Kocurek, B., *Promoting Medication Adherence in Older Adults … and the Rest of Us.* Diabetes Spectrum, 2009. **22**(2): p. 80.

132. Bastani, P., et al., *Medication Adherence among the Elderly: Applying Grounded Theory Approach in a Developing Country.* Journal of Pharmaceutical Policy and Practice, 2021. **14**(1): p. 55.

133. Wang, A., et al., *Nutraceuticals and Osteoarthritis Pain.* Pharmacology & Therapeutics, 2018. **187**: p. 167-179.

134. Trč, T. and J. Bohmová, *Efficacy and Tolerance of Enzymatic Hydrolysed Collagen (EHC) Vs. Glucosamine Sulphate (GS) in the Treatment of Knee Osteoarthritis (KOA).* International Orthopaedics, 2011. **35**(3): p. 341-348.

135. Crowley, D.C., et al., *Safety and Efficacy of Undenatured Type II Collagen in the Treatment of Osteoarthritis of the Knee: A Clinical Trial.* International Journal of Medical Sciences, 2009. **6**(6): p. 312-321.

136. Verhoeckx, K., et al., *General Introduction* in *The Impact of Food Bioactives on Health*, K. Verhoeckx, et al., Editors. 2015, Springer. p. viii-xi.

137. Brayden, D.J., *Evolving Peptides for Oral Intake.* Nature Biomedical Engineering, 2020. **4**(5): p. 487-488.

138. Simons, V.S., et al., *Comparative Analysis of Peptide Composition and Bioactivity of Different Collagen Hydrolysate Batches on Human Osteoarthritic Synoviocytes.* Scientific Reports, 2018. **8**(17733).

139. Alegría, A., G. Garcia-Llatas, and A. Cilla, *Static Digestion Models: General Introduction*, in *The Impact of Food Bioactives on Health: In Vitro and Ex Vivo Models*, K. Verhoeckx, et al., Editors. 2015, Springer International Publishing: Cham. p. 3-12.

140. Mackie, A., A.-I. Mulet-Cabero, and A. Torcello-Gómez, *Simulating Human Digestion: Developing Our Knowledge to Create Healthier and More Sustainable Foods.* Food & Function, 2020. **11**(11): p. 9397-9431.

141. Guo, L., et al., *In Vitro Assessment of the Multifunctional Bioactive Potential of Alaska Pollock Skin Collagen Following Simulated Gastrointestinal Digestion.* Journal of the Science of Food and Agriculture, 2015. **95**(7): p. 1514-1520.

142. Egger, L., et al., *The Harmonized Infogest in Vitro Digestion Method : From Knowledge to Action.* Food Research International, 2016. **88**(Par B): p. 217-225.

143. Escudero, E., M.A. Sentandreu, and F. Toldrá, *Characterization of Peptides Released by in Vitro Digestion of Pork Meat.* Journal of Agricultural and Food Chemistry, 2010. **58**(8): p. 5160-5165.

144. Sayd, T., et al., *Combined in Vivo and in Silico Approaches for Predicting the Release of Bioactive Peptides from Meat Digestion.* Food Chemistry, 2018. **249**: p. 111-118.

145. Shigemura, Y., et al., *Identification of Food-Derived Elastin Peptide, Prolyl-Glycine (Pro-Gly), in Human Blood after Ingestion of Elastin Hydrolysate.* Journal of Agricultural and Food Chemistry, 2012. **60**(20): p. 5128-5133.

146. Kawaguchi, T., P.N. Nanbu, and M. Kurokawa, *Distribution of Prolylhydroxyproline and Its Metabolites after Oral Administration in Rats.* Biological & Pharmaceutical Bulletin, 2012. **35**(3): p. 422-427.

147. Lea, T., *Caco-2 Cell Line*, in *The Impact of Food Bioactives on Health: In Vitro and Ex Vivo Models*, K. Verhoeckx, et al., Editors. 2015, Springer, Cham. p. 103-111.

148. Feng, M. and M. Betti, *Transepithelial Transport Efficiency of Bovine Collagen Hydrolysates in a Human Caco-2 Cell Line Model.* Food Chemistry, 2017. **224**: p. 242-250.

149. Larregieu, C.A. and L.Z. Benet, *Drug Discovery and Regulatory Considerations for Improving in Silico and in Vitro Predictions That Use Caco-2 as a Surrogate for Human Intestinal Permeability Measurements.* The American Association of Pharmaceutical Scientists Journal 2013. **15**(2): p. 483-497.

150. Cheng, K.C., et al., *Development of a High-Throughput in Vitro Assay Using a Novel Caco-2/Rat Hepatocyte System for the Prediction of Oral Plasma Area under the Concentration Versus Time Curve (Auc) in Rats.* Journal of Pharmacological and Toxicological Methods, 2006. **53**(3): p. 215-218.

151. Zhang, M., et al., *The Dipeptide Pro-Gly Promotes IGF-1 Expression and Secretion in HepG2 and Female Mice Via PepT1-JAK2/STAT5 Pathway.* Frontiers in Endocrinology, 2018. **9**(424).

152. La Fata, G., et al., *Recent Development of Prebiotic Research-Statement from an Expert Workshop.* Nutrients, 2017. **9**(12): p. 1376.

153. Matt, S.M., et al., *Butyrate and Dietary Soluble Fiber Improve Neuroinflammation Associated with Aging in Mice.* Frontiers in Immunology, 2018. **9**: p. 1832.

154. Li, Z., et al., *Butyrate Reduces Appetite and Activates Brown Adipose Tissue Via the Gut-Brain Neural Circuit.* Gut, 2018. **67**(7): p. 1269-1279.

155. Mollica, M.P., et al., *Butyrate Regulates Liver Mitochondrial Function, Efficiency, and Dynamics in Insulin-Resistant Obese Mice.* Diabetes, 2017. **66**(5): p. 1405-1418.

156. Chang, Y., et al., *Short-Chain Fatty Acids Accompanying Changes in the Gut Microbiome Contribute to the Development of Hypertension in Patients with Preeclampsia.* Clinical Science, 2020. **134**(2): p. 289-302.

157. Saresella, M., et al., *Alterations in Circulating Fatty Acid Are Associated with Gut Microbiota Dysbiosis and Inflammation in Multiple Sclerosis.* Frontiers in Immunology, 2020. **11**(1390).

158. Ma, N. and X. Ma, *Dietary Amino Acids and the Gut-Microbiome-Immune Axis: Physiological Metabolism and Therapeutic Prospects.* Comprehensive Reviews in Food Science and Food Safety, 2019. **18**(1): p. 221-242.

159. Wallace, J.L., J.P. Motta, and A.G. Buret, *Hydrogen Sulfide: An Agent of Stability at the Microbiome-Mucosa Interface.* American Journal of Physiology: Gastrointestinal and Liver Physiology, 2018. **314**(2): p. 143-149.

160. Sun, L., et al., *Purification of Antioxidant Peptides by High Resolution Mass Spectrometry from Simulated Gastrointestinal Digestion Hydrolysates of Alaska Pollock (Theragra Chalcogramma) Skin Collagen.* Marine Drugs, 2016. **14**(10): p. 186.

161. Bianchi, M.A., et al., *Ability of a High-Total Antioxidant Capacity Diet to Increase Stool Weight and Bowel Antioxidant Status in Human Subjects.* British Journal of Nutrition, 2010. **104**(10): p. 1500-1507.

162. Ao, J. and B. Li, *Amino Acid Composition and Antioxidant Activities of Hydrolysates and Peptide Fractions from Porcine Collagen.* Food Science and Technology International, 2012. **18**(5): p. 425-434.

163. Silverstein, A.M., et al., *Toward Understanding the Role of Cartilage Particulates in Synovial Inflammation.* Osteoarthritis and Cartilage, 2017. **25**(8): p. 1353-1361.

164. Di Bernardini, R., et al., *Antioxidant and Antimicrobial Peptidic Hydrolysates from Muscle Protein Sources and by-Products.* Food Chemistry, 2011. **124**(4): p. 1296-1307.

165. Emwas, A.-H., et al., *Recommended Strategies for Spectral Processing and Post-Processing of 1D ^{1}H-NMR Data of Biofluids with a Particular Focus on Urine.* Metabolomics, 2018. **14**(3): p. 31.

166. Cao, X., et al., *Why Is It Challenging to Predict Intestinal Drug Absorption and Oral Bioavailability in Human Using Rat Model.* Pharmaceutical Research, 2006. **23**(8): p. 1675-1686.

167. Musther, H., et al., *Animal Versus Human Oral Drug Bioavailability: Do They Correlate?* European Journal of Pharmaceutical Sciences, 2014. **57**(1): p. 280-291.

168. Lacroix, I.M.E., et al., *Investigation into the Bioavailability of Milk Protein-Derived Peptides with Dipeptidyl-Peptidase Iv Inhibitory Activity Using Caco-2 Cell Monolayers.* Food & Function, 2017. **8**(2): p. 701-709.

169. Wang, B. and B. Li, *Effect of Molecular Weight on the Transepithelial Transport and Peptidase Degradation of Casein-Derived Peptides by Using Caco-2 Cell Model.* Food Chemistry, 2017. **218**: p. 1-8.

170. Guo, Y., et al., *Transepithelial Transport of Milk-Derived Angiotensin I-Converting Enzyme Inhibitory Peptide with the RLSFNP Sequence.* Journal of the Science of Food and Agriculture, 2018. **98**(3): p. 976-983.

171. Sadeghi Ekbatan, S., et al., *Biotransformation of Polyphenols in a Dynamic Multistage Gastrointestinal Model.* Food Chemistry, 2016. **204**: p. 453-462.

172. Gaisawat, M.B., et al., *Probiotic Supplementation in a Clostridium Difficile-Infected Gastrointestinal Model Is Associated with Restoring Metabolic Function of Microbiota.* Microorganisms, 2019. **8**(1): p. 60.

173. Tiedemann, K., et al., *Regulation of Osteoclast Growth and Fusion by mTOR/raptor and mTOR/rictor/Akt.* 2017. **5**.

174. Paiva, K.B.S. and J.M. Granjeiro, *Chapter Six - Matrix Metalloproteinases in Bone Resorption, Remodeling, and Repair*, in *Progress in Molecular Biology and Translational Science*, R.A. Khalil, Editor. 2017, Academic Press. p. 203-303.

175. Hata, S., et al., *Effect of Oral Administration of High Advanced-Collagen Tripeptide (HACP) on Bone Healing Process in Rat.* Journal of Hard Tissue Biology, 2008. **17**(1): p. 17-22.

176. Bernardo, M.L.R. and A.C. Azarcon Jr., *A Randomized Controlled Trial on the Effects of Oral Collagen Treatment on the Medial Knee Joint Space and Functional Outcome among Veterans Medical Center Patients Diagnosed with Osteoarthritis of the Knee* in *Philippine Academy of Rehabilitation Medicine Proceedings* 2012. p. 1-8.

177. Flick, T.G., et al., *Solution Additives That Desalt Protein Ions in Native Mass Spectrometry.* Analytical Chemistry, 2012. **84**(17): p. 7511-7517.

178. Jehmlich, N., et al., *Comparative Evaluation of Peptide Desalting Methods for Salivary Proteome Analysis.* Clinica Chimica Acta, 2014. **434**: p. 16-20.

179. Chen, D., et al., *Osteoarthritis: Toward a Comprehensive Understanding of Pathological Mechanism.* Bone Research, 2017. **5**(1): p. 16044.

180. Brodkorb, A., et al., *Infogest Static in Vitro Simulation of Gastrointestinal Food Digestion.* Nature Protocols, 2019. **14**(4): p. 991-1014.

181. Zanaboni, G., et al., *Use of Capillary Zone Electrophoresis for Analysis of Imidodipeptides in Urine of Prolidase-Deficient Patients.* Journal of Chromatography B: Biomedical Sciences and Applications, 1996. **683**(1): p. 97-107.

182. Mikšík, I., et al., *Capillary Electromigration Methods for the Study of Collagen.* Journal of Chromatography B, 2006. **841**(1-2): p. 3-13.

183. Xiang, Y., et al., *Gut-on-Chip: Recreating Human Intestine in Vitro.* Journal of tissue engineering, 2020. **11**(2041731420965318).

184. Steinway, S.N., et al., *Human Microphysiological Models of Intestinal Tissue and Gut Microbiome.* Frontiers in Bioengineering and Biotechnology, 2020. **8**(725).

185. An, F., et al., *A Laminated Microfluidic Device for Comprehensive Preclinical Testing in the Drug Adme Process.* Scientific Reports, 2016. **6**(1): p. 25022.

186. Kimura, H., et al., *An on-Chip Small Intestine-Liver Model for Pharmacokinetic Studies.* J Lab Autom, 2015. **20**(3): p. 265-273.

187. Imura, Y., K. Sato, and E. Yoshimura, *Micro Total Bioassay System for Ingested Substances: Assessment of Intestinal Absorption, Hepatic Metabolism, and Bioactivity.* Analytical Chemistry, 2010. **82**(24): p. 9983-9988.

188. Feng, M. and M. Betti, *Both PepT1 and GLUT Intestinal Transporters Are Utilized by a Novel Glycopeptide Pro-Hyp-CONH-GlcN.* Journal of Agricultural and Food Chemistry, 2017. **65**(16): p. 3295-3304.

189. Bruno, B.J., G.D. Miller, and C.S. Lim, *Basics and Recent Advances in Peptide and Protein Drug Delivery.* Therapeutic Delivery, 2013. **4**(11): p. 1443-1467.